Aston University

Some parts of this thesis may have been removed for copyright restrictions.

If you have discovered material in AURA which is unlawful e.g. breaches copyright, (either yours or that of a third party) or any other law, including but not limited to those relating to patent, trademark, confidentiality, data protection, obscenity, defamation, libel, then please read our Takedown Policy and contact the service immediately

Investigation into visual defects attributed to Vigabatrin.

Miriam Conway

Doctor of Philosophy

Aston University

December 2003

The copy of the thesis has been supplied on the condition that anyone who consults it is understood to recognise that its copyright rests with its author and that no quotation from the thesis and no information derived from it may be published without proper acknowledgement.

Thesis Summary

Vigabatrin (VGB) is a transaminase inhibitor that elicits its antiepileptic effect by increasing GABA concentrations in the brain and retina. Over recent years evidence has accumulated to suggest a strong association between VGB therapy and visual field defects. To date, no-one has established why a significant proportion of the population remain protected from visual disturbances or why pathology is reported to remain confined to the peripheral retina. This investigation aims to:

- Assess whether certain factors predispose patients to develop severe visual field loss.
- Develop a sensitive algorithm for investigating the progression of visual field loss.
- Determine the most sensitive clinical regimen for diagnosing VGB-attributed visual field loss.
- Investigate whether the reports of central retinal sparing are accurate.

The investigations have resulted in a number of significant findings:

- The anatomical evidence in combination with the pattern of visual field loss suggests that the damage induced by VGB therapy occurs at retinal level, and is most likely a toxic effect.
- The quantitative algorithm, designed within the course of this investigation, provided increased sensitivity in determining the severity of visual field loss.
- Maximum VGB dose predisposes patients to developing severe visual field loss.
- The SITA Standard algorithm was found to be as sensitive and significantly faster, in diagnosing visual field defects attributed to VGB, when compared to the Full Threshold algorithm. The Full Threshold algorithm was found to be the most repeatable between visits.
- The normal SWAP 10-2 database provided an effective method of differentiating SWAP defects.
- SWAP, FDT and the mfERG have increased sensitivity in detecting visual field loss attributed to VGB. The pattern of visual field loss from these investigations suggests that VGB produces a diffuse effect across the retina including subtle central abnormalities and more severe peripheral defects.
- Abnormalities detected using the mfERG have suggested that VGB adversely affects the photoreceptors Müller, amacrine and ganglion cells in the retina.

An urgent review of the manufacturers recommended maximum dose for VGB is required, as it is currently based on the efficacy of the drug and not its toxicological side effects. White-white perimetry significantly underestimates the prevalence of visual field abnormalities attributed to VGB and fails to detect subtle deficits in the central retina. The optional clinical regimen for detecting visual field loss attributed to VGB should include SWAP, using Program 10-2, and FDT. Patients with confirmed visual field loss who need to be identified for visual field progression are recommended to undergo visual field examination using the Full Threshold algorithm and have their results analysed using the quantitative algorithm.

Acknowledgements

I would like to thank each of my supervisors, Paul Furlong, Sarah Hosking and Robert Cubbidge for their intellectual input throughout the course of this research. Their help was greatly appreciated, in particular for encouraging me and commenting on the final draft of this thesis.

Thanks to all the staff at Aston University, particularly Andrea Scott for her technical advice with electrophysiology and Professor Graham Harding for his constructive comments on my multifocal electroretinogram chapter.

I am grateful to all my participants for their time and patience in each of the studies.

Finally, I am very much indebted to my family, fellow post-graduate students and Andrew for their moral support throughout the period of this research.

Table of Contents

List of Tables

List of Figures

List of Equations

1. Introduction: to visual field damage in epilepsy

1.1. Definition of Epilepsy

The word epilepsy is derived from the Greek verb *epilamvanein* meaning *to be seized, to be taken hold of*, or *to be attacked*. The term is related to a group of symptoms arising from a wide variety of abnormal brain functions. A diagnosis is based on two or more epileptic seizures, which are unprovoked by any immediately identifiable cause. Those individuals demonstrating only febrile or neonatal seizures are excluded from this category.

1.2. Epileptic seizures

A seizure is the clinical expression resulting from the excessive firing of a set of neurones in the brain. The seizures are not a disease in themselves, but a symptom of the many different disorders that may affect the brain. The clinical expression consists of sudden, temporary phenomena, which may include alterations in consciousness, motor sensory, autonomic, or apparent psychic occurrences.

1.3. Types of Epileptic Seizure

Classification of the different types of seizures is vital in terms of making the correct treatment choice, administering useful advice to each patient (prognosis, clinical course, treatments) and the advancement of knowledge. In 1981 the Commission on Classification and Terminology of the International League against Epilepsy developed a classification of epileptic seizures (*International Classification of Epileptic Seizures*) based on a number of factors. Partial and generalised seizures are grouped separately. Other distinguishing factors included aetiologies, a detailed history and electroencephalography (EEG) results. In recent years this classification has been criticised by neurologists for its simplicity and inflexibility. Few patients diagnosed with epilepsy appear to fall into an exact category, patients may move from one syndrome to another, within their epileptic condition. A revised classification entitled the *International Classification of Epilepsies and Epileptic Syndromes* (ICE) however, now exists to help address some of the original difficulties.

1.3.1. Partial Seizure

Partial seizures are those that remain confined to one area of the brain. In a simple partial seizure the patient remains in a fully conscious state and may develop a number of symptoms depending on the exact location of the abnormal activity. If they have motor

symptoms, portions of their body may be involved in focal seizure activity. If they have autonomic symptoms they may complain of symptoms such as vomiting, pallor, flush or sweating. If they have somatosensory or special sensory symptoms they may complain of numbness, hallucinations or olfactory sensations such as a bad odour.

1.3.2. Complex partial seizure

The main characteristic of a complex partial seizure is impairment of consciousness, which may or may not be associated with automatisms. Automatisms are co-ordinated adapted involuntary motor activity occurring during a state of clouding of the consciousness and usually followed by amnesia of the event. An example of an automatism would be fumbling with their clothing or scratching themselves whilst having the seizure and afterwards being unaware that the event ever occurred.

1.3.3. Partial seizure evolving to secondarily generalised

This type of seizure may take several different routes. Simple partial seizures evolving into generalised seizure, complex partial seizures evolving into generalised seizures, or simple partial evolving into complex partial evolving into generalised seizure.

1.3.4. Generalised seizure

This group of seizures is thought to originate from the involvement of both hemispheres in the brain and are broken into sub-groups according to the seizure type. The hallmark of a typical absence seizure is the interruption of the ongoing activity. Absences may be associated with an impairment of consciousness only, or they may have a mild clonic, atonic, or tonic component of autism. Tonic clonic seizures were previously called grand-mal seizures and are the most frequently encountered of the generalised seizures. There is a sudden sharp tonic contraction of muscle, the patient then falls to the ground in a tonic state and lies there rigidly. The tonic state gives way to the clonic convulsive movements, at the end of the seizure the muscles relax and the patient usually remains in an unconscious state for a while. Myoclonic Jerks are single or multiple, sudden brief shock like contractions, that may be generalised, limited to the face or trunk or target specific muscle groups. Clonic Seizures are generalised convulsive seizures that lack a tonic component. In a Tonic seizure a rigid violent muscle contraction occurs, because of this the limbs may be placed in a strained position. While in Atonic seizure sudden diminution in muscle tone may lead to a head drop or even a fall.

1.3.5. Unclassified

Lists any seizure that is not classified, due to insufficient data.

1.3.6. Infantile Spasm

Certain seizure types are specific to the paediatric community. Infantile spasms, also known as West's syndrome, usually begin between 3 and 12 months of age and usually stop between 2 to 4 years old. The disorder has unique features including the spasms themselves, hypsarrhythmia (multifocal spikes, disorganised background and burst-suppression) on the EEG and possible developmental delay. The seizures, or spasms, consist of a sudden jerk followed by stiffening, in some spells, the arms and legs might be extended and the trunk bends forward. The prognosis for this particular syndrome is generally poor with many children subsequently developing other seizure types and/or cognitive impairment (Appleton, 2001). The treatment is initiated immediately after diagnosis in an aggressive manner, in an attempt to control the seizures and prevent mental retardation.

1.4. Incidence of epilepsy and different seizures

Epilepsy is a relatively common neurological condition, which is believed to affect around 300,000 people in the UK and an estimated 40 million world-wide (The National Society for Epilepsy April 2003). The greatest incidence of epilepsy appears to be in the first few months, after the first year the prevalence falls dramatically. The incidence remains fairly stable in the middle range of ages, in the older age group there is another sharp increase (Hopkins & Shorvon, 1995). The incidence of specific types of seizure is known to vary: data from one longitudinal study documented that over 50% of their investigated cases were classified with partial seizures (Hauser, Annegers, & Kurland, 1993).

1.5. Risks associated with epilepsy

A number of risks are associated with epilepsy. Injuries may occur as the result of an actual seizure or more commonly, from a fall through loss of consciousness. Injury is normally soft tissue with or without laceration, occasionally however fractured skulls or subdural haematomas are also reported. Prevalence studies suggest that children with epilepsy are approximately 7.5 times more likely to drown or nearly drown than children who do not develop the condition (Kemp & Sibert, 1993). Patients with uncontrolled epilepsy find that their jobs and hobbies such as: driving, working with heavy machinery, electricity or swimming, are severely restricted. Their autonomy may be severely limited by the psychological stigma which is still associated with the condition. A study of epilepsy at work revealed that 81% of patients demonstrating less than one seizure per year were employed compared with the 47% of patients who had more than one seizure per year (Rodin, 1982).

1.6. Mortality of Epilepsy

The largest cause of death in epilepsy are the conditions underlying its pathology, i.e. stroke, cerebral tumour and other diseases. In a population of patients diagnosed with epilepsy, 14% of deaths were related to the epilepsy itself, 15% were from cerebral tumour, 16% from heart diseases and 55% from other non-specified causes (Tennis *et al.*, 1995). Zielinski (1974) has reported that approximately 25% of patients died from causes directly related to the seizures with a further 10% of the population dying from a result of suicide. The suicide rate was approximately five times the expected rate and was probably due to the large number of psychological disadvantages associated with epilepsy and its treatments.

1.7. The Prognosis of Epilepsy

For the majority of individuals the condition is self-limiting and the seizures usually stop. In one retrospective study, it was reported that 15 years after diagnosis, 76% of those who were diagnosed with epilepsy, had not had a seizure in the last 5 years and over 50% were off treatment altogether (Annegers, Hauser, & Elveback, 1979). Hospital based studies suggest that between 60% and 95% of patients treated with monotherapy enter at least one-year remission at the onset of therapy, however, those with partial epilepsy do less well (Shorvon, 1982). The above data suggests that for the majority of patients their epilepsy is a temporary condition.

1.8. Chronic Epilepsy

The clinic course for patients with long-standing epilepsy is very different. Small improvements in seizure frequency are occasionally seen, however, relapse is common. Epilepsy has been previously divided into the following four outcome groups (Shorvon, 1991). Excellent prognosis is thought to represent 20-30% of all cases, including those patients with relatively few seizures and self-limiting epilepsy. Good prognosis is thought to represent 30-40% of all cases, including patients with seizures that are easily controlled and where spontaneous remission is possible. Uncertain prognosis is thought to represent 10-20% of all cases, including those patients where drug therapy is progressive and the treatment might result in seizure control. Poor prognosis is thought to represent 20% of all cases, including those patients where intensive drug therapy is largely unsuccessful and surgery is often not possible. This group includes severe childhood syndromes such as Lennox-Gastaut syndrome, West syndrome and Sturge–Weber syndrome.

1.9. Treatment for epilepsy

There are approximately 40 distinct epilepsy syndromes. The large numbers and varying aetiologies ensures that epilepsy is a difficult neurological problem to control.

1.9.1. Pharmacological treatment

The choice of drug is primarily dependent upon the type of seizure and/or syndrome. Certain drugs are more responsive within specific types of seizure. Duration of treatment and expense are other important considerations, as certain drugs are too expensive and others are toxic only after a specific period of time. Monotherapy is the preferred method of treatment because systemic interaction with other drugs is not possible. Multiple drug therapy however, is frequently necessary. The toxicological side effects of any pharmacological treatment are extremely significant and may vary depending on the quantity of drug, systemic interactions with alternative anti epileptic drugs (AEDs), gender, body mass and genetic variability of an individual patient. The majority of early antiepileptic medications were discovered to have many of their anti-seizure properties by chance, these drugs are usually referred to as first generation antiepileptic drugs. In the last 20 years significant progress has been made on manufacturing and designing treatments specifically for those patients diagnosed with epilepsy. These anticonvulsants are usually referred to as second-generation drugs and have been actively discovered through screening, structure variation from existing medication or based on a specific scientific rational. Three possible strategies are thought to exist for preventing epileptic seizures: stabilising the membrane and preventing depolarisation by action on the ion channel, increasing GABAergic transmission or decreasing excitatory amino acid (EAA) transmission.

1.9.2. Alternative treatments

A number of alternative treatments including: surgery, vagal nerve stimulation, yoga, massage and homeopathy are also available to the patient. However, even with such a vast range of treatments, satisfactory seizure control is achieved in an estimated 66% of the epilepsy population (Hauser & Hesdorffer, 1990). The optimum treatment is complete seizure control with nil side effects. For the majority of patients this goal is unobtainable and each treatment's therapeutic efficacy must be weighed against its toxic side effects.

1.10. Vigabatrin (VGB)

Vigabatrin (Sabril) is the first of a new generation of anti-epileptic medication, which was purposely designed with a specific scientific rationale of preventing epileptic seizures. As a direct consequence VGB is one of the few anti-epileptic drugs (AEDs) whose mechanism of action is known. The drug was first licensed in the UK in 1989 and is now marketed in over 64 countries world wide and administered to over 170,00 patients. The drug was never licensed in America because pre clinical animal trials revealed cases of microvaculation (Arezzo *et al.*, 1989; Butler, Ford, & Newberne, 1987).

VGB is also known as γ-vinyl GABA or d1-4aminohex-5-enoic acid, its chemical structure closely resembles GABA itself. The drug works by binding itself irreversibly (irreversible

suicide inhibitor) to the active site of GABA aminotransferase, resulting in the inhibition of GABA breakdown, subsequently increasing the overall GABA concentration levels in the brain.

Gamma-aminobutyric acid (GABA) is the major inhibitory neurotransmitter in the brain and a loss of GABA inhibition results in recurrent epileptogenesis. GABA is synthesized from glutamate by the enzyme GAD or glutamic acid decarboxylase, in the presynaptic nerve terminal. GABA acts through three separate receptors (GABA-A, GABA-B and GABA-C) in the retina and its effects are diverse. Presynaptic inhibition occurs when GABAergic nerve terminals release GABA onto presynaptic nerve terminals resulting in a corresponding reduction in neurotransmitter release. Postsynaptic inhibition is mediated by the interaction of the neurotransmitter with specific postsynaptic receptors. GABA's inhibitory action is limited through an active reuptake of GABA into the presynaptic nerve terminals and surrounding glial cells.

Previous investigations into VGB have revealed that a dose of 50mg/kg of VGB per day results in a 200-300% increase in the GABA CSF brain tissue (Ben-Menachem *et al.*, 1991). VGB also accumulates in the retina, where it is reported to produce a proportionally greater increase in the GABA concentrations when compared with the brain (Sills *et al.*, 2001). Immunocytochemical evidence has suggested that GABA specifically accumulates in the amacrine cell bodies, Müller cells and inner plexiform layer of VGB-treated animals (Neal *et al.*, 1989). Active transport of immunolabelled VGB has been reported in the amacrine and Müller cells of rabbits cats and monkeys (Crook & Pow, 1997; Pow, Baldridge, & Crook, 1996). Neal *et al.* (1989) have indicated that GABA accumulates in retinal cells which do not normally possess enough endogenous GABA to be detected through immunochemistry. They hypothesised that long-term inhibition of GABA transaminase may cause an accumulation of GABA in the glial Müller cells at a rate that might exceed their catabolism. Conversely, not all GABA-influencing AEDs result in significant accumulation of retinal GABA. Tiagabine has been documented to produce comparatively lower concentration levels of GABA in the retina when compared to the brain (Sills *et al.*, 2001). Sills *et al.* (2001) investigated the concentration effects of VGB in the rat brain and eye compared against those of gabapentin and topiramate. VGB concentrations were reported to be 18.5-fold higher in the retina than those in the brain in contrast gabapentin and topiramate did not accumulate appreciably in the retina. These findings suggest that the grossly elevated GABA concentrations in the retina might be specific to VGB itself and not the mechanisms that increase GABA concentrations.

VGB is water-soluble and oral administration is rapidly distributed throughout the body. The drug is not expected to act with any of the other AEDs because it is not influenced by cytochrome P-450 dependent enzymes (Richens, 1991). Despite this, an interaction

between phenytoin and VGB has been reported (Rimmer & Richens, 1989). Poor potentiation across the blood brain barrier means that large doses of VGB are often necessary to achieve a satisfactorily level of seizure control (Mattson *et al.*, 1995). Authors have postulated that brain absorption enhancers, may facilitate its efficacy (Dimitrijevic *et al.*, 2001). VGB is not metabolised in humans and so is excreted unchanged within the urine, with a plasma elimination half-life of 5-7 hours. The pharmacokinetics of VGB however, is not a realistic guide to its duration of action. Concentration levels of GABA in the retina might take several days to return to normal, after administering just a single dose of VGB (Richens, 1991).

1.10.1. The efficacy of VGB

The efficacy of any antiepileptic medication is usually described as its ability to prevent epileptic seizures. Before VGB was licensed in the UK, six double-blind studies were initiated throughout Europe (Gram, Klosterskov, & Dam, 1985; Loiseau *et al.*, 1986; Remy, Favel, & Tell, 1986; Rimmer & Ritchens, 1984; Tartara *et al.*, 1986; Tassinari *et al.*, 1987). In four of the studies, approximately one half of the VGB recipients experienced at least a 50% reduction in seizure frequency (Gram *et al.*, 1985; Loiseau *et al.*, 1986; Rimmer & Ritchens, 1984; Tartara *et al.*, 1986). Patients with partial epilepsy found the treatment to be particularly effective. Favourable reports on long-term efficacy have also been documented, with many studies suggesting at least 55% of recipients maintain their clinical benefits through time (Dam, 1989; Pederson *et al.*, 1985). Studies in the paediatric community report a similar efficacy to that of the adult population (Dulac *et al.*, 1991; Heranz *et al.*, 1991; Uldall *et al.*, 1991). Children with partial seizures again appear to respond more favourably to the treatment when compared to those patients with generalised seizures.

Infantile Spasms is one of the epilepsy syndromes found in childhood, it is also one of the most refractory types of epilepsy. The principle cause of infantile spasms is tuberous sclerosis (Jeavons & Bower, 1974): the children in this group are particularly difficult to treat and are consequently vulnerable to high levels of mental retardation. Until the advent of VGB, Adrenocorticotrophic hormone (ACTH) was considered the drug of choice for treating these children. ACTH however, has also major side effects associated with its use (Riikonen & Donner, 1980). A number of studies now suggest that VGB is better tolerated and more effective in treating Infantile Spasms, when compared to ACTH (Cossette, Riviello, & Carmant, 1999; Vigevano & Cilio, 1997).The best results have been reported in those patients with infantile spasms due to tuberous sclerosis (Chiron *et al.*, 1991; Chiron *et al.*, 1997). VGB is now currently recommended as the drug of choice for children with infantile spasms (Sankar & Wasterlain, 1999).

1.10.2. The side effects associated with VGB

Before any drug is licensed in the UK, an evaluation of their associated toxicological side effects is undertaken. Ring & Reynolds (1992) have summarised the 10 most frequently reported adverse events, which were documented in the six double blind European studies (Gram *et al.*, 1985; Loiseau *et al.*, 1986; Remy *et al.*, 1986; Rimmer & Ritchens, 1984; Tartara *et al.*, 1986; Tassinari *et al.*, 1987). The principal side effect was drowsiness, reported in 27% of the VGB-treated population followed by fatigue, irritability, dizziness, headache, depression confusion, poor concentration, abdominal pain and anorexia. It of significant importance to note that within one of the placebo control groups 13% of the patients also demonstrated drowsiness, indicating that some of the side effects might be of a psychological nature. In a multi-centre study consisting of 254 patients 75% were reported to complain of no obvious side effects (Remy & Beaumont, 1989).

1.10.3. Intramyelinic oedema in animals

Numerous studies have documented evidence that has shown that prolonged administration of VGB produces varying levels of microvaculation in the white matter of the brains of rats (Butler *et al.*, 1987; Qiao *et al.*, 2000), mice (Graham, 1989) and dogs (Arezzo *et al.*, 1989; Schroeder *et al.*, 1992). The change is caused by the separation of the outer lamellar sheath of myelinated fibres and is characteristic of intramyelinic oedema (IME). The canine species was most severely affected by VGB followed by the rat and mouse, the results from monkeys were equivocal (Butler, 1989). There is evidence that in the rat and dog species, the lesion is reversible upon cessation of its use (Arezzo *et al.*, 1989; Butler, 1989; Qiao *et al.*, 2000). Two mechanisms have been postulated for producing IME and myelin toxicity: a direct VGB induced toxic effect, or a toxic effect induced by the increased GABA concentrations (Cohen *et al.*, 2000). The second postulation is more likely as other GABA-T inhibitors have also produced IME (John *et al.*, 1987).

1.10.4. Intramyelinic oedema in humans

Cases of IME in animal toxicology studies have led many investigators to carry out a series of clinical examinations into the human population. Techniques included evoked potentials (Cohen *et al.*, 2000; Hammond, Rangel, & Wilder, 1988; Liegeosis-Chauvel *et al.*, 1989), Magnetic Resonance Imaging (MRI) (Cohen *et al.*, 2000) neurological examination/cognitive testing (Cohen *et al.*, 2000) and autopsy (Cohen *et al.*, 2000; Hauw *et al.*, 1988). Results from these examinations have consistently revealed no indications of IME in humans. In fact, Cohen et al (Cohen *et al.*, 2000). have stated that after an estimated 350,00 patient-years of VGB exposure no case of IME has ever been identified.

1.11. Visual assessment and consequences of VGB

1.11.1. Visual acuity

Visual acuity specifically tests a patient's ability to resolve high-contrast, high spatial frequency detail. In clinical terms visual acuity describes the patients ability to resolve separate points and recognise patterns. In 1862, Dr. Hermann Snellen, a Dutch ophthalmologist developed a chart for measuring visual acuity. The chart consists of a number of black graded letter sizes constructed on a grid and presented upon a white background. The Snellen notation system enables the size of the letter to be calculated in terms of the distance at which one element of the construction grid subtends 1 minute of arc. The most widely used method for describing the resolving power of the eye is the Snellen fraction D/d: where (D) indicates the distance between the observer and chart and (d) is the Snellen size of the letter (the distance where I unit of the construction grid subtends I minute of arc). The grid system for constructing letters is the most widely used however in this system the choice of letters, the spacing and the luminance of the chart may vary. The Snellen chart has been criticised for its lack of standardisation between the number of letters on each line and also spaces between each of the letters (Bailey & Lovie, 1976). The LogMAR (LOGarithm of the Minimal Angle of Resolution) chart employs a logarithmic progression of letter spaces and sizes allowing increased consistency between each measurement. An acuity of 6/9 in Snellen notation equates to an MAR of 1.5 minutes (9/6). Alternatively, a decimal notation is achieved by dividing the Snellen fraction 0.67.

1.11.1.1. Visual acuity in patients receiving VGB

Although constant (Krauss, Johnson, & Miller, 1998) or transient (Agarwal, Gulati, & Sihota, 2000) "blurred vision" was occasionally complained of by VGB recipients. The majority of studies report normal visual acuities (Daneshvar *et al.*, 1999; Eke, Talbot, & Lawden, 1997; Hardus *et al.*, 2000b; Ruether *et al.*, 1998). On the rare occasions where reduced visual acuity has been documented, it is unknown whether the individuals already demonstrated abnormal responses before initiating VGB treatment (Krauss *et al.*, 1998; Lawden *et al.*, 1999; Miller *et al.*, 1999).To date, there is no information to suggest that VGB has any adverse effect on refractive error.

1.11.2. Investigation of Contrast sensitivity

Contrast sensitivity is a measurement of a patient's ability to perceive differences in contrast over a range of spatial frequencies. At birth contrast sensitivity is approximately $1/30^{th}$ of its eventual level, it develops rapidly during the first few months of life and reaches adult level at approximately 3-months of age (Held, 1988). At around 40-50 years contrast sensitivity again starts to decline (Owsley, Sekuler, & Siemsen, 1983). Visual deprivation during the first 8 years is thought to result in a loss of contrast sensitivity affecting, either all the spatial frequencies or limited to the high spatial frequencies (Hess & Howell, 1977).

Contrast sensitivity measurement may identify abnormalities not detected through visual acuity assessment. Investigators have reported contrast sensitivity to be preferentially reduced by the glaucoma disease process when it was compared against high contrast visual acuity (Hawkins *et al.*, 2003). Others have reported contrast sensitivity to be more sensitive in detecting early cataract when it was compared against high contrast visual acuity (Elliott, Hurst, & Weatherill, 1991; Elliott & Situ, 1998). Lennerstrand & Lundh (1984) reported significant improvement in the contrast sensitivity measurement of amblyopia treated patients, despite no change in high contrast visual acuity. In addition, contrast sensitivity provides a useful measurement with which to monitor the progression of a disease. Certain pathologies appear to demonstrate selective spatial frequency deficits, whereas others show more uniform loss over a wide range of spatial frequencies (Table 1.1; Townsend, 2003). The test may also provide a more realistic insight into the degree of visual disability.

Contrast threshold is the ability to perceive a sinusoidal grating of a given spatial frequency for at least 50% of the time: its reciprocal is defined as contrast sensitivity. The logarithmic value of contrast sensitivity is plotted on the vertical axis and the spatial frequency is plotted on the horizontal to produce a contrast sensitivity curve (Figure 1.1). Numerous test plates, charts and slides are capable of providing accurate contrast sensitivity measurements. Arden plates were the first commercially available contrast sensitivity plates. The test consists of a booklet of seven plates, with one sine wave grating on each plate. The patient views the test, plate by plate and is requested to point out when they first note the appearance of bars. Arden plates are not commonly used today as they are negatively affected by ambient lighting conditions and false positive results (Owsley *et al.*, 1983). VistTech charts (VCTS) were the first contrast sensitivity test to be mounted on the wall and consist of six rows of sine waves grating patches. Each row presents a grating of different spatial frequency, with contrast decreasing from left to right. Gratings are tilted to specific orientations and the participant is requested to identify the correct orientation. The test-retest reliability of the VCTS is reported as problematic, particularly at low and high spatial frequencies (Rubin, 1988). The Pelli-Robson chart consists of eight rows of letters with two triplets of letters per row. Contrast decreases from top (near 100%) to bottom (less than 1%) and in 0.15-log unit for each triplet of letters. Test-retest reliability is reported as good (Rubin, 1988), nevertheless, some investigators suggest the VCTS and CSV-1000 are superior to letter contrast sensitivity charts as they assess the broad-contrast-sensitivity from low to high spatial frequencies (Ginsburg & Cannon, 1984).

The CSV-1000 (Vector vision Dayton OH, USA) is one popular method for measuring contrast sensitivity (Figure 1.2). The technique yields high sensitivity, good repeatability and is now successfully employed for monitoring a wide range of retinal diseases. The test provides a fluorescent luminance source that retroilluminates a translucent chart and

automatically calibrates to a constant 85 cd/m^2. The participant is requested to view four rows of sine waves, which are presented at a spatial frequency of either 3, 6, 12 or 18 cycles per degree. Each row is made up of eight-paired circular patches showing different levels of contrasts. In each pair of circles, one circle contains the sine wave the other is left blank. The participant is asked to identify which circle (top or bottom) contains the sine wave. The contrast across each row slowly decreases from left to right. The last pair of circles at which the participant is able to correctly identify the sine wave, is taken as the contrast threshold for that particular spatial frequency. The process is then repeated for the other three rows (spatial frequencies). For statistical analysis the manufacturers recommend that contrast sensitivity data be converted into a logarithmic scale to account for a skew that occurs in the normal population. The test-retest variability of the CSV-1000 is reported as favourable (Pomerance & Evans, 1994).

1.11.2.1. Contrast sensitivity in patients receiving VGB

Contrast sensitivity appears to be reduced over a range of spatial frequencies for a proportion of adult patients, exposed to VGB (Nousiainen, Kalviainen, & Mantyjarvi, 2000a; Roff Hilton *et al.*, 2002). (Roff Hilton *et al.*, 2002) reported that 94% of their investigated participants (patients exposed to VGB) experienced an abnormality of contrast sensitivity, that was predominantly evident at the higher spatial frequencies. (Nousiainen *et al.*, 2000a) identified 13% (4 patients) of their investigated cohort who experienced more than two standard deviations in reductions of their contrast sensitivity measurement when compared with normal healthy controls. They did not specify which spatial frequency was particularly affected, however they did find a positive correlation between the contrast sensitivity values and the extents of the visual fields in linear regression ($R = 0.498$, $p = 0.05$ in the right eye, $R = 0.476$, $p = 0.06$ in the left eye).

Table 1.1. Spatial frequency deficits in selected ocular disorders adapted from Townsend (2003).

Figure 1.1. The contrast sensitivity curve adapted from Gilchrist (1988). Threshold contrast sensitivity plotted against spatial frequency.

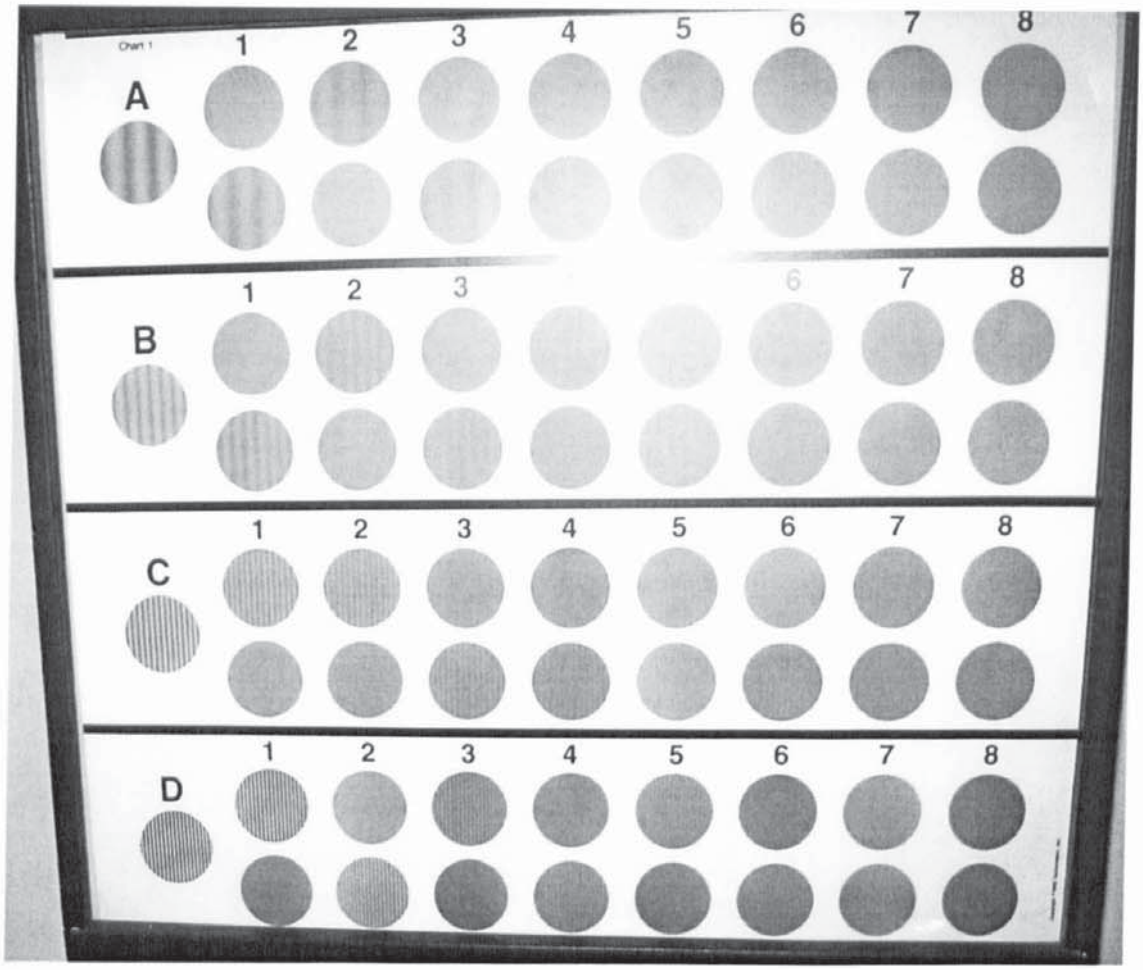

Figure 1.2. Illustrating the CSV-1000 test plate for contrast sensitivity.

1.11.3. Colour vision

Colour vision is one useful test for measuring retinal function, abnormalities might occur long before any other clinical sign is detectable (Adams *et al.*, 1982; Drance *et al.*, 1981). Congenital colour deficiency preferentially affects the medium (M) and long (L) wavelength sensitive cones (Iregren, Andersson, & Nylen, 2002), the condition is normally bilateral and will not change through time. Acquired abnormalities are monocular or bilateral, they are frequently unequal between the two eyes and might be secondary to either ocular or systemic pathologies. Short wavelength (S) cones are particularly vulnerable to the exposure of various drugs and chemicals (Iregren *et al.*, 2002). Changes in colour vision may provide useful information on the progression of the pathology and provide a good indicator for initiating treatment

Colour visions tests are designed to identify and differentiate between congenital and acquired abnormalities. Charts are based on psychophysical principles and there is now a wide range of techniques available for identifying those individuals with colour defects (screening tests) and also estimating the severity of the colour defect. The simplicity of the pseudoisochromatic plates ensures that they are the most commonly used technique for screening colour vision. Hue discrimination and colour matching tests require increased time patience and discrimination.

Pseudoisochromatic plates are based on spots or patches of colour in the same isochromatic zone. The spots are positioned into an easily recognisable figure. Patients with colour deficiency falsely identify all the spots as the same colour (pseudoisochromatic) and cannot distinguish the figure. The Ishihara pseudoisochromatic plates are the most widely used screening test for identifying those with red-green colour defects. The plates were not designed to detect tritan abnormalities, making them less useful for the detection of acquired abnormalities.

The Standard Pseudoisochromatic Plates (SPP2) are intended for the identification of acquired colour deficiency. Patients with acquired tritanopic abnormalities often fail both red-green and tritanopic designs. The participant is requested to identify 12 numbered plates. Two of the plates are used for demonstration purposes; the remaining plates detect red-green, tritan or scotopic abnormalities.

Hue discrimination tests are based on a number of colour samples, which are individually placed inside small caps. Participants are requested to place the caps in order, in accordance with their hue: the more colours the greater the information and the longer the examination duration. Young children and those adults with developmental delay are usually not capable of carrying out such a test. The Farnsworth-Munsell (FM) 100-Hue is a complete circle of hues taken from a special series of Munsell samples. The step sizes (colour

differences) are smaller in the blue-green range and errors most commonly occur at this point. The differences in the step sizes are shown by the variations in the spatial radiations. Computer based programs are available to help with data analysis. Classification of colour deficiency is based on the on the position severity and numbers of clusters. The FM 100-hue is not designed for screening as only those with moderate to severe abnormalities are identified (Birch, 2001).

1.11.3.1. Colour vision in patients receiving VGB

Deficiencies in colour perception are commonplace in VGB patients. The nature of the defect, however, is equivocal. Using Farnsworth Munsell 100-hue, a non-specific impairment of foveal colour sensitivity has been reported in a number of patients receiving VGB (Krauss *et al.*, 1998; Nousiainen *et al.*, 2000a; Nousiainen, Kalviainen, & Mantyjarvi, 2000b; Roff Hilton *et al.*, 2002). Abnormal red-green colour perception has been detected with the Ishihara pseudoisochromatic plates (Lawden *et al.*, 1999; Manucheri *et al.*, 2000) and the Lanthony Desaturated Panel D15 Test (Besch, Sarfan, & Kurtenbach, 2000; Ruether *et al.*, 1998), in patients exposed to VGB with confirmed visual field constriction. The non-specific nature of the colour vision abnormalities in VGB patients may be a consequence of the varying dosage and duration of VGB treatment. It should be remembered that many patients receive VGB as part of a combination drug therapy and that many other anti-epileptic drugs are known to cause colour vision impairment (Lopez, Thompson, & Rabinowicz, 1999; Mecarelli, Rinalduzzi, & Accornero, 2001; Nousiainen, Mantyjarvi, & Kalviainen, 2000c; Nousiainen *et al.*, 2000b; Paulus, Scharwtz, & Steinhoff, 1996). Perhaps the most conclusive evidence that VGB causes colour vision impairment arises from colour perimetry. Patients were requested to press a switch when they perceived a local change on the screen other than changes in colour or brightness. Using this method of investigation, Mecarelli *et al.* (2001) reported that VGB produced a selective deficit for blue contrast perception in a group of healthy volunteers after the administration of a single oral dose of VGB.

1.11.4. Ocular Examination

Ophthalmoscopy is performed as part of a routine eye examination. Observation of the red reflex should be carried out noting any defects of the media including the cornea, anterior chamber, crystalline lens and vitreous. At the retinal plane the optic disc should be visualised and the blood vessels can be followed to the equator and back. A scan of the retina is then carried out quadrant-by-quadrant and the macula examined.

1.11.4.1. Ophthalmic findings in patients receiving VGB

A number of authors have reported a "pale optic disc" or "mild optic nerve pallor", in VGB patients which have been attributed to damage in the nerve fibres of retinal ganglion cells (Kalviainen & Nousiainen, 2001). Krauss *et al.* (1998) have reported narrowing of the retinal arterioles, surface wrinkling retinopathy and abnormal macular reflexes. Atrophy and

tessellation of the peripheral retina have also, occasionally been documented (Eke *et al.*, 1997; Lawden *et al.*, 1999). To date, one histopathological study has been (Ravindran *et al.*, 2001) carried out on a patient with confirmed visual field loss, which was attributed to VGB treatment. On withdrawal of VGB therapy, a 41-year-old male experienced repeated seizures, had a cardiopulmonary arrest and died. Histology of the retina revealed that the peripheral retina showed significant loss of ganglion cells and partial loss of cell nuclei from both the inner and outer retinal layers. This cell loss was most extensive in the peripheral retina and the macular area was significantly less affected which correlated well with the visual field loss observed in the patient. It was concluded that the quantity of cell atrophy would indicate that the visual field loss was irreversible.

1.11.5. Electrophysiology Investigations

Electroretinogram

The retina is a complex neuronal network consisting of numerous rods and cones that are linked to bipolar, ganglion cells and two types of interneurones called horizontal and amacrine cells. Surrounding these neurones, are the Müller cells. The ERG (electroretinogram) is a flash-evoked potential, recorded at or near the cornea when a light electrically activates the retinal cells. The functions of the various preganglionic neurones are determined by manipulating the flash intensities, wavelength, rate of stimulation and state of light and dark adaptation. In 1989 the International Society for Clinical Electrophysiology of Vision (ISCEV) produced a series of guidelines to help standardise this recording (Marmor *et al.*, 1989). They defined five major responses; rod response, maximal combined response, oscillatory potentials (OPs), cone response and 30Hz flicker response Figure 1.3. Stimulus intensity is positively correlated with amplitude size and negatively correlated with latency. A cone dominant response is produced when the eye is light adapted (photopic ERG) or by rapidly flickering the stimulus (30Hz), as the rods are unable to respond at this frequency. Oscillatory potentials are accentuated through altering the filter bandwidths and manipulating the high and low frequency filters. If the eye is dark-adapted a rod dominant (scotopic ERG) is produced. ISCEV guidelines recommend that all records be carried out with maximal pupil dilation.

An early receptor potential (ERP) is recorded from the outer segments of photoreceptors. The a-wave is generated by the hyper polarisation of many photoreceptors. The origin of the b-wave is more spatially complex. A spot of light on the centre of one class of bipolar cell hyperpolarises it, however, on its surround it produces the opposite response. In other classes of bipolar cell the opposite occurs. Many authors now believe the b-wave to reflect mainly the activity from the Müller cells (Falk, 1991; Kline, Ripps, & Dowling, 1978). The OPs are thought to result from the feedback between the amacrine and bipolar cells and or feedback from ganglion to amacrine cells (Tzekov & Arden, 1999). They are particularly susceptible to damage through ischaemia.

Electro-oculogram

The EOG is a recording of the standard electrical potential between the relatively positive cornea and the negative posterior pole of the eye. Many structures are believed to contribute to this potential, however, it is mainly generated at the junction between the photoreceptors and the pigment epithelium. Arden & Barrada (1962) developed a test of retinal function, which is based on the changes between light and dark and is known as the Arden Index (Equation 1.1). Requesting the patients to move their eyes to the right and left assess the EOG the size of the potential is proportional to the degree of rotation.

$$ArdenIndex = \frac{LightPeak}{DarkTrough} \times 100$$

Equation 1.1. Arden index

An EOG record provides a quantitative assessment about the functioning of the outer retinal layers. The light/dark ratio is dependent on changes in the retinal-pigmented epithelium (RPE), photoreceptor activity and RPE-photoreceptor attachment. In central retinal artery occlusion the ratio may be reduced as it supplies the middle and inner layers of the retina including the RPE.

Aston University

Illustration removed for copyright restrictions

Figure 1.3. Diagram of the five basic ERG reposes adapted from Marmor *et al.* (1999).

1.11.5.1. Electroretinogram (ERG) and the Electro-oculogram (EOG) in patients receiving VGB

VGB administration is thought to cause a dual effect in the human retina. Previous authors have reported either a reduction in the Arden index of the EOG (Besch *et al.*, 2002; Comaish *et al.*, 2002; Eke *et al.*, 1997) abnormalities of the photopic ERG b wave (Bayer *et al.*, 1990; Harding *et al.*, 1995), reduced oscillatory potentials amplitudes (Besch *et al.*, 2002; Comaish *et al.*, 2002; Eke *et al.*, 1997; Harding *et al.*, 2000a; Harding *et al.*, 2000b; Krauss *et al.*, 1998; Van der Torren, Graniewski-Wijnands, & Polak, 2002) or reduced 30-Hz flicker amplitude (Harding *et al.*, 2002; Krauss *et al.*, 1998; Miller *et al.*, 1999). The reduction of the Arden Index is thought to be a temporary physiological response, induced by the elevated retinal GABA levels. After cessation of VGB treatment, participant's responses returned to normal levels (Comaish *et al.*, 2002; Coupland *et al.*, 2001; Graniewski-Wijnands & Van der Torren, 2002; Harding *et al.*, 1999) even when the visual field defects persisted. ERG abnormalities are generally considered to be the progressive effects relating to the VGB-associated VFDs themselves. One possible exception to this rule may be the amplitude of photopic b-wave. Harding *et al.* (2002) suggest that a reduction in the amplitude of photopic b-wave correlates with several anti-epileptic drugs and not VGB specifically. The parameters that were associated with severe VFDs were abnormalities of the photopic a-wave latency, 30Hz a-wave latency or 30Hz a-b amplitude. These effects were present in participants both currently or previously treated with VGB, suggesting that the cone pathways are irreversibly affected in those participants with severe visual field loss.

1.11.5.2. Visual Evoked Potential

The visual evoked potential (VEP) is the mass potential, which is generated as the result of visual stimulation. The signals are recorded between a reference electrode over the non - visual part of the brain and the occipital cortex. As the signals are small they are averaged together, flash or pattern stimuli may be presented. A series of peaks and troughs are evident in the recording, the amplitudes and latencies are compared against normal control values. The VEP is useful in the identification and diagnosis of both retinal and neural neuropathies.

1.11.5.3. Visual Evoked Potential (VEP) in patients receiving VGB

Extensive investigations of the visual evoked responses of patients treated with VGB were carried out. Concerns initially stemmed from the reports of IME in the pre clinical animal toxicity trials, and later because of the evidence of visual field constriction. The majority of evidence suggests that VGB does not adversely affect the integrity of the VEP response (Eke *et al.*, 1997; Harding *et al.*, 1995; Krauss *et al.*, 1998; Lawden *et al.*, 1999; Liegeosis-Chauvel *et al.*, 1989; Ruether *et al.*, 1998; Wild *et al.*, 1999a). In fact, a number of studies have documented normal VEPs, even in those patients with confirmed visual field loss (Eke *et al.*, 1997; Krauss *et al.*, 1998; Lawden *et al.*, 1999; Ruether *et al.*, 1998; Wild *et al.*, 1999a). Individual cases of abnormal VEPs have occasionally been documented (Daneshvar

et al., 1999; Gross-Tsur *et al.*, 2000; Miller *et al.*, 1999). These deficits however were probably not related to the treatment itself as no baseline reading was carried out before initiating the treatment.

1.11.6. The visual field

The clinical visual field can be defined as the entire space that an eye can see in a given instant. A normal monocular visual field extends to 60 degrees superiorly, 75 degrees inferiorly, 100 degrees temporally and 60 degrees nasally (Anderson & Patella, 1992). The extent of the visual field is limited by each participant's facial anatomy, as the nose the cheek and eyebrow all limit the field of view. Its boundary however, is only one aspect, as sensitivity is not uniform across the entire visual field. Sensitivity is greatest at the centre (fovea) and then decreases towards the periphery. Traquair (1938) linked the visual field to an " island of vision surrounded by a sea of blindness". Any stimuli, which fall outside the field of view fall into the sea, and any that are seen lie in the boundaries of the island. A physiological blind spot, approximately 5.5 degrees wide and 7.5 degrees high, exists 15 degrees temporal to fixation and 1.5 degrees below the horizontal meridian (Reed & Drance, 1972). The blind spot consists of an area lacking all photoreceptors and is caused by the convergence of retinal nerve fibres at the optic nerve head. See Figure 1.4 for the normal hill of vision.

Measurement of the hill of vision

The minimum brightness at which a patient can detect a stimulus is referred to as the visual threshold. The reciprocal of differential light threshold is defined as sensitivity. Every point in a visual field has its own threshold of sensitivity. Perimetry is a non-invasive measurement of the field of vision on a curved surface or measuring the differential light threshold sensitivity across the retina. The height and shape of the normal visual field is dependent upon the age of the subject and also the colour, size and duration of the stimulus. A field defect is described as any clinically significant departure from the normal shape of the hill of vision. An area of reduced sensitivity is termed a relative a scotoma, while one with no light perception is called an absolute scotoma. An overall loss of threshold sensitivity across the retina is termed diffuse loss and loss in the peripheral retina (greater than 30 degrees) is called contraction.

Factors influencing the field of vision

Facial contours may limit the size of a visual field as patients with narrow palpebral apertures or large frontal, zygomatic or maxilla bones may all show smaller visual field sizes. Patients with ptosis need their lids held open to avoid visual field loss in their superior periphery (Meyer *et al.*, 1993). Changes in pupil size affect the intensity of both the stimulus and the background. The effect of both pupil miosis and pupil mydriasis was investigated in ten normal subjects using the Dicon automated perimeter (Wood *et al.*, 1988). Sensitivity was

reported to improve with increases in pupil size. Spherical defocus results in a reduction of sensitivity that is greater at the periphery when compared to fixation (Atchison, 1987).

Long examination times, occasionally induce fatigue effects in a clinically normal population. The effects usually manifest themselves, as an abnormal reduction of threshold sensitivity. The effects are greater in an elderly population, increasing eccentricity (Hudson, Wild, & O' Neill, 1994), or locations adjacent to visual field defects (Holmin & Krakau, 1979). Several methods are available for overcoming the effects of tiredness: patients may pause the test when they feel tired, regular breaks may be taken or a shorter algorithm chosen.

A learning effect may occur in both normal (Wood *et al.*, 1987) and glaucomatous populations (Werner *et al.*, 1990), whereby the threshold sensitivity is reported to increase either between or during perimetric examinations. The effect is reported to lessen with increasing number of visits (Wood *et al.*, 1987), suggesting that it is advisable to exclude the first examination at the very least.

1.11.6.1. Standard techniques for measuring the visual field

The two standard methods for measuring a visual field are kinetic and static perimetry.

Kinetic perimetry

Kinetic perimetry is based on targets that move in and out of the field of vision. The patient is requested to respond when small circular targets either appear or disappear from their field of vision. Lines joining points of equal sensitivity are called isopters and are plotted by the perimetrist.

Goldmann perimetry

Goldmann perimetry is one type of kinetic perimetry. The participant is asked to either monocularly or binocularly fixate on a central target in a hemispherical bowl. Small targets (usually white) are moved along different field meridians towards a central fixation point. The number of meridians, the speed and the target size are chosen by the perimetrist. The participant is requested to indicate when they detect a stimulus and their isopters of vision (their visual field) are plotted by the perimetrist. The examination time is dependent upon the ability of the participant, the type of field test and the perimetrist's experience.

Figure 1.4. Illustrating the normal hill of vision adapted from (Hayley, 1993).

Static perimetry

In static perimetry the target is kept in the same location while the intensity of the stimulus varies. This technique not only measures the boundary of vision but also the threshold sensitivity at each location. Manual static perimetry is very time consuming, however, with the advancement of technology most static perimetry is now computerised (Humphrey Field Analyser, Dicon, Henson and Octopus perimeters).

The differences between static and kinetic perimetry

Kinetic perimetry is performed rapidly, the equipment is relatively inexpensive and patients usually find that the test is relatively easy to complete. Conversely, kinetic techniques are known to experience a number of limitations. Moving stimuli are detected more peripherally than static stimuli because of a type of successive lateral spatial summation (Greve, 1973). The position of the field isopters is highly influenced by patient reaction time (Lynn, 1969). A stimulus velocity of five degrees per second in the peripheral visual field and two degrees per second in the central visual field has been suggested as appropriate (Greve, 1973). The technique is vulnerable to false positive results and examiner related bias, as there are no computer programmes to standardise the technique. Investigators have reported that patients demonstrating visual field loss through static perimetry are 13.4 times more likely to demonstrate abnormalities in kinetic perimetry in one year when compared against subjects with no defects (Katz *et al.*, 1995). Other studies have reported static perimetry to be superior to various methods of kinetic perimetry in detecting small isolated areas of focal loss in glaucomatous eye disease (Drance, Wheeler, & Patullo, 1967; Lynn, 1969). Agarwal *et al.* (2000) have documented that static perimetry using the Humphrey Field Analyser is superior to kinetic perimetry using the Goldmann perimeter, when detecting progression of visual field loss in primary open angle glaucoma.

1.11.7. Automated static perimetry

1.11.7.1. The Humphrey Field Analyser (HFA)

The HFA is a type of computerised static perimetry. The participant is asked to, either monocularly or binocularly, fixate on a central target in a hemispherical bowl. At fixed positions, a light of a pre-determined threshold is presented. The location, threshold, colour, size and order of the stimulus may be altered. The threshold is varied in accordance with the algorithm that was chosen. After the test is completed a visual field printout is produced. The printout reports the measured threshold sensitivity at each field location. The duration of the field test is dependent upon the particular test and the participant's ability. The HFA offers a number of different test patterns, strategies and parameters. It is the choice of the clinician as to which test is considered most appropriate.

Background and stimulus parameters for the HFA

In static perimetry attenuation of the light is expressed in decibels (dB). In terms of retinal sensitivity 0 dB corresponds to 10.000 apostilib (asb) or the maximum stimulus luminance. One decibel is equal to 0.1 log unit; accordingly 10 dB is equal to a 1-log unit and 20 dB is equal to a 2-log unit attenuation of the maximum possible stimulus luminance (i.e. a 10-fold and a 100-fold reduction). The HFA uses the same background illumination (31.5 apostilib) as the Goldmann perimeter. The bright background is thought to produce a test that is less susceptible to stray light and produce shorter examination times, as each patient requires less time to adapt to the bright background. The dynamic range equates to the range of maximum stimulus luminance of the perimeter and the threshold stimulus luminance of an eye with normal sensitivity (Frankhauser, 1979). In the HFA the projected stimuli may be varied in intensity over a range of more than 5.1 log units or 51 decibels (between 0.08 and 10.000 apostilib). There are five stimulus sizes available for use in the HFA, which correspond to the Goldmann perimeter stimuli I to V. In addition, the HFA provides up to one log unit of stimulus range brighter than the Goldmann perimeter. Unless otherwise chosen the HFA defaults to stimulus size III which subtends an angle of 0.43 °. The default size was chosen as it was expected to be small enough to plot the smallest of scotomas and large enough to be unaffected by residual refractive error (Frankhauser, Koch, & Roulier, 1972). The HFA employs a default stimulus duration of 200ms.

1.11.8. Threshold algorithms for automated static perimetry

The HFA provides several algorithms that maybe used to plot threshold sensitivities. The algorithm that is chosen is dependent upon the ocular pathology, the available time and the ability of the patient.

1.11.8.1. The Full Threshold algorithm

Patient responses are often uncertain or inconsistent at the boundary of visibility-invisibility. When this occurs the intensity of the stimulus may be adjusted so as to increase the likelihood of seeing the stimulus. A graph may then be plotted indicating the percentage frequency with which a stimulus is seen according to its intensity. This graph is called a frequency-of-seeing curve (Figure 1.5). The stimulus luminance at which the frequency of perception is 50% is defined as the threshold. The Full Threshold algorithm initially determines the thresholds at 4 primary seed locations, which are placed nine degrees from both the horizontal and vertical meridians. Each location starts at predetermined threshold of 25dB. A 4-2dB staircase is used, which means that there is a change in stimulus brightness in 4dB steps until the first reversal is achieved and then in 2dB steps until the second reversal is achieved. A double crossover is used to determine the last seen threshold. Thresholds in the immediately adjacent locations are determined by starting at a threshold, which is 2dB brighter than what is expected after determining the primary seed locations. In addition to the four primary seed locations there are another six locations where the

threshold is determined twice. These pre-selected points are used to determine the short-term fluctuation (test-retest difference). Whenever the measured threshold departs from 5dB or more from the expected value, the analyser rebrackets it. The second measurement is printed in parentheses below the first. These additional double determinations are not included in the short-term fluctuation calculation.

1.11.8.2. The Suprathreshold algorithm

The suprathreshold algorithm determines whether the threshold sensitivity at a particular location is better than certain pre-selected criterion. The algorithm detects the location of abnormalities but does not quantify the depth of defect. If there is only one stimulus presentation at each location the test duration is short. In certain strategies if the stimulus is not visible the depth of defect may be further categorised. One of the three methods described below are used for setting the level of stimulus intensity for suprathreshold testing.

Age-corrected screenings

Stimuli are based on thresholds 8dB (0.8 log unit) more intense than the mean age-corrected normal sensitivity at each test location.

Threshold related screenings

Stimuli are based on the second highest threshold sensitivity made at four standard locations at the beginning of the test. The luminance of the subsequent suprathreshold stimuli are based upon thresholds that are 6dB more intense than the expected threshold sensitivity at each location after adjusting for sector and eccentricity.

Single Intensity screenings

Stimuli of constant luminance are presented at all locations in the visual field. Stimuli intensity is selected to represent some standard of quantifying disability.

In the HFA, default parameters are set so that missed stimuli are automatically repeated before locations are recorded as not seeing. The perimetrist is able to choose whether such locations are further categorised.

- *In the two-zone mode*, points which are missed twice are marked with a black symbol indicating abnormal sensitivity at that location.

- *In the three-zone mode*, points which are missed twice are then exposed to a maximal luminance of 10,000-asb (0dB). If the maximal stimulus luminance is not seen, the location is categorised as an absolute scotoma, but if the maximal luminance is seen, the location is categorised as having a relative defect.

Figure 1.5. The frequency of seeing curve adapted from (Anderson & Patella, 1992).

- *In the quantify defects mode,* the stimuli are intensified in 4dB steps, until seen and then decreased in 2dB steps until not seen. Only the points which are missed are thresholded, if lots of points are missed the test becomes long and tiring.

1.11.8.3. The FASTPAC algorithm

The FASTPAC algorithm utilises a 3dB step size and a single crossover. Because of the single crossover FASTPAC is more vulnerable to false positive responses. The starting point for the 4 primary seed locations is identical to Full Threshold, however for the secondary points the starting point is 2dB dimmer than the expected threshold, when the expected value is an odd number, and 1 dB brighter when the expected value is an even number. FASTPAC is reported to have higher intra-test variability (short-term fluctuation), which allows for the shorter examination duration.

1.11.8.4. Swedish Interactive Threshold Algorithm (SITA)

Until the advent of SITA, automated perimetry relied upon the standard staircasing procedures described above to determine each participant's threshold sensitivity. The size of the steps and the number of crossovers was thought to determine the sensitivity and duration of each field test. A test of high sensitivity was considered to be one of small step sizes and a large number of crossovers. This procedure also ensures a longer examination duration, which may induce fatigue in some participants compromising the reliability of their results.

The SITA algorithm was developed with a specific rationale of significantly reducing examination duration, without significantly altering the quality of the test results. The algorithm is based on probability models, of both normal and glaucomatous visual field test results. Each model includes age-corrected normal values, frequency of seeing curves and correlations between specific threshold values at different test point locations. The algorithm initially determines the thresholds at 4 primary seed locations using a traditional 4-2dB staircasing procedure with two reversals. These seed locations are used to determine the sensitivities at immediately adjacent locations. Posterior probability functions are recalculated after each stimulus exposure at each test point and each neighbouring test point. The updated probability functions allow new maximum posterior estimates of threshold sensitivity values for both normal and glaucomatous visual fields. The model changes and develops as the patient responds to each stimulus allowing a new estimated threshold to be presented and the staircase to continue. Once a predetermined error level of uncertainty is reached, error related factor (ERF), the staircase is stopped.

This new method of estimating a threshold at each location, before any stimuli are presented is the primary explanation for the substantial reduction of examination duration. Other factors include adjusting the presentation rates of the stimuli in accordance with the patient's

reaction time. Postprocessing which allows some of the information to be processed after the test is completed. Quicker staircase thresholding when there is high confidence that the threshold determined is correct. Determining false positive results by using the periods when no positive answers are expected. All account for the substantial reduction in examination duration.

1.11.8.5. SITA Fast

SITA Fast was designed with the specific rationale of reducing the testing time even further. The algorithm initially determines the thresholds at 4 primary seed locations using a traditional 4-2dB staircasing procedure with two reversals. The values obtained at these locations are used to calculate the points at immediately adjacent locations. At neighbouring locations a 4dB staircasing procedure is used and the staircase is stopped when one positive response was achieved provided that the measurement error is smaller than the stipulated ERF, if not, a single reversal is carried out. Second staircases are used if the estimated value is more than 12dB away from the predicated normal valued. The main difference between the two SITA strategies is that in SITA Fast the stimulus sequence is interrupted an earlier stage than SITA Standard (Bengtsson & Heijl, 1998). This is achieved by increasing the ERF cut-off value in SITA Fast, resulting in lower test accuracy and reduced examination times. (Bengtsson & Heijl, 1998) have reported that SITA Fast has between 30-34% fewer stimulus exposures than FASTPAC in both normal and glaucomatous visual field tests.

Efficacy and reliability of SITA Standard and SITA Fast

Previous investigations have revealed that SITA Standard and SITA Fast reduce examination durations by approximately 50%, when compared against the Full Threshold and FASTPAC algorithms respectively (Bengtsson & Heijl, 1998; Bengtsson, Heijl, & Olsson, 1998). In addition to their shortened test times, less between-subject (Bengtsson & Heijl, 1999a; Wild *et al.*, 1999c) was reported when each SITA strategy was compared against the Full Threshold algorithm. Authors have postulated that SITA's narrower confidence limits, which are used to define normality, produces the lighter more even grey-scale printouts that are typically associated with the strategies (Bengtsson & Heijl, 1999a; Shirato *et al.*, 1999; Wild *et al.*, 1999c). In both SITA strategies the normal hill of vision appears to be slightly higher and slightly flatter than the Full Threshold algorithm (Bengtsson & Heijl, 1999a; Wild *et al.*, 1999c). Authors have postulated that Full Threshold's lower mean sensitivity thresholds might be caused by a slight fatigue effect induced by the longer examination times when compared against the SITA strategies (Bengtsson & Heijl, 1999b; Wall *et al.*, 2001). Statistically deeper defects were evident in both SITA strategies when a population of patients with stable primary open angle glaucoma were assessed with Full Threshold, SITA Standard and SITA Fast (Wild *et al.*, 1999b). The reproducibility of SITA Fast is slightly inferior to either SITA Standard or Full Threshold, which is unsurprising after considering the

trade-off between speed and accuracy (Sekhar *et al.*, 2000). Findings suggest when transferring from one algorithm to another, it is advisable to carry out a baseline examination as the differences described above prevent a direct comparison between algorithms.

1.11.9. Statistical analysis of perimetric data

1.11.9.1. STATPAC

STATPAC is the trademark for Humphrey software, which performs a number of statistical analyses and is also available for use in a personal computer. STATPAC compares threshold values, obtained in a visual field examination, against normal age-corrected threshold values. Global visual field indices and probability maps can then be generated.

1.11.9.2. Global Indices in the HFA

The HFA provides 4 Global indices including: Mean deviation (MD), Pattern Standard Deviation (PSD), Short-term Fluctuation (SF) and Corrected Pattern Standard Deviation (CPSD). Each global index provides an average figure for the entire visual field. The Mean deviation (MD) index is the average sensitivity away from a weighted mean of all the age-corrected normal values. The Pattern Standard Deviation (PSD) index represents the standard deviation around the mean that constitutes the MD index. The Short-term Fluctuation (SF) index is a measurement of the within-subject or intra-test variability. The Corrected Pattern Standard Deviation (CPSD) index is the SF value subtracted from the PSD value in an attempt to remove the normal variability in the test.

1.11.9.3. Graphical Presentation of Perimetric Data.

A number of graphical methods have been developed to illustrate the spatial location and severity of a visual field defect.

Numeric data

Raw test results are displayed as a map of decibel threshold sensitivity values. Double determinations of thresholds are illustrated as two values of sensitivities. Total Deviation plot, is a map showing the difference between a patient's measured threshold sensitivity and the their age-matched normal threshold, for each field location. A positive figure indicates that the sensitivity is better than normal and a negative value indicates that the sensitivity is below the age-matched normal value. Pattern Deviation plot is used to determine localised defects, which are masked by a generalised depression. Threshold sensitivity values (raw results) are adjusted in accordance with the "general height" of the hill. The general height of the hill is determined as the deviation from the normal age-matched 85^{th} percentile best point.

Grey scale

The grey scale is a visual representation of the numeric data or a picture representing the field isopters. Sensitivity values are represented by shades of grey, ranging from black to white. Each step of the pattern corresponds to a change of 5dB sensitivity. The map was produced in an attempt to provide an immediate idea of the size and seriousness of defect. Disadvantages include inter-test variations between perimeters resulting in different shades of grey.

Probability plots

Probability plots graphically illustrate the level of statistical probability associated with a given visual field abnormality compared to the normal reference field. The Total Deviation probability plot indicates locations where deviations exceed those found in less than 5%, 2%, 1% or 0.5% of an age-matched population. The darkest shades of grey represent the greatest deviation. The Pattern Deviation probability plot indicates locations where deviations exceed those found in less than 5%, 2%, 1% or 0.5% of an age-matched population after they have been adjusted for generalised loss or gains. Again the darkest shades of grey represent the greatest deviation.

1.11.9.4. Reliability Indices of the perimetric data

The HFA provides data about the accuracy of each field test, through a series of reliability indicators. Fixation losses, indicates the proportion of times that a participant responds to stimuli that are presented in their blind spot. The visual field is usually classed as unreliable if the number of fixation losses exceeds 20%, above this rate the sensitivity and specificity of the test is reported to deteriorate (Sanabria, Feuer, & Anderson, 1991). False positives, indicates the proportion of stimuli that a participant responds to even though there is no actual light. False negative, indicates the proportion of visible stimuli that the participant fails to respond to. A visual field is normally classed as unreliable if the number of false-positive or false-negative answers exceed 33%, above this rate the sensitivity and specificity of the test is reported to deteriorate (Sanabria *et al.*, 1991).

1.11.9.5. The severity of visual field loss

An accurate knowledge of each patient's degree of pathology is essential for making decisions with regards to their clinical management. A number of agencies rely upon the *Guide to Evaluation of Permanent Impairment* to determine the extent of visual disability (Cocchiarella & Anderson, 2002). The visual field is evaluated using stimulus size-III 4e for Goldmann perimetry and stimulus size-III-10dB for the HFA, to quantify the area over which the selected stimulus is seen. Subtle relative defects may be missed, as this method is only capable of quantifying the extent of visual field. The Esterman grid method (Esterman, 1968) is another popular method of grading the extent of visual field loss. The technique was originally designed to score monocular or binocular visual fields in kinetic perimetry however,

in more recent years this test has been adapted to use in the HFA. The Esterman grid consists of a grid of either 100 unequal rectangles (monocular) or 120 rectangles (binocular). Greater weight is given to the areas that are considered most disabling. The number of rectangles that are found in the patient's visual field boundary are counted and this number represents the percentage of retained field. In static perimetry the global index MD maybe considered useful for classifying cases of diffuse visual field loss. Conversely, for cases of localised visual field loss the MD index is less useful as the abnormalities might be completely missed. Several studies have devised a more complex scoring system for use in automated perimetry. Each classification is based on the number, location and probability levels, for the abnormalities in a given visual field for both glaucomatous eye disease (Advanced Glaucoma Intervention Study 2, 1994; Hodapp, Parish, & Anderson, 1993) and VGB (Wild *et al.*, 1999a). Once the severity is noted changes in levels may be considered as evidence of progression.

1.11.9.6. Monitoring the progression of visual field loss

Early detection of pathology is extremely beneficial with regards to patient management, however the majority of clinicians find the interpretation of visual field loss extremely difficult. Inter-test variation (fluctuation) may mimic visual field progression and lead to misdiagnosis. Other factors, which confound detection of progression, include *fatigue and learning effects*. Numerous statistical packages are now available to use, in the majority of automated perimeters, in order to help facilitate analysis. These include the grey-scale print out, Total or Pattern Deviation plots, visual field indices and specific statistical algorithms.

The most widely used criterion for identifying visual field progression is examination of a series of visual field printouts through time, after taking into account the typical visual field loss which is associated with that specific ocular disease. Such analysis however, is highly dependent on the ability of the patient and the examiner. In glaucomatous eye disease authors have reported that global visual field indices such as MD might not be considered as clinically reliable for the interpretation of visual field changes (Chauchan, Drance, & Douglas, 1990) because small localised defects will be missed. To overcome some of these difficulties a wide variety of statistical analyses have been designed to differentiate between true progression and fluctuation. There are currently three statistical algorithms for use in conjunction with the HFA. A univariate linear regression (ULR) of the global index MD versus time enables the detection of the rate of progression through the slope of the regression line. This analysis requires a series of at least five to six fields in order to make reasonable estimates (Krakau, 1985) and it is thought to be relatively insensitive to small-localised defects, as it uses a global measure of MD. In ULR analysis it is important that each patients normal decline in threshold sensitivity with age is accounted for, as visual field progression may mimic a normal decline in threshold sensitivity with age. In addition, Wild *et al.* (1997) state that ULR may either seriously under or overestimate the rate of progression if the

decline is non-linear. Glaucoma Change Probability analysis (GCP) is an algorithm which detects progressive field loss in all the locations where the level of change exceeds the normal test-retest variation produced by stable glaucoma. Progressor Programme uses a linear regression analysis to derive a slope of change against time to follow-up for each individual test location in the entire visual field (Birch, Wishart, & O'Donnell, 1995).

Previous research has indicated that there is a high level of disagreement between the different algorithms for determining visual field progression (Birch *et al.*, 1995; Wild *et al.*, 1997). Birch *et al.* (1995) have reported that ULR identified progression in only 11% of a glaucomatous population, compared against 23% through Glaucoma change probability analysis or 26% through Progressor Programme. Wild *et al.* (1997) concur with these findings, stating that a regression of MD (ULR) against time to follow-up is a poor indicator of localised progressive visual field loss. However, they also documented that in cases of good quality data the ULR technique identified visual field progression before that of the GCP analysis.

1.11.9.7. Visual field loss in patients receiving VGB

Individual cases of visual field loss attributed to VGB treatment have been reported since its introduction over 20 years ago. The incidence however, was then thought to be 0.1% of the population and consequently was not thought to be of clinical significance (Martinez & Noack, 1997). Interest again arose in 1997, when Eke *et al.* (1997) reported on a series of three patients, all showing severe persistent constriction of the visual field which they attributed to VGB treatment. Since then a body of evidence has accumulated which suggests that VGB is associated with concentric visual field loss. Despite this evidence no direct causative relationship has been established between VGB therapy and visual field loss. To date, only one study has investigated the incidence of visual field defects in VGB monotherapy. The authors reported a correlation between visual field constriction and VGB treatment (Nousiainen *et al.*, 2000b), however a causative relationship was not established, as a baseline visual field examination was not initiated before the participants were entered into the trial. In the adult population, the prevalence of visual field constriction ranges between 17% (Hardus *et al.*, 2000b) and 60% (Toggweiler & Wieser, 2001) of the recipient population. In the paediatric community it ranges between 19% (Vanhatalo *et al.*, 2002) and 71% (Russell-Eggitt *et al.*, 2000). It is reasonable to assume that some of the disparity in these figures arises from the various methodological differences between the studies. Risk factors or selection biases might also have prejudiced their incidences. The slightly larger range in the paediatric community probably reflects the smaller sample sizes and lack of Cupertino that is characteristically associated with participants in this group. Extrapolation of the true incidence of VGB-attributed field defects is confounded by the small number of participants who are willing and capable of participating in research and is particularly true for patients receiving VGB monotherapy.

Stability of visual field loss

The consensus of medical opinion is that visual field loss present in patients receiving VGB treatment is irreversible (Hardus *et al.*, 2000a; Nousiainen, Mantyjarvi, & Kalviainen, 2001; Schmidt *et al.*, 2002). However, there are a number of individual case studies which have suggested otherwise (Giordano *et al.*, 2000; Krakow *et al.*, 2000; Vanhatalo *et al.*, 2002; Versino & Veggiatt, 1999). It is interesting to note that Goldmann perimetry was the technique employed in all the studies that documented recovery. Goldmann perimetry is susceptible to variations in the speed of the stimulus (Lynn, 1969) and the depth of defect (Drance *et al.*, 1967; Heijl, 1976; Lynn, 1969). It can be argued therefore, that the reported recovery in the visual field may be attributed to testing artefacts, arising from an originally poor testing technique. A number of investigators have suggested recovery documented in younger patients might have been due to plasticity in their neural system (Giordano *et al.*, 2000; Vanhatalo *et al.*, 2002; Versino & Veggiatt, 1999). After reviewing their protocols it appears equally probable that improvement might have been caused by a better test performance on subsequent visits. All studies failed to include a protocol that accounted for the visual field learning effect which is well documented in Wood *et al.* (1987). Neither was any measure of visual field reliability such as fixation monitoring and false positive and negative catch trials incorporated into their experimental protocols.

The stability of the visual field loss after continued VGB therapy is equivocal. Some authors have indicated that visual field loss is stable in patients who continue long-term VGB therapy (Nousiainen *et al.*, 2001; Paul *et al.*, 2001), whilst others have reported visual field progression (Hardus *et al.*, 2000a).

The pattern of visual field loss

Studies using Goldmann perimetry, describe a typical VGB-associated defect as concentric contraction of the peripheral visual field (Figure 1.6). Studies using static automated perimetry, describe a typical defect as concentric contraction of the peripheral visual field with relative temporal sparing (Figures 1.7 & 1.8). As in glaucomatous eye disease (Drance *et al.*, 1967; Lynn, 1969) kinetic perimetry fails to detect shallow scotomas in the nasal visual field. Some investigators have suggested that static automated perimetry using a central 30 degree spatial grid fails to detect mild deficits in the extreme peripheral visual field (Kalviainen & Nousiainen, 2001), however they do not specify how peripheral. No normative threshold values are available on the Humphrey Field Analyser for spatial test grids measuring beyond 30 degrees. This necessitates the use of a suprathreshold-screening program beyond 30 degrees.

Risk factors associated with severity of visual field loss.

A number of studies have attempted to determine what risk factors, if any, influence the severity of visual field loss. A review of the findings (Table 1.2) reveals that no risk factor is

consistently correlated. Confounding conclusions were again probably caused by the studies varied protocols. Differences included: inclusion criteria, the type of perimetry, the algorithm, the field size, the learning effect, catch trials to ensure reliability, the fatigue effect and the methodology that was used to define the severity. A defined visual field protocol is necessary if other studies are to attempt to compare findings. Goldmann perimetry is consequently not advisable as there is less standardisation when compared to the computerised forms of perimetry.

1.11.10. Non-standardised investigation of the visual field

1.11.10.1. Short-Wavelength Automated Perimetry (SWAP)

SWAP was originally developed with the specific scientific rationale of improving the detection of visual field loss in glaucoma. The motivation behind the technique was initially based on the discovery that early on in the glaucomatous disease process, blue-yellow deficits are present (Adams *et al.*, 1982; Drance *et al.*, 1981). Since colour vision testing is essentially a measure of foveal function, it was suggested that a more sensitive test might be revealed if SWS pathway function could be measured across the visual field. Early attempts at isolating the SWS pathway did not reveal satisfying results (Hart *et al.*, 1984; Mare, 1972). In the late 1980's, two independent laboratories isolated the short-wavelength sensitive pathway, using a two-colour increment threshold technique and showed that the technique was useful for the detection of glaucomatous eye disease (Johnson *et al.*, 1993b; Johnson, Adams, & Brandt, 1993a; Sample & Weinreb, 1990; Sample *et al.*, 1993).

How SWAP works

SWAP tests SWS function by saturating the red cones, green cones and rods using a high luminance yellow background, while preferentially stimulating the blue cones using a blue violet stimulus. The background and stimulus parameters for SWAP are now standardised and consist of a 440 nm narrowband stimulus of angular subtense 1.74° and 200 ms duration, presented against a high luminance (100 cdm-2) broadband yellow background transmitting wavelengths greater than 530 nm. Studies have shown that approximately 1.5 log units of SWS isolation can be obtained using these parameters (Cubbidge & Wild, 2001; Sample *et al.*, 1996). SWAP is carried out using the HFA.

Efficacy of SWAP

A number of studies have shown SWAP to be an effective tool in the detection of glaucoma and other retinal diseases (Johnson *et al.*, 1993b; Sample *et al.*, 1993). Using this method, glaucomatous visual field defects have been detected up to five years earlier than by using standard perimetry (Johnson *et al.*, 1993b). Results have also indicated that SWAP yields a greater sensitivity in the monitoring of visual field progression (Johnson *et al.*, 1993a; Sample & Weinreb, 1992).

Figure 1.6. Goldmann kinetic visual field illustrating typical VGB associated visual field loss for a 34-year-old male patient (right eye) adapted from Lawden *et al.* (1999).

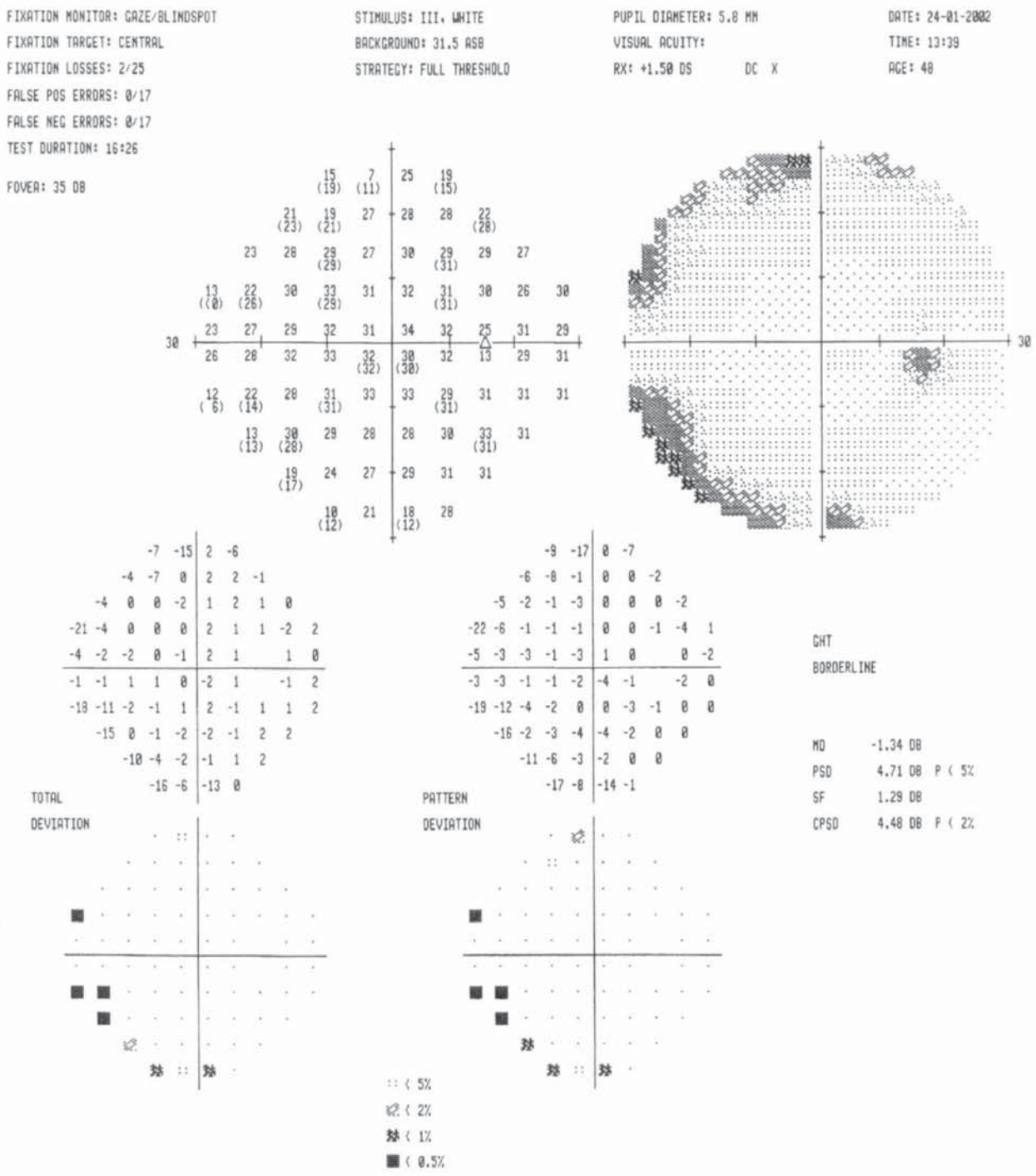

Figure 1.7. Static automated white-white perimetry (HFA) illustrating typical mild VGB associated visual field loss for a 48-year-old female patient (right eye).

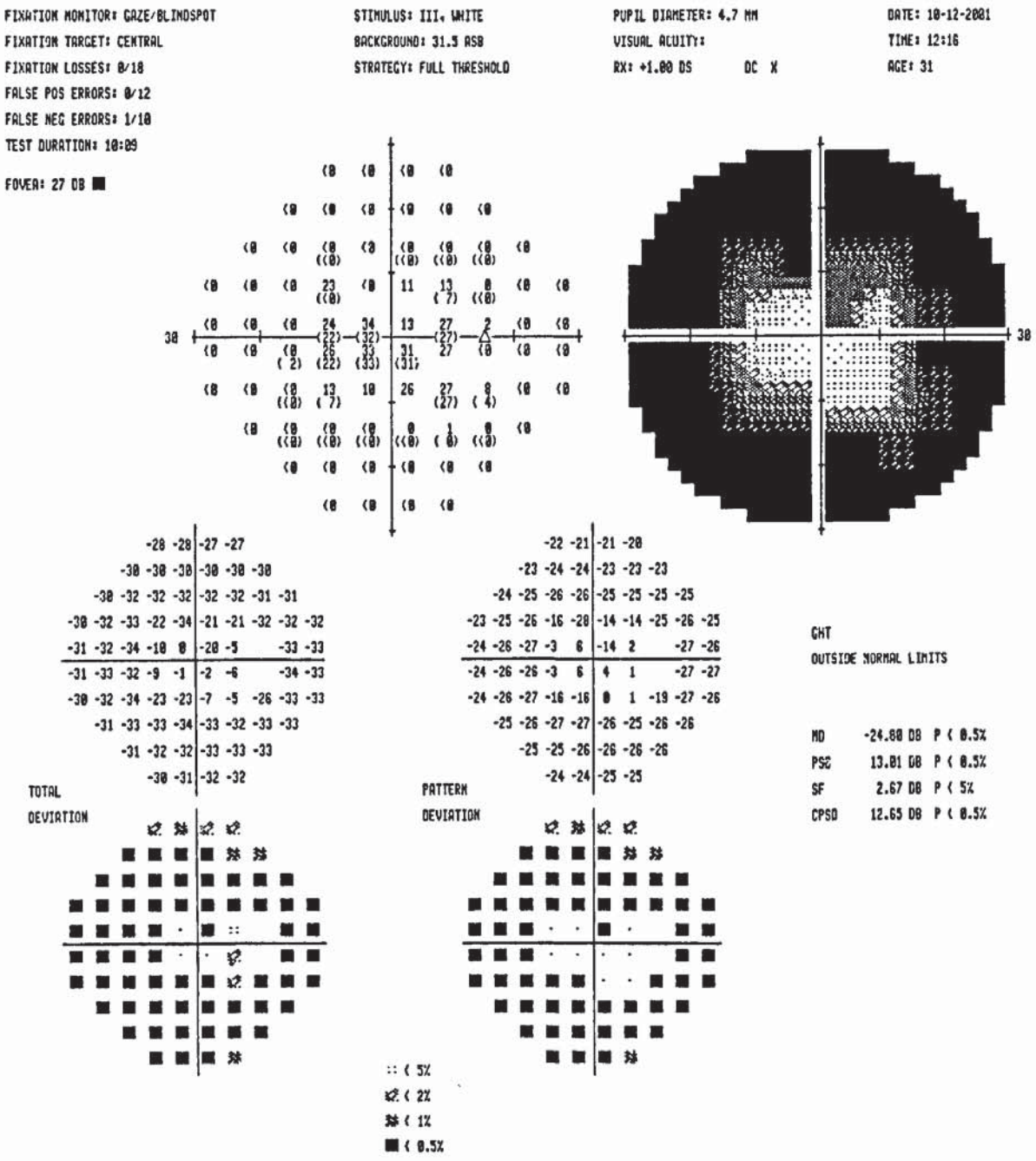

Figure 1.8. Static automated white-white perimetry (HFA) illustrating typical severe VGB associated visual field loss for a 31-year-old female patient (right eye).

	Arndt *et al.*, (2002) (64)	Hardus *et al.*, (2001) (92)	Hardus *et al.*, (2000b) (157)	Kalviainen *et al.*, (1999a) (32)	Manucheri *et al.*, (2000) (21)	Newman, Tocher, & Acheson, (2002) (100)	Nousiainen *et al.*, (2001) (60)	Toggweiler & Wieser, (2001) (15)	Wild *et al.*, (1999a) (88)
1. Cumulative VGB Dose	-	$p < 0.001$	-	NS	$p = 0.002$	NS	NS	-	NS
2. Daily VGB Dose	-	NS	-	NS	-	-	-	-	NS
3. Concomitant AEDs	$p < 0.001$	NS	NS	-	-	-	-	-	NS
4. Duration of VGB treatment	$p < 0.001$	NS	$p = 0.021$	NS	-	NS	NS	$p = 0.006$	-
5. Age	-	-	NS	-	NS	-	NS	-	NS
6. Gender	-	$p = 0.026$	$p = 0.004$	-	NS	$p < 0.01$	NS	-	Increased incidence
7. Smoking	-	-	-	-	NS	-	-	-	-

Table 1.2. Summary table showing results from previous visual field studies showing both significant (p values included) and non-significant (NS) correlations between the severity of field loss and (1)cumulative VGB dose (2) daily VGB dose (3) concomitant AEDs (4) duration of VGB treatment (5) age (6) gender and (7) smoking. A black line indicates that the correlation was not attempted: number in brackets equals the sample size.

Pathways mediating stimulus detection in SWAP

The output of the retina is conveyed via the retinal ganglion cells to the Lateral Geniculate Nucleus (LGN). P-ganglion cells project to the parvocellular layers and M-ganglion cells project to the magnocellular layers of the LGN. SWAP is mediated by the small bistratified ganglion cells (Dacey, 1993) and were originally thought to terminate in the parvocellular layers. The P-cells constitute the majority of retinal ganglion cells, their axon diameters are relatively small and they have slower conduction velocities. P-cells show increased responsiveness to high spatial frequencies and low temporal frequencies. They process information on colour, high spatial frequency and fine pattern discrimination. Recent work with monkeys now suggests that the small bistratified cell axons project to the interlaminar koniocellular layers (a third geniculocortical pathway; Martin *et al.*, 1997).

Theories surrounding the efficacy of SWAP

A number of theories have been put forward to explain why SWAP detects abnormalities before standard (white-white) perimetry. Histological studies have shown that large optic nerve fibres are preferentially lost in humans who have glaucomatous eye disease (Quigley, Dunkelberger, & Green, 1988). The larger ganglion cells were thought to be more vulnerable to mechanical and/or physiological insult as they were positioned at the weakest area of the optic nerve head and consequently more susceptible to damage (Miller & Quigley, 1988). Since ganglion cells mediating the SWS pathway have a larger diameter than other P-cells (Dacey, 1993) it was postulated that selective damage of the larger ganglion cells would result in preferential damage of the SWS pathway (Quigley, 1994). This theory has become more controversial in recent years, as psychophysical evidence now suggests that M-cells may be preferentially damaged (Anderson & O'Brien, 1997). An alternative explanation is the "fragile receptor hypothesis" which states that s-cones are in some way more vulnerable to damage by light, chemicals or retinal disease (Sperling, Johnson, & Harwerth, 1980). Or the "reduced redundancy hypothesis" which is based on the knowledge that in the retina there are proportionally less s-cones than either m or l-cones (Curcio *et al.*, 1991). If a disease process equally damages all chromatic pathways, then due to the relative paucity of the s-cones initially there functional (psychophysical) response was affected to a greater extent (Johnson, 1994).

1.11.10.2. SWAP in patients receiving VGB

Examination using a SWAP 10-2 programme revealed that 14 eyes of eight patients showed visual field abnormalities (Roff Hilton *et al.*, 2002). Each patient's test results were compared against a normal extrapolated database. Examination using the SWAP 30-2 programme revealed defects in eight of nine investigated patients, including two with normal white-white 30-2 visual fields (Daneshvar *et al.*, 1999). Each patient's test results were compared with age-matched normative values that had been obtained as part of prior studies (Johnson *et al.*, 1988).

1.11.10.3. Frequency doubling Technology (FDT)

FDT was originally designed to detect visual field loss caused by glaucoma and other ocular diseases. The field test was based on the rationale that a technique which measures a specific subset of ganglion cells, might detect damage earlier than one which measures the entire retinal population. Instead of presenting lights of varied intensities to the patient, a sinusoidal grating is presented. This grating has a low spatial frequency (0.25 cycles per degree), which undergoes a rapid counterphase flicker of 25Hz. The combination of the low spatial frequency accompanied by the high temporal frequency produces an apparent frequency doubling effect, meaning the number of black and white bands appears to be double what is actually physically present (White *et al.*, 2002) Figure 1.9.

How FDT works

Participants are asked to monocularly view a screen of 40 degrees eccentricity. No occlusion is necessary as the viewfinder slides from side to side, automatically occluding one eye. A stimulus pattern of the central 20-degrees (C-20), or the central 20-degrees including an extra 10-degree nasal step (N-30) is shown. At the standard testing distance, each square stimuli measure approximately 10-degrees and the central circle measures approximately 5-degrees. The frequency-doubling stimulus randomly presents itself at predetermined locations, for a maximum duration of 720ms. FDT has both screening and Full Threshold modes. In Full Threshold modality the threshold is defined as, the contrast necessary to perceive the stimulus. A Modified Binary Search (MOBS) staircase procedure is used, whereby the contrast is increased in targets that are unseen and then decreased until unseen (the same bracketing procedure that is used in standard perimetry). Testing may be carried out under normal room illumination, no refractive correction (up to seven dioptres) is necessary and the accuracy is unaffected by pupil size. Reliability characteristics are determined using the same procedures (fixation losses, false positive and negative responses) that are used in conventional perimetry.

Results are printed using a thermal printer, which is incorporated into the machine. FDT also provides a normal age-matched database. The normal database consists of approximately 750 eyes of more than 450 participants who were aged between 18 and 88 years. From the normal database a statistical model is produced, which is used to determine each persons Total and Pattern Deviation Probability Plot. These plots are based on the same techniques, which are used in conventional perimetry. Results can therefore be interpreted in a similar way as conventional Full Threshold Standard Perimetry. Manufacturing guidelines recommend that one training session should be included, in order to avoid misinterpretation of the results through a learning effect.

Efficacy of FDT

FDT compares favourably to conventional (white-white) perimetry, in its ability to detect glaucomatous field defects. In fact, a number of studies have supported that FDT detects glaucomatous visual field loss at an earlier stage in the disease than conventional white-white perimetry (Landers, Goldberg, & Graham, 2000; Maddess *et al.*, 2000; Soliman *et al.*, 2002). FDT is significantly shorter than standard perimetry, in diseased (Munoz-Negrete *et al.*, 2003) and non-diseased participants (Balwantry & Johnson, 1999). In neuro-ophthalmic disorders, optic neuropathies are detected with equal sensitivity and specificity to white-white perimetry, however, hemianopic and quadrantanopic defects are occasionally misdiagnosed due to a failure to detect abnormalities along the vertical meridian (Wall, Neahring, & Woodward, 2002). Adults with reading difficulties (dyslexia) have reported lower sensitivities to the frequency doubling illusion when compared against a normal control group (Pammer & Wheatley, 2001). FDT is reported to yield higher sensitivity when the Full Threshold mode is employed, however, the examination duration is also significantly longer (Burnstein, Ellish, & Higginbotham, 2000). FDT shows less test-retest variability than standard perimetry, when either eccentricity or severity of defect was increased (Balwantry & Johnson, 1999). Both short and long-term fluctuations appear equivocal to those recorded in standard perimetry (lester *et al.*, 2000). The main disadvantage of this technique is the large stimulus size (10-degrees) suggests localised damage might not be detected with this technique. In fact, an investigation of macular degeneration revealed that FDT's stimulus size is not small enough to detect localised lesions in the macula (Sheu *et al.*, 2002). To overcome this problem, Johnson, Cioffi, & Van Buskirk, (1999) carried out FDT using smaller target sizes and a 24-2 stimulus presentation. They reported greater sensitivity when using the 24-2 pattern. Unfortunately, the examination duration was approximately twice as long to complete.

Theories surrounding the efficacy of FDT

The relative paucity of the M_y cells makes them a population, which is very vulnerable to damage (redundancy theory) (Johnson, 1994). Alternatively, their larger axon diameters might be preferentially damaged through ocular disease (selective damage theory) (Anderson & O'Brien, 1997).

1.11.10.4. FDT in patients receiving VGB

To date, there have been no studies investigating VGB associated visual field loss using FDT.

Figure 1.9. Diagram illustrating the frequency doubling response adapted from Johnson *et al.* (1998).

Figure 1.10. A schematic comparison of the full-field and the multifocal paradigms adapted from Hood *et al.* (1997).

1.11.10.5. The Multifocal Electroretinogram (mfERG) and its application

In 1992 Sutter and Tran developed the Visual Evoked Response Imaging System (VERIS)(Sutter & Tran, 1992). This new technique simultaneously records the electrical activity from multiple cone-driven areas (mfERG) see Figure 1.10. Its shortened examination duration allows over 100 retinal areas to be measured inside seven minutes (Hood, 2000). It is not feasible to measure the same number of areas, during the same recording session, using conventional focal techniques. Retinal topography is known to vary with eccentricity. Rod density peaks at a similar eccentricity as the optic disc (between 157,900-188,600 cells/mm^2), numbers then decrease to 30,000 cells/mm^2 towards the periphery (Curcio *et al.*, 1990). Cone density reports a density that ranges between 100,000-324,000 cells/mm^2 at the fovea, decreasing to as low as between 4,700-7,000 cells/mm^2 at the extreme nasal periphery (Curcio *et al.*, 1990). Knowledge of the normal functional topography across the retina is vital to understanding any disease processes. The mfERG enables this information to be collated and used in a database in order to determine whether any responses, in any retinal area, fall outside the normal range. The full-field ERG by contrast, measures the summed electrical activity of cells across the entire retina. The mfERG is particularly useful in cases of localised disease, as numerous defects are frequently too small to be detected with full-field recording. Centres occasionally use it to differentiate between diseases, which affect the outer retina from those, which damage either ganglion cells or the optic nerve. Others have used it as a tool to follow the effects from clinical intervention (Palmowski *et al.*, 2002; Radtke *et al.*, 2002; Theodossiadis *et al.*, 2002).

Recording the mfERG

As with a full-field ERG the technique involves a measurement of the potential difference between two electrodes (active and reference). The active electrode is placed close to the cornea and the reference near the outer canthus of the eye. Pupils are fully dilated prior to testing and the appropriate reading correction paced in front of the tested eye. The alternate eye is occluded. The patient is asked to place their chin on a chin rest and a view a stimulus array consisting of multiple hexagons located on a CRT monitor. Each hexagon is scaled inversely with the gradient of cone receptors (response density scaled), so that focal responses of approximately equal amplitude are obtained (Sutter & Tran, 1992). This scaling procedure produces similar response amplitudes and signal-to-noise ratio across the retina. The hexagon pattern is flashed from black to white according to a pseudo-random binary m-sequence. The m-sequence is a simple binary stimulation assuming the states of 0 and 1 (flash and non-flash). A binary m-sequence of the order n is a cyclic sequence of $2^n - 1$. A longer m-sequence will extend the examination duration and result in a more reliable recording. Each m-sequence may be broken down into segments of equal length; shorter segments are considered more comfortable for the patient. Recording times of greater than four minutes were thought to be impractical for the current patient population and consequently not used. Each frame of the m-sequence was changed every 13.33 ms (75Hz).

The contrast, colour and number of hexagons in each stimulus array may be altered. An array that uses a large number of hexagons and reduced contrast will produce responses with small signal amplitude, which are vulnerable to noise. A brief examination of blue and yellow isoluminant stimuli revealed responses of such low signal amplitudes, that they were indiscernible from noise variations. It was subsequently decided to use an array that consisted of 61-hexagons that was alternated between black and white at high contrast. Cross correlation between the pseudo-random binary m-sequence and each response cycle (in real time) allows the extraction of each local response contribution. The average signal for each segment is then amplified and band-passed filtered in order to remove any extraneous electrical noise.

Corneal electrodes

As in a full-field ERG, the VERIS may be recorded with a number of different types of corneal electrode. Mohidin, Yap, & Jacobs (1997) compared the mean response amplitudes for the jet contact lens, gold foil, carbon fibre and DTL electrodes. The contact lens electrode produced the largest response amplitude followed by the gold foil, DTL and the carbon glide. The carbon glide produced significantly higher coefficients of variation or less repeatability between tests. Many research departments prefer to use contact lens electrode (typically the Burian Allen), as the larger response amplitudes result in a better signal-to-noise ratio. Conversely, some negative aspects are also associated with its use. The optics may increase the amount of stray light, a prismatic effect may be induced if the contact lens is incorrectly fitted, there is a greater associated risk to corneal abrasion and significantly less comfort when compared with other electrodes. After reviewing the literature for each type of electrode, it was decided to use the DTL fibre as this protocol promised better levels of patient recruitment and retention due to the significant improvement in comfort.

The mfERG and its spatial resolution

Light scatter from neighbouring stimulus elements may adversely affect the recording. Authors have hypothesised that no clearly defined blind spot suggests poor spatial resolution (Kretschmann *et al.*, 2000). Hood, (2000) has refuted these allegations stating that in the 103-hexagon display there is no guarantee that a hexagon will fall entirely in the optic disc.

First and second order Kernels

The first order kernel (response waveform) is obtained by adding all the records following a white stimulus and subtracting all the records following a black stimulus. The responses specific to that hexagon are built up, while the effects from other hexagons are eliminated. The second order kernel (response waveform) is a measure of how the response is influenced by the adaptation to successive flashes. If the response to a flash preceded by a flash, is not the same, as the response to a flash preceded by no flash then the system is not completely linear and a second order kernel is present. The upper bold arrow in Figure 1.11

indicates the response to a flash preceded by a flash: the lower bold arrow indicates the response to a flash preceded by no flash. If the two waveforms are not identical then a second order kernel is present, which is calculated by subtracting one response from the other. The first slice of a second order kernel is the effect from an immediately preceding flash; the second slice is a flash, which are two frames away. The shape of the second order kernel provides information about the adaptive mechanisms of the retina. The first-order kernel response is believed to originate predominantly in the outer retina and partly within the inner retina (Bearse & Sutter, 1996; Sutter & Tran, 1992). The second-order kernel response is believed to originate predominantly from the inner retina and partly from the outer retina (Bearse & Sutter, 1996; Palmowski *et al.*, 1997). Recent studies have reported reduced second order kernels in conditions such as diabetic retinopathy (Mita-Harris, 2001; Palmowski *et al.*, 1997) and glaucoma (Chan & Brown, 1999).

1.11.10.6.Analysis of mfERG

The mfERG recording may be analysed in different ways. The trace array displays individual waveforms for each stimulus element. The averages tool allows individual waveforms to be grouped with other traces showing similar response characteristics. Responses are typically grouped into rings or quadrants. In cases where concentric pathology is present a ring analysis might be considered most appropriate, while for other types of pathology a quadrant analysis might be better. In averages normalised, the amplitudes for each stimulus element in a group are added together and the result is divided by the root mean square: each group trace will have approximately the same vertical excursion (unit = nV). In averages response density scaled, the responses for each stimulus element are added together and the result is divided by the total solid angle of all the elements in a group (unit = nV/deg^2). In averages sum of groups, the amplitudes in each group are added together providing a cumulative response for that group (unit = nV). The scalar product is an artificial number representing the correlation between a template and an actual trace. The computer program compares the resultant waveform point by point with the mean normal waveform. The differences between the two waveforms in terms of both implicit time and amplitude produce a scalar product (essentially a correlation coefficient). If normal files are used a template is created from the mean of the selected group. If no normal files are selected a template is created from within the same recording using responses. Using the editing procedure you can define how the reference file is calculated. As the centre hexagon is always compared to itself then this element will produce the highest response. The response density is the scalar product divided by the area of that element (nV/deg^2). Scalar product analysis is advisable in recordings demonstrating smaller amplitudes and a poorer signal-to-noise ratio (Keating, Parks, & Evans, 2000; Sutter & Tran, 1992).

Figure 1.11. Diagram illustrating the difference between the first and the second order kernel adapted from Sutter & Bearse (1999) (black = flash, white = non flash, grey = 50-50 chance of flash or non flash).

Choosing an appropriate analysis technique is both dependent on the specific disease and the quality of data. The averages tool is not advisable in cases that show small areas of localised damage. Conversely, individual traces are occasionally too noisy to reveal any details of interest unless they are averaged together. Because the DTL fibre produces small signal amplitudes and VGB is associated with concentric visual field (not localised to one small area) loss, it was decided to use both the averages tool and scalar product analysis

The typical waveform of a normal mfERG response

The waveform of the first-order response is typically biphasic: an initial negative deflection (N1) followed by a positive peak (P1) Figure 1.12. N1 is thought to be comprised of some of the same components as the a-wave of a full-field ERG record (Hood, 2000; Hood & Li, 1997). P1 is thought to be comprised of some of the same components as the b-wave and oscillatory potentials of a full-field ERG record (Hood, 2000; Hood & Li, 1997). The summed mfERG response however, bears only a superficial resemblance to that from a typical full-field ERG (Hood & Li, 1997). Its positive peak is earlier and its waveform lacks the multiple positive components of a full-field recording. Altering the mfERGs filter bandwidths, to the same settings as a full-field recording, makes little difference to its appearance (Hood, 2000). The summed mfERG response however, can be manipulated to look more like that of a full-field recording, by reducing the temporal density of flashes so that seven steps of solid background follows one-step of the m-sequence (Hood & Li, 1997). These adjustments produce a summed waveform with a multi-peaked component that is similar to the b wave and oscillatory potentials within a full-field recording.

The mfERG and damage to the outer retina

Diseases, which affect the outer segment of the cone photoreceptors, are associated with either reductions in response density amplitudes (Chan & Brown, 1998; Kretschmann *et al.*, 1998a; Kretschmann *et al.*, 1998b; Piao *et al.*, 2000) and or implicit time delays (Kretschmann *et al.*, 1998b; Piao *et al.*, 2000; Seeligr *et al.*, 1998). The mfERG has been used successfully to diagnose maculopathies such as Stargardt's Maculopathy (Kretschmann *et al.*, 1998a), Occult Macular Dystrophy (Piao *et al.*, 2000), Age-Related Macular Degeneration (Bearse & Sutter, 1996; Kretschmann *et al.*, 1998a) and dystrophies such as Retinitis Pigmentosa (Chan & Brown, 1998; Kondo *et al.*, 1995; Seeligr *et al.*, 1998) and Myopia (Kawabata & Adachi-Usami, 1997). Their visual field loss, appears to correlate closely with the topography of their mfERG responses (Kondo *et al.*, 1995; Kretschmann *et al.*, 2000; Palmowski *et al.*, 2001; Wildberger & Junghardt, 2002). Beyond the outer segment, the damage is postulated to produce either large delays (e.g. <7 ms) or relatively large response amplitudes with moderate delays (e.g. >4 ms) (Hood, 2000).

The mfERG and damage to the inner retina

Glaucoma is a progressive disease, which leads to ganglion cell death and reduced visual sensitivity. Controversy has surrounded the mfERGs ability, to successfully detect glaucomatous damage. Some studies have documented altered mfERG amplitudes (Chan & Brown, 1999), implicit times (Hasegawa *et al.*, 2000) and waveform changes (Bearse & Sutter, 1996; Hasegawa *et al.*, 2000; Hood *et al.*, 1999; Hood *et al.*, 2000). Others have reported no change (Vaegan & Buckland, 1996; Vaegan & Sanderson, 1997). Sutter & Bearse (1999) have hypothesised that an mfERG response is composed of two separate identifiable components a larger retinal component (RC) and a smaller optic nerve head component (ONHC). The RC remains constant throughout the entire recording. The ONHC varies with distance from the fovea producing naso-temporal variations, which are thought to reflect the inner retinal (ganglion, amacrine cell) activity. Studies have reported that some patient's with confirmed glaucomatous field damage, also demonstrate reduced naso-temporal variations (Hasegawa *et al.*, 2000; Hood, 2000; Hood *et al.*, 1999). Conversely, there appears to be no correlation between abnormal mfERG responses and the areas of field loss (Fortune, Johnson, & Cioffi, 2001). One study has reported normal mfERG responses despite significant glaucomatous field loss (Hood, 2000). Incongruities suggest that ganglion cells are not solely responsible for the ONHC which led Hood (2000) to postulate two possibilities. Patients who demonstrate abnormal naso-temporal variations have damage that is beyond the ganglion cell body. Alternatively, mfERG responses are also dependent upon the integrity of the Müller cells or the myelin sheath near the optic nerve head.

Animal evidence indicating an inner retinal component

Several studies have reported large naso-temporal asymmetry in the mfERG recordings from monkeys (Frischman *et al.*, 2000; Hood *et al.*, 1999). After administration of Tetrodotoxin (TTX), a chemical which blocks the action potentials from all ganglion cells some amacrine cells and possibly the interplexiform cells, the naso-temporal variations were eliminated. Multifocal ERG responses were recorded in five monkeys, after experimentally inducing glaucoma (Frischman *et al.*, 2000). As visual field loss progressed the first order kernel responses lost their naso-temporal asymmetry, the second order kernel responses were almost eliminated. Animal evidence appears to be at least partially consistent with the ONHC theory (Sutter & Bearse, 1999).

1.11.10.7.The mfERG in patients receiving VGB

Studies have previously investigated VGB associated abnormalities using the mfERG (Besch *et al.*, 2000; Harding *et al.*, 2000a; Lawden *et al.*, 1999; Mackenzie & Klistorner, 1998; Ponjavic & Andreasson, 2001; Ruether *et al.*, 1998)., however the results have varied as to which parameter is primarily affected and why. To date only one other study has investigated the second-order responses in VGB-treated subjects (Besch *et al.*, 2002).

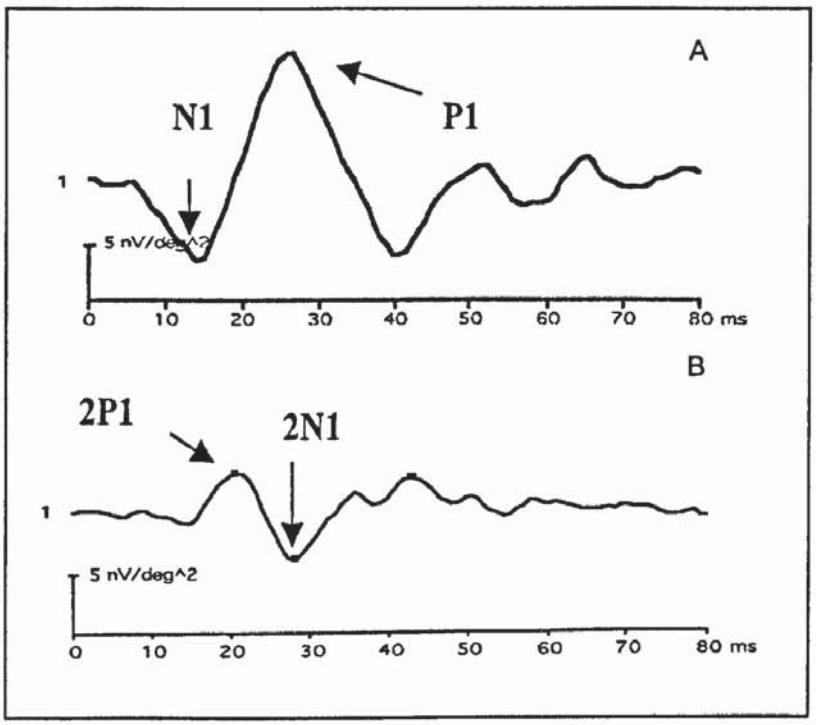

Figure 1.12. Multifocal electroretinograms from the left eye of a 26-year-old female. **(A)** An "All trace" wave obtained by averaging the sum of the waves of the first-order kernel. **(B)** An "All trace" wave obtained by averaging the sum of the waves of the second-order kernel.

2. Rationale and Logistics

2.1. Rationale

Current literature suggests that although some of the information surrounding VGB's toxicology has been identified, a number of questions remain unanswered. It is of critical importance to determine why the pathology appears to affect only a proportion of the patients exposed to the treatment and why there are some claims of central retinal sparing. One hypothesis for this occurrence is that other risk factors besides the drug itself are correlated with its pathology. An alternative hypothesis is that the current techniques are insufficient for detecting all the abnormalities associated with VGB.

2.2. Aims

To investigate both hypotheses so that safer treatment regimes and monitoring practices might be designed.

The first part of this thesis focused on determining which risk factors, if any, significantly alter the severity of visual field loss. Several studies have already attempted to answer this question. However, these studies vary in their methodologies and their findings are not robust. The initial part of this study concentrated on designing an algorithm that was capable of precisely quantifying the severity of visual field loss attributable to VGB therapy. This algorithm was incorporated into a suitable visual field protocol and used to establish which risk factors act as predictors of visual field loss.

Visual field testing is the current "gold standard" clinical investigation for the detection and monitoring of abnormalities associated with VGB. The most commonly used techniques are the Goldmann Perimeter and automated static perimetry, using a white-white Full Threshold algorithm. Goldmann perimetry is frequently criticised for its relative insensitivity, vulnerability to false positive results and its potential for examiner related bias. Full Threshold white-white perimetry has also been criticised for its lack of sensitivity and long examination times. The next aim of the thesis was to establish an optimum clinical regimen for detecting visual field loss attributed to VGB and for those patients with confirmed visual field loss, to determine the optimum clinical regimen for identifying visual field progression. The following studies were consequently designed to explore whether a more efficient, sensitive or specific method of investigating the abnormalities associated with VGB treatment could be found.

The Swedish Interactive Threshold Algorithms (SITA Standard and SITA Fast) represent a new generation of thresholding algorithms specifically designed to reduce examination times

without any significant alteration in accuracy, when compared to the Full Threshold and FASTPAC algorithms respectively. Both SITA algorithms (SITA Standard and SITA Fast) might reduce examination times and enable patients that were previously unable to carry out long examinations to be regularly monitored with perimetry. A study was consequently designed to evaluate the clinical effectiveness of the Full Threshold, SITA Standard and SITA Fast algorithms in detecting visual field loss attributed to VGB.

The typical appearance of VGB-attributed visual field loss, measured using white-white perimetry, is bilateral and presents as concentric peripheral constriction that is most severe nasally with relative sparing of the temporal and central visual field. These results are in contrast to the reports from colour vision (Krauss *et al.*, 1998; Manucheri *et al.*, 2000; Roff Hilton *et al.*, 2002), contrast sensitivity (Nousiainen *et al.*, 2000a; Roff Hilton *et al.*, 2002; Perron *et al.*, 2002) and SWAP (Roff Hilton *et al.*, 2002) investigations which have indicated that VGB-mediated toxicity extends to the central visual field. White-white perimetry employs a white stimulus presented against a white background. In recent years, evidence has accumulated to suggest that this technique is relatively insensitive for detecting subtle abnormalities, due to the achromatic nature of the stimulus, which simultaneously stimulates all visual pathways. Short-Wavelength Automated Perimetry (SWAP) and Frequency Doubling Technology (FDT) are two relatively new perimetric techniques, which have been designed to investigate specific visual pathways and expected to detect damage at an earlier stage than the standard (white-white) stimulus.

A study was consequently designed to evaluate the relative effectiveness of white-white perimetry, SWAP and FDT in the detection of visual field loss attributed to VGB. FDT was measured using Program N-30 as this algorithm enabled the examination of the nasal visual field out to 30-degress. SWAP has failed to gain wide spread acceptance in the routine clinical investigation of retinal disease due to its inherent greater between- and within-subject variability (Cubbidge, Hosking, & Embleton, 2002). The central 10-degrees is known to produce smaller between- and within-subject variability (Cubbidge *et al.*, 2002), however the Humphrey Field Analyser (HFA) does not provide a normal database for SWAP within the central 10 degrees. A normal empirical SWAP 10-2 database was collected and then used to construct global visual field indices and probability analyses sensitive to diffuse and focal visual field loss. Analysing visual field tests without this knowledge is inherently dangerous because subtle abnormalities might be confused with normal physiological variations.

Research at the Department has previously developed a successful linear interpolation procedure to extrapolate normal SWAP sensitivity for each of the remaining stimulus locations of the 10-2 program from an existing 30-2 normal database (also known as the extrapolated database). A secondary aim was to compare the detection and quantification of

VGB-attributed visual field loss after using the empirically derived and extrapolated normal SWAP 10-2 databases to analyse results.

The multifocal electroretinogram (mfERG) is a technique which allows over 100 retinal areas to be measured inside approximately seven minutes. The results are presented in similar way to a conventional visual field examination; the areas of localised damage are plotted topographically on a field map. Unlike a conventional visual field examination, the mfERG also provides additional information relating to the site of pathology, enabling a differentiation between damage in the inner and outer retinal layers. The initial aim was to collect a normal database of mfERG results to calculate whether any responses from VGB treated patients fell outside a normal range. This procedure was used to determine whether a more specific or sensitive analysis of the abnormalities associated with VGB treatment could be found.

2.3. Logistics

All of the research was conducted in the Neurosciences Research Institute, at Aston University, Birmingham and with the approval from the Aston University Human Science Ethical Committee. A detailed drug history was obtained from each patients hospital notes after requesting permission from the patient, their hospital consultant physician and obtaining approval from each Hospitals Ethical Committee.

The normal participants were recruited from the staff, students, and general public. Each participant was given a detailed verbal and written explanation of the study. Before they were formally enrolled, written informed consent was obtained and they were given the opportunity to ask any questions. No problems were experienced in either the recruitment or retention of patients in the normal SWAP-10-2 study (chapter 5). A high drop out rate was found within the normal mfERG study (chapter 7) as several patients found the procedure either too uncomfortable or too difficult to complete (Table 2.1). All subjects and patients were free to withdraw from the studies at any time without prejudice.

The participants who were diagnosed with epilepsy and exposed to VGB therapy were recruited from the neurology clinics at the Queen Elizabeth Medical Centre in Birmingham, Queens Medical Centre in Nottingham and the Neurophysiology Department Aston University in Birmingham. Each participant was given a detailed explanation about the study and his or her written informed consent was obtained prior to enrolment. Patient recruitment was confounded by a failure to meet the strict inclusion criteria. Patients diagnosed with epilepsy frequently have other medical problems besides the seizures themselves and are either not capable of carrying out such long complicated research procedures or have pathology that would interfere with their test results (Table 2.1). Participant retention was also difficult, as the participants were frequently too unwell or too tired to attend their follow-

up visits (Table 2.1). This factor necessitated studies consisting of small number of visits and an assessment of repeatability was consequently not attempted for the majority of techniques. All subjects and patients were free to withdraw from the studies at any time without prejudice.

All studies ran concurrently therefore data analysis was carried out at the end of a two year research period. As a direct consequence the SITA algorithm, which is suggested in this thesis as the algorithm of choice for the detection of VGB attributed field loss in white-white perimetry, was not used in subsequent chapters.

Chapter number	The percentage of participants who were unable to complete the study	Reasons for failure
3	17.95% (7)	Inter-cranial pathology, high catch trials and tiredness
4	27.27% (6)	Inter-cranial pathology and high catch trials
5	2.99% (2)	Repeatable field defects
6	8.33% (2)	High catch trials and tiredness
7	26.09% (6)	Poor control of blinking and lack of comfort
8	23.53% (4)	Poor control of blinking

Table 2.1. Indicating the percentage of patients that failed to meet the inclusion criteria or accurately complete the study. The number inside the brackets equals the actual number of participants.

3. Identification of risk factors for VGB-attributed visual field loss using a new quantitative algorithm for visual field classification.

Aim: To develop a quantitative algorithm to determine the severity of visual field loss attributable to VGB therapy. To incorporate this algorithm into a suitable visual field protocol and use it to establish which risk factors act as predictors of visual field loss. **Methodology:** The sample comprised of 32 patients (mean age 37.8 years ±14.5years) diagnosed with epilepsy and exposed to VGB therapy. Each participant underwent standard white-white perimetry on either eye, using Program 30-2 Full Threshold algorithm on the Humphrey Field Analyser. Defect maps were constructed for each eye (right, left and combined) illustrating the percentage of patients with a visual field defect defined by a significant Total Deviation probability greater than the 5% significance at each stimulus location. A severity algorithm was then applied to quantify the visual field loss in terms of the both spatial area and depth of defect. This algorithm was used to quantify the severity of visual field loss for each patient (right eye, left eye and combined eyes) and compared to a qualitative classification previously designed Wild *et al.*, (1999a). A simultaneous multiple regression analysis was used to determine whether the severity of visual field loss was significantly correlated to a number of predictor variables including: cumulative VGB dose, maximum VGB dose, duration of VGB treatment and gender. **Results:** Thirty-seven eyes of 32 patients (57.8%) presented with a clinically significant defect. The severity of visual field loss ranged from 0 (no abnormalities) to 0.92 (where 1 equals all 74-field locations exhibiting abnormalities at $p< 0.005$ within shape probability analysis). A comparison between the two methods of classifications (qualitative-quantitative) revealed that in terms of quantifiable visual field loss there was little distinction between those patients diagnosed with mild visual field loss and those diagnosed with severe. The regression model indicated that maximum VGB dose was the only factor to be significantly correlated with severity of visual field loss: right eye ($p = 0.035$), left eye ($p = 0.030$) and combined ($p = 0.030$). **Conclusion:** The pattern of visual field loss illustrated by the defect maps along with previously reported anatomical evidence suggests that the damage induced by VGB therapy occurs at retinal level and is most likely a toxic effect. Results suggest that the quantitative analysis is useful for identifying the progression of visual field loss. Maximum VGB dose was significantly correlated with severity of visual field loss. This finding is important, as it indicates that patients who receive low doses of VGB are at reduced risk of developing severe visual field loss.

3.1. Introduction

Considerable evidence now exists to suggest a strong association between vigabatrin (VGB) and visual field loss. The typical appearance of VGB-associated visual field loss is bilateral and presents as concentric peripheral constriction that is most severe nasally with relative sparing of the temporal and central visual field (Hosking *et al.*, 2003; Roff Hilton *et al.*, 2002; Wild *et al.*, 1999a). The prevalence of visual field defects in the VGB-treated epilepsy population range from 17% (Hardus *et al.*, 2000b) to 71% (Russell-Eggitt *et al.*, 2000). It is unclear why a certain proportion of the population appears to remain protected from visual disturbances. It is possible however, that other factors besides the drug itself protect or expose patients to visual dysfunction.

A number of investigations have tried to establish which factors, if any, contribute to the aetiology of VGB (Arndt *et al.*, 1999; Arndt *et al.*, 2002; Hardus *et al.*, 2000b; Hardus *et al.*, 2001; Kalviainen *et al.*, 1999a; Malmgren, Ben-Menachem, & Frisen, 2001; Manucheri *et al.*, 2000; Newman *et al.*, 2002; Nicolson *et al.*, 2002; Nousiainen *et al.*, 2001; Toggweiler & Wieser, 2001; Wild *et al.*, 1999a). Current findings suggest that none of the investigated factors consistently correlate with the severity of visual field loss (Table 1.2). Cumulative VGB dose, duration of VGB treatment, concomitant anti epileptic drugs (AEDs) and gender are all factors previously documented as having both statistically significant relationships and null effects (Arndt *et al.*, 1999; Arndt *et al.*, 2002; Hardus *et al.*, 2000b; Hardus *et al.*, 2001; Kalviainen *et al.*, 1999a; Malmgren *et al.*, 2001; Manucheri *et al.*, 2000; Newman *et al.*, 2002; Nicolson *et al.*, 2002; Nousiainen *et al.*, 2001; Toggweiler & Wieser, 2001; Wild *et al.*, 1999a). The only factors to have shown agreement between studies are: age, VGB daily dose and smoking; and were documented to have no relationship with severity of visual field loss (Arndt *et al.*, 1999; Arndt *et al.*, 2002; Hardus *et al.*, 2000b; Hardus *et al.*, 2001; Kalviainen *et al.*, 1999a; Malmgren *et al.*, 2001; Manucheri *et al.*, 2000; Newman *et al.*, 2002; Nicolson *et al.*, 2002; Nousiainen *et al.*, 2001; Toggweiler & Wieser, 2001; Wild *et al.*, 1999a). To date, the relationship between the severity of visual field loss and maximum VGB dose has not been investigated. This is despite VGB's increasing association with visual toxicity. Descriptions of the various protocols employed by previous studies for investigating the visual field loss are presented in Table 3.1. It is highly probable that gross differences in methodologies (sample sizes, investigative procedures) account for at least some of the inconsistencies between studies. The majority of investigations failed to employ an adequate protocol, which would ensure accuracy and repeatability between studies. It is reasonable to assume therefore, that false results, examiner related bias and the fatigue effect (Hudson *et al.*, 1994) have prejudiced at least some of their results.

Identification and quantification of the severity of visual field loss is a vital step towards the successful management of VGB-treated patients, as even the most experienced clinicians find it difficult to accurately determine the true severity of visual field loss. To date, no perimetric testing protocol has gained widespread acceptance for the quantification of VGB-attributed field loss. Studies have previously used the Estermann Suprathreshold Screening method (Esterman, 1968), measurement of Goldmann field isopters (Arndt et al., 2002; Hardus et al., 2000a; Hardus et al., 2001; Kalviainen et al., 1999; Newman et al., 2002; Nousiainen et al., 2001; Toggweiler et al., 2001; Wild et al., 1999) or a classification based on clinical observations (Wild *et al.*, 1999a), for quantifying the severity of visual field loss. None have attempted to include a calculation based on both eyes, despite the consistent reports of the bilateral nature of the visual field loss.

While the classification designed by Wild *et al.* (1999a) is the most advanced method to date (Table 3.2), for quantifying the severity of VGB associated visual field loss, this classification is also subject to a number of limitations. The analysis is quite time consuming, as the perimetrist is required to evaluate each visual field based on the number and position of stimulus locations exhibiting abnormality at either $p< 0.01$ or $p< 0.005$ on shape probability analysis. It does not include those locations exhibiting abnormalities at either $p< 0.02$ or $p< 0.05$ within the analysis and may consequently miss subtle changes in threshold sensitivity. In addition, the algorithm does not take into account the typical bilateral symmetrical nature of a VGB associated abnormality and is susceptible to missing subtle abnormalities in the visual field; interocular symmetry strongly suggest a VGB-related defect.

Establishing which factors contribute to the aetiology of VGB will enable practitioners to determine which patients are more vulnerable to visual dysfunction and aid the design of safer treatment guidelines. The ideal severity algorithm should be sensitive enough to detect subtle changes in the visual field loss, as well as including changes in depth and area of defect, whilst excluding visual field loss unrelated to VGB therapy. A new classification based on improving these limitations should enable clinicians to determine whether progression of visual field loss does occur.

	Arndt *et al.*, (2002)	Hardus *et al.*, (2001)	Hardus *et al.*, (2000b)	Kalvialnen *et al.*, (1999a)	Manucherl *et al.*, (2000)	Newman *et al.*, (2002)	Nousialnen *et al.*, (2001)	Toggweiler & Wieser, (2001)	Wild *et al.*, (1999a)
Full Threshold Static Perimetry	(99 point screening)+ Goldmann	Goldmann	Peritest Static perimetry+ Goldmann	Goldmann	Humphrey (120 point screening)	Goldmann	Goldmann	Goldmann	Humphrey (30-2) + Goldmann
Manual Kinetic Perimetry (Goldmann)	✓	✓	✓	✓	✓	✓	✓	✓	✓
Reliability Catch Trials Considered	✓	x	x	x	x	x	x	x	✓
Fatigue Effect Considered	x	x	x	x	x	x	x	x	✓
Learning Effect Considered	x	x	x	x	x	x	x	x	x
Exclusion Criteria Employed	✓	x	x	x	x	x	x	x	x

Table 3.1. Visual field investigation protocols used in studies of visual field loss in patients receiving VGB.

3.2. Aims

To develop a quantitative algorithm to determine the severity of visual field loss attributable to VGB therapy. To incorporate this algorithm into a visual field protocol and use it to establish which risk factors act as predictors of visual field loss.

3.3. Methodology

3.3.1. Patients and inclusion criteria

Thirty-nine patients: 25 female, 14 male (mean age 38.2; ±13.9 years: range 16 to 66 years) previously diagnosed with epilepsy and who were either currently, or had previously received VGB, were invited to take part in the study. All patients had previous experience of at least one visual field test on a Humphrey Field Analyser. Inclusion criteria consisted of a logMAR visual acuity of 0.1 or better (6/6 Snellen equivalent), a distance refractive error of less than ±6.00 dioptres of sphere or ±2.5 dioptres of astigmatism, absence of intra-cranial pathology which is known to effect the visual pathway or any known ocular pathology which was unrelated to VGB therapy.

3.3.2. Ethical approval and informed consent

All patients were asked for their written informed consent. A detailed drug history was obtained from their hospital notes after requesting permission from the patient and their hospital consultant physician (see section 2.3).

3.3.3. Experimental procedures: visual fields

In accordance with previous investigations, this study was unable to review a large cohort of VGB recipients more than once due to recruitment difficulties and the long travelling distances requested of the patients. In an attempt to minimise the perimetric learning effect (Wood *et al.*, 1987), all patients had undergone at least one visual field examination within the last six months using the Humphrey Field Analyser (HFA). Each participant underwent standard white-white perimetry on either eye using white-white automated static perimetry with the Humphrey Field Analyser (Carl Zeiss Ltd, Hertfordshire, UK); Program 30-2, Full Threshold algorithm, Goldmann stimulus size III, stimulus duration 200 ms. The HFA model 750 (software version A10.2.) was employed and the head tracking option enabled. A 30-minute break between visual field tests was introduced in order to minimise any fatigue-related bias (Hudson *et al.*, 1994).

Table 3.2. Guidelines for a qualitative classification of the severity of visual field loss for static threshold perimetry out to 30° eccentricity adapted from Wild *et al.* (1999a).

Additionally, rest periods were introduced during individual visual field examinations where necessary, as epileptic patients are particularly susceptible to fatigue. The order, with which eyes were tested, was randomised between subjects. Catch trials of less than 20% fixation losses, less than 33% false positives and less than 33% false negatives were employed to ensure reliability of patient responses (Heijl & Krakau, 1975). If any results fell outside these criteria, they were invited back to repeat their examination on a different day. Subsequently, if the visual field results again fell outside the reliability criteria they were removed from the study.

3.4. Analysis

3.4.1. Visual field defect maps

Defect maps were constructed for all the right eyes (Figure 3.1) and all the left eyes (Figure 3.2), illustrating the percentage of patients with a visual field defect defined by a significant Total Deviation probability greater than the 5% significance at each stimulus location. A mean defect map was also constructed by averaging the results from the right and left eyes (Figure 3.3).

3.4.2. Severity algorithm

Each stimulus location in the Total Deviation probability map was weighted for both depth of defect and its spatial location. Visual field locations were weighted for depth, to ensure that the diagnostic algorithm not only considered changes in the area of visual field loss but also accounted for changes in the threshold sensitivity. The weighted depth severity was calculated by grading the locations according to their significance levels as follows

Weighting	Defect significance
0	not significant
1	**p<0.05**
2	**p<0.02**
3	**p <0.01**
4	**p <0.005**

Table 3.3. Weighing for severity algorithm according to defect significance.

Stimulus locations were weighted for their spatial severity in order to emphasise the peripheral visual field abnormalities typically associated with VGB treatment. Using the mean defect map produced (Figure 3.3), each stimulus location was then graded according to the frequency of defect occurrence, the greater the frequency the higher the applied weight according to the following rules.

Weighting	Frequency
1	0 to 25% frequency
2	26% to 50% frequency
3	>50% frequency

Table 3.4. Weighting for severity according to spatial location.

The overall defect severity for each stimulus location in the visual field was determined by multiplying the depth severity weighting by the spatial severity weighting and totalling the values for all 74 stimulus locations (i.e. all the stimulus locations in the 30-2 spatial grid, excluding the locations immediately above and below the blind spot). The overall defect severity was divided by the maximum defect severity (all 74-field locations exhibiting abnormalities at $p< 0.005$ within shape probability analysis) in order to place on a scale between zero (no defect) and one (maximum defect severity).

A combined defect severity was achieved by adding the overall defect severity for the right and left eyes together and then totalling the values for all 74 stimulus locations (i.e. all the stimulus locations in the 30-2 spatial grid, excluding the locations immediately above and below the blind spot). The overall combined defect severity was divided by the maximum combined defect severity (all 148-field locations exhibiting abnormalities at $p< 0.005$ within shape probability analysis) in order to place on a scale between zero (no defect either eye) and one (maximum combined defect severity). A Student's paired *t*-test was used to investigate the differences between the severity recorded between the right and left eyes.

3.4.3. Comparison between classifications

The severity of each visual field test was calculated both quantitatively using the severity algorithm outlined above, and qualitatively using the guidelines previously proposed by (Wild *et al.*, 1999a).

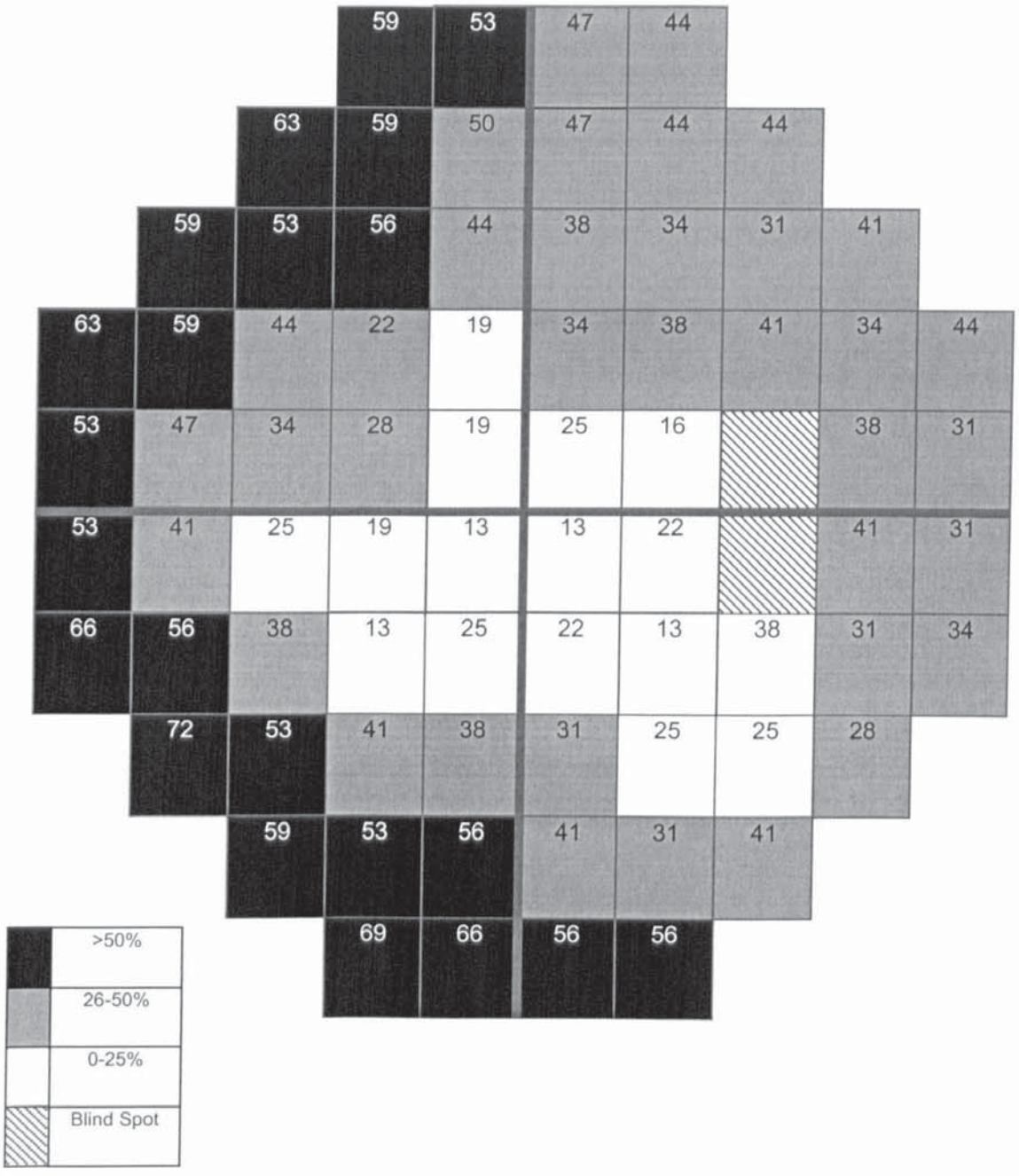

Figure 3.1. Defect Map showing the percentage of patients with a significant Total Deviation (TD) at each stimulus location for the Right Eye. Locations were reported as defective if their threshold values fell outside age matched normal values, found in less than 5% of the population.

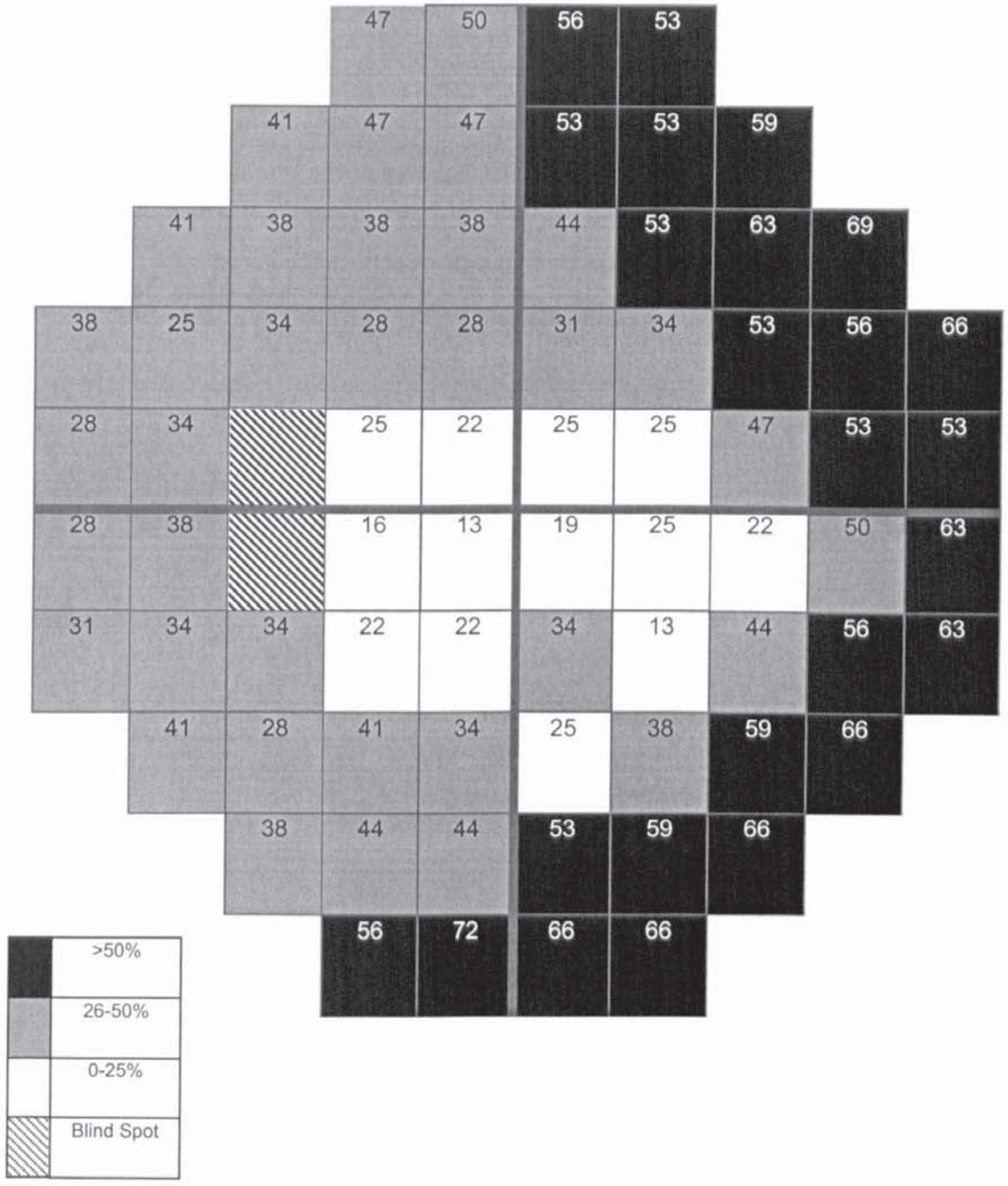

Figure 3.2. Defect Map showing the percentage of patients with a significant Total Deviation (TD) at each stimulus location for the Left Eye. Locations were reported as defective if their threshold values fell outside age matched normal values, found in less than 5% of the population.

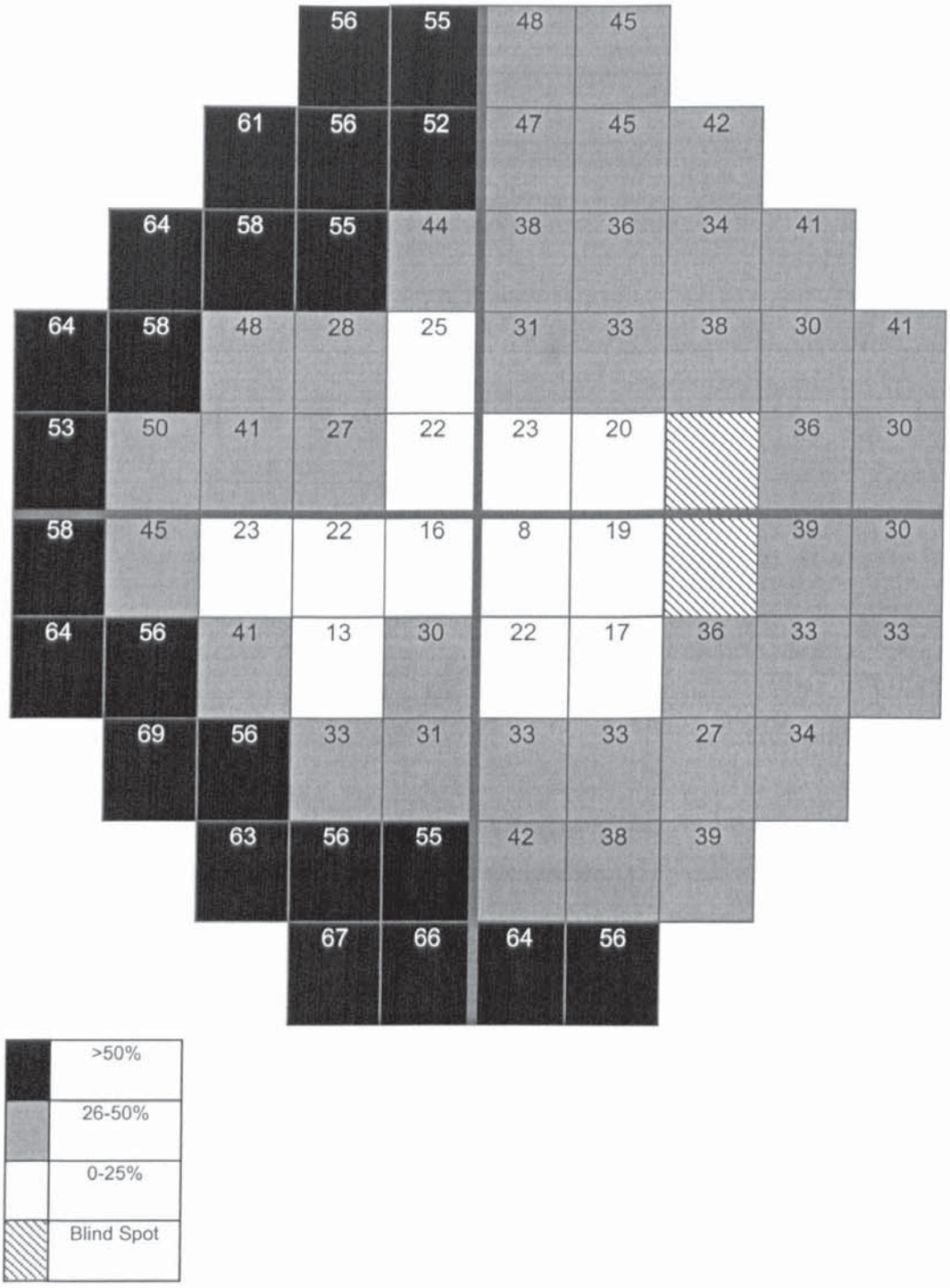

Figure 3.3. Defect Map showing the percentage of patients with a significant Total Deviation (TD) at each stimulus location Mean of Right and Left eyes. Locations were reported as defective if their threshold values fell outside age matched normal values, found in less than 5% of the population. The left eye has been inflected to a right eye in this analysis. Correlation between VGB therapy and visual field loss

3.4.4. Correlation between VGB therapy and visual field loss

A simultaneous multiple regression model, was used to explore the relationship between the severity of visual field defect and a number of potential predictor variables: cumulative VGB dose, maximum VGB dose, duration of VGB treatment and gender.

3.5. Results

Following the strict inclusion criteria it was necessary to remove two patients who had undergone temporal lobe surgery. Two further patients were removed due to poor patient reliability defined by numbers of fixation losses, false positive and negative catch trials exceeding the defined criteria for normality. An additional three patients were removed from data analysis because of an inability to complete the visual field testing as a result of excessive fatigue. Consequently, 32 patients: 21 female 11 male (mean age 37.8 years; ±14.5 years; range 16 to 66 years) were included for data analysis. Patient's concomitant medication other than VGB is presented in Table 3.5.

3.5.1. Visual field defect maps

The defect maps are presented in Figures 3.1, 3.2 and 3.3. The peripheral visual field, particularly on the nasal side showed the greatest number of defects. The central visual field particularly along the horizontal meridian remained relatively unaffected. Furthermore, the visual field loss in the right eye (Figure 3.1) closely mirrors in the visual field loss in the left eye (Figure 3.2), in terms of both the spatial location and frequency of occurrence of visual field loss. A Student's paired t-test showed that there was no statistical difference between the severity recorded between the right and left eyes ($p = 0.914$).

3.5.2. Comparison between classifications

An evaluation between the two methods of classification yielded good agreement between no defects and severe defects Table 3.6 & 3.7. However, there was little agreement between two methods of classification for those patients with mild or moderate visual field loss. Some of the patients diagnosed with mild visual field loss yielded greater visual field loss defined quantitatively using the severity algorithm than patients with either moderate or severe visual field loss. In terms of quantifiable loss there was little distinction between each nominal level of classification (mild, moderate and severe).

Patient number	Carbamazepine	Sodium Valporate	Clobazam	Levetiracetam	Topiramate	Lamotrogine	Phenytoin	Gabapentin	Other
1	X			X					
2	X	X				X			
3						X			
4		X							
5	X		X			X		X	
6		X		X					
7	X								
8			X			X			
9	X					X			
10									
11						X			
12	X					X		X	
13	X			X					
14	X			X					
15	X			X					
16						X			
17	X			X					
18	X	X				X	X		X
19						X			
20	X	X					X		
21							X		X
22		X				X		X	X
23	X	X	X			X		X	X
24	X							X	
25					X	X			
26					X				
27	X			X					X
28									
29					X				
30									
31		X							
32	X					X	X		

Table 3.5. Concomitant epileptic medication (other than VGB)

Right eye (quantitative classification)	Right eye (qualitative classification)
0	Normal
0	Normal
0	Normal
0	Normal
0	Normal
0.01	Normal
0.01	Normal
0.02	Normal
0.04	Normal
0.04	Normal
0.04	Normal
0.06	Normal
0.1	Normal
0.11	Normal
0.23	Mild
0.32	Moderate
0.33	Moderate
0.33	Mild
0.34	Severe
0.37	Mild
0.45	Severe
0.50	Severe
0.55	Severe
0.66	Severe
0.70	Severe
0.72	Severe
0.83	Severe
0.83	Severe
0.87	Severe
0.89	Severe
0.92	Severe
0.92	Severe

Table 3.6. The results for each patients visual field test (right eye), classified quantitatively with the present severity algorithm (in ascending order) and qualitatively using the guidelines for VGB severity classification taken from Wild *et al.*, (1999a).

Left eye (quantitative classification)	Left eye (qualitative classification)
0	Normal
0	Normal
0	Normal
0	Normal
0	Normal
0.01	Normal
0.02	Normal
0.02	Normal
0.04	Normal
0.06	Normal
0.06	Normal
0.09	Normal
0.14	Mild
0.14	Normal
0.22	Mild
0.27	Mild
0.36	Moderate
0.37	Moderate
0.38	Moderate
0.46	Severe
0.46	Severe
0.51	Severe
0.51	Severe
0.56	Severe
0.71	Severe
0.76	Severe
0.78	Severe
0.79	Severe
0.84	Severe
0.86	Severe
0.91	Severe
0.92	Severe

Table 3.7. The results for each patients visual field test (left eye), classified quantitatively with the present severity algorithm (in ascending order) and qualitatively using the guidelines for VGB severity classification taken from Wild *et al.* (1999a).

Patient number	Cumulative VGB dose (grams)	Duration of VGB treatment (weeks)	Maximum VGB dose (grams)	Gender	Severity Right eye	Severity Left eye	Severity Combined eyes
1	8543.5	494	2.5	Female	0.10	0.06	0.08
2	2527	121	3	Male	0.01	0.09	0.05
3	6840.75	461	2.5	Male	0.00	0.00	0.00
4	2485	184	2	Female	0.83	0.84	0.84
5	1039.5	99	1.5	Female	0.33	0.37	0.35
6	3872.75	430	2	Female	0.50	0.51	0.50
7	6818	487	2	Female	0.23	0.22	0.23
8	2576	342	1	Female	0.32	0.56	0.44
9	5418	387	2	Male	0.55	0.51	0.53
10	6531	280	4	Male	0.70	0.71	0.71
11	3136	230	2.5	Female	0.01	0.00	0.01
12	7693	314	3.5	Female	0.92	0.92	0.92
13	7318.5	484	3	Male	0.33	0.38	0.36
14	1827	192	1.75	Female	0.04	0.14	0.09
15	3976	284	2	Female	0.00	0.00	0.00
16	2446.5	197	2	Female	0.00	0.02	0.01
17	3794	170	3.5	Male	0.45	0.46	0.45
18	2359	337	1	Female	0.00	0.00	0.00
19	1246	178	1	Male	0.04	0.02	0.03
20	13013	491	5.5	Male	0.66	0.78	0.72
21	2765	145	3	Female	0.92	0.79	0.86
22	5572	271	4	Female	0.83	0.91	0.87
23	11599	635	6	Male	0.34	0.46	0.40
24	10899	527	3	Female	0.06	0.01	0.04
25	6793.5	468	2.5	Female	0.04	0.04	0.04
26	7672	387	3.5	Male	0.89	0.86	0.88
27	6230	445	2	Female	0.11	0.14	0.12
28	2492	357	1	Female	0.00	0.00	0.00
29	8386	392	3	Female	0.37	0.27	0.32
30	5572	354	2.5	Female	0.02	0.06	0.04
31	3654	247	3	Female	0.87	0.76	0.82
32	3815	368	3	Male	0.72	0.36	0.54

Table 3.8. Cumulative VGB dose, duration of VGB treatment, maximum VGB dose, gender and severity of visual field loss for each of the 32 patients exposed to VGB.

Predictor variable	Standardised coefficients (beta values)	Significance (p values)	Correlation (zero-order)	Correlation (part)
Cumulative VGB dose (grams)	-0.187	0.690	0.147	-0.064
Duration of VGB (weeks)	-0.195	0.567	-0.116	-0.093
Maximum VGB dose (grams)	**0.702**	**0.035**	**0.465**	**0.356**
Gender	0.077	0.675	-0.166	0.068

Table 3.9. Table showing right eye outcome of simultaneous multiple regression analysis using cumulative VGB dose, maximum VGB dose, duration of VGB treatment and gender to predict severity of visual field loss

Predictor variable	Standardised coefficients (beta values)	Significance (p values)	Correlation (zero-order)	Correlation (part)
Cumulative VGB dose (grams)	-0.127	0.782	0.174	-0.044
Duration of VGB (weeks)	-0.235	0.483	-0.108	-0.112
Maximum VGB dose (grams)	**0.709**	**0.030**	**0.491**	**0.360**
Gender	0.101	0.575	-0.156	0.089

Table 3.10. Table showing left eye outcome of simultaneous multiple regression analysis using cumulative VGB dose, maximum VGB dose, duration of VGB treatment and gender to predict severity of visual field loss

Predictor variable	Standardised coefficients (beta values)	Significance (p values)	Correlation (zero-order)	Correlation (part)
Cumulative VGB dose (grams)	-0.154	0.738	0.162	-0.053
Duration of VGB (weeks)	-0.220	0.513	-0.113	-0.105
Maximum VGB dose (grams)	**0.711**	**0.030**	**0.483**	**0.360**
Gender	0.090	0.620	-0.162	0.079

Table 3.11. Table showing combined eyes outcome of simultaneous multiple regression analysis using cumulative VGB dose, maximum VGB dose, duration of VGB treatment and gender to predict severity of visual field loss

3.5.3. Correlation between VGB therapy and visual field loss

Cumulative VGB dose, maximum VGB dose, duration of VGB treatment, gender and severity of visual field loss for each of the 32 patients is presented in Table 3.8. Using simultaneous multiple regression to determine the severity of field loss, a significant model emerged for the right eye ($p = 0.035$), left eye ($p = 0.022$) and combined ($p = 0.025$) after using the following predictor values: cumulative VGB dose, maximum VGB dose, gender and duration of VGB treatment, (Tables 3.9, 3.10 and 3.11). The total regression equation accounted for 20.6% of the variance for the right eye and 23.8% of the variance for the left eye and 22.9% of the variance for the combined in the prediction of the dependent variable (severity of visual field loss). Further inspection of the correlation revealed that maximum VGB dose was the only significant predictor within each model for the right eye ($p = 0.035$), left eye ($p = 0.030$) and combined ($p = 0.030$). No other predictor variables reached statistical significance. The beta value for maximum VGB dose, within each model implied that some of the predictive power initially found (right eye = 0.702, left eye = 0.709, combined = 0.711) was due to the variance it shared with other predictors (right eye part correlation = 0.356, left eye part correlation = 0.404, combined part correlation = 0.360). Cumulative VGB dose and duration of VGB treatment also showed significantly larger beta values than part correlations. This suggests that any shared variance between these variables and severity of field loss might be accounted for largely by maximum VGB dose. The zero-order correlation suggested that maximum VGB dose (right eye = 0.465, left eye = 0.491, combined = 0.483) had more predictive power when it was considered independently from the other predictive factors. A graph of severity of visual field loss versus maximum VGB dose illustrates that once an outlying participant (number 23) was removed from the analysis, the correlation became stronger (Figure 3.4).

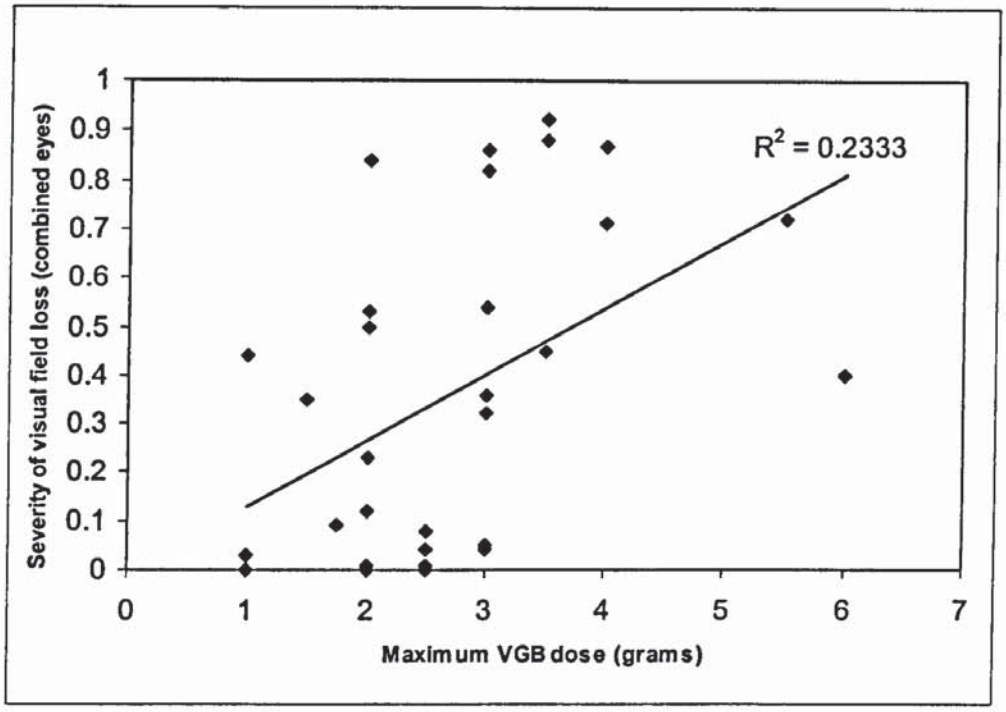

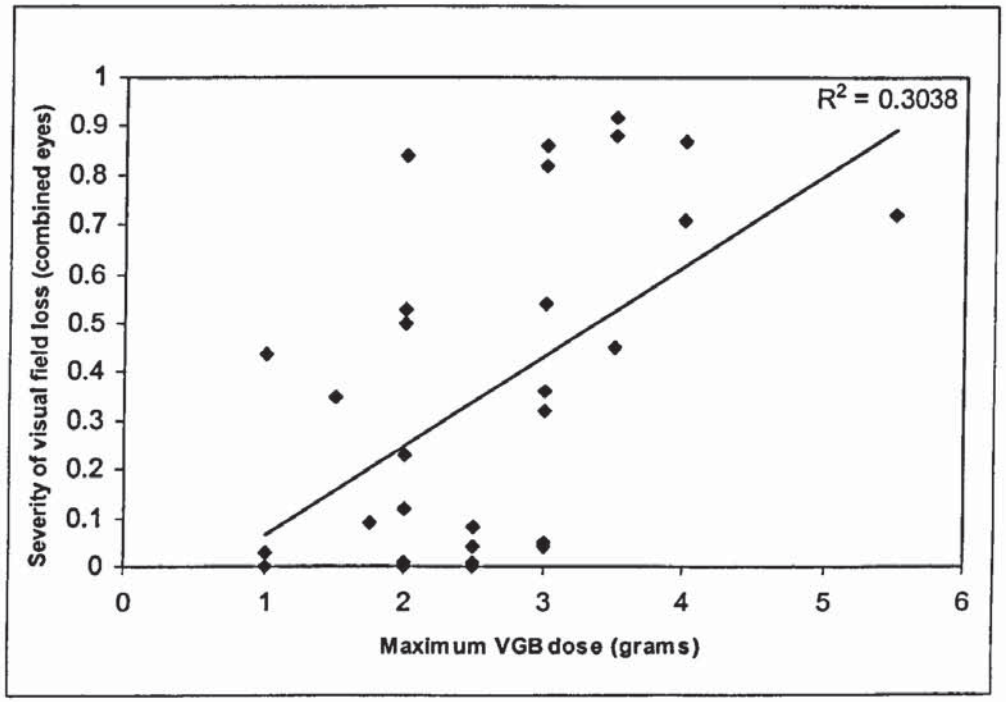

Figure 3.4 Graph showing severity of visual field loss versus maximum VGB dose with (top) and without participant 23 (bottom).

3.6. Discussion

3.6.1. Visual field defect maps

Diagnosing cases of mild visual field loss attributed to VGB therapy has previously proven difficult because the pattern of field loss mimics testing artefacts induced by fatigue or misalignment of the corrective lens position. The defect maps presented in this study confirm the findings of Daneshvar *et al.*, (1999); Lawden *et al.*, (1999); Ravindran *et al.*, (2001); Versino & Veggiatt, (1999) and Wild *et al.*, (1999a) that VGB therapy induces a bilateral, symmetrical defect. The findings from this study suggest that all VGB recipients should undergo regular field examinations of both eyes, as monocular field loss or field loss that does not mirror that of the contralateral eye implies the defect is not associated with VGB treatment.

Figures 3.1 & 3.2 indicate that the temporal visual field is significantly less affected by VGB treatment. This finding is concordant with previous investigations which employed automated static perimetry to quantify the severity of visual field loss (Lawden *et al.*, 1999; Mackenzie & Klistorner, 1998; Russell-Eggitt *et al.*, 2000; Wild *et al.*, 1999a). The nasal visual field, corresponding to the temporal retina, showed the greatest frequency of defects, whilst the central visual field and corresponding retina was least affected, particularly along the horizontal field meridian. This unique pattern of visual field loss appears to closely follow the normal physiological variations of human photoreceptor populations. Specifically, the greatest density of human photoreceptors occurs at the fovea, followed by a steep decline in photoreceptor population towards the periphery. The nasal retina is approximately 40-45% more populated than the temporal retina and there is a band of high cone density along the horizontal field meridian (Curcio *et al.*, 1990; Jonas, Schneider, & Naumann, 1992). Figure 3.5 illustrates the normal density of human photoreceptors along the horizontal and vertical meridians. This anatomical evidence, in combination with the pattern of visual field loss, would suggest that the damage to the visual pathway induced by VGB therapy occurs at the retinal level and is most likely a toxic effect.

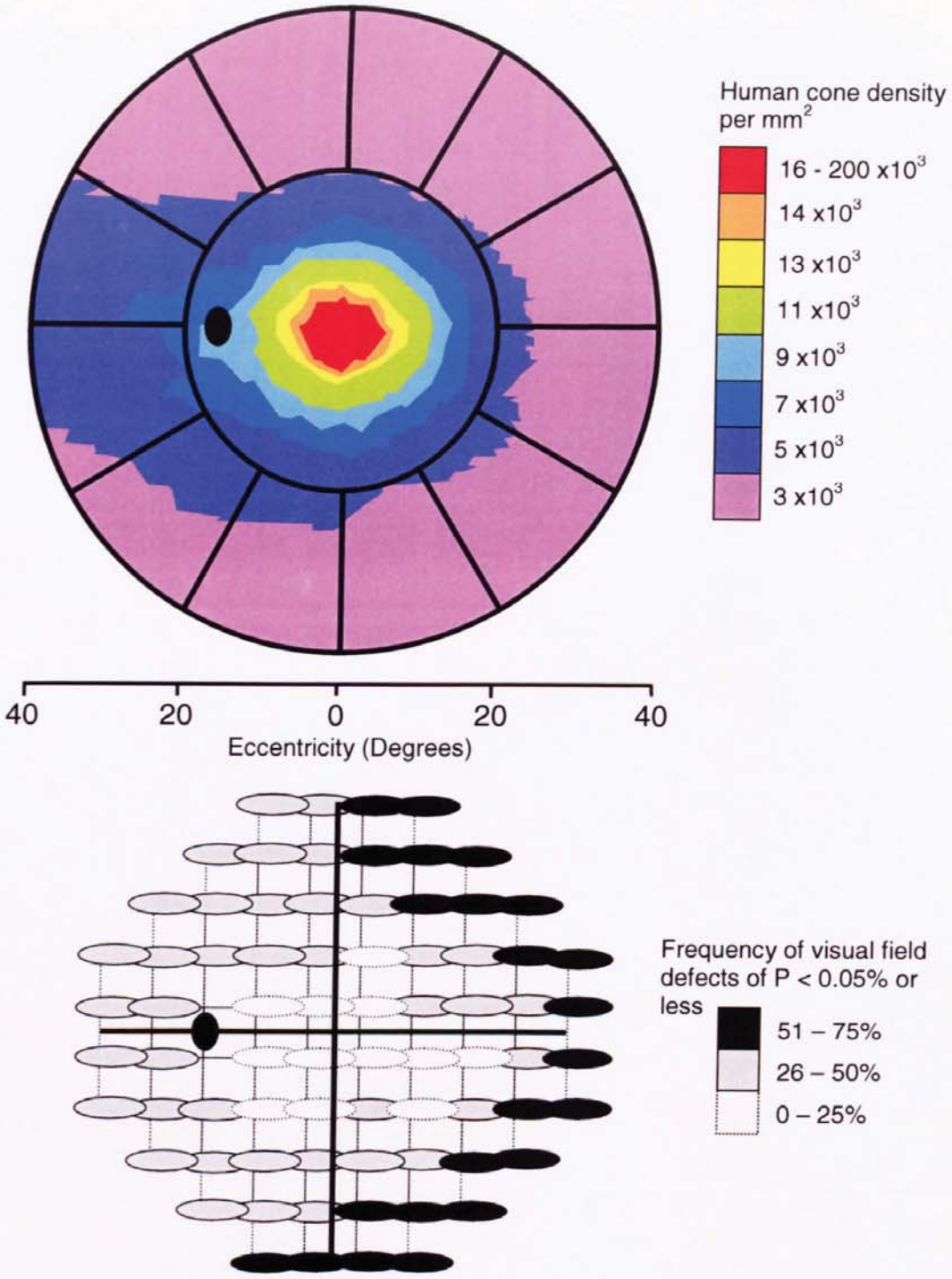

Figure 3.5 Correlation between normal human retinal cone density (from seven individuals between 27 and 44 years of age), displayed for a left eye in standard perimetric projection (Top) and the mean frequency of VGB induced visual field loss shown as a left eye as a function of spatial location in the 30-2 spatial grid of the HFA (Bottom). The incidence of visual field defect increases as a function of decreasing cone density. The retinal cone density map has been adapted from the data of Curcio *et al.* (1990).

Investigations using manual Goldmann Perimetry document a typical VGB associated field defect, as concentric constriction with no temporal sparing (Hardus *et al.*, 2000b; Kalviainen *et al.*, 1999a). Their results suggest that manual kinetic perimetry is a relatively insensitive technique for visual field investigation, as it fails to detect the subtle abnormalities which occur in the nasal visual field. Such findings are not surprising as investigations of glaucomatous eye disease have shown that static perimetry is superior to kinetic perimetry at detecting small isolated areas of focal loss (Drance *et al.*, 1967; Lynn, 1969). Manual kinetic perimetry is capable of measuring field loss beyond the central 30 degrees (Hardus *et al.*, 2000b; Hardus *et al.*, 2001; Wild *et al.*, 1999a) but was not used in this study because of its inherent lack of sensitivity (Drance *et al.*, 1967; Lynn, 1969). Automated static perimetry should therefore be used when investigating patients undergoing VGB treatment.

3.6.2. Comparison between classifications

The classification designed by Wild *et al.* (1999a) has the advantage of producing a clinical diagnosis for each visual field examination. However, the results in Tables 3.6 and 3.7 indicate that such a nominal classification may lead to erroneous diagnoses. In terms of quantifiable loss there appears to be little distinction between patients diagnosed with mild visual field loss and patients diagnosed with severe. Practitioners that use the nominal classification may incorrectly presume progression of visual field loss has occurred through minor changes in threshold sensitivities. A patient's classification may change from a diagnosis of mild visual field loss to a diagnosis of moderate visual field loss, through relatively minor changes in threshold sensitivity at one visual field location. Using the severity algorithm, it is possible to derive a numerical cut-off for differentiating abnormal visual fields from normal visual fields. However this type of analysis should be used in conjunction with a quantitative key used to ensure that practitioners are aware of the true progression which has occurred. Analyses of a larger cohort of VGB-treated patients would enable statistically significant bandings differentiating between early, moderate or severe defects.

3.6.3. Correlation between VGB therapy and visual field loss

Within the present study the only factor to reach statistical significance with severity of visual field loss was maximum VGB dose. This correlation is important in light of VGB's pre-clinical success for treating substance abuse of alcohol, cocaine and nicotine (Gerasimov *et al.*, 2000; Schiffer *et al.*, 2000; Schiffer, Marsteller, & Dewey, 2003). VGB works through decreasing dopamine (DA) levels resulting in a diminished response to the many drugs, which are known to elevate DA in the mesocorticolimbic system (Schiffer *et al.*, 2000). Schiffer *et al.* (2003) concluded that sub-chronic low dose VGB (50mg/kg per day) potentiates and extends the

inhibition of cocaine induced increases in DA, when compared against larger doses of VGB. These findings suggest that VGB might be less dangerous for treating patients with substance abuse, as the smaller treatment doses should reduce the risk of severe visual field defects.

It is important to remember that the correlation between severity of visual field loss and maximum VGB dose is a trend, which accounts for a proportion of the variance within the model and other risk factors are necessary to explain the complete relationship. Pre-existing ischaemia might also be linked to the severity of visual field loss, as previous evidence suggests that ocular blood flow is reduced in patients receiving VGB (Hosking *et al.*, 2003; Roff Hilton *et al.*, 2002). Other possibilities include concomitant AEDs and their systemic interactions or the catabolism of VGB. Unfortunately, small participant numbers and the diversity of medication have meant that an investigation between severity of defect and concomitant medication was not possible in this study. However, the majority of literature suggests that concomitant medication is not correlated with severity of defect (Hardus *et al.*, 2000b; Hardus *et al.*, 2001; Wild *et al.*, 1999a). The only exception was reported by (Arndt *et al.*, 1999) who postulated that a combination of Valporate (VPA) and VGB led to increased retinal toxicity. Their initial postulation was based on two patients (Arndt *et al.*, 1999) and later confirmed by a larger study (Arndt *et al.*, 2002).

The link between cumulative VGB dose and severity of field loss is equivocal. A number of other studies have documented, both significant relationships (Hardus *et al.*, 2001; Manucheri *et al.*, 2000) and null effects (Kalviainen *et al.*, 1999a; Newman *et al.*, 2002; Nicolson *et al.*, 2002; Nousiainen *et al.*, 2001; Wild *et al.*, 1999a) between cumulative VGB dose and severity of visual field loss. All previous investigations of VGB treatment and visual field loss have failed to include maximum VGB dose as an independent variable. In these studies it is unclear which proportion of each significant relationship with cumulative VGB dose was due to its shared variance with maximum VGB dose. The results from this study suggest that cumulative dose does indeed share some of its predictive power with the other variables. Independently however, this particular risk did not reach statistical significance. This finding implies that different conclusions may have been found if the earlier studies (Hardus *et al.*, 2001; Manucheri *et al.*, 2000) were repeated, including maximum dose as an independent variable.

Although gender was not correlated with the severity of visual field loss, a number of other studies have reported a preponderance of visual field defects in male patients (Hardus *et al.*, 2000b; Hardus *et al.*, 2001; Nicolson *et al.*, 2002; Wild *et al.*, 1999a). These findings could be partly explained by the statistical analyses used in these studies, which failed to account for differences in drug treatment regimes between the genders (Nicolson *et al.*, 2002; Wild *et al.*, 1999a). Adopting an inappropriate statistical analysis could also explain some of the ambiguous

findings reported for the duration of VGB treatment. Hardus *et al.* (2001) concluded that the duration of VGB treatment was not significantly correlated with the severity of field loss, after they included cumulative VGB dose as an independent variable. In an earlier investigation, by the same group, a significant correlation was reported (Hardus *et al.*, 2000b).

The relationship between severity of field loss, and either cigarette smoking or mean daily VGB dose has not been investigated. Exploration of these variables is unfeasible, as the majority of those patients who smoked (nine patients) varied the number of cigarettes smoked in a given day and for a large number of the patient sample, the VGB dose varied on a monthly basis.

3.7. Conclusions

Patients exposed to VGB should undergo automated static perimetry examinations in both eyes at regular intervals. After assessing the visual field examination for adequate reliability, they should be analysed using the severity algorithm described in this Chapter.

The severity algorithm:

- Produces a quantitative index of the defect based on both severity and location
- Weights locations which are most likely to be effected by VGB more strongly than those which do not, thereby reducing artifactual abnormalities in the visual field.
- The combined calculation emphasises defects mirror imaged in the contralateral eye, by adding the severity for the right and left eye together, which is a stronger indication of VGB induced visual field loss.
- Could be incorporated into the HFA as an additional statistical analysis, or adapted for use in other automated perimeters.

The pathophysiology behind VGB's toxicity is currently not understood. The results from this study suggest that VGB causes a toxic effect on the retina as the pattern of visual field loss appears to be correlated with the documented distribution of retinal cone density. If VGB damage is due to a retinal toxic effect, then the implication is that it should affect the entire retina. The achromatic nature of the stimulus and background used in standard automated perimetry may render it relatively insensitive for the investigation of the central visual field. More sensitive measures of retinal function may reveal abnormalities in the more central retina (See

Chapter 6). The manufacturer of VGB currently recommends that the highest dose of VGB should not exceed 3 g/day (Electronic Medicines Compendium 2003) because no additional efficacy is achieved beyond this level. Indeed, the findings from this study suggest that patients receiving larger doses of VGB are more susceptible to severe visual field loss. Clinicians should bear this in mind when future treatment guidelines are designed. Further research to investigate the complete mechanism surrounding the field loss is still necessary. It is advisable that future studies use a clearly defined investigation of the visual field consisting of strict inclusion criteria, accurate techniques for measuring threshold sensitivities, an assessment of patient reliability and a suitable algorithm for measuring the severity of visual field loss. Such a defined protocol should improve repeatability between studies allowing a more accurate comparison between results. Factors relating to VGB dosage should not be analysed in isolation, as their shared variance must also be included in any statistical analysis. VGB is primarily used as an add-on treatment and the patients treated with this drug are frequently treated with at least one other AED. Studies with significantly larger participant numbers are necessary if an accurate investigation of drug interactions, between VGB associated field loss and concomitant AEDs, is to occur.

4. Evaluation of the SITA algorithm in the visual field analysis of patients exposed to Vigabatrin.

Aim: To determine the between- and within-algorithm differences in perimetric sensitivity for the Full Threshold, the SITA Standard and the SITA Fast algorithm in a population of patients diagnosed with epilepsy and exposed to VGB therapy. To evaluate the clinical utility of all three algorithms in detecting visual field loss attributed to VGB therapy. **Methodology:** The sample comprised one randomly selected eye of 16 patients (mean age 39.3 years ±14.5 years) diagnosed with epilepsy and exposed to VGB therapy. The first visit was a familiarisation session and the results were not included in the subsequent analysis. At the second and third visit the test eye was examined with three algorithms (Full Threshold, SITA Standard and SITA Fast) using the Humphrey Field Analyser and Program 30-2. Repeated measures analysis of variance was used to determine whether there was any significant difference between the examination duration, MD or PSD as a function of algorithm type or the order of the visit (second or third). The pointwise group mean difference in sensitivity between- each pair of algorithms at the second visit and for a given algorithm between the second and third visit, for each of the 74 stimulus locations was calculated. The pointwise difference in threshold sensitivity for all patients for each pair of algorithms (between-algorithm) at the second visit and for a given algorithm at the second and third visit (within-algorithm), was calculated and expressed as a function of the reference algorithm. **Results:** The average examination duration for the Full Threshold algorithm was 937.1 seconds, for the SITA Standard algorithm 449 seconds and for the SITA Fast algorithm 279.4 seconds. This difference was found to be statistically significant between algorithms ($p < 0.001$). The group mean sensitivity (MS) for SITA Standard was 0.8dB higher and group MS for SITA Fast 1.6dB higher when compared to the Full Threshold algorithm. Between-algorithm comparisons revealed that in terms of both spatial location and threshold sensitivity, SITA Fast's threshold sensitivities were the least comparable to either Full Threshold or SITA Standard. Within-algorithm comparisons revealed that in terms of both spatial location and threshold sensitivity at the second visit that Full Threshold was the most repeatable algorithm. **Conclusions:** SITA Standard is the algorithm of choice for the clinical diagnosis of VGB-attributed field loss. The algorithm is considerably quicker than the Full Threshold algorithm, less vulnerable to fatigue and easier to perform. Patients with confirmed visual field loss who need to be identified for visual field progression are recommended to undergo perimetry using the Full Threshold algorithm, as the highest repeatability is expected to aid the detection of progression.

4.1. Introduction

Examination of epilepsy patients using perimetry has proven vital for the detection of abnormalities associated with VGB treatment. To date, no other test has been shown to be either as sensitive or as specific at detecting the visual field loss. Medical practitioners recommend that all VGB recipients be regularly tested with either Goldmann perimetry or white-white automated static perimetry (Kalviainen & Nousiainen, 2001; Wild *et al.*, 1999a). Goldmann perimetry is dependent on the technique of the perimetrist and, as a direct consequence there is little standardisation between patients and visits. White-white automated perimetry is believed to have greater uniformity and sensitivity when compared to Goldmann perimetry (Drance *et al.*, 1967; Heijl, 1976; Lynn, 1969), unfortunately, the longer examination time means that a significant proportion of patients are unable to complete the visual field examination.

In psychophysics, it is common to employ a staircase with many crossovers of the threshold in order to gain an accurate estimate of the threshold. In perimetry, this is not possible because the large numbers of stimulus locations which require threshold estimation would inevitably entail an impracticably long test duration. Therefore, in perimetry, abbreviated staircase procedures are employed. The Full Threshold algorithm, which utilises a 4-2 dB staircase, crossing the threshold twice, has gained widespread acceptance as the optimal staircase strategy in visual field examination. Using the Full Threshold algorithm, it is not uncommon for a visual field examination to take 13 minutes or longer to complete in each eye, which inevitably leads to patient fatigue and places a high demand on patient attention in order to gain clinically acceptable results. In the early 1990's a number of visual field testing algorithms were developed with the aim of reducing test time without loss in accuracy of threshold estimation. In the HFA, FASTPAC was developed, utilising a 3 dB staircase and a single crossing of the threshold. This algorithm resulted in significantly reduced examination times, of the order of a 40% reduction over the Full Threshold algorithm, but at the expense of an increase in the intra-test variability, defined by the short-term fluctuation (Flanagan *et al.*, 1993). Furthermore, simulation studies of FASTPAC have shown that the threshold is underestimated if the initial stimulus presentation is below threshold and overestimated if the initial stimulus presentation is above threshold (Glass, Schaumberger, & Lachenmayr, 1995). A full description of the Full Threshold and FASTPAC algorithms is provided in sections 1.11.8.1 & 1.11.8.3.

All of the methods for estimating the threshold described above assume that the psychometric function governing frequency-of-seeing is an increasing function. Additionally, these staircase procedures are non-parametric, since they do not require prior knowledge regarding the nature of the threshold response. Parametric methods of estimating the threshold require knowledge of the general form of the psychometric function which governs the probability of stimulus detection. In theory, they offer a reduced examination time but

without loss in accuracy. QUEST (quick estimation by sequential testing) (Watson & Pelli, 1983) and ZEST (zippy estimation by sequential testing) (King-Smith *et al.*, 1994) are examples of parametric methods of threshold estimation commonly used in psychophysical experiments. These methods are based upon maximum likelihood probability. After each stimulus presentation using the maximum likelihood method, the most likely estimate of the threshold is calculated and this becomes the intensity for the next presentation. The final estimate of the threshold is designated as the most likely value of the threshold calculated after the last stimulus presentation. Vingrys & Pianta (1999) have described how a bimodal Probability Density Function (PDF) improves the efficiency of ZEST implementation for perimetry. They have argued that SITA's use of two PDFs complicates the decision-making process regarding termination and placement of stimulus intensity. In the late 1990's, parametric methods of estimating the threshold were applied to perimetry and a new generation of algorithms became commercially available, namely; SITA (Swedish Interactive Thresholding Algorithms)(Bengtsson & Heijl, 1998; Bengtsson *et al.*, 1997). The goal of SITA is a perimetric examination which significantly reduces the testing time without any reduction in accuracy. The algorithm is based on age-matched models of normal and glaucomatous visual field behaviour. Using posterior probability calculations the model changes and develops as the patient responds to each stimulus allowing a new estimated threshold to be presented and the staircase to continue. A full description of the method of threshold estimation using SITA algorithms can be found in sections 1.11.8.4 & 1.11.8.5.

SITA Standard and SITA Fast have already shown themselves to be sensitive algorithms in both normal (Bengtsson & Heijl, 1999a; Wild *et al.*, 1999c) and glaucomatous populations (Budenz *et al.*, 2002),(Sekhar *et al.*, 2000; Sharma *et al.*, 2000) and in consequence have replaced the Full Threshold and FASTPAC algorithms as the threshold strategies of choice for clinical visual field examination. Patients with compressed optic neuropathies and optic neuritis have nerve fibre bundle defects similar to glaucoma, both SITA algorithms should map the defects accurately. In patients where visual field loss does not conform to the pattern of visual field loss found in glaucoma, it could be argued that SITA may not be able to determine any visual field loss accurately, since the threshold modelling is based upon normal and glaucomatous models. Before the SITA strategies should be employed for clinical investigation of patients receiving VGB, it is vital to establish whether or not they are an efficient family of algorithms for this purpose.

4.2. Aim

To determine the between- and within-algorithm differences in perimetric sensitivity for Full Threshold, SITA Standard and SITA Fast algorithm in a population of patients diagnosed with epilepsy and exposed to VGB therapy. To evaluate the clinical utility of all three algorithms in detecting visual field loss attributed to VGB therapy.

4.3. Methodology

4.3.1. Patients and inclusion criteria

Twenty-two patients: 12 females and 10 males (mean age 38.5 years; ±13 5 years: range 16 to 61), previously diagnosed with epilepsy and who were either currently, or had previously received VGB, were invited to take part in the study. Inclusion criteria consisted of logMAR visual acuity of 0.1 or better (6/6 Snellen equivalent), distance refractive error of not greater than ±6.00 dioptres of sphere or ±2.5 dioptres of astigmatism, absence of intra-cranial pathology which may effect the visual pathway or any known ocular pathology which was unrelated to VGB therapy.

4.3.2. Ethical approval and informed consent

Written informed consent was obtained from all the patients. A detailed drug history was obtained from their hospital notes after requesting permission from the patient and their hospital consultant physician (see section 2.3).

4.3.3. Experimental procedures: visual fields

Each patient attended for three visits in order to complete the study. At the first visit patients completed one visual field on each eye using white-white automated static perimetry with the Humphrey Field Analyser (Carl Zeiss Ltd, Hertfordshire, UK); Program 30-2, Full Threshold algorithm, Goldmann stimulus size III, stimulus duration 200 ms. The HFA model 750 (software version A10.2.) was employed and the head tracking option enabled. The results from this visit were not included in the subsequent data analysis in order to reduce any possible bias induced by the perimetric learning effect (Wood *et al.*, 1987). One randomly selected eye of each patient was then assigned to one of four randomised protocols which determined the order of perimetric examination for the remaining visits (Table 4.1). The study's unconventional order protocol was chosen in an attempt to produce equal fatigue within all three algorithms by ensuring each session produced similar examination durations.

Protocol	First Session	Rest Period	Second Session
A	Full Threshold	30-minutes	SITA Standard, SITA Fast
B	Full Threshold	30-minutes	SITA Fast, SITA Standard
C	SITA Standard, SITA Fast	30-minutes	Full Threshold
D	SITA Fast, SITA Standard	30-minutes	Full Threshold

Table 4.1. Protocol illustrating the four randomly-assigned sequence options of perimetric examination.

At the second and third visit the test eye was examined with three algorithms (Full Threshold, SITA Standard and SITA Fast) using the Humphrey Field Analyser, Goldmann stimulus size III and Program 30-2. For each patient, the order of the visual field examination and the eye assigned remained constant over the two visits. Each session of the visual field examination was separated by a 30-minute rest period to minimise the influence of patient fatigue (Hudson *et al.*, 1994). In addition, rest periods were given to patients during each individual visual field examination when required. Fixation losses of less than 20% using the Heijl-Krakau method (Heijl & Krakau, 1975) and false positive and negative catch trials of less than 33% were employed to ensure reliability of patient responses. If any patient fell outside these reliability criteria, they were re-examined on a different day. If they failed to meet the reliability criteria at this visit, they were removed from subsequent analysis.

4.4. Analysis

The visual field data for all left eyes was inflected into right eye format in order to facilitate data analysis, and for all visual fields, the two stimulus locations immediately above and below the blind spot were removed from the analysis. The pointwise group mean threshold sensitivity and the associated standard deviation (SD), for the Full Threshold, SITA Standard and SITA Fast algorithms, for each of the 74 stimulus locations was determined.

4.4.1. Global analysis

One-way analysis of variance (between-subject) was used to determine whether there was any significant difference between mean deviation (MD) and pattern standard deviation (PSD), in any of the three algorithms resulting from the various sequence options of perimetric examination. Repeated measures analysis of variance was used to determine whether there were any significant differences between the examination duration, MD or PSD as a function of algorithm type or the order of the visit.

4.4.2. Sensitivity and specificity analysis

All visual fields in visit two were classified as either normal or abnormal, using criteria which were specifically designed for the interpretation of VGB-attributed visual field loss (Wild *et al.*, 1999). This criterion was based on over 25 spontaneous consecutive reports of visual field loss attributed to VGB and 63 patients from an open label extension trial, making the study one of the largest investigations of visual field loss attributed to VGB to date. This classification was applied to all visual field tests within the present study to produce a distribution of defects, by patient, for Full Threshold, SITA Standard and SITA Fast. The classification designed in Chapter 3 was not employed because a significant number of patients in the present study were used to derive the classification (Table 4.2). Sensitivity and specificity was calculated for both SITA algorithms with respect to the Full Threshold algorithm, which was assigned as the "gold standard" algorithm, for the detection of VGB-attributed visual field loss. Full Threshold was assigned the "gold standard" algorithm as it is the most widely used algorithm for investigating VGB-attributed field loss. Sensitivity was defined as the proportion of diseased individuals (as classified by the Full Threshold algorithm) that were identified as diseased individuals by the SITA Standard and the SITA Fast algorithm. Specificity was defined as the proportion of non-diseased individuals (as classified by the Full Threshold algorithm) who were identified as non-diseased by the SITA Standard and the SITA Fast algorithm.

4.4.3. Spatial analysis

The pointwise group mean difference in sensitivity, between each pair of algorithms at the second visit and the associated SD, for each of the 74 stimulus locations was determined. Similarly, the pointwise group mean difference in sensitivity, between the second and third visit for each algorithm and associated SD, for each of the 74 stimulus locations was determined. This analysis enabled a sensitivity comparison of the differences, within- and between-algorithms in terms of their spatial location.

Patient	Chapter 3	Chapter 4	Chapter 6	Chapter 8
1	✓		✓	✓
2				
3	✓		✓	✓
4	✓			
5	✓			
6	✓	✓		
7	✓			✓
8	✓	✓	✓	
9	✓		✓	
10	✓			
11	✓		✓	
12	✓		✓	✓
13	✓	✓		
14	✓	✓	✓	✓
15	✓			
16	✓		✓	
17	✓			
18	✓	✓		✓
19	✓	✓		
20	✓	✓		
21	✓	✓	✓	
22	✓			
23	✓	✓		
24	✓	✓		
25	✓		✓	
26	✓		✓	✓
27	✓		✓	✓
28	✓	✓	✓	
29	✓		✓	
30	✓		✓	✓
31	✓		✓	
32	✓			
33		✓	✓	✓
34		✓		
35		✓		
36		✓	✓	✓
37		✓	✓	✓
38			✓	✓

Table 4.2. Table showing the number of patients exposed to VGB who participated in each study.

4.4.4. Threshold Analysis

The 10th, 50th and 90th percentiles of the difference between each pair of algorithms at the second visit (between-algorithm) and the difference between each given algorithm at the second and third visit (within-algorithm), as a function of the threshold sensitivity of the reference algorithm at each stimulus location was calculated for all patients (Wild *et al.*, 1999b). This analysis was repeated for the Total Deviation sensitivities.

4.5. Results

Following the strict inclusion criteria, it was necessary to remove two patients who had visual field loss not attributed to VGB. Another two patients were removed because they yielded poor patient reliability, defined by fixation losses and false positive and negative catch trials. Consequently, the results of the remaining 16 volunteers were analysed: 10 females and six males (mean age 39.3 years; ±14.5 years: range 18 to 61). All visual fields were within the reliability criteria of <33% false positive and negative catch trials and <20% fixation losses. The average time between the first and second visits was 11.4 days ± 5.5 days. The average time between the second and third visits was 10.4 days ± 9 days. Patient's concomitant medication other than VGB is presented in Table 4.3.

The pointwise group mean sensitivities and the SDs, for each threshold algorithm, at each of the 74 stimulus locations are presented in Figures 4.1 to 4.3. The pointwise group mean sensitivities were greatest in magnitude for the SITA Fast algorithm, followed by the SITA Standard algorithm and then the Full Threshold algorithm. The group mean sensitivity (MS) for SITA Standard algorithm was 0.8 dB higher than that for the Full threshold algorithm. The group mean (MS) for SITA Fast algorithm was 1.6 dB higher than that for the Full threshold. Between-subject variability expressed by SDs were fairly similar between all three algorithms. Standard deviations were largest within the locations most frequently affected by VGB treatment (See section 3.5.1).

4.5.1. Global analysis

Group mean values for MD and PSD and their associated SDs for the four randomly-assigned sequence options of perimetric examination are given in Table 4.4. The results from six separate (between-subject) one-way analyses of variance showed that the algorithm order was not significant, for either the MD or PSD at the second visit (Table 4.5). Group mean values for (MD, PSD and examination times) and their associated SDs for each algorithm at the second and third visit are presented in Table 4.6. A repeated measures analysis of variance (Table 4.7) revealed that neither variable had an effect on PSD. However, algorithm type was found to have an effect on MD. A significant effect was also found between examination duration and algorithm type. On average SITA Standard was 52.1% faster than the Full Threshold algorithm and SITA Fast was 70.2% faster than the Full Threshold algorithm.

Patient number	Carbamazepine	Sodium Valporate	Clobazam	Levetiracetam	Topiramate	Lamotrogine	Phenytoin	Gabapentin	Other
1							X		X
2	X	X	X			X		X	X
3						X			X
4									
5		X		X					
6	X							X	
7	X			X					
8	X				X				
9						X			
10	X			X					
11			X			X			
12	X								
13	X	X				X	X		X
14				X					
15	X	X					X		
16			X			X		X	

Table 4.3. Concomitant epileptic medication (other than VGB).

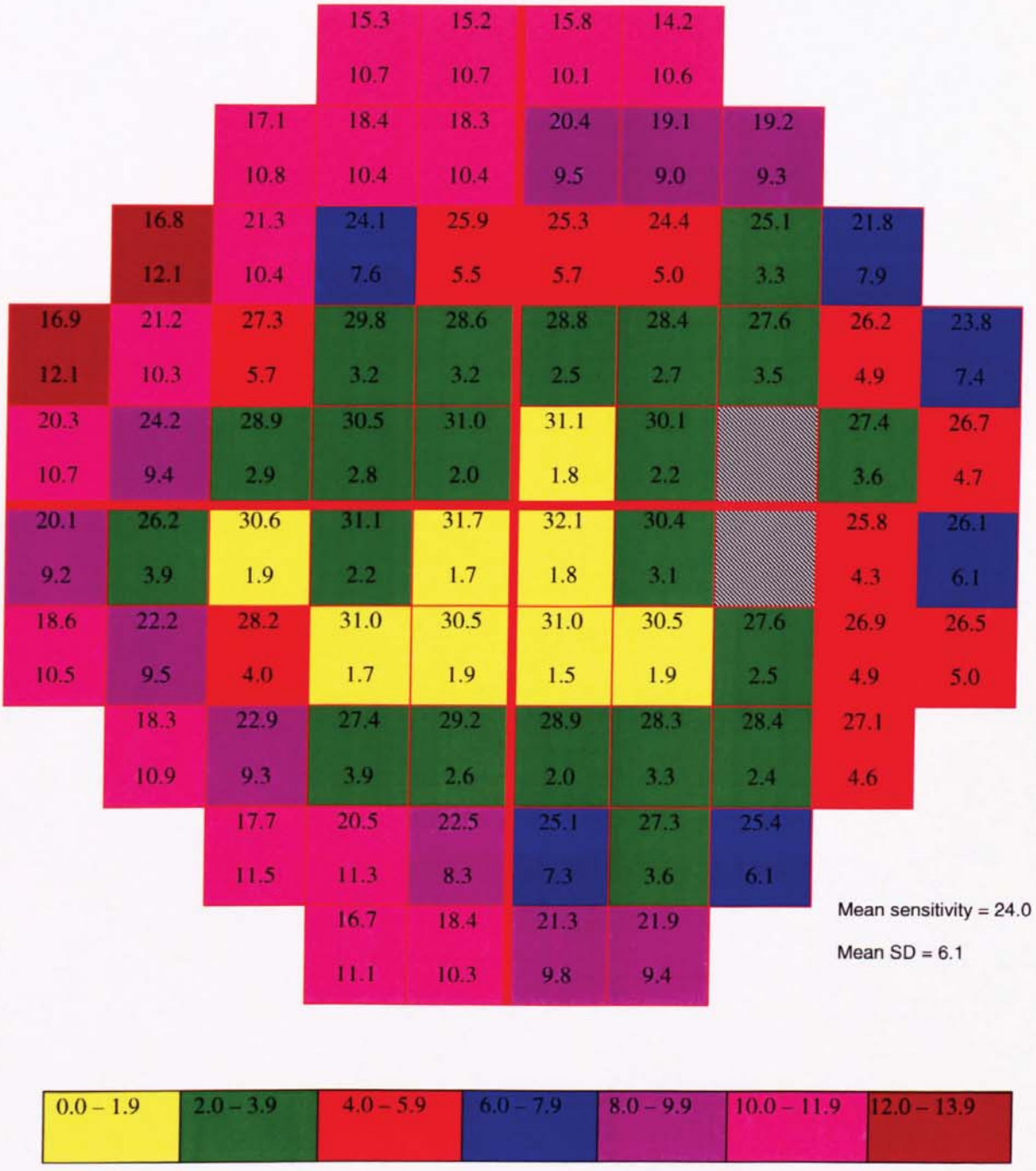

Figure 4.1. Schematic visual field plot showing the group mean sensitivity and the SD (colour coded key) for Full Threshold (dB) at each of the stimulus locations on the second visit.

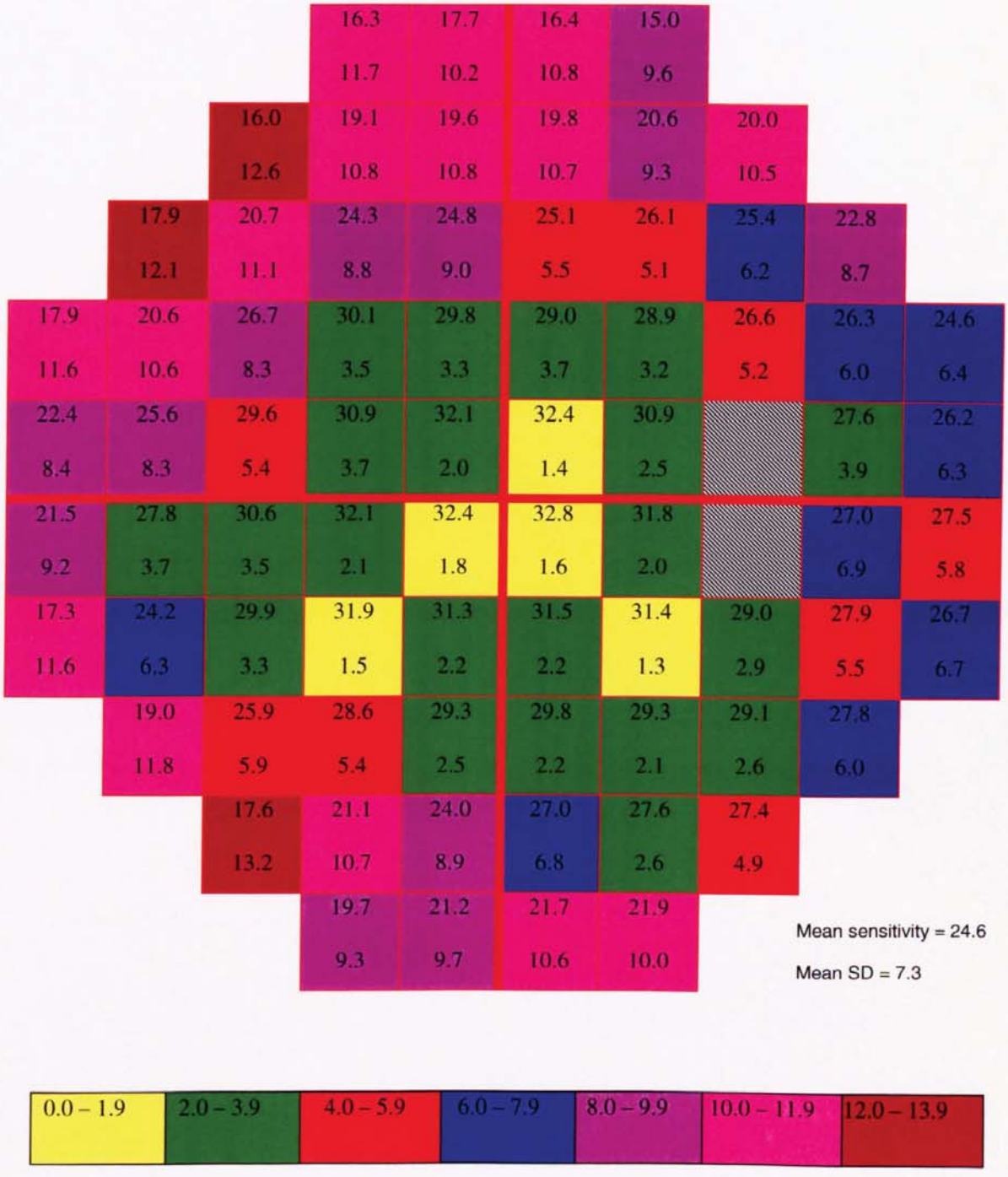

Figure 4.2. Schematic visual field plot showing the group mean sensitivity and the SD (colour coded key) for SITA Standard (dB) at each of the stimulus locations on the second visit.

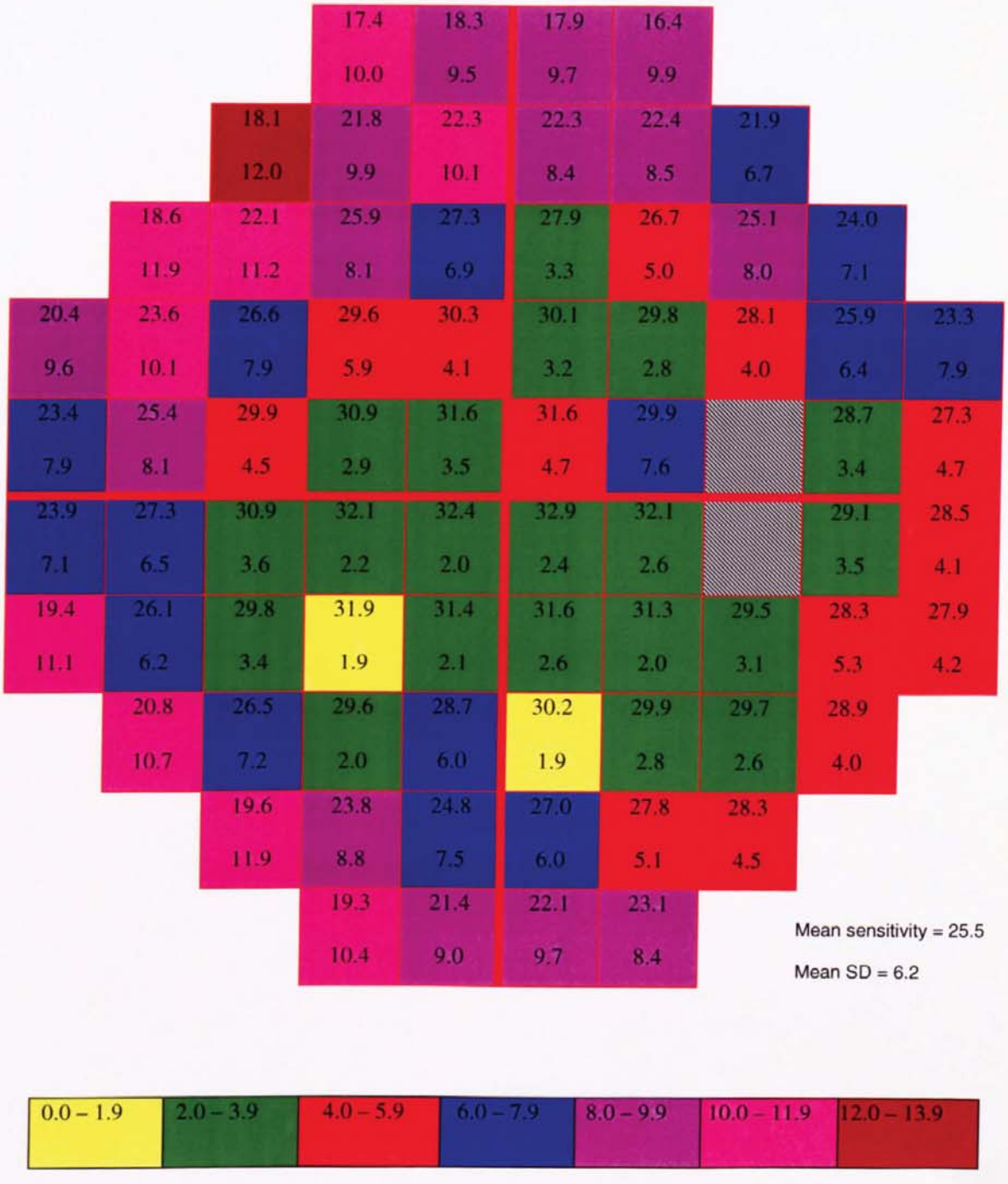

Figure 4.3. Schematic visual field plot showing the group mean sensitivity and the SD (colour coded key) for SITA Fast (dB) at each of the stimulus locations on the second visit.

Protocol	MD Full Threshold	MD SITA Standard	MD SITA Fast	PSD Full Threshold	PSD SITA Standard	PSD SITA Fast
A	-6.28 (4.71)	-6.76 (5.09)	-6.43 (5.13)	5.65 (4.90)	5.86 (4.61)	5.97 (5.66)
B	-3.31 (2.81)	-3.90 (3.11)	-3.57 (3.63)	4.88 (2.46)	4.97 (2.47)	5.18 (3.12)
C	-2.97 (4.00)	-3.79 (2.67)	-2.21 (2.25)	4.01 (3.71)	4.57 (4.24)	3.64 (3.16)
D	-4.29 (5.29)	-5.10 (4.56)	-4.44 (6.38)	4.05 (4.86)	4.05 (4.23)	3.96 (4.50)

Table 4.4. Table showing the group mean and standard deviation (in brackets) for MD and PSD, within each algorithm, as a function of the assigned sequence options of perimetric examination.

	Full Threshold	SITA Standard	SITA Fast
MD	p = 0.700	p = 0.708	p = 0.679
PSD	p = 0.933	p = 0.924	p = 0.866

Table 4.5. Table showing the results from one–way ANOVAs investigating whether the sequence of the algorithm was a significant factor to the MD or PSD of a specific test (Full Threshold, SITA Standard, SITA Fast) at the second visit.

	MD (dB)	PSD (dB)	Examination times (seconds)
Full Threshold visit 1	-4.24 (4.00)	4.70 (3.67)	937.06 (157.90)
Full Threshold visit 2	-4.89 (3.79)	4.89 (3.51)	956.63 (165.09)
SITA Standard visit 1	-4.89 (3.79)	4.89 (3.51)	449 (80.94)
SITA Standard visit 2	-5.06 (4.98)	4.95 (3.97)	464.13 (99.43)
SITA Fast visit 1	-4.25 (4.46)	4.78 (3.91)	279.38 (79.21)
SITA Fast visit 2	-4.34 (4.25)	4.63 (3.64)	282.34 (67.31)

Table 4.6. Table showing the group mean and standard deviation (in brackets) for MD, PSD and examination times for each algorithm at each visit.

	MD	PSD	Examination Time
Visit	p = 0.172	p = 0.847	p = 0.242
Algorithm	**p = 0.049**	p = 0.511	**p < 0.001**
Visit * algorithm	p = 0.665	p = 0.575	p = 0.545

Table 4.7. Table showing the results from repeated measures analysis of variance investigating whether the algorithm type or order of visit had a significant effect to either MD, PSD or examinations time.

Patient Number	Full Threshold	SITA Standard	SITA Fast
1	**Defect**	**Defect**	**Defect**
2	**Defect**	**Defect**	**Defect**
3	No defect	No defect	No defect
4	No defect	No defect	No defect
5	**Defect**	**Defect**	**Defect**
6	No defect	No defect	No defect
7	**Defect**	**Defect**	**Defect**
8	No defect	**Defect**	No Defect
9	No defect	No defect	No defect
10	No defect	No defect	**Defect**
11	**Defect**	**Defect**	**Defect**
12	No defect	No defect	**Defect**
13	No defect	No defect	No defect
14	**Defect**	**Defect**	No Defect
15	**Defect**	**Defect**	**Defect**
16	No defect	**Defect**	No defect

Table 4.8. Table showing the distribution of defects by patient for Full Threshold, SITA Standard and SITA Fast visual fields.

	SITA Standard	SITA Fast
Sensitivity	100%	85.7%
Specificity	77.8%	77.8%

Table 4.9. The sensitivity and specificity for SITA Standard and SITA Fast algorithms after assigning Full Threshold the "gold standard" for the detection of VGB-attributed field loss.

4.5.2. Sensitivity and specificity analysis

The distribution of defects, by patient, for Full threshold SITA Standard and SITA Fast is presented in Table 4.8. High sensitivity was found when SITA Standard and SITA Fast was compared against the current "gold standard" Full Threshold algorithm. Slightly reduced

specificity was found when either SITA algorithm was compared against Full Threshold. The results are presented in Table 4.9.

4.5.3. Spatial Analysis

Results for this analysis are presented in Figures 4.4 to 4.9. The between-algorithm group mean difference in sensitivity was greatest when Full Threshold was compared against SITA Fast (average mean of differences -1.6 dB) and the least difference was yielded when SITA Standard was compared against Full Threshold or SITA Fast (average mean of differences -0.8dB). Peripheral stimulus locations yielded the largest SDs. Between-visit comparisons revealed that the smallest between-visit variability was demonstrated by Full Threshold (average mean of differences –0.6dB) with both the SITA Standard (average mean of differences -0.8dB) and the SITA Fast algorithm (average mean of differences –0.7dB) producing more variability. These results indicate that Full Threshold results are the most reproducible.

4.5.4. Threshold Analysis

Results for this analysis are presented in Figures 4.10 to 4.13. Between-algorithm comparisons (Full Threshold versus SITA Standard, Full Threshold versus SITA Fast and SITA Standard versus SITA Fast) revealed that the percentile range was narrow for threshold sensitivities greater than 20 dB. For sensitivities less than 20 dB, the percentile range became wider and more variable, particularly when SITA Standard was compared against SITA Fast. Between-algorithm comparisons (Full Threshold versus SITA Standard and Full Threshold versus SITA Fast) showed that the 50^{th} percentile exhibited a negative value for the majority of threshold sensitivities, indicating that threshold sensitivities were comparatively higher within the SITA algorithms. However, after threshold sensitivities were adjusted for the normal variation of sensitivity that occurs with age i.e. the Total Deviation sensitivity, the 50^{th} percentile yielded a positive value, particularly when Full Threshold algorithm was compared against SITA Standard (Figure 4.11). Between-visit (within-algorithm) comparisons showed that the percentile range was narrow for threshold sensitivities greater than 20 dB, after which the range became wider and more variable particularly for the SITA Fast algorithm.

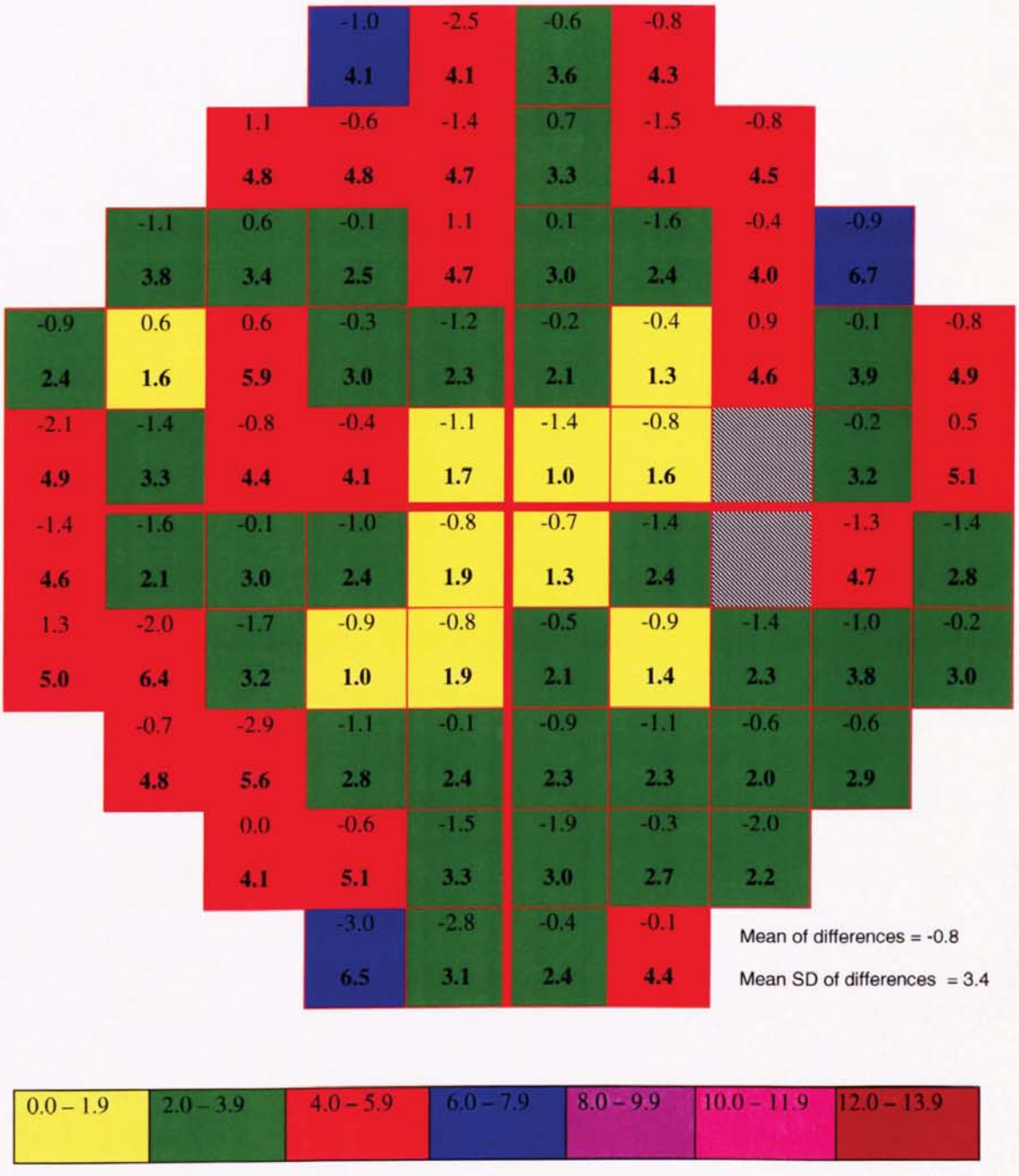

Figure 4.4. Schematic visual field plot showing the group mean difference in sensitivity and the SD (colour coded key) of the differences (bold) between Full Threshold visit two and SITA Standard visit two in dB at each of the 74 stimulus locations.

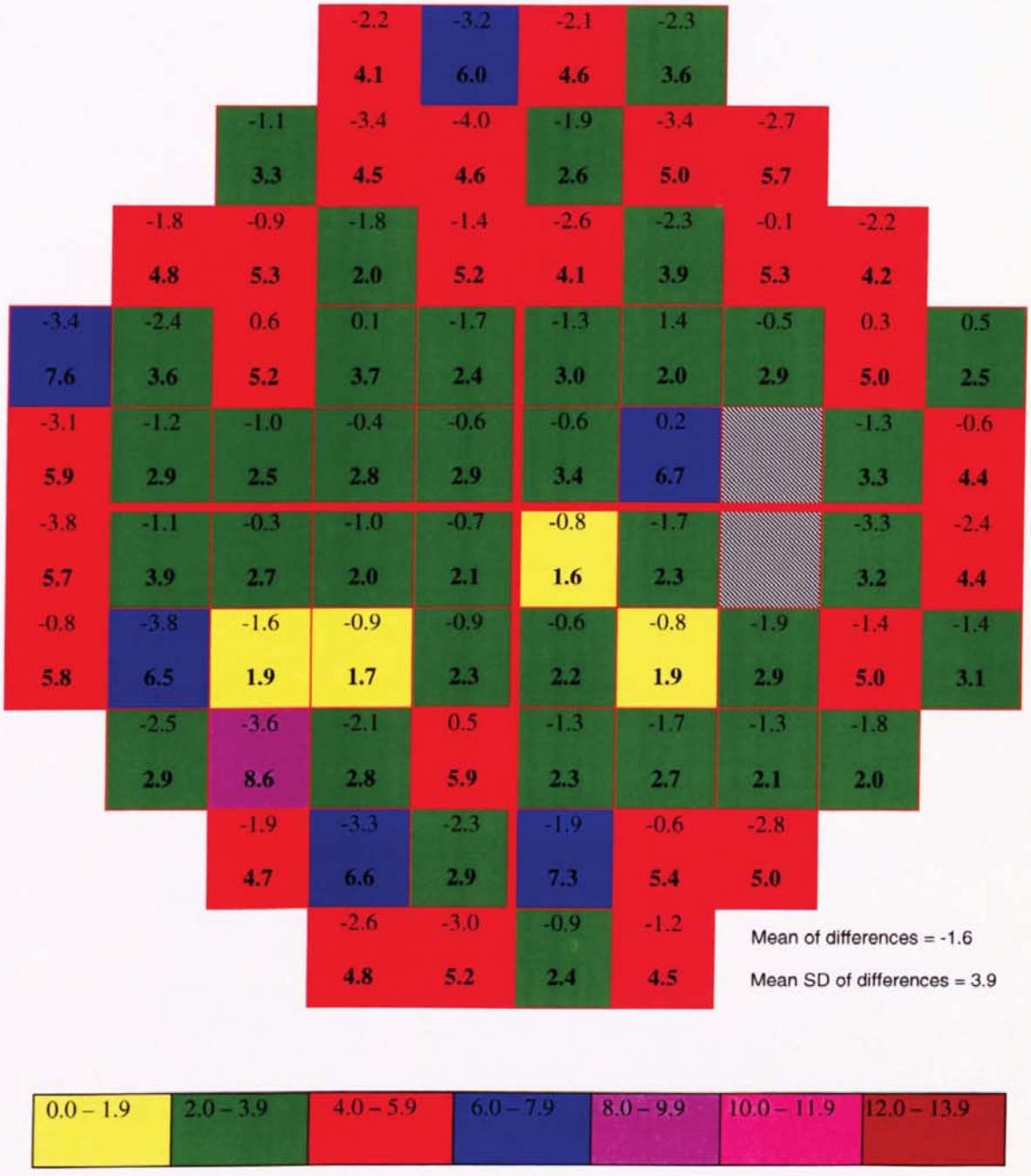

Figure 4.5. Schematic visual field plot showing the group mean difference in sensitivity and the SD (colour coded key) of the differences (bold) between Full Threshold visit two and SITA Fast visit two in dB at each of the 74 stimulus locations.

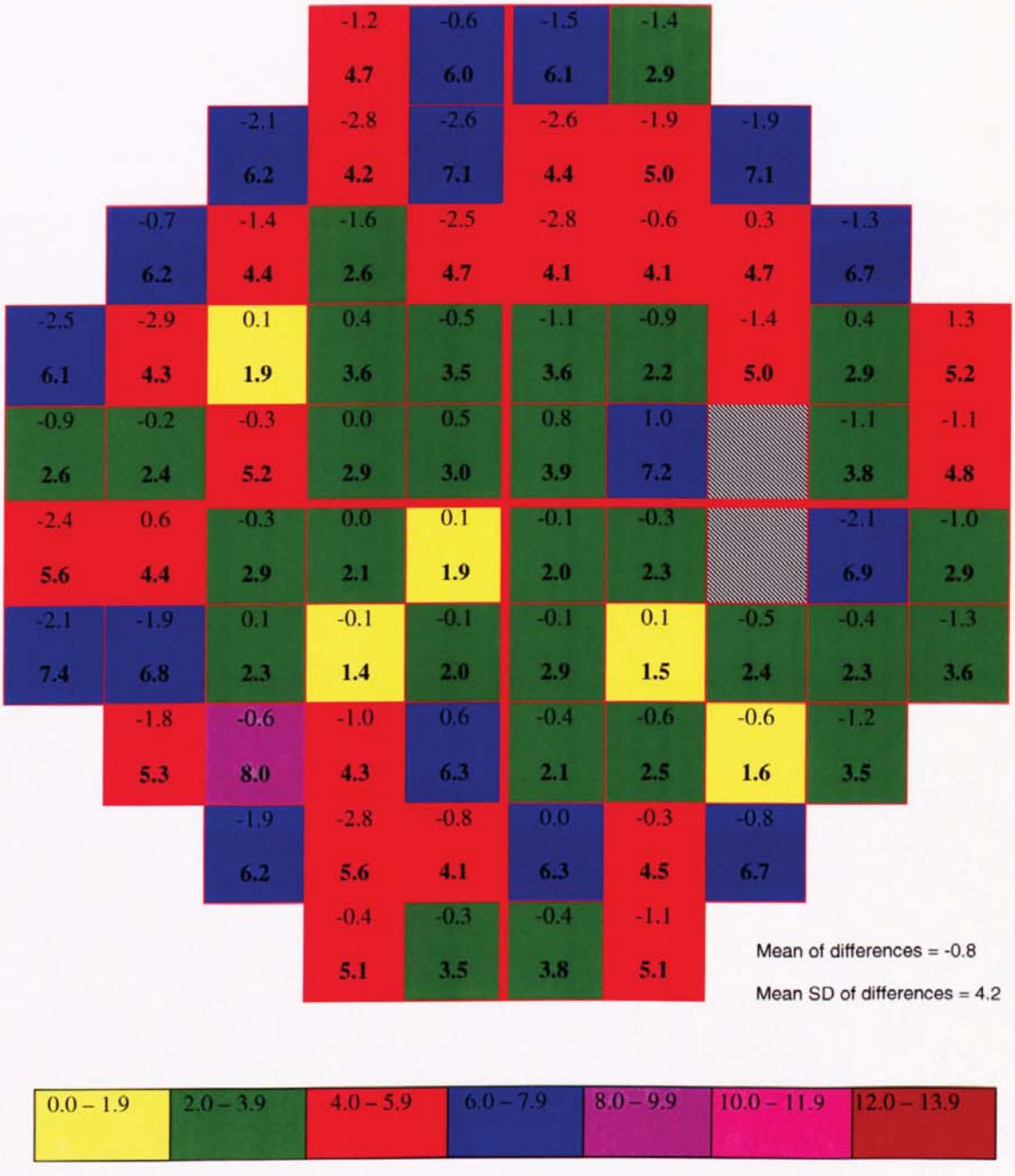

Figure 4.6. Schematic visual field plot showing the group mean difference in sensitivity and the SD (colour coded key) of the differences (bold) between Sita Standard visit two and SITA Fast visit two in dB at each of the 74 stimulus locations.

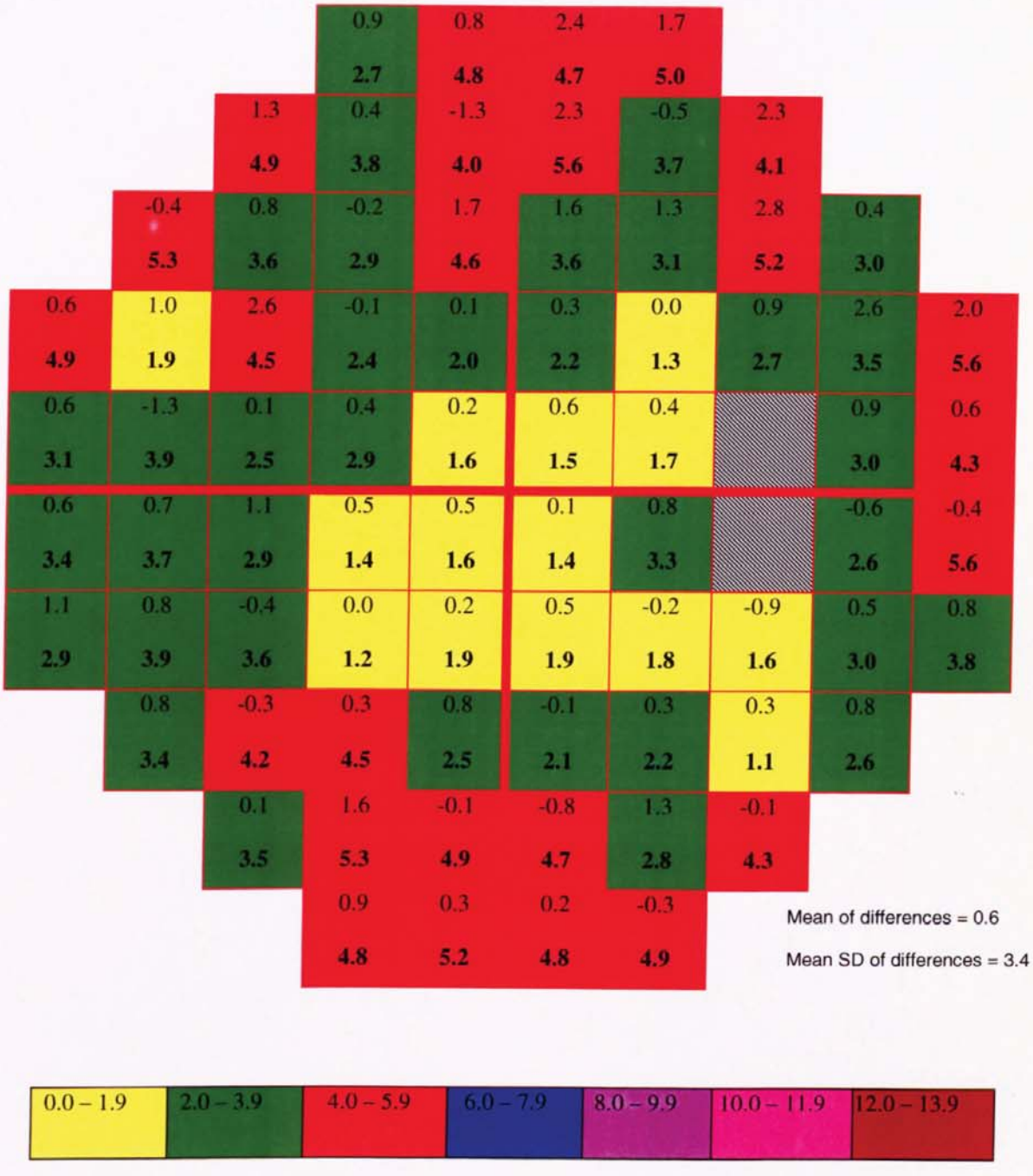

Figure 4.7. Schematic visual field plot showing the group mean difference in sensitivity and the SD (colour coded key) of the differences (bold) between Full Threshold visit two and Full Threshold visit three in dB at each of the 74 stimulus locations.

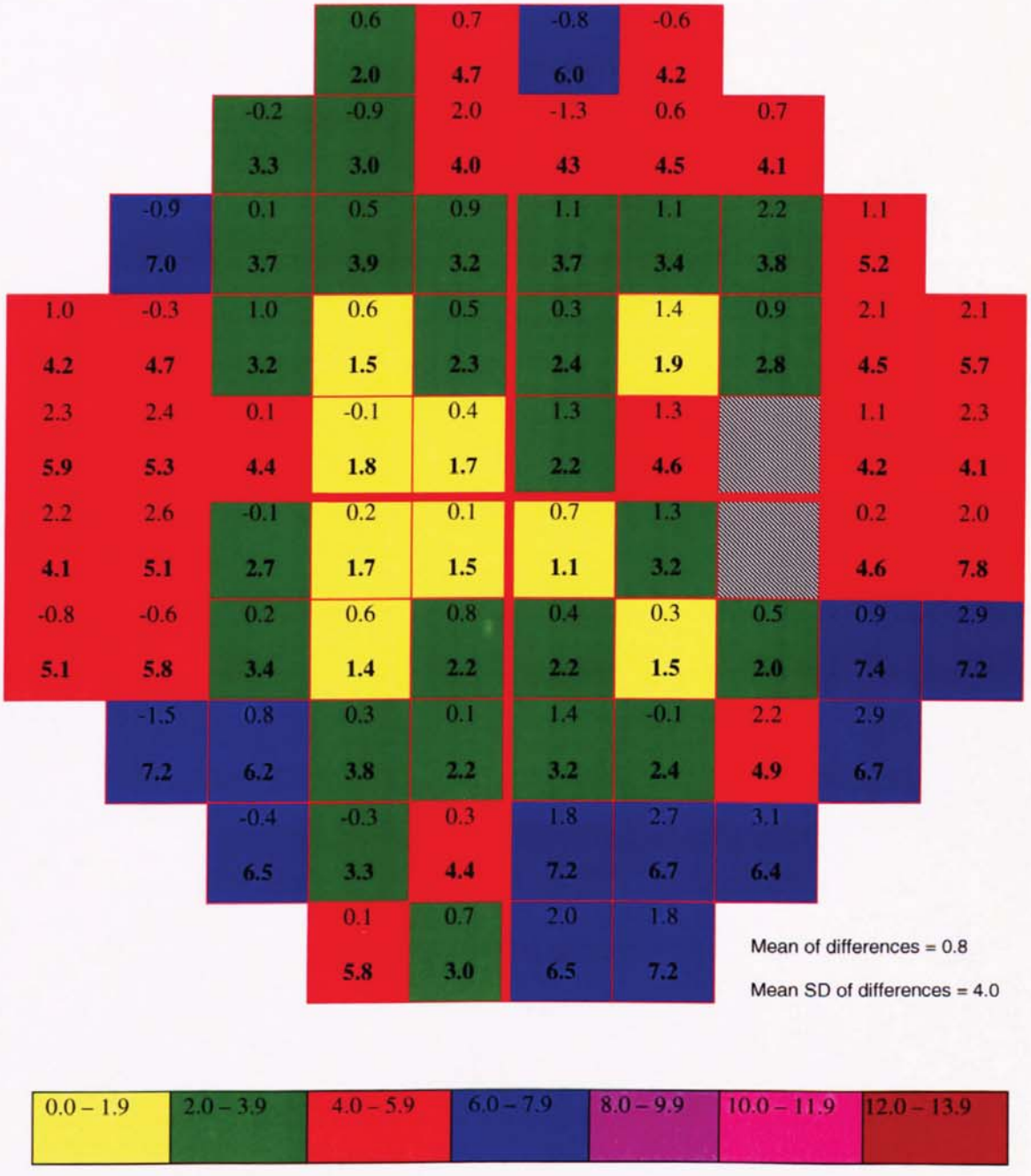

Figure 4.8. Schematic visual field plot showing the group mean difference in sensitivity and the SD (colour coded key) of the differences (bold) between SITA Standard visit two and SITA Standard visit three in dB at each of the 74 stimulus locations.

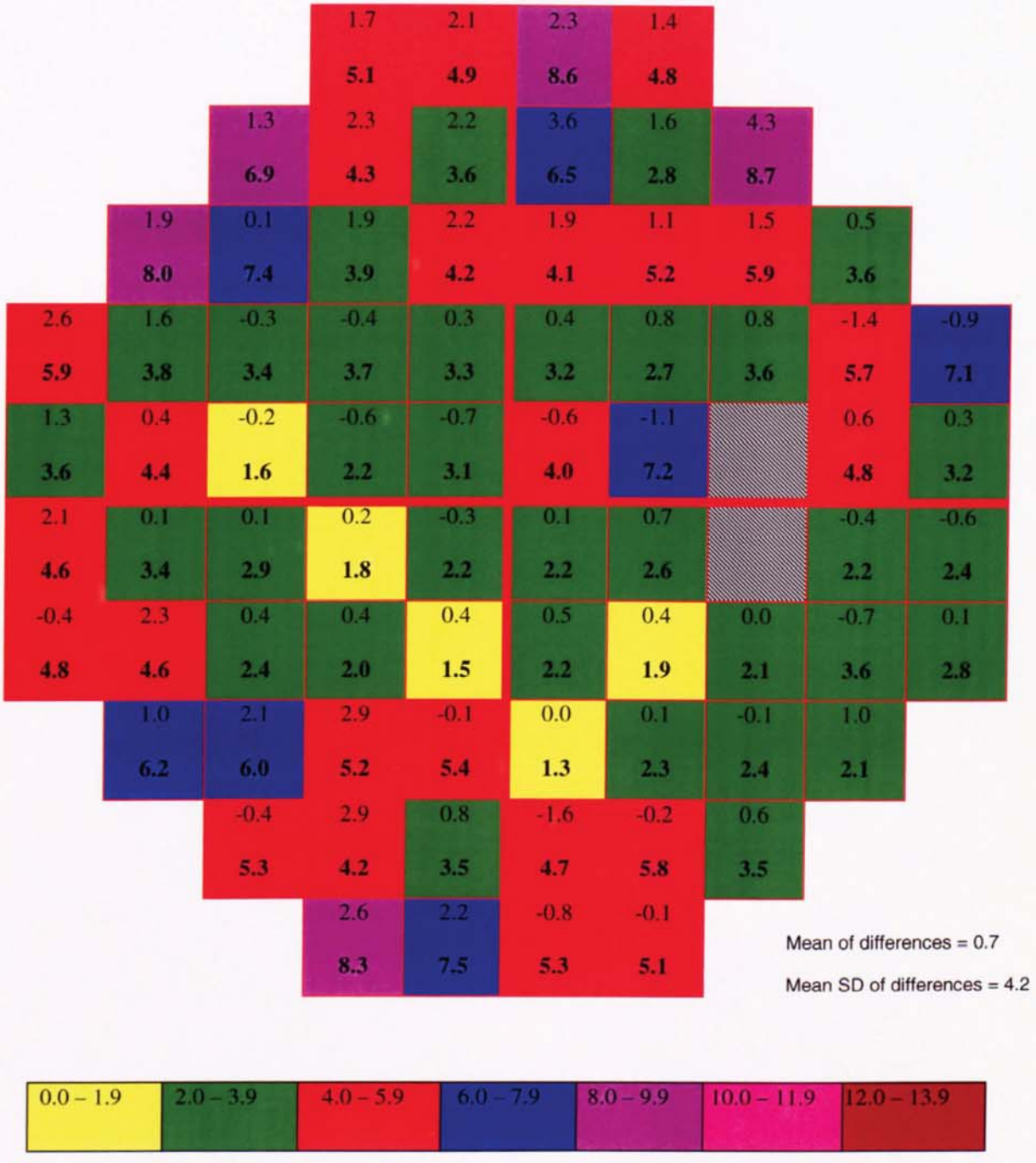

Figure 4.9. Schematic visual field plot showing the group mean difference in sensitivity and the SD (colour coded key) of the differences (bold) between SITA Fast visit two and SITA Fast visit three in dB at each of the 74 stimulus locations.

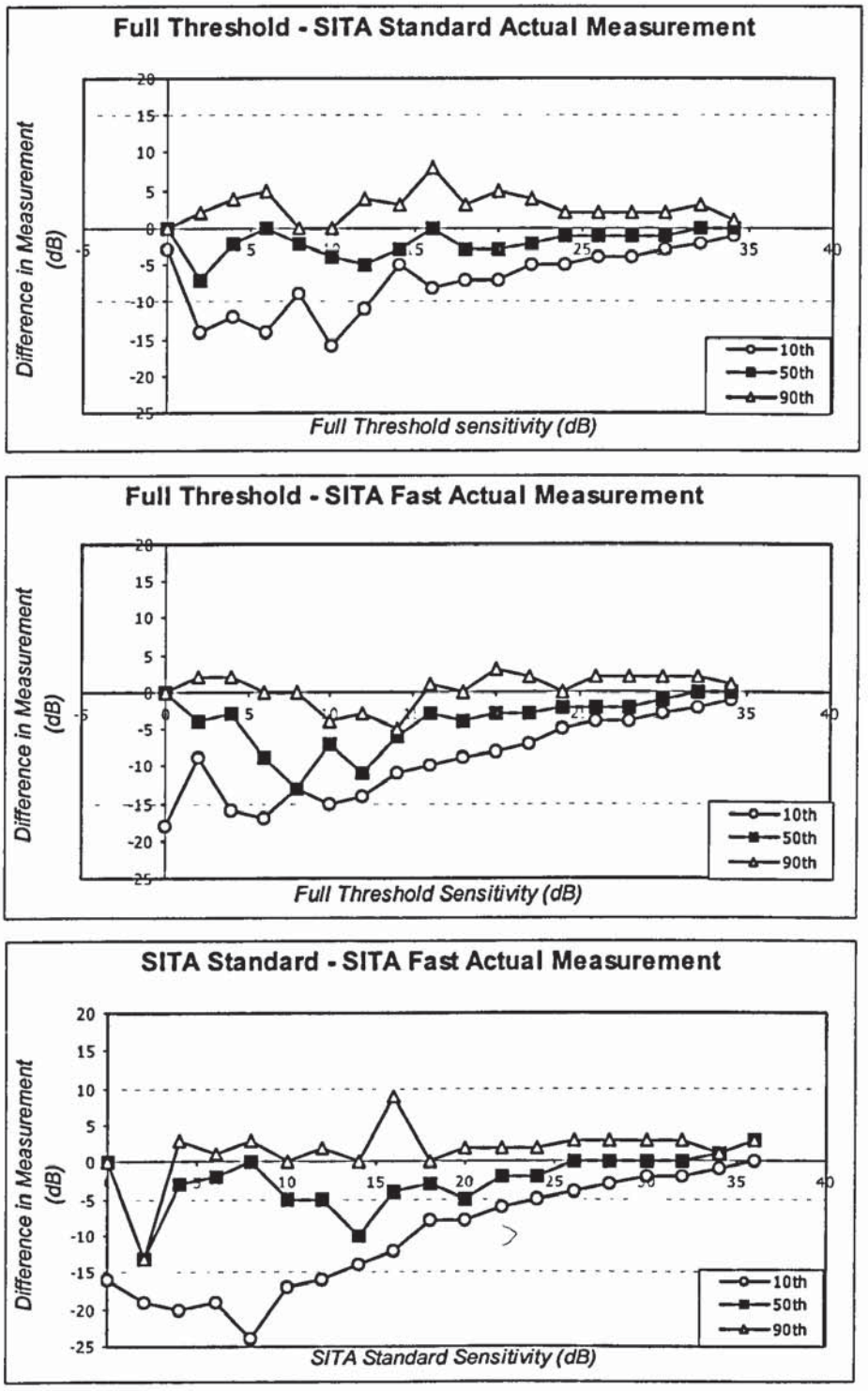

Figure 4.10. The 10th 50th and 90th percentiles of the distribution of the actual measurement (AM) differences in sensitivity across all locations between each pair of algorithms at the second visit as a function of the reference algorithm at the given location at the second visit for all patients.

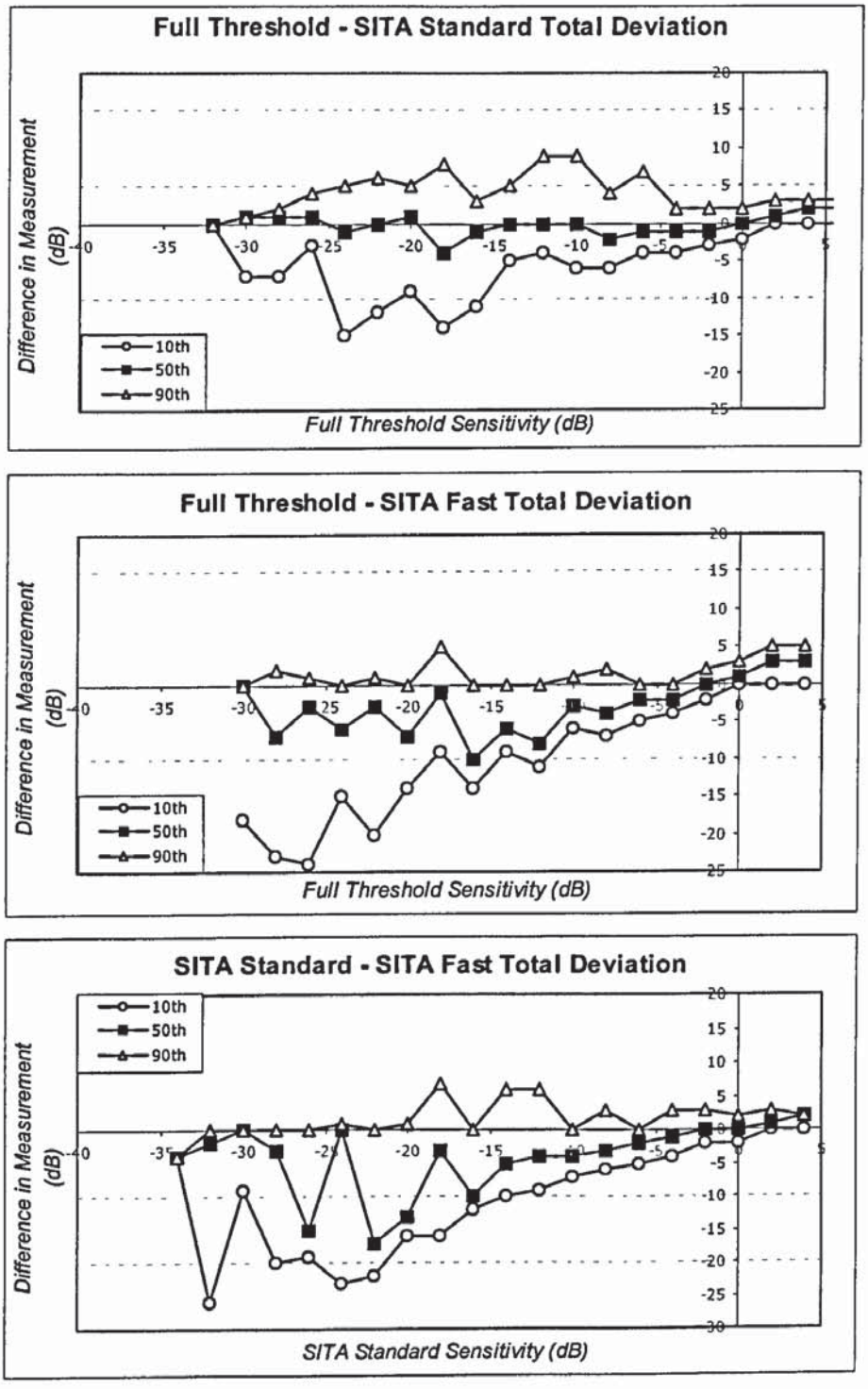

Figure 4.11. The 10th 50th and 90th percentiles of the distribution of the differences in Total Deviation (TD) sensitivity across all locations between each pair of algorithms at the second visit as a function of the reference algorithm at the given location at the second visit for all patients.

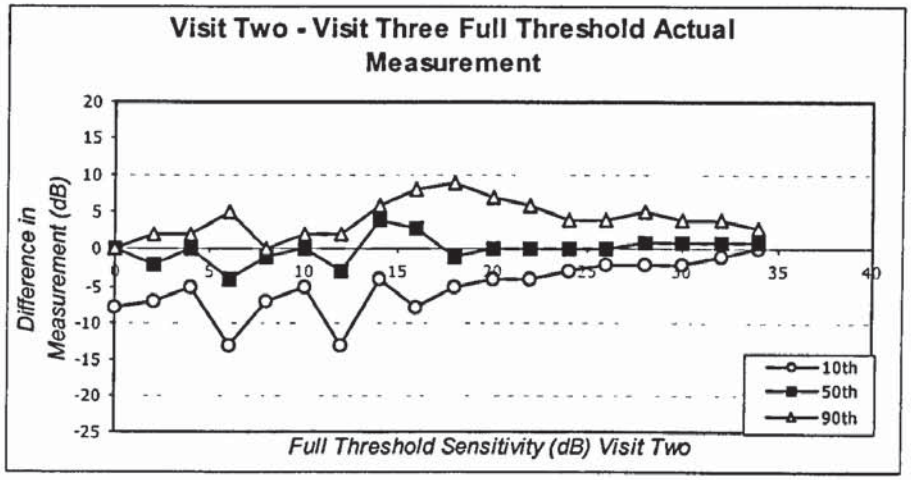

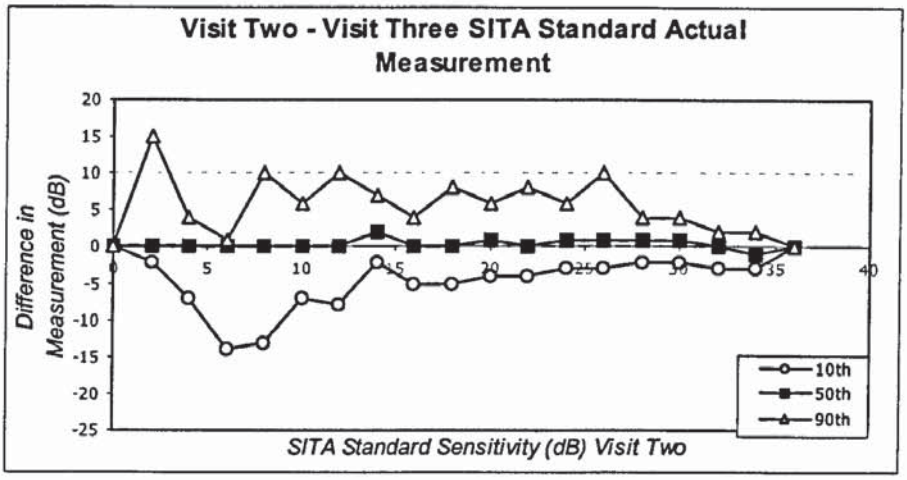

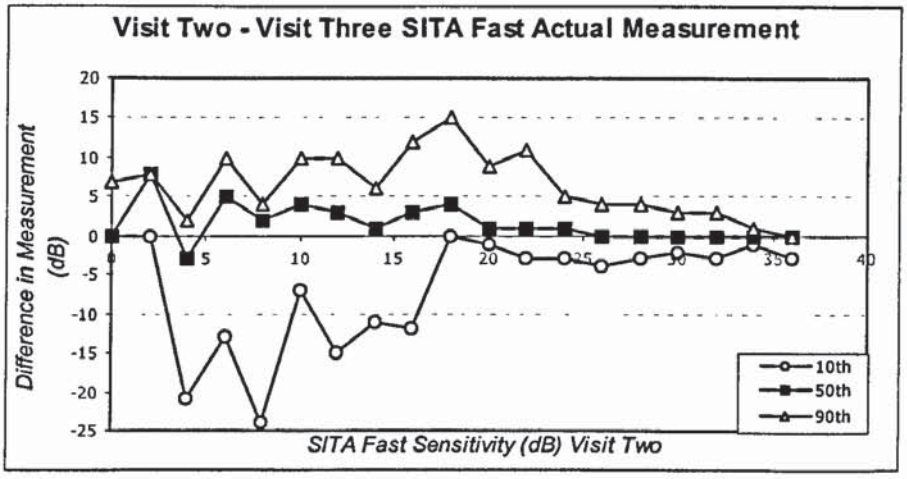

Figure 4.12. The 10th 50th and 90th percentiles of the distribution of actual measurement (AM) differences in sensitivity across all locations for a given algorithm between the second and third visit for all patients.

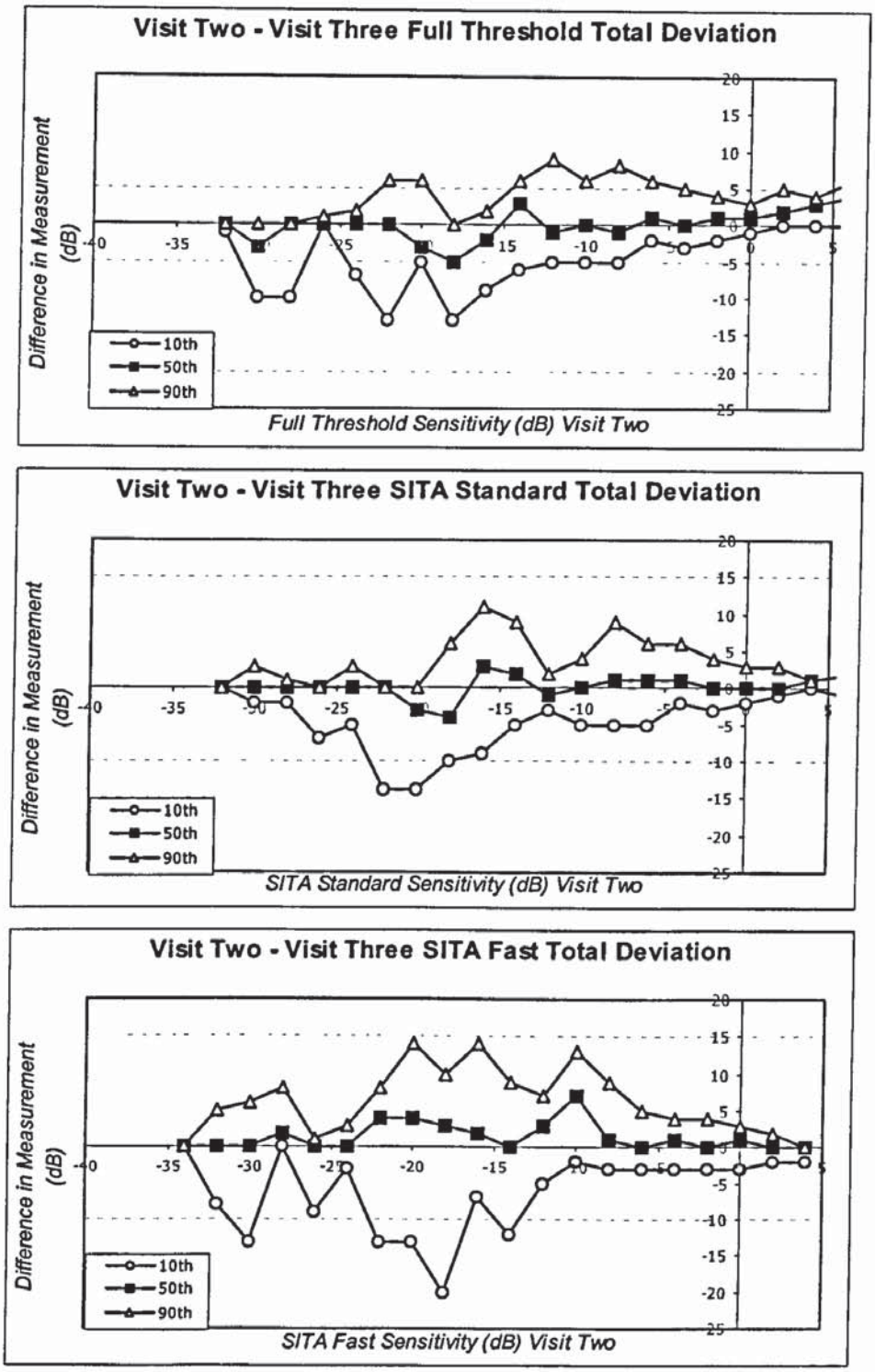

Figure 4.13. The 10th 50th and 90th percentiles of the distribution of Total Deviation (TD) differences in sensitivity across all locations for a given algorithm between the second and third visit for all patients.

4.6. Discussion

The group mean pointwise sensitivities, for SITA Standard were on average 0.8 dB greater and for SITA Fast 1.6 dB greater, than the Full Threshold algorithm. These results are concordant with findings in both normal (Bengtsson & Heijl, 1999a; Shirato *et al.*, 1999; Wild *et al.*, 1999c) and glaucomatous populations (Sharma *et al.*, 2000; Shirato *et al.*, 1999; Wild *et al.*, 1999b). The lower sensitivity of the Full Threshold algorithm could relate to a fatigue effect induced by the longer examination duration of the Full Threshold algorithm (Bengtsson & Heijl, 1999b; Wall *et al.*, 2001). Alternatively, the initial stimulus presentation intensity of SITA might also contribute to the higher overall sensitivities (Shirato *et al.*, 1999). The results from this study suggest that the latter hypothesis is more likely, as the order of the field tests was not significant to the overall threshold sensitivity within each algorithm. Furthermore, the protocol design of this study ensured that the duration of each examination was similar and therefore any fatigue effects would be expected to be comparable. The between-subject variability, when expressed as the SD of the group mean pointwise sensitivity, was similar for all three algorithms. This finding contradicts the trends in normal populations, which have reported narrower between-subject variations in both SITA strategies (Bengtsson & Heijl, 1999a; Wild *et al.*, 1999c). Nevertheless, the findings of this study are concordant with studies examining optic neuropathies and hemianopias, which report little difference after comparing the probability analysis data of SITA Standard and the Full Threshold algorithms (Wall *et al.*, 2001). The disparity between these findings and those of glaucomatous populations probably relates to the underlying design of the SITA algorithms which are optimised for glaucoma detection since they are based on models of normal and glaucomatous visual fields and do not specifically model neurological or toxicological damage to the visual field.

4.6.1. Global analysis

Investigations of glaucomatous eye disease have reported that SITA Standard yields a marginally greater group mean PSD than either Full Threshold or SITA Fast algorithms and that MD is more negative when a given algorithm is examined at the second visit (Wild *et al.*, 1999b). The results from this study would suggest that PSD does not vary significantly as a function of algorithm type or the order of the visit. MD does significantly alter as a function of algorithm type. Closer inspection of the averages for each algorithm across visits revealed that MD was slightly more negative for the SITA Standard algorithm. The reduced examination times of SITA compared with the Full Threshold algorithm are in accordance with the findings of others (Budenz *et al.*, 2002; Sekhar *et al.*, 2000; Wild *et al.*, 1999b), confirming improved clinical viability of the SITA algorithms.

4.6.2. Sensitivity and specificity analysis

In this study, both SITA strategies yielded high sensitivity when compared against the current "gold standard" Full Threshold algorithm. This finding confirms that of other studies of glaucoma patients where a sensitivity of greater than 95% has been reported (Budenz *et al.*, 2002). Nevertheless, it should be remembered that care must be taken when analysing the sensitivity or specificity of any technique, since the assumption that Full Threshold is the "gold standard" algorithm for the detection of VGB pathology may be incorrect. However, this analysis does allow a direct comparison to be made with the algorithm, which up until now has been considered the "gold standard". It is possible that the lower specificity indicates that both SITA algorithms are more sensitive than the Full Threshold algorithm in terms of diagnosing abnormalities. In fact, computer simulations of normal and glaucomatous visual fields have shown SITA Standard to be more accurate when compared with the Full Threshold algorithm (Bengtsson *et al.*, 1997).

4.6.3. Spatial analysis

Peripheral stimulus locations, particularly those most frequently damaged by VGB yielded the largest SDs, indicating that the greatest between subject variability occurred in this region. Results probably reflect in part the difference between patients with normal visual fields and those with VGB-attributed field loss and also the greater normal variation of threshold sensitivities at these peripheral locations (Katz & Sommer, 1986).The between-algorithm group mean difference was largest when SITA Fast was compared against the Full Threshold algorithm. This finding confirms that the threshold sensitivities of the SITA Fast algorithm are not comparable to those of the Full Threshold algorithm. Between-visit comparisons yielded the lowest variability for the Full Threshold algorithm. This finding suggests that in terms of reproducibility, the Full Threshold algorithm is the most accurate for delineating visual field loss induced by VGB.

4.6.4. Threshold analysis

Between- and within-algorithm comparisons showed that the percentile range became wider and more variable for threshold sensitivities below 20 dB. Wild *et al.* (1999b) reported similar results and concluded that the large variability might be explained by the small number of points for deviations within this range. This finding could also be explained by the hypothesis that the defects found in white-white automated static perimetry, associated with VGB therapy, are steeply bordered. It is reasonable to assume that large changes in the threshold, corresponding to the variability of the percentiles, could be induced by relatively minor head adjustments. Indeed short-term fluctuation is known to be higher in or around deeply bordered scotomas (Flammer *et al.*, 1984). This hypothesis could also account for the removal of two patients from the study. Patients were excluded because of their high false negative rate, even though their concentration levels appeared excellent. The head tracking

option was enabled, however as this procedure has not been clinically tested it was thought to be insufficient for discounting the present hypothesis.

The negative 50th percentile indicates that both SITA strategies produce higher threshold sensitivities when compared against the Full Threshold algorithm. Nevertheless, it is of importance to note that the negative trend disappears once threshold sensitivities were adjusted for age (Total Deviation values). This finding indicates that the negative trend is of little clinical significance, as any diagnosed abnormality should be based upon Total or Pattern Deviation plots.

The percentile range was greatest in magnitude and most variable when SITA Fast was compared with the Full Threshold or SITA Standard algorithm. These results are as expected since the SITA Fast algorithm was designed to be comparable to the FASTPAC algorithm and not to the Full Threshold or the SITA standard algorithms (Bengtsson & Heijl, 1998). Indeed the only difference in algorithm design between SITA Standard and SITA Fast is that the threshold determination procedure is terminated at a lower level of accuracy (defined by the standard error function) than that of SITA Standard in order to reduce the examination time of SITA Fast against that of SITA Standard (Bengtsson & Heijl, 1998). Within-algorithm comparisons yielded slightly greater between-visit variability for the SITA Fast algorithm than either the Full Threshold or SITA Standard algorithms, illustrating that the SITA Fast algorithm was the least repeatable algorithm in terms of threshold sensitivity. The Full Threshold algorithm showed the least between-visit variability indicating that this algorithm was the most repeatable in terms of the threshold sensitivity.

4.7. Conclusions

The choice of algorithm used in perimetry is a compromise between the speed of the test and its repeatability. Increased examination times could lead to a degradation in the quality of the data due to patient inattention and fatigue (Hudson *et al.*, 1994). Such reduced repeatability makes it difficult to decide when true visual field progression has occurred. SITA Fast offers the most profound reduction in examination duration, followed by SITA Standard and Full Threshold. The Full Threshold algorithm showed highest repeatability in terms of threshold sensitivities. The clinical recommendation from these results is that SITA Fast should not be routinely used for the investigation of patients with suspected or confirmed visual field loss induced by VGB therapy. SITA Fast may however, have a role for use in patients who are particularly affected by the drowsiness side effects of the anti-epileptic medications and are only able to undergo a few minutes of testing. The SITA Standard algorithm offers a satisfactory alternative to Full Threshold for the clinical evaluation of VGB-attributed field loss. The algorithm is faster to complete than the Full Threshold algorithm, is less vulnerable to the influence of fatigue and easier to perform. Patients with confirmed

visual field loss who need to be identified for visual field progression are recommended to undergo visual field examination using the Full Threshold algorithm, as the highest repeatability of this algorithm should enable practitioners to detect visual field progression at an earlier stage than either SITA strategy.

5. Validation of an empirically derived normal database for short-wavelength automated perimetry (SWAP) 10° visual fields: to classify VGB central defects.

Aim: To define and validate a normal empirical database for the SWAP 10-2 program to be used to identify defects in the central visual field of VGB-treated patients. **Methodology:** The sample comprised 65 clinically normal subjects (mean age 46.92 years ±17.57 years). Examination of the visual field was undertaken on one eye of each subject for each of two visits, with the Humphrey Field Analyser Program 10-2: using white-white automated perimetry and short wavelength automated perimetry (SWAP). Univariate linear regression was used to determine age-corrected normal thresholds for SWAP at each stimulus location. Total and Pattern Deviation maps were constructed and the predication limits of SWAP normality for each stimulus location were ascertained for significance at 95%, 98%, 99% and 99.5%. **Results:** Univariate linear regression revealed an inverse correlation between MS and age for white-white perimetry and SWAP (adjusted r^2= 0.482 $p<0.001$ white-white: adjusted r^2= 0.292 $p<0.001$ SWAP). Mean global short-term fluctuation values for white-white perimetry were 2.06dB and for SWAP 2.84dB. SWAP consistently showed higher coefficients of variability across the entire visual field when compared to white-white perimetry. Examination times for white-white perimetry were on average 10.44% faster than those for SWAP; this difference was shown to reach statistical significance ($p<0.001$). **Conclusions:** SWAP yields greater between-subject and within-subject variability than white-white perimetry. The normal database provides an objective tool for differentiating abnormalities from normal physiological variations.

5.1. Introduction

Short-wavelength automated perimetry (SWAP) is a method of visual field investigation based upon chromatic adaptation of the visual system. A blue light stimulus is used to preferentially stimulate the short-wavelength sensitive (SWS) pathway while a high luminance yellow background is employed to adapt the remaining chromatic pathways and rods. SWAP is thought to be more sensitive for detecting early glaucomatous abnormalities (Sample, 2000) and identifies progression one to three years prior to detection by white-white perimetry (Johnson *et al.*, 1993a; Sample & Weinreb, 1992). Studies have reported a significant relationship between optic nerve damage: measured via Heidelberg Retina Tomography (HRT) (Tsai *et al.*, 1995) or retinal nerve fibre layer (RNFL) photographic evaluation (Polo *et al.*, 2002), and visual field loss in SWAP. These studies have exhibited a high level of correspondence between the location of optic nerve damage and the location of the focal visual field abnormalities in SWAP. In more recent years, SWAP has been successfully utilised in the investigation of diabetes (Hudson *et al.*, 1998b; Lutze & Bresnick, 1994), patients who are HIV-positive (Plummer *et al.*, 1996) and those with neuro-ophthalmic disorders (Keltner & Johnson, 1995). These studies report that SWAP offers improved sensitivity for the detection of visual defects when compared with standard white-white perimetry. In epilepsy, Roff Hilton *et al.* (2002) have documented that approximately 87.5% of VGB recipients demonstrated SWAP abnormalities in the central 10 degrees. A detailed description of SWAP and its associated efficacy is discussed in section 1.11.10.1.

Since the introduction of automated visual field tests, examiners have found it increasingly difficult to interpret results. Cases of mild visual field loss are particularly problematic, as they must be differentiated from normal physiological variations. Collating a normal database of results facilitates the analysis by enabling computer programs to calculate and graphically display statistical age-matched indices of normality on a global level and for each stimulus location within the visual field.

The current Humphrey Field Analyser (HFA) does not provide a normal database for the SWAP 10-2 program. Studies have previously produced normal databases for the 68 stimulus locations of the 10-2 spatial grid using statistical procedures which extrapolated sensitivity values by interpolating sensitivity from locations of known sensitivity (Cubbidge *et al.*, 2002; Hudson *et al.*, 1998b). Extrapolating the data in this way assumes that the sensitivity profile across the 10-2 field is the same as that of the 30-2 field. If thresholds do not follow the same pattern a false normative database would be set up leading to incorrect statistical indices of normality for each location. Furthermore, the degree of short-term fluctuation in the field either hasn't been measured (Hudson *et al.*, 1998b) or has been assumed to be the same as the 30-2 field (Cubbidge *et al.*, 2002).

5.2. Aims

To define and validate a normal empirical database for the SWAP 10-2 program to be used to identify defects in the central visual field of VGB-treated patients.

5.3. Methodology

5.3.1. Participants and inclusion criteria

Sixty-seven normal subjects: 32 female 35 male were invited to take part within the study. The subjects were evenly stratified for age (mean age 47.15 years; ±17.6 years: range 22 to 79). Inclusion criteria consisted of logMAR visual acuity of 0.1 or better logMAR (6/6 Snellen equivalent), distance refractive error of not greater than ±6.00 dioptres of sphere or ±2.5 dioptres of astigmatism, lenticular changes not greater than NC3, N03, C1or P1 defined using the Lens Opacities Classification System (LOCS) III (Chylack, Wolfe, & Singer, 1993), intraocular pressure less than 22mmHg in either eye, absence of retinal pathology found by digital fundus photography (ImageNet Topcon, Newbry, UK) absence of a tritanopic colour vision defect (Standard Pseudoisochromatic Plates 2), no systemic medication known to affect the visual field, no previous ocular surgery or trauma, no history of diabetes or no family history of diabetes mellitus or glaucoma.

5.3.2. Ethical approval and informed consent

Written informed consent was obtained for all the normal participants (see section 2.3).

5.3.3. Experimental procedures: visual fields

At each visit one eye of each participant completed two visual field tests. The field tests, using the Humphrey Field Analyser (Carl Zeiss Ltd, Hertfordshire, UK), were white-white automated static perimetry using Program 10-2 (Goldmann stimulus size III) and SWAP using Program 10-2(Goldmann stimulus size V). The background and stimulus parameters for SWAP are now standardised and consist of a 440 nm narrowband stimulus of angular subtense 1.74° and 200 ms duration, presented against a high luminance (100 cdm-2) broadband yellow background transmitting wavelengths greater than 530 nm. Studies have shown that approximately 1.5 log units of SWS isolation can be obtained using these parameters (Cubbidge & Wild, 2001; Sample *et al.*, 1996). The fluctuation option for SWAP was enabled. The software version of the HFA was A10.2. Both visual field tests were carried out using the FASTPAC algorithm, which uses a 3 dB single staircase reversal. In 30-degree SWAP, this algorithm yields greater staircase efficiency and reduced between-subject variability when compared to the 4-2 dB Full Threshold algorithm, which is the standard staircase design in conventional perimetry (Wild *et al.*, 1998). Before carrying out SWAP, each participant underwent three minutes of light adaptation to allow adaptation of

the medium- and long-wavelength sensitive pathways, thus isolating the short-wavelength sensitive pathway. The order of the visual field examinations and the eye assigned, was randomised between subjects in order to eliminate order effects, but remained constant over the two visits. The results from visit one were discarded to reduce the influence of learning (Wood *et al.*, 1987) and a rest period of 10 minutes between visual field tests was allowed to reduce the influence of fatigue (Hudson *et al.*, 1994).

5.3.4. The Lens Opacities Classification System (LOCS III)

LOCS III consists of six slit lamp images for grading nuclear colour and nuclear opalescence, five retroillumination images for grading cortical cataract and five retroillumination images for grading subcapsular cataract. The set of standards is prepared as a set of slides for grading standardised photographic images of opacity.

5.4. Analysis

5.4.1. Building an empirical statistical database

Before the data from the 65 age-stratified normal subjects could be used to determine the prediction limits of normality for SWAP using standard parametric statistics, it was necessary to establish that the data fell within the parameters of a normal distribution. A Kolmogorov-Smirnoff test was used to determine whether the centiles of the observed data matched the centiles within a normal distribution. Out of the 68 field locations found within the 10-2 algorithm, 64 exhibited a statistically normal distribution. As the majority of points within the 10-degree field exhibited a Gaussian distribution of normal sensitivity for SWAP prediction limits of normality were determined using standard parametric statistical methods.

Age-corrected normal thresholds for SWAP at each stimulus location were determined from the univariate linear regression of sensitivity with age. Total Deviation maps were calculated by subtracting the age-matched normal sensitivity from the measured sensitivity at each stimulus location. The general height of the hill of vision was extracted from the Total Deviations in order to calculate a Pattern Deviation probability map by calculating the 85^{th} percentile of the Total Deviation, termed the elevator, and subtracting from the Total Deviation at each stimulus location. Using Equation 5.1 the prediction limits of SWAP abnormality were ascertained where, a, represents the age corrected threshold sensitivity, SE, represents the standard error and the integer, n, represents the weighted value appropriate for that significance level. For the following significance levels 95%, 98%, 99% and 99.5% and probability maps of Total and Pattern Deviation were constructed.

$$y=a-(SE*n)$$

Equation 5.1. Prediction limits for SWAP (Bullman, 1997).

Using these significance levels it was possible to determine what deviations (measured age-matched threshold) exceeded those found in less than 5%, 2%, 1% or 0.5% of the population. These statistical procedures were applied to both the empirical and extrapolated databases.

5.4.2. Comparison of the SWAP 10-2 and the white-white 10-2 database

The four Global indices including: Mean deviation (MD), Pattern Standard Deviation (PSD), Short-term Fluctuation (SF) and Corrected Pattern Standard Deviation (CPSD) were calculated for white-white perimetry. Univariate linear regression of mean sensitivity versus age was carried out for each of the 68 locations for both white-white perimetry and SWAP. The global short-term fluctuation was determined by measuring the threshold twice at 10 pre-selected field locations (Figure 5.1) for both white-white perimetry and SWAP using Equation 5.2 where, x_{j1}, represents the first measurement of sensitivity and, x_{j2}, the second. The integer, n, represents the number of locations where a double determination of threshold is undertaken.

$$SF = \sqrt{\frac{1}{n}\frac{\sum_{j=1}^{n}(x_{j2}-x_{j1})^2}{2n}}$$

Equation 5.2. The short-term fluctuation index for the Humphrey perimeter (Heijl, Lindgren, & Olsson, 1987).

The mean sensitivity and one standard deviation of the group mean sensitivity was calculated for each of the 68 positions within white-white perimetry and SWAP. The coefficient of variation (CoV) was calculated as the SD divided by mean and were determined for each of the 68 locations for both white-white perimetry and SWAP. Standard deviation as opposed to standard error was used as this calculation gives a better picture of the range of variation. Student's paired *t*-tests were used to determine whether there was any significant difference between types of perimetry and their: examination times, false positives false negatives and fixation losses.

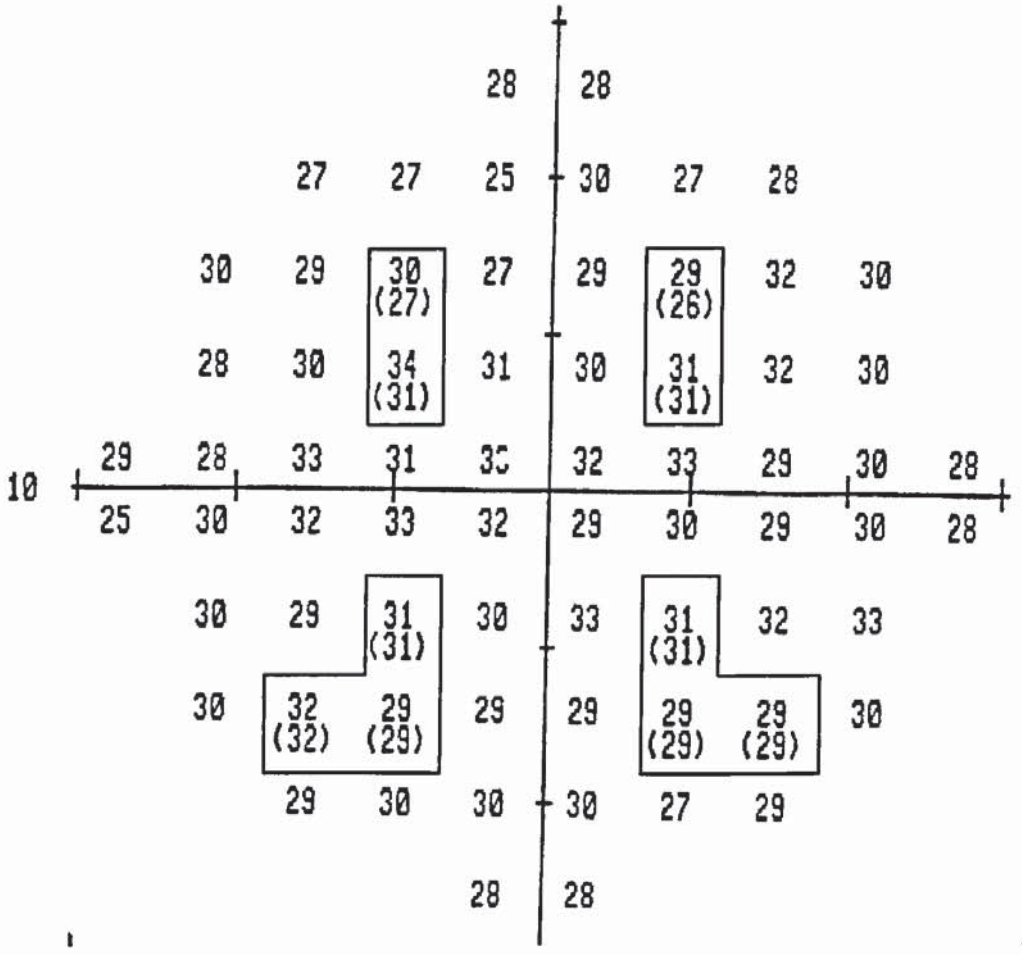

Figure 5.1. Showing the 10 locations used to determine the short-term fluctuation within the 10-degree field.

5.5. Results

Out of 67 participants who met the inclusion criteria, 8 demonstrated small areas of visual field loss with conventional perimetry. The defects were repeatable in two of the cases and their data was subsequently removed from the study. The results of the remaining 65 participants were analysed, 32 female and 33 male (mean age 46.92 years; ±17.57 years; range 22 to 79). All white-white and SWAP visual fields fell within the visual field reliability criteria of <33% false positive and negative catch trials and <20% fixation losses. The average time between the first and second visit was 17.12 days: (SD) 14.59 days.

5.5.1. Comparison of the SWAP (empirical) and white-white normal 10-2 databases

The group mean global indices for white-white perimetry were as follows: MD 0.14 dB, PSD 1.63 dB, SF 1.47 and CPSD 0.67dB. Univariate linear regression revealed an inverse correlation between mean sensitivity (MS) and age for both white-white perimetry and SWAP (Figure. 5.2). The correlation accounted for 48% of the variance within white-white perimetry, but only 29% of the variance within SWAP (adjusted r^2= 0.482, p<0.001 white-white: adjusted r^2 =0.292 p<0.001 SWAP). The average age-decline in MS, for the entire visual field, was greater for SWAP (-0.89 dB per decade) than for white-white perimetry (–0.45dB per decade). The normal age-decline in MS was consistent throughout the entire visual field for both types of perimetry (Figure 5.3). The global SF values were (mean 2.06 dB; SD 0.59 dB; range 0.95 dB to 3.48 dB) for white-white perimetry and (mean 2.84 dB; SD 0.94 dB; range 1.34 dB to 6.84 dB) for SWAP. Mean threshold sensitivity for white-white perimetry was 31.87 dB and for SWAP 27.72dB. The mean sensitivities were slightly lower within the superior hemifield for both types of perimetry (Figure 5.4). The standard deviations (SDs) of group mean sensitivity were slightly higher within the superior hemifield for both types of perimetry (Figure 5.4). Because the decibel scale is referenced to the maximum stimulus luminance of the perimeter, the decibel scale in SWAP cannot be directly compared to that of conventional perimetry. Thus, in order to make a comparison of the between-subject variability between perimetry types, the coefficient of variability was used. This statistic enables a comparison between white-white deviations derived from distributions which differ in the magnitude of their measurement scales. SWAP consistently showed higher CoVs across the entire visual field when compared to white-white perimetry (Figure 5.5). The CoVs for SWAP were on average twice as large as those found for white-white perimetry. Examination duration was significantly different between tests p<0.001. White-white examination times were on average 10.44% faster than those for SWAP. Between tests, there was no significant difference in the parameters that were used to determine visual field reliability (fixation losses p=0.956; false positives p=0.195; false negatives p=0.094).

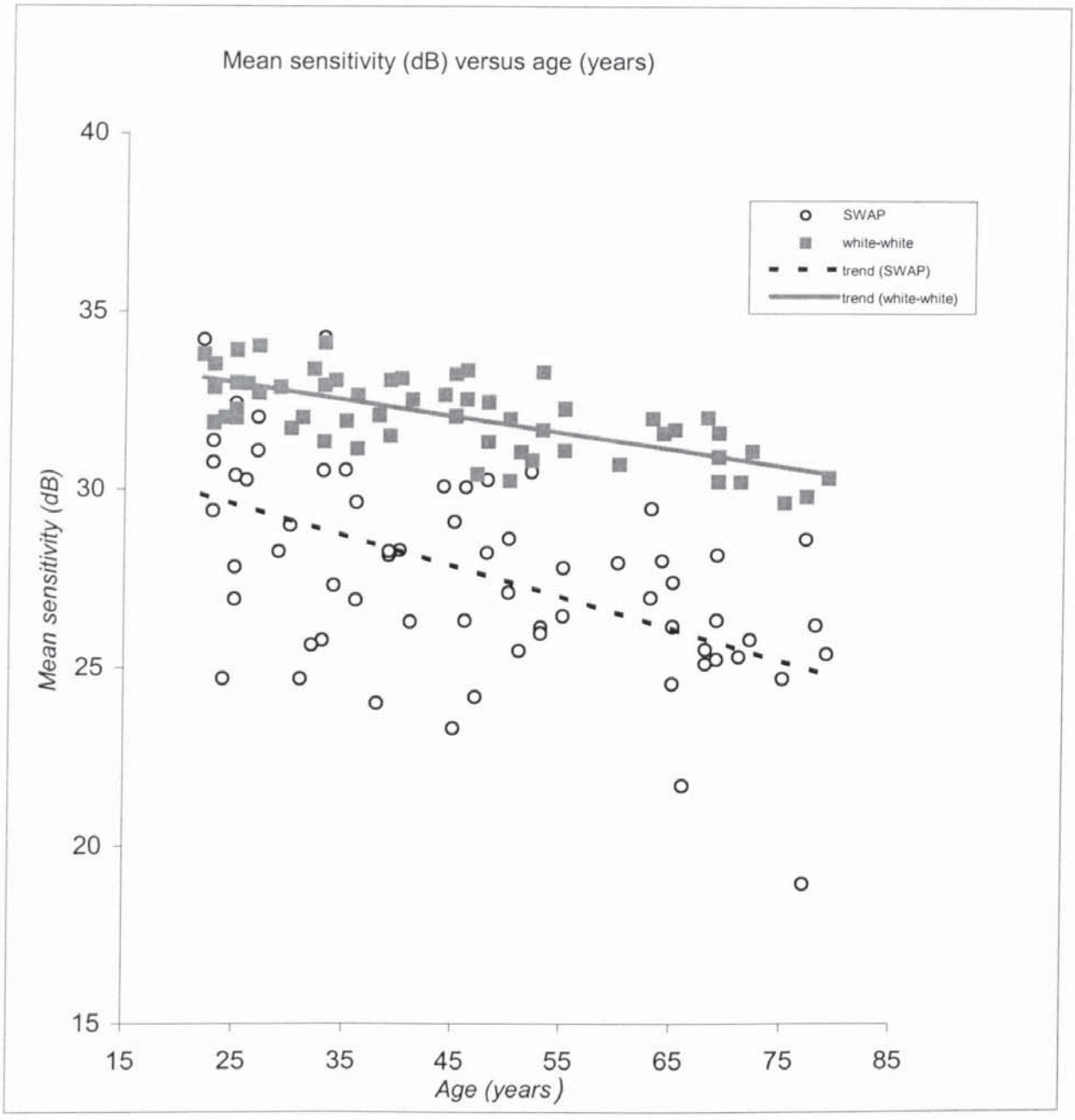

Figure 5.2. Scatterplot showing mean sensitivity versus age for SWAP and white-white perimetry.

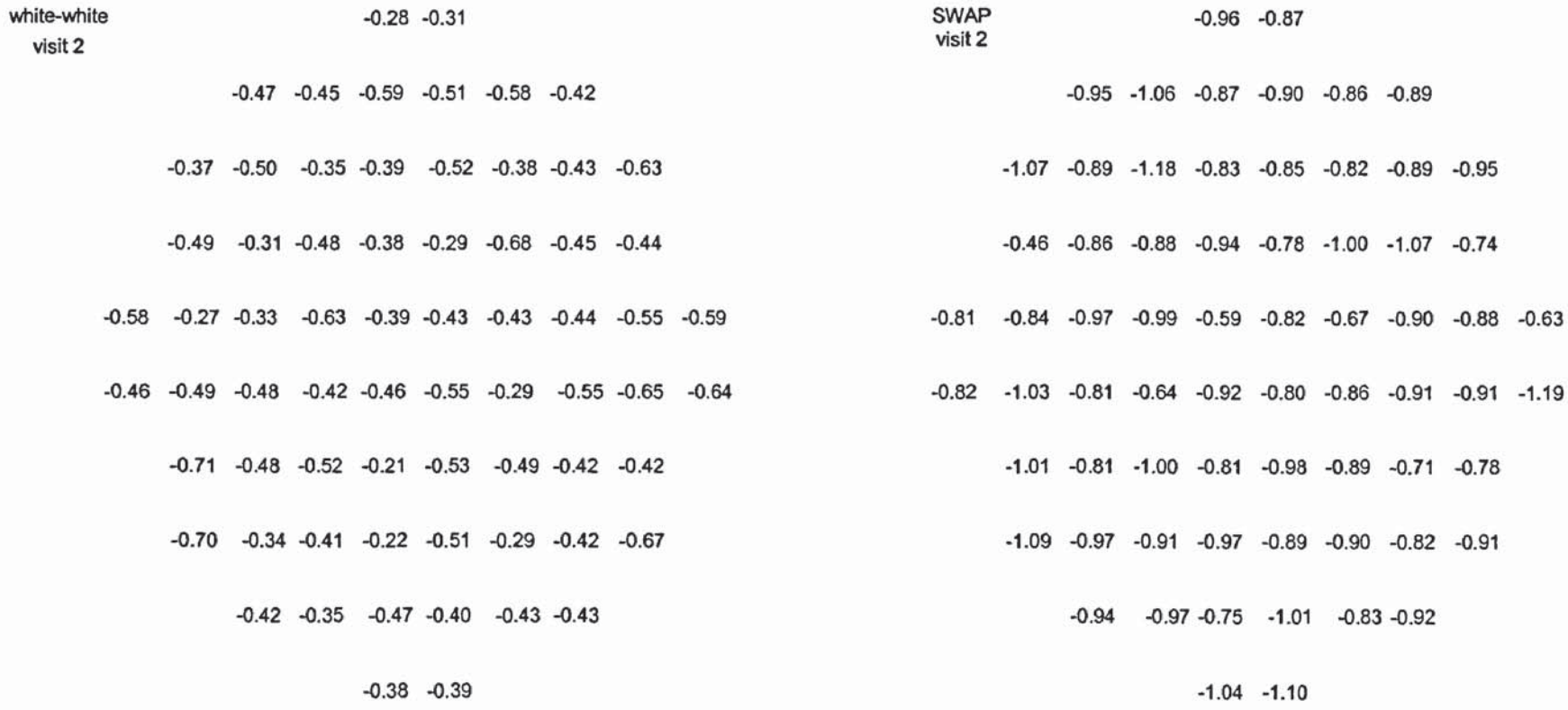

Figure 5.3. Pointwise group mean decibel loss per decade for white-white (left) and SWAP (right).

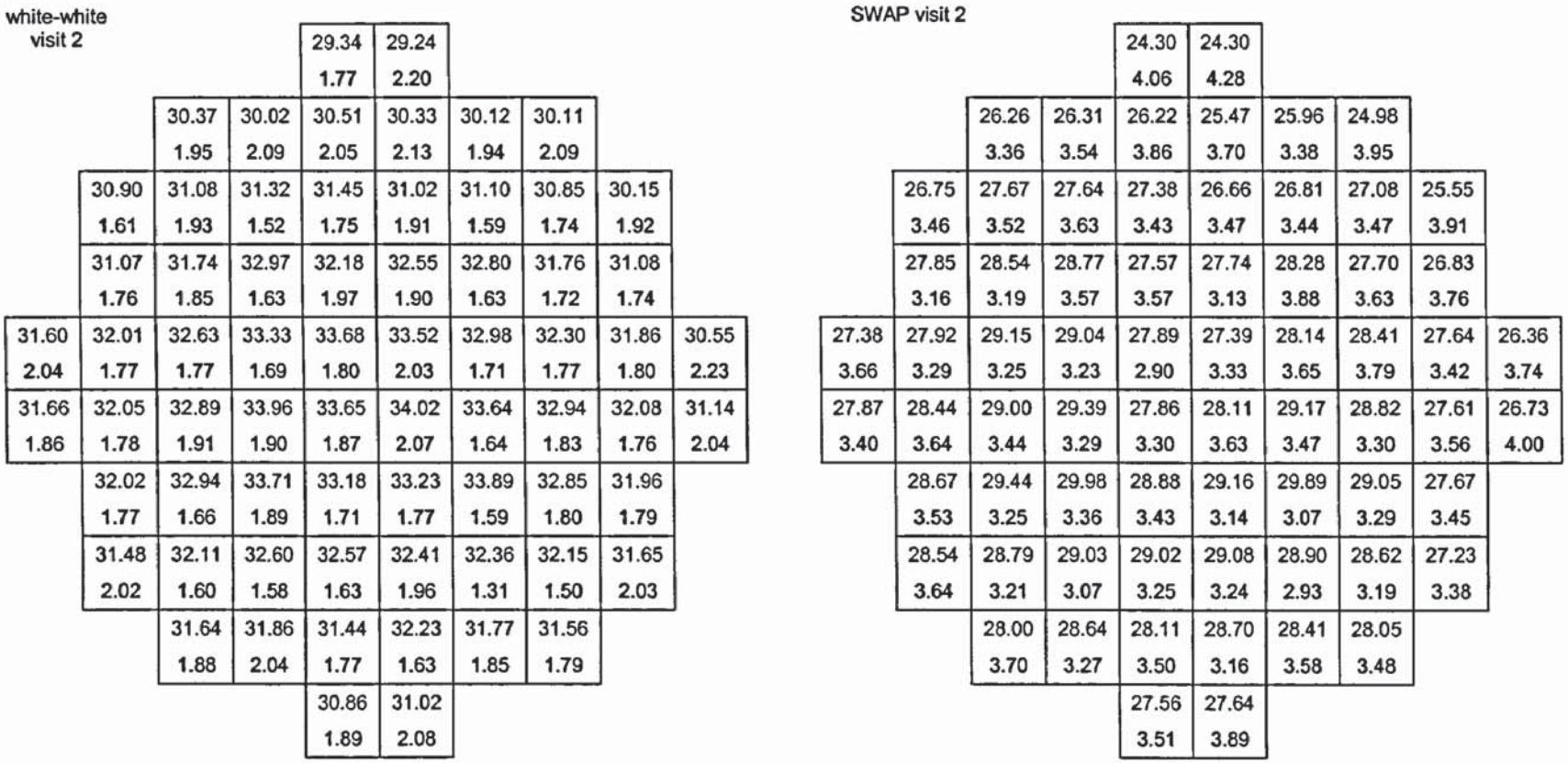

Figure 5.4. The mean threshold sensitivity (dB) ± one standard deviation for each stimulus location for white-white perimetry (right) and SWAP (left)

white-white visit 2

				6.03	7.53				
		6.42	6.97	6.73	7.01	6.43	6.96		
	5.20	6.22	4.87	5.57	6.16	5.12	5.63	6.38	
	5.66	5.83	4.95	6.12	5.83	4.98	5.43	5.59	
6.46	5.55	5.42	5.08	5.35	6.06	5.19	5.47	5.66	7.30
5.87	5.55	5.80	5.58	5.56	6.08	4.88	5.56	5.48	6.56
	5.52	5.04	5.60	5.16	5.34	4.68	5.49	5.60	
	6.41	4.97	4.85	5.01	6.05	4.06	4.66	6.41	
		5.94	6.39	5.62	5.07	5.81	5.66		
				6.12	6.71				

SWAP visit 2

				16.70	17.61				
		12.79	13.45	14.73	14.51	13.02	15.80		
	12.92	12.72	13.15	12.53	13.03	12.82	12.81	15.31	
	11.36	11.19	12.40	12.95	11.27	13.71	13.12	14.02	
13.37	11.79	11.14	11.12	10.40	12.17	12.98	13.35	12.38	14.19
12.19	12.81	11.86	11.18	11.83	12.90	11.88	11.47	12.89	14.98
	12.32	11.05	11.19	11.88	10.78	10.26	11.31	12.46	
	12.76	11.13	10.57	11.21	11.14	10.12	11.13	12.43	
		13.20	11.41	12.44	11.00	12.61	12.41		
				12.74	14.07				

Figure 5.5. The coefficients of variation (%) at each individual stimulus location for white-white perimetry (left) and SWAP (right).

5.6. Discussion

All white-white 10-2 visual fields were normal, as defined by probability analysis STATPAC and confirmed with group mean global indices. A normal age-correlated reduction of threshold sensitivity (-0.45 dB per decade for white-white: -0.89 dB per decade SWAP) was evident for both types of perimetry. This finding is concordant with numerous studies, previously carried out on clinically normal participants (Heijl, Lindgren, & Olsson, 1987b; Johnson *et al.*, 1988; Wild *et al.*, 1998) and is thought to reflect an age-related reduction in the photoreceptor population, retinal neurones and retinal pigment epithelial cells (Curcio *et al.*, 1993; Gao & Hollyfield, 1992). In fact, one study reports a significant correlation between the decline in density of the photoreceptor population and a loss of white-white perimetric threshold sensitivity with increasing age (Panda-Jonas, Jonas, & Jakobczyk-Zmija, 1995).

A comparatively greater age-decline in threshold sensitivity was evident when SWAP results were compared against those from white-white perimetry. Studies have previously attributed the steeper decline in SWAP sensitivity to pre-receptoral absorption, i.e. the preferential absorption of the SWAP stimulus by the ocular media and macular pigment (Johnson *et al.*, 1988; Johnson & Marshall, 1995; Wild *et al.*, 1995). Some controversy exists as to whether it is acceptable to correct for the absorption of the short-wavelength stimulus. The technique was previously advocated on the grounds that between-subject variability was reduced (Wild *et al.*, 1998). Findings however, have not been replicated (Johnson *et al.*, 1988). It should be remembered that any correction of short wavelength perimetric thresholds for pre-receptoral absorption increases the perimetric sensitivity artificially. The influence of correction of SWAP for macular pigment absorption on the normal prediction limits is currently unknown. Considerable within-subject variability exists in the measurement of macular pigment absorption (Hammond, Jr. & Fuld, 1992; Wild & Hudson, 1995), but the within-subject variability of measurements of ocular media absorption are not known. It is possible that high within-subject variability in ocular media absorption measurements could account for the equivocal nature of whether correction reduces the between-subject variability of SWAP. Correction for pre-receptoral absorption does not take into account the difficulty in stimulus detection arising from the reduced stimulus contrast, nor the influences of backward and forward light scatter on stimulus detection. Furthermore, methods that utilise retinal adaptation to measure macular pigment and ocular media absorption assume normal retinal function (Sample *et al.*, 1988; Wild *et al.*, 1995; Wild *et al.*, 1998; Wild & Hudson, 1995) which is unlikely in the presence of retinal disease. Objective measures of lenticular absorption exist (Johnson *et al.*, 1993c; Teesalu *et al.*, 1997) but these are not appropriate in the clinical setting. If the correction for ocular media absorption does not reduce the between-subject variability of SWAP (Johnson *et al.*, 1988; Wild & Hudson, 1995), it could be considered a superfluous clinical procedure, especially as the increased examination time necessitated by these measurements decreases the viability of SWAP clinically.

The gradients (age-related decline in threshold sensitivity) documented for each location remained fairly consistent throughout the entire visual field for both types of perimetry and may be contrasted with investigations of the 30-degree field which revealed comparatively steeper gradients across all field locations for both SWAP (Johnson & Marshall, 1995; Wild *et al.*, 1998) and white-white perimetry (Heijl *et al.*, 1987b). These findings appear to confirm that the profile of a normal 10-degree field is much flatter than its 30-degee counterpart. Pearson's correlation coefficient revealed that white-white perimetry enabled a more accurate prediction of MS based on age. The increased between-subject variability of SWAP is the most likely cause for the weaker correlation. Despite this finding SWAP may still preferentially detect subtle abnormalities when compared against white-white perimetry (Roff Hilton *et al.*, 2002).

Short-term fluctuation (SF) is a measurement of the test-retest variability or within-subject variability. The locations where double determinations of threshold sensitivity occurred for the SF measurement in SWAP yielded approximately 25% more variability than those recorded for white-white perimetry. Evidence from earlier studies report that the SF for SWAP in the 30-degree visual field, ranged between 17% (Wild *et al.*, 1998) and 55% (Kwon *et al.*, 1998). However, as each visual field test is known to use a different measurement scale this type of comparison should be approached with caution. The studies design currently prevented a comparison of long-term fluctuations. Other investigators have reported that SWAP in the 30 degree visual field yields a greater long-term fluctuation than white-white perimetry (Blumenthal *et al.*, 2000; Hutchings *et al.*, 2001). These reports suggest that it may be difficult to separate whether true defect progression has occurred. However, the long-term fluctuation of SWAP in the 10-degree field is currently unknown.

The standard deviation of the mean sensitivity was plotted to determine the between-subject variability across all field locations for both types of perimetry. Both types of perimetry reported greater variations in the superior field and were probably caused by blinking. Katz & Sommer (1986) have previously stated that the likelihood of missing a stimulus is greater superiorly than inferiorly which probably reduces overall threshold sensitivity. Between-subject variations remained consistent throughout the entire 10-degree field for white-white perimetry. For SWAP between-subject variations were found to increase towards the edge of the 10-degree field. Present data implies that for SWAP between-subject variability increases with increasing eccentricity.

Each type of perimetry possesses a different measurement scale for stimulus luminance. The coefficient of variation (the SD divided by the mean) was used to express the difference in between-subject variability at each stimulus location for both SWAP and white-white perimetry. Throughout the entire visual field SWAP consistently reported larger CoVs or higher between–subject variability than white-white perimetry. In addition, investigations

using SWAP 30-2 algorithm revealed consistently larger between–subject variability (Wild *et al.*, 1998) when compared with present SWAP 10-2 results. In fact, after a linear interpolation procedure was used to extrapolate normal SWAP 10-2 sensitivities from a normal 30-2 database, slightly greater CoVs were recorded across all locations (Cubbidge *et al.*, 2002).

Increased between-subject variability influences the sensitivity of a test. A greater variation between subjects means that wider confidence limits of normality are produced. A proportionately higher reduction in sensitivity is then necessary, before a reduction of sensitivity was recognised as an abnormal defect. Present results suggest that white-white perimetry produces narrower confidence limits of normality than short wavelength perimetry.

SWAP may have produced a greater between-subject variability than white-white perimetry for a number of reasons. Possibilities include greater variations in s-cone photoreceptor densities (Curcio *et al.*, 1990) or different amounts of s-cone damage induced by prolonged UV radiation (Ham *et al.*, 1982). The SWAP 30-2 algorithm (Wild *et al.*, 1998) and the linear interpolation procedure (Cubbidge *et al.*, 2002) may have produced greater between-subject variability due to slightly different population characteristics between studies.

The examination duration for white-white perimetry (Program 10-2) was on average 10.4% faster than the examination duration for SWAP. This figure was reported to increase to 15% when a 30-2 algorithm was used (Wild *et al.*, 1998). Increased examination times leads to visual fatigue and as a consequence could lead to greater numbers of false negatives and a possible decrease in mean sensitivity (Hudson *et al.*, 1994). This study did not find a significant difference between types of perimetry and false positive, false negative or fixation losses. These findings suggest that fatigue did not seriously affect the perimetric sensitivity.

5.7. Conclusions

The 10-2 algorithm for SWAP yielded less between-subject variability, was proportionately shorter and fluctuated less with age than the 30-2 algorithm. Reducing the between subject variability means that narrower confidence limits of normality are produced, resulting in a smaller reduction in threshold sensitivity being required before it is recognised as abnormal. These results suggest that SWAP 10-2 may be more sensitive than SWAP 30-2, in delineating abnormalities and may be of value in the investigation of VGB. SWAP yields greater between-subject and within-subject variability than white-white perimetry, however, its increased sensitivity may still render it a superior diagnostic test to conventional perimetry. The normal variation of threshold sensitivities between-subjects in conjunction with normal variation of threshold sensitivities across the retina confounds the interpretation of visual field loss. The normal SWAP 10-2 database provides a method of differentiating SWAP defects in the VGB-treated population through construction of probability maps for

diffuse and focal visual field loss. This database may be used in the clinical investigation of other drug toxicities. It could also be used for the investigation of diseased states affecting the central retina including age-related macular degeneration and diabetic maculopathy.

6. Investigation of Vigabatrin attributed visual field defects with three clinical perimetric protocols.

Aim: To evaluate the effectiveness of white-white automated perimetry, short-wavelength automated perimetry (SWAP) and frequency doubling technology's (FDT) ability to detect VGB-attributed visual field loss and to establish a battery of tests for screening patients exposed to VGB treatment for visual abnormalities. **Methodology:** The sample comprised 22 patients (mean age 37.7 years ±16.7 years) diagnosed with epilepsy and exposed to VGB therapy. Each patient underwent a battery of tests on either eye including high contrast visual acuity (EDTRS logMAR chart), contrast sensitivity (CSV-1000) and colour perception (Standard Pseudoisochromatic Plates part 2). For each of two visits, one randomly selected eye was administered white-white automated perimetry Program 30-2 (Humphrey Field Analyser), SWAP Program 10-2 (Humphrey Field Analyser) and FDT Program N-30 (Frequency Doubling Technology). Multiple regression was used to determine whether there was any significant relationship between contrast sensitivity deficits at any of the spatial frequencies, and the severity of visual field loss measured using each diagnostic protocol. Each visual field was classified as normal or abnormal using a series of guidelines outlined in the study. A repeated measures analysis of variance was used to determine whether there was any significant difference between examination duration and perimetry type. **Results:** Thirty six eyes out of a potential 43 investigated eyes yielded abnormal contrast sensitivity measurements in at least one or more spatial frequencies. All spatial frequencies (3, 6, 12 and 18 cycles/ degree) were equally affected. Contrast sensitivity deficits were not correlated with the severity of visual field loss for each diagnostic protocol ($p= 0.221$ white-white; $p= 0.347$ SWAP; $p= 0.630$ FDT). Visual field abnormalities were found in a total of 13 eyes (59%) out of a potential 22 investigated eyes. White-white automated perimetry detected abnormalities in nine eyes, SWAP detected abnormalities in ten eyes and FDT also detected abnormalities in ten eyes. A significant difference was observed between examination duration and perimetry type ($p< 0.001$). SWAP and FDT's combined examination duration was on average 13.4% faster than that for white-white perimetry. **Conclusions:** SWAP and FDT have increased sensitivity for the detection of VGB-attributed field loss, when compared against conventional white-white automated static perimetry. A screening battery consisting of contrast sensitivity measurement, SWAP and FDT should yield maximum sensitivity.

6.1. Introduction

Standard (static, white-white) perimetry and Goldmann perimetry are the most frequently recommended techniques, for diagnosing and monitoring VGB associated abnormalities (Kalviainen & Nousiainen, 2001; Wild *et al.*, 1999a). These tests are thought to be successful to a degree, however there is now a large body of evidence to suggest that they do not detect the more subtle abnormalities that are also associated with the treatment. Investigations with Goldmann perimetry and/or white-white perimetry typically reveal a concentric constriction of the peripheral visual fields. These results were in contrast to the numerous, colour vision (Krauss *et al.*, 1998; Manucheri *et al.*, 2000; Roff Hilton *et al.*, 2002), contrast sensitivity (Nousiainen *et al.*, 2000a; Perron *et al.*, 2002; Roff Hilton *et al.*, 2002) and SWAP (Roff Hilton *et al.*, 2002) investigations, which report significant central abnormalities.

Further evidence for the inefficacy of white-white perimetry arises from investigations of glaucoma, which report that visual field loss only becomes manifest after significant ganglion cell death has occurred (Pederson & Anderson, 1980; Quigley, Dunkelberger, & Green, 1989). The relative insensitivity that is demonstrated by white-white perimetry is probably explained in part, by its lack of specificity. The achromatic stimulus and background conditions simultaneously stimulate all retinal ganglion cells meaning that substantial damage must occur to the visual system before defects are detected. In recent years, a series of new perimetric testing strategies have been developed with the aim of detecting visual field deficits at an earlier stage than can be accomplished with white-white perimetry. Two of these techniques are: Short-Wavelength Automated Perimetry (SWAP) and Frequency Doubling Technology (FDT). Both techniques test specific visual pathways and may therefore yield-increased sensitivity due to the relative reduction in their target cell population.

6.1.1. Short-wavelength automated perimetry (SWAP)

A detailed description of SWAP and its associated efficacy is outlined in section 5.1

6.1.2. Frequency doubling technology (FDT)

FDT is a method of visual field investigation based upon evaluating visual pathways that are responsive to high rates of flicker and rapid motion. An apparent frequency doubling illusion is produced when a sinusoidal grating is modulated rapidly in temporal counterphase. The illusion is thought to be mediated by magnocellular retinal ganglion cells which demonstrate non-linear response properties (My cells) (Maddess & Henry, 1992). Investigators have reported that the FDT perimeter is a compact inexpensive perimeter, whose transportability, tolerance to refractive errors, and rapid test times make it a suitable candidate for visual field screening (Anderson & Johnson, 2003). The majority of research studies suggest that FDT

detects glaucomatous damage at an earlier stage (Landers *et al.*, 2000; Maddess *et al.*, 2000; Soliman *et al.*, 2002) than standard white-white perimetry. In neuro-ophthalmic disorders, optic neuropathies are detected with equal sensitivity and specificity to white-white perimetry, only, hemianopic and quadrantanopic defects have a tendency to be misdiagnosed due to a failure of FDT to detect abnormalities along the vertical meridian (Wall *et al.*, 2002). The technique shows less test-retest variability than standard perimetry, when either eccentricity or severity of defect is increased (Balwantry & Johnson, 1999). The magnitude of short- and long-term fluctuation, is equivocal between testing strategies (Iester *et al.*, 2000). A detailed description of the FDT perimeter and its associated efficacy can be found in section 1.11.10.3.

6.2. Aims

To evaluate the effectiveness of white-white Perimetry, SWAP and FDT's ability to detect VGB-attributed field loss and to establish a battery of tests to screen patients for reduced visual function as a result of VGB therapy. A secondary aim was to compare the interpretation of SWAP 10-2 visual fields using an empirical and extrapolated normal database.

6.3. Methodology

6.3.1. Patients and inclusion criteria

Twenty-four patients: 18 female, 6 male (mean age 37.6 years, ±16.1years: range 17 to 66), previously diagnosed with epilepsy and who were either currently, or had previously received VGB, were invited to take part in the study. Inclusion criteria consisted of a distance refractive error of not greater than ±6.00 dioptres of sphere or ±2.5 dioptres of astigmatism, absence of a congenital red-green colour vision defect (measured using Ishihara Plates under controlled illumination), absence of intra-cranial pathology which is known to effect the visual pathway or any known ocular pathology which was unrelated to VGB therapy.

6.3.2. Ethical approval and informed consent

Written informed consent was obtained from all the patients. A detailed drug history was obtained from their hospital notes after requesting permission from the patient and their hospital consultant physician (see section 2.3).

6.3.3. Experimental procedures

On the first visit each subject underwent a battery of tests: visual acuity, contrast sensitivity and colour vision.

6.3.4. Visual acuity

Visual acuity was measured monocularly using a high contrast EDTRS logMAR chart (Vector Vision, Dayton OH, USA). The LogMAR (LOGarithm of the Minimal Angle of Resolution) chart employs a logarithmic progression of letter spaces and sizes allowing increased consistency between each measurement. The Snellen chart was not used in this study because the lack of standardisation between the number of letters on each line and also the spaces between each of the letters, results in poor uniformity between measurements (Bailey & Lovie, 1976).

6.3.5. Contrast sensitivity

Contrast sensitivity is a measurement of a patient's ability to perceive differences in contrast over a range of spatial frequencies and has greater clinical significance than standard measures of visual acuity. Investigators have reported contrast sensitivity to be more sensitive than visual acuity for detecting abnormalities associated with glaucoma (Hawkins *et al.*, 2003), cataract (Elliott *et al.*, 1991; Elliott & Situ, 1998) and amblyopia (Lennerstrand & Lundh, 1984). There are numerous test plates, charts and slides available for making contrast sensitivity measurements. In this study contrast sensitivity was measured on the first visit, using the CSV-1000 (Vector Vision Dayton OH, USA). This test provides a quick and accurate tool for assessing broad-contrast sensitivities from low to high spatial frequencies (Ginsburg & Cannon, 1984). The technique is reported to detect subtle changes in contrast sensitivity: after refractive surgery (Ghaith *et al.*, 1998); regaining metabolic control in diabetics with and without retinopathy (Verrotti *et al.*, 1998) and treatment changes in glaucoma (Pomerance & Evans, 1994). Test-retest variability of the CSV-1000 is favourable (Pomerance & Evans, 1994) and a detailed description of the CSV-1000 is provided in section 1.11.2.

6.3.6. Colour perception

Colour vision plates are capable of identifying both congenital and acquired abnormalities. The Ishihara pseudoisochromatic plates were used to exclude any participant with a congenital or acquired red-green colour vision defect. However, these plates are not designed to detect tritan colour vision defects. Consequently, Standard Pseudoisochromatic Plates part 2 (SPP2) were used to assess whether any congenital acquired foveal tritanopic abnormalities were present. The Farnsworth Munsell (FM) 100-Hue was not used in this study because the longer examination times and the demand for increased discrimination were considered to be beyond the capabilities of the present patient cohort. All colour vision testing was carried out monocularly at 75cms, using a Sol Source daylight desk lamp (Gretag Macbeth) angled at 90°, to illuminate the plates.

6.3.7. Visual fields

At each visit, one eye of each participant completed three different types of perimetry. The order of the field tests and the eye assigned, alternated between subjects but remained constant over the two visits. To reduce the influence of the learning effect (Wood *et al.*, 1987), results from visit one were discarded from all the analyses. A break of 10-minutes was administered between field tests to reduce the effects from fatigue (Hudson *et al.*, 1994). Additionally, rest periods were introduced during individual visual field examinations where necessary, as epileptic patients are particularly susceptible to fatigue. Catch trials of less than 20% fixation losses, less than 33% false positives and less than 33% false negatives were employed to ensure reliability of patient responses. If any participant's results fell outside these criteria, they were invited back to repeat their visual field test. If the results again fell outside the reliability criteria they were removed from the study.

6.3.8. White-white perimetry

White-white perimetry was measured using program 30-2 Full Threshold, Goldmann stimulus size III on the Humphrey Field Analyser (Carl Zeiss Ltd, Hertfordshire, UK). Kinetic perimetry was not used as it was considered to be less sensitive than automated static perimetry in detecting areas of localised visual field loss (Drance *et al.*, 1967; Lynn, 1969) and more vulnerable to examiner related bias (Lynn, 1969). A detailed explanation of the disadvantages of manual kinetic perimetry is given in section 1.11.6.1 Suprathreshold static perimetry detects the location of abnormalities but does not quantify the depth of defect (section 1.11.8.2). The standard algorithm for diagnosing early glaucomatous abnormalities is the Full Threshold algorithm because of the post-examination statistical analyses provided by this testing strategy (Mills *et al.*, 1994). Consequently, the 30-2 Full Threshold algorithm was used in this study in order to ensure that the mild abnormalities associated with VGB treatment were detected.

6.3.9. SWAP

SWAP was measured using program 10-2 FASTPAC, Goldmann stimulus size V on the Humphrey Field Analyser (Carl Zeiss Ltd, Hertfordshire, UK). The 3dB single reversal algorithm (FASTPAC) was employed, as this algorithm yields increased staircase efficiency compared to the white-white 4-2 dB Full Threshold algorithm in SWAP and furthermore, reduced between-subject variability when compared to the 4-2 dB Full Threshold algorithm (Wild *et al.*, 1998). For SWAP, the central 10-degrees was measured because the reduced field size is thought to produce smaller between- and within- subject variability (Blumenthal *et al.*, 2000; Kwon *et al.*, 1998; Wild *et al.*, 1995; Wild *et al.*, 1998), increasing the overall sensitivity of the test. SWAP sensitivities were not corrected for the absorption of the short-wavelength stimulus by the ocular media because the increased examination time significantly decreases the viability of SWAP clinically (section 5.6). Global visual field

indices and Total and Pattern Deviation probability maps were constructed using the normal database described in Chapter 5.

6.3.10. FDT

Frequency Doubling Perimetry Technology was measured using Program N-30 and the Full Threshold algorithm (Carl Zeiss Ltd, Hertfordshire, UK). Even though examination durations are longer in Full Threshold mode (typically four minutes per eye), the Program also yields higher sensitivity (Burnstein *et al.*, 2000) and was therefore used in the present study. The N-30 is similar to the C-20 Program and differs only in the addition of two 10-degree diameter stimulus locations presented above and below the horizontal midline between 20 and 30 degrees which encompasses the nasal visual field which is most frequently affected by VGB therapy (section 3.5.1).

6.4. Analysis

6.4.1. Classification of visual fields

Each visual field was classified as normal or abnormal using a number of criteria, which are defined below. White-white visual fields were classified using criteria which were specifically designed for the interpretation of VGB-attributed visual field loss See Table 3.2 (Wild *et al.*, 1999a). FDT results were classified using criteria that were originally designed to interpret glaucomatous field loss using a Full Threshold C-20 program (Sponsel *et al.*, 1998): as there are currently no criteria for classifying any type of abnormality with the N-30 program. An alternative FDT classification based on neuro-ophthalmic visual field loss is available, however this method was thought to be less reliable as it was based on non-retinal abnormalities (Thomas *et al.*, 2001). To date, there are no criteria for classifying any type of abnormality with the SWAP 10-2 program.

6.4.2. Evaluation of empirical and extrapolated normal SWAP 10-2 databases in VGB-treated patients

A previous investigation in the Department has evaluated VGB-attributed visual field loss in the central 10 ten degrees using SWAP (Roff Hilton *et al.*, 2002). The patient data was analysed with reference to a database of normal sensitivities, extrapolated from the normal 30-2 profile in SWAP (Cubbidge *et al.*, 2002). However, this approach assumes that the profile of the hill of vision within the extrapolated area is the same as the peripheral locations from which it is derived. Therefore it is possible that some of the VGB-attributed visual field loss of (Roff Hilton *et al.*, 2002) could have been artifactual in nature. A comparison between the empirically derived (Chapter 5) and mathematically extrapolated databases was made by constructing Total and Pattern Deviation probability maps for both databases, using the

methodology outlined in section 5.4.1 Two SWAP 10-2 visual fields (for a given eye) were then classified for abnormality by an experienced perimetrist (RC) based on depth and locations of diffuse and focal loss.

6.4.3. Statistical analysis

An Independent sample *t*-test was used to compare visual acuity differences between those patients who presented with a defect and those that did not. The severity of each visual field test (white-white perimetry, SWAP when analysed with an empirical database, SWAP, when analysed with an extrapolated database and FDT) was calculated by determining the percentage of locations with a defect of significance level < 5% within the Total Deviation probability field plot. This calculation is most similar to the measurement previously used by Nousiainen *et al.* (2000a). A multiple regression was used to determine whether there was any relationship between contrast sensitivity deficits at any of the spatial frequencies investigated, and the severity of visual field loss (measured with white-white perimetry, SWAP when analysed with an empirical database and FDT). Pearson's correlation coefficient was used to explore the interactions between the severity of visual field loss defined by the extrapolated and empirically derived databases respectively. A repeated measures ANOVA was used to determine whether there was any significant difference between examination duration and perimetry type. Sensitivity and specificity was calculated for both FDT and SWAP with respect to white-white perimetry, which was assigned as the "gold standard" algorithm, for the detection of VGB-attributed visual field loss. Sensitivity was defined as the proportion of diseased individuals that were identified as diseased individuals by the screening test. Specificity was defined as the proportion of non-diseased individuals who were identified as non-diseased by the screening program.

6.5. Results

Following the strict inclusion criteria it was necessary to remove two patients from the study: one due to poor reliability (high catch trials), the other due to an inability to complete the visual field test due to tiredness. Consequently 22 patients (17 female, 5 male: mean age 37.7 years, ±16.7 years: range 17 to 66) remained in the study. Due to the presence of amblyopia, one subject failed to complete the high contrast LogMAR visual acuity, spatial contrast sensitivity and colour vision tests, with both eyes. Therefore, contrast sensitivity data for 43 eyes is presented. The average time between the first and second visit was 16.2 days (SD) 11.9 days. Patient's concomitant medication other than VGB is presented in Table 6.1.

All 22 subjects successfully completed three types of perimetry and their reliability criteria fell inside the parameters of <33% false positive and negative catch trials and <20% fixation losses.

6.5.1. Visual acuity and contrast sensitivity

The group mean high contrast LogMAR visual acuity was 0.01 ± 0.10, which is consistent with a Snellen visual acuity of 6/6. There was no statistical difference in the visual acuity, between the group of patients with a confirmed visual field defect and those without, for white-white perimetry (p=0.904), SWAP (p=0.565) and FDT (p=0.797). A comparison of contrast sensitivity with age-stratified normal data (Arend *et al.*, 1997; Pomerance & Evans, 1994) revealed that out of 43 investigated eyes, 36 yielded abnormal contrast sensitivity measurements for at least one spatial frequency. The percentage of defects at each spatial frequency is shown in Table 6.2. Defects were prominent at each spatial frequency. No correlation was found to be statistically significant (Table 6.3) within the multiple regression model of severity of visual field defect (white-white, SWAP, FDT) and contrast sensitivity deficit for each of the spatial frequencies.

6.5.2. Colour perception

No colour defects were detected using either the Ishihara pseudoisochromatic plates or the (SPP2).

6.5.3. Visual fields

A table of the quantity of visual field abnormalities (detected using white-white automated perimetry, SWAP when analysed using the empirical database, SWAP when analysed using the extrapolated database and FDT) for 22 individual eyes is presented in Table 6.4. Visual field loss consistent with VGB treatment was found in 13 eyes out of 22 patients (59%). Individually, SWAP and FDT detected abnormalities in approximately 77% (10 out of a possible 13) of the group, whilst white-white perimetry detected only 69% (9 out of a possible 13). If SWAP and FDT are considered together then their combined sensitivity increased to 100%, as SWAP and FDT detected an additional 30.1% (4 out of 13) VGB abnormalities not detected with white-white perimetry. Approximately 73% of the investigated patients yielded the same results using all three types of perimetry. Results from this table have also indicated that all SWAP 10-2 visual fields were classified into the same category, regardless of the database that was used to analyse the results. In addition, Pearson's correlation coefficient revealed a significant positive correlation ($p < 0.001$, adjusted $r^2 = 0.821$) between the severity which was determined from the empirical database and the severity which was determined from the extrapolated database. A significant difference was observed ($p<0.001$) between examination duration and perimetry type. Group mean examination times for each algorithm and their associated standard deviation is presented in Table 6.5. SWAP's examination durations were on average 44.2% faster than those for white-white perimetry. FDT's examination durations were on average 69.2% faster than those for white-white perimetry. The combined examination time for SWAP and FDT together was on average 13.4% faster than that for white-white perimetry. High sensitivity and specificity was found for

Patient number	Carbamazepine	Sodium Valporate	Clobazam	Levetiracetam	Topiramate	Lamotrogine	Phenytoin	Gabapentin	Other
1	X			X					
2						X			
3					X				
4		X				X		X	X
5									
6					X				
7						X			
8						X			
9	X			X					
10				X			X		
11			X			X		X	
12	X	X				X	X		X
13		X							
14									
15			X			X			
16						X			
17	X					X			
18	X	X				X	X		X
19				X					
20	X			X					X
21	X					X	X		
22					X	X			

Table 6.1. Concomitant epileptic medication (other than VGB).

Patient number	Visual acuity Right eye	Contrast sensitivity measurement				Visual acuity Left eye	Contrast sensitivity measurement			
		3 cycles/ degree	6 cycles/ degree	12 cycles/ degree	18 cycles/ degree		3 cycles/ degree	6 cycles/ degree	12 cycles/ degree	18 cycles/ degree
1	0		✓			0				
2	-0.1					-0.2				✓
3	-0.2	✓	✓			-0.2	✓	✓	✓	
4	0.04	✓	✓	✓	✓	0.1	✓	✓	✓	✓
5	AMBLYOPIC	AMBLYOPIC	AMBLYOPIC	AMBLYOPIC	AMBLYOPIC	0.12	✓	✓	✓	✓
6	0.04	✓	✓	✓	✓	0.04		✓	✓	✓
7	-0.1	✓	✓	✓	✓	-0.1	✓	✓	✓	✓
8	0.02					0.02				
9	0.04	✓	✓	✓	✓	0.04	✓	✓	✓	✓
10	0.04	✓	✓	✓		0.04	✓	✓	✓	
11	0	✓	✓	✓	✓	0	✓	✓	✓	
12	0.04					0				
13	0.16	✓	✓	✓		0.08	✓	✓	✓	
14	0.02		✓	✓	✓	0.12	✓	✓	✓	✓
15	0.04	✓	✓	✓	✓	0.04	✓	✓	✓	✓
16	0	✓	✓	✓		0.2	✓	✓	✓	✓
17	-0.18					-0.24			✓	
18	0	✓	✓	✓		0	✓	✓	✓	
19	0			✓		0.08	✓	✓		✓
20	0	✓	✓	✓	✓	0	✓	✓	✓	✓
21	0.06	✓	✓	✓		0.04	✓	✓	✓	✓
22	0.06	✓	✓	✓	✓	0.06	✓	✓	✓	✓
% OF EYES SHOWING ABNORMALITY		66.7%	76.2%	71.4%	42.9%		72.7%	77.3%	77.3%	59.1%

Table 6.2. Showing the visual acuity and contrast sensitivity measurement of 43 eyes.

	Contrast sensitivity spatial frequency			
	3 cycles/degree	6 cycles/degree	12 cycles/degree	18 cycles/degree
Severity white-white perimetry	p = 0.484	p = 0.354	p = 0.841	p = 0.058
Severity SWAP (analysed using the empirical database)	p = 0.710	p = 0.349	p = 0.886	p = 0.840
Severity FDT	p = 0.891	p = 0.165	p = 0.926	p = 0.235

Table 6.3. Table showing the correlations between the severity of visual field loss using three protocols, and contrast sensitivity measurement at each of the spatial frequencies.

Participant number	White-white perimetry	SWAP (analysed using the empirically derived normal database)	SWAP (analysed using the extrapolated normal database)	FDT
1	No defect	**Defect**	**Defect**	No defect
2	No defect	No defect	No defect	No defect
3*	**Defect**	**Defect**	**Defect**	**Defect**
4	**Defect**	**Defect**	**Defect**	**Defect**
5*	No defect	No defect	No defect	No defect
6*	**Defect**	**Defect**	**Defect**	**Defect**
7	No defect	No defect	No defect	No defect
8	No defect	No defect	No defect	No defect
9*	No defect	No defect	No defect	No defect
10	No defect	No defect	No defect	**Defect**
11	**Defect**	**Defect**	**Defect**	**Defect**
12*	No defect	No defect	No defect	No defect
13*	**Defect**	**Defect**	**Defect**	**Defect**
14*	No defect	No defect	No defect	No defect
15	**Defect**	**Defect**	**Defect**	No defect
16	No defect	No defect	No defect	No defect
17*	**Defect**	No defect	No defect	**Defect**
18	**Defect**	**Defect**	**Defect**	**Defect**
19*	No defect	No defect	No defect	**Defect**
20*	**Defect**	**Defect**	**Defect**	**Defect**
21*	No defect	**Defect**	**Defect**	No defect
22*	No defect	No defect	No defect	No defect

Table 6.4. Table showing the visual field abnormalities with white-white perimetry, SWAP analysed using the empirically derived normal database, SWAP analysed using the extrapolated normal database and FDT protocols for each patient. (* indicates those patients who were receiving VGB).

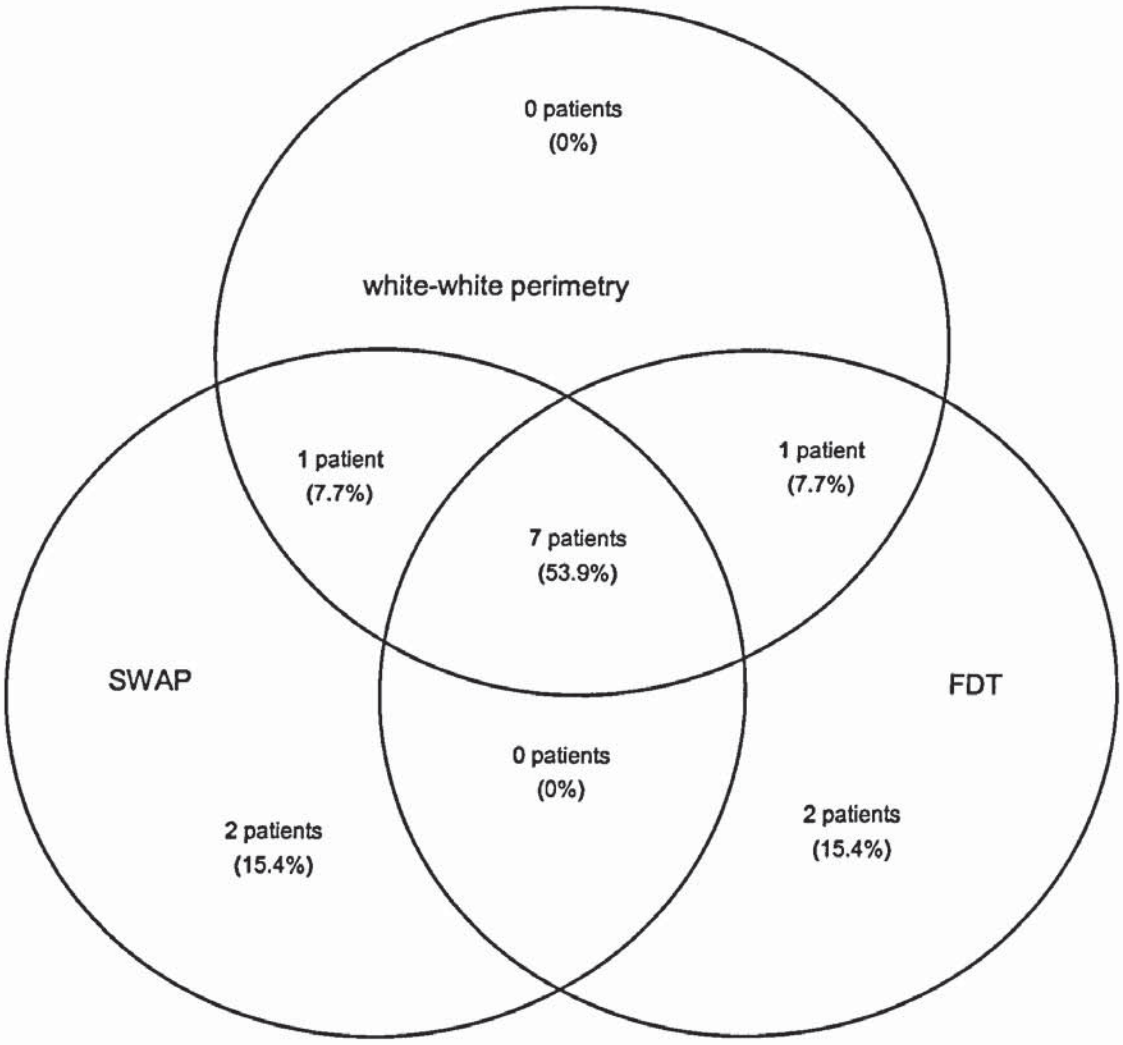

Figure 6.1. Venn diagram illustrating the relationship between three different types of perimetry in those patients demonstrating an abnormal field test. The number in brackets represents the percentage of abnormalities detected.

Algorithm	Group mean examination times (seconds)
White-White	898.5 (173.7)
SWAP	501.1 (63.5)
FDT	276.9 (21.1)

Table 6.5. Table showing the group mean examination times for each algorithm (standard deviation in brackets).

	FDT	SWAP
Sensitivity	88.9%	88.9%
Specificity	84.6%	84.6%

Table 6.6. Table showing the sensitivity and specificity for FDT and SWAP after assigning Full Threshold the "gold standard" for the detection of VGB-attributed field loss.

both FDT and SWAP, the results are presented in Table 6.6. Visual field loss was evident in both current and previous VGB recipients.

6.6. Discussion

6.6.1. Visual acuity and contrast sensitivity

No significant relationship between high-contrast visual acuity and visual field defect, defined by any type of perimetry was evident within the present study. These results highlight the need for a full comprehensive eye examination, as visual acuity measurement alone will fail to detect any abnormalities relating to VGB treatment. Contrast sensitivity is a measurement of a patient's ability to perceive differences in contrast over a range of spatial frequencies and has greater clinical sensitivity than standard measures of visual acuity. Previous investigators have reported contrast sensitivity to be more sensitive than high contrast visual acuity for detecting abnormalities associated with glaucoma (Hawkins *et al.*, 2003), cataract (Elliott, Hurst, & Weatherill, 1991; Elliott & Situ, 1998) and amblyopia (Lennerstrand & Lundh, 1984). Present results are concordant with earlier studies, as over 75% of the investigated eyes demonstrated an abnormal contrast sensitivity measurement for at least one spatial

frequency, despite normal high contrast visual acuity measurement (< 0.1)(Elliott & Situ, 1998; Hawkins *et al.*, 2003; Lennerstrand & Lundh, 1984). It is also evident from the results that contrast sensitivity deficits were detected in large number of patients who demonstrated no visual field abnormality through any of the perimetric testing strategies. This data strongly suggests that VGB has a large affect on visual performance even before abnormalities are detected through perimetry. The speed of this technique (approximately one minute per eye) combined with its high sensitivity suggest that this is an ideal tool for detecting VGB recipients for visual dysfunction, particularly if included as part of a screening battery of tests. A similar high prevalence of reduced contrast sensitivity is in agreement with the findings of (Roff Hilton *et al.*, 2002) suggesting that VGB produces a greater effect on visual function than was previously considered. Nousiainen, Kalviainen, & Mantyjarvi (2000) previously reported a significant correlation between contrast sensitivity deficits and severity of visual field loss in epilepsy patients receiving VGB. Their findings are particularly interesting as they suggest that contrast sensitivity might be an alternative technique, for monitoring those patients who are unable to carry out long complicated visual field examinations. Unfortunately, a significant correlation between contrast sensitivity deficits and severity of visual filed loss was not replicated in this study. Incongruities may have arisen because of the different perimetric techniques and contrast sensitivity measurements between the two studies.

6.6.2. Colour perception

Many investigators consider colour vision to be a useful indicator of retinal function. Such abnormalities may occur long before any other clinical sign is detectable. Investigations with the Farnsworth-Munsell 100-hue have previously revealed a non-specific impairment of foveal colour sensitivity in a proportion of the VGB-treated patients (Krauss *et al.*, 1998; Nousiainen *et al.*, 2000a; Nousiainen *et al.*, 2000b; Roff Hilton *et al.*, 2002). A selective blue impairment has been detected using colour perimetry, after a group of healthy volunteers were administered a single 2,000 mg dose of VGB (Mecarelli *et al.*, 2001). Previous findings indicate that VGB is associated with significant colour abnormalities (Krauss *et al.*, 1998; Mecarelli *et al.*, 2001; Nousiainen *et al.*, 2000a; Nousiainen *et al.*, 2000b; Roff Hilton *et al.*, 2002). With the exception of colour perimetry, these colour vision tests are measures of foveal function and as such do not reflect damage to the retina as a whole. It is not surprising therefore, that the Ishihara Plates and SPP2 plates are relatively insensitive techniques and failed to detect any abnormalities, even in patients with confirmed visual field defects.

6.6.3. Visual fields

The results from this study show a prevalence of white-white perimetry defects of approximately 41%. This finding is in agreement with a number of investigations, which used either Goldmann perimetry, or white-white perimetry to detect VGB associated abnormalities

(Daneshvar *et al.*, 1999; Miller *et al.*, 1999; Wild *et al.*, 1999a). Using SWAP and FDT together, shows a prevalence of visual field constriction of approximately 59%. This finding along with contrast sensitivity evidence provides further support to the hypothesis that white-white perimetry is a relatively insensitive technique for the detection of visual field loss. Therefore, a greater prevalence of abnormalities might be revealed if these sensitive examination procedures were employed.

Studies that use either Goldmann perimetry or white-white perimetry to quantify VGB associated field loss, document concentric contraction of the peripheral visual fields, with relative sparing both temporally and centrally. This information has led many investigators to concentrate on techniques which investigated the peripheral visual field. The relative insensitivity of white-white perimetry could mask underlying damage to the central visual field. It is now evident that central visual field damage occurs in patients undergoing anti-epileptic therapy (Krauss *et al.*, 1998; Manucheri *et al.*, 2000; Nousiainen *et al.*, 2000a; Perron *et al.*, 2002; Roff Hilton *et al.*, 2002). This study has shown that the short-wavelength sensitive pathway in the central ten degrees is significantly impaired in patients undergoing VGB treatment. Indeed, approximately 77% of the total abnormalities lie within the central 10-degrees. These findings confirm earlier reports from (Roff Hilton *et al.*, 2002) and are of particular concern clinically as central defects may arguably result in greater visual difficulties than peripheral abnormalities. The patient examples presented in Figures 6.2 and 6.3 highlight this clinical finding. In both patients white-white perimetry was comparatively less sensitive for detecting VGB-attributed visual field loss. The pattern of visual field loss, shown by SWAP and FDT, indicates that VGB produces diffuse visual field loss across the entire retina, including subtle central defects and more severe peripheral deficits.

Established visual field loss using conventional perimetry was evident in a number of patients who had ceased VGB treatment, before entering the study. The longest duration without VGB treatment was 98-months, suggesting that the visual field loss was at the very least persistent if not irreversible. Approximately 27% of the investigated patients yielded a different classification (normal or abnormal) for at least one of the visual field tests (Table 6.4). These incongruities may have arisen because the criterion that was used to define an abnormal visual field test was different between each type of perimetry due to the different stimulus configurations. Secondly, each type of perimetry used a different field size and algorithm strategy. Furthermore, and most significantly, each type of perimetry is based on a different psychophysical design. White-white perimetry is an achromatic response, mediated by the parasol and midget ganglion cells which terminate in the parvocellular and magnocellular layers respectively. The FDT illusion is mediated by the My retinal ganglion cell division of the magnocellular pathway. SWAP is mediated by the small midget bistratified ganglion cells (Dacey, 1993) which were originally thought to terminate in the parvocellular

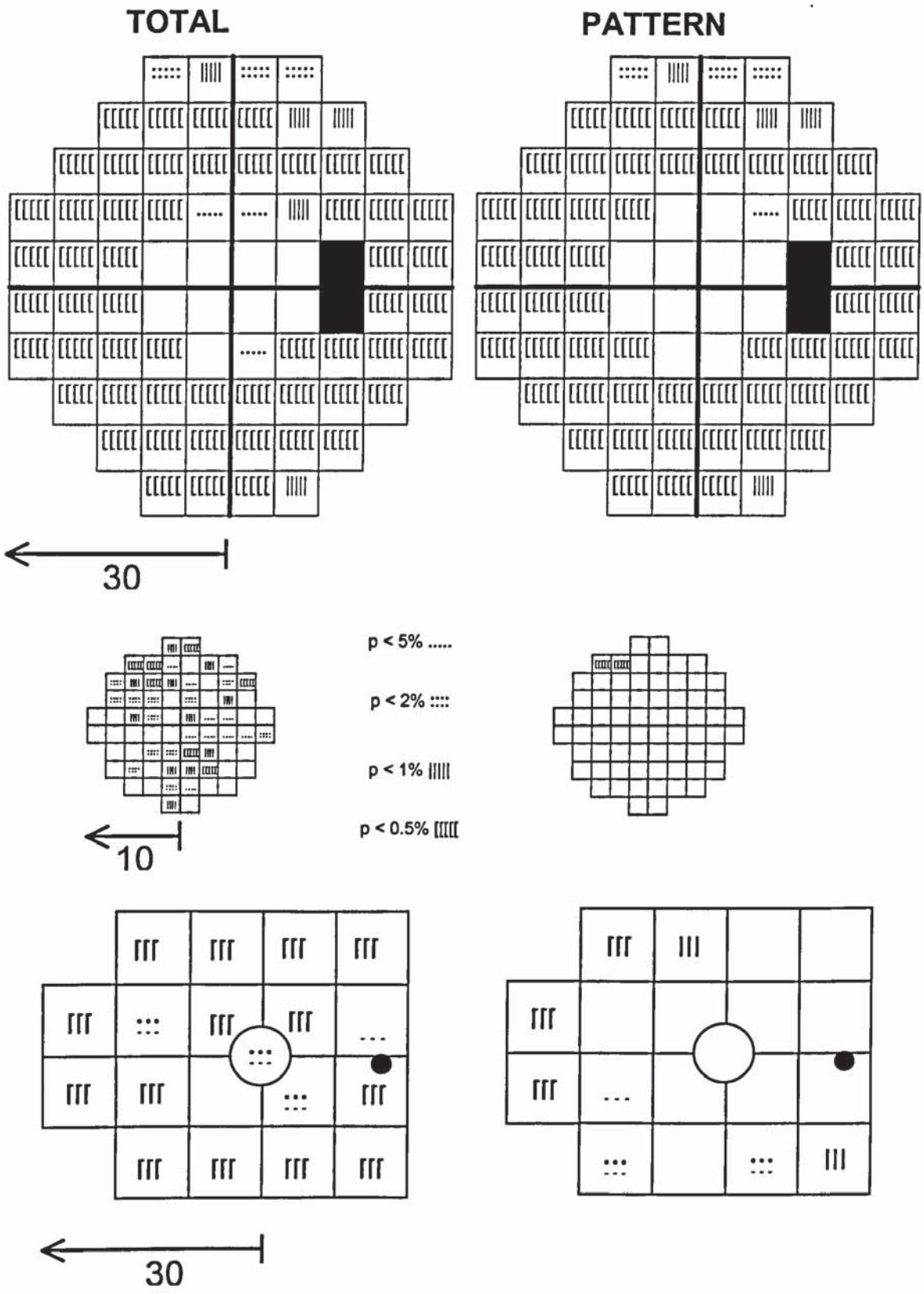

Figure 6.2. Illustration showing the Total and Pattern Deviation plots for the right eye of a 31 year old female (participant 3) exposed to VGB treatment, demonstrating severe visual field loss for white-white 30-2 (top), SWAP 10-2 (middle) FDT N30 (bottom).

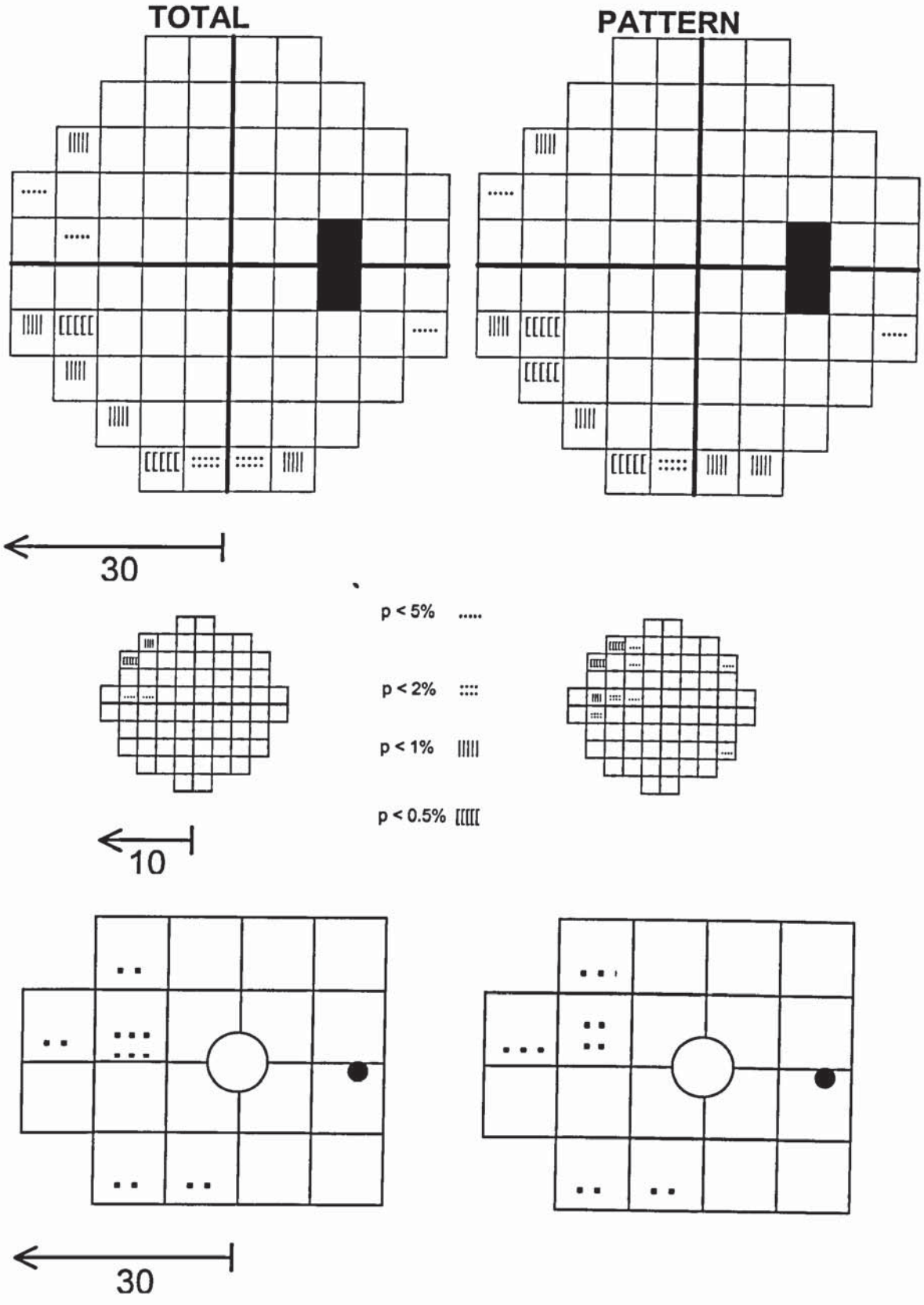

Figure 6.3. Illustration showing the Total and Pattern Deviation plots for the right eye of a 48 year old female (participant 20) exposed to VGB treatment, demonstrating mild visual field loss white-white 30-2 (top), SWAP 10-2 (middle) and FDT N30 (bottom).

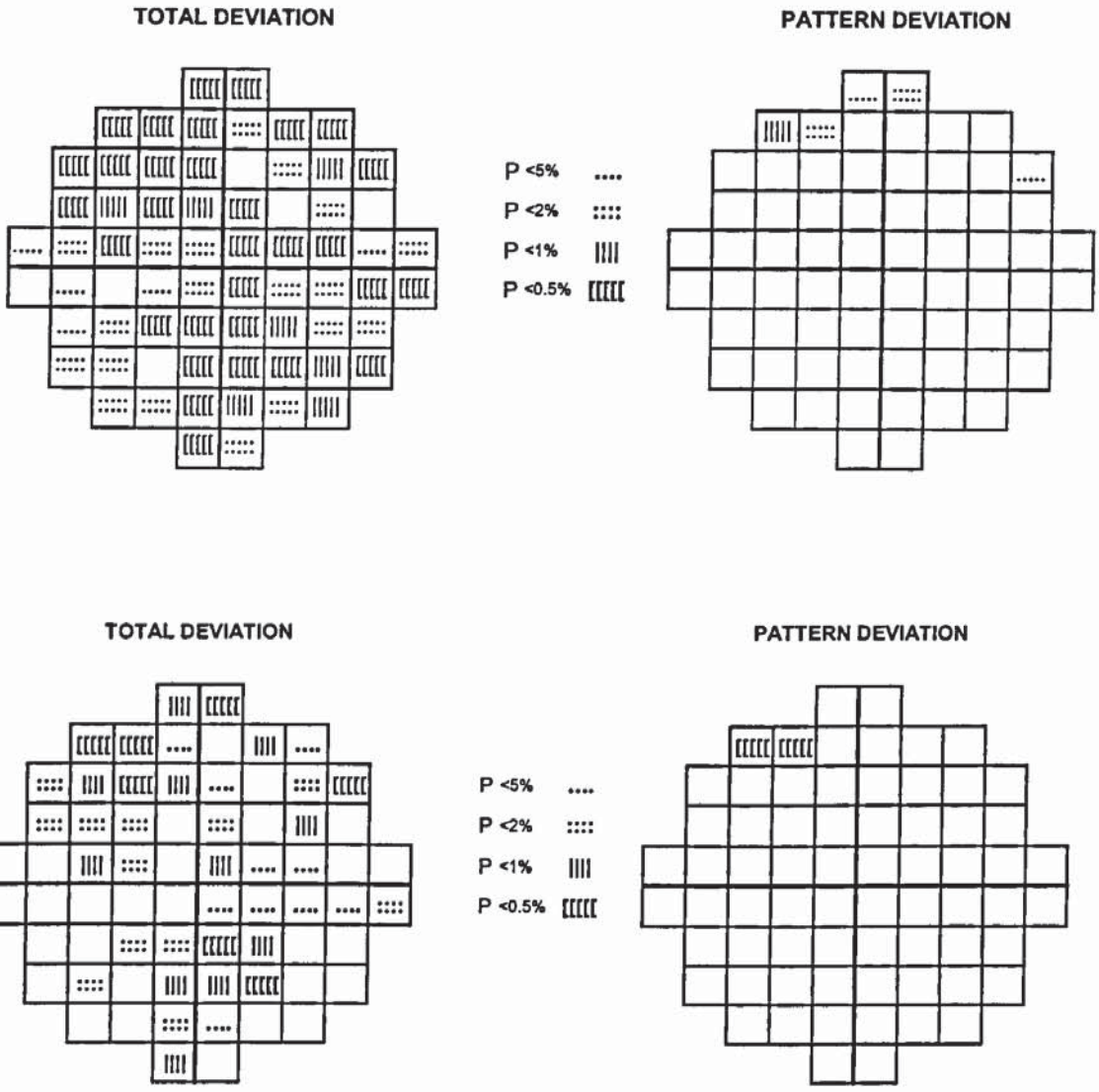

Figure 6.4. Schematic illustration showing the Total and Pattern Deviation plots for SWAP 10-2 analysed with an extrapolated database (top) SWAP 10-2 analysed with an empirical database (bottom) for the right eye of a 31 year old female exposed to VGB demonstrating severe visual field loss.

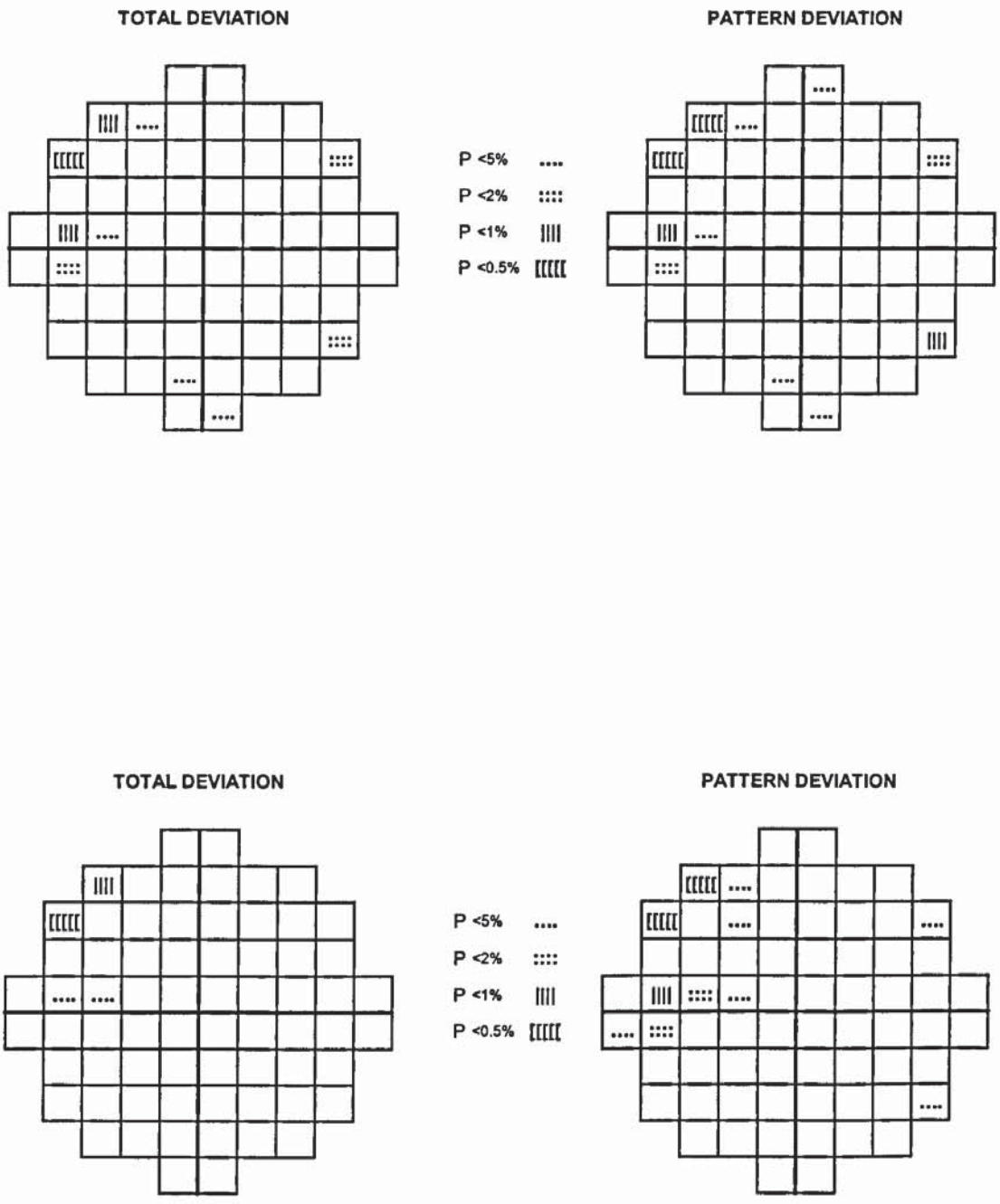

Figure 6.5. Schematic illustration showing the Total and Pattern Deviation plots for SWAP 10-2 analysed with an extrapolated database (top) SWAP 10-2 analysed with an empirical database (bottom) for the right eye of a 38 year old female exposed to VGB demonstrating mild visual field loss.

layers. However, recent work in primates now suggests that midget ganglion cells project to the interlaminar koniocellular layers (a third geniculocortical pathway; Martin *et al.*, 1997). In this study both SWAP and FDT strategies yielded high sensitivity (88.9%) and slightly reduced specificity (84.6%) when compared against the current "gold standard", white-white perimetry. SWAP and FDT's reduced specificity might be caused by both techniques detecting high numbers of false positive defects. Nevertheless, extreme care must be taken when analysing the sensitivity or specificity of a given technique. In this case, the assumption that white-white perimetry is the "gold standard" examination for the detection of VGB pathology could be incorrect. Individually, SWAP and FDT each detected 77% of the total abnormalities while white-white perimetry detected 69%. It is of particular interest to note that 100% sensitivity was achieved by carrying out both SWAP and FDT together. These results might therefore suggest that SWAP and FDT's lower specificity indicates that both examinations are more sensitive than white-white perimetry in terms of diagnosing abnormalities. In addition, evidence from glaucoma and macular eye disease studies, indicates that SWAP (Hudson *et al.*, 1998a; Johnson *et al.*, 1993b) and FDT (Yamashiro *et al.*, 2001), are capable of detecting visual field loss at an earlier stage than white-white perimetry. A number of theories exist to explain why these techniques are more sensitive than white-white perimetry.

Histological studies have shown that large optic nerve fibres are preferentially lost in glaucomatous eye disease (Quigley *et al.*, 1988). The larger ganglion cells are thought to be more vulnerable to mechanical and/or physiological insult as they are positioned at the weakest area of the optic nerve head and therefore more susceptible to damage (Miller & Quigley, 1988). It has been postulated that since ganglion cells mediating the SWAP pathway have larger diameters than other P-cells (Dacey, 1993) selective damage would result in preferential damage of the SWAP pathway (Quigley, 1994). This selective damage theory has become more controversial in recent years as psychophysical evidence now suggests that M-cells (cells that mediate the FDT illusion) are preferentially damaged (Anderson & O'Brien, 1997). An alternative explanation is the fragile receptor hypothesis which states that s-cones are in some way more vulnerable to damage by light, chemicals or retinal disease (Sperling *et al.*, 1980). The most probable hypothesis is that of reduced redundancy which suggests that damage equally affects all visual pathways, but is preferentially detected by the more redundant populations because of their relative paucity (Johnson, 1994). SWAP and FDT both test specific visual pathways and are thought to yield-increased sensitivity due to the relative redundancy of their target cell population.

Results have indicated that both the empirically derived and the extrapolated normal databases are equally effective for diagnosing and monitoring VGB-associated abnormalities, as each database revealed the same classification (Table 6.4) or overall severity level ($p < 0.001$). An example of two patients demonstrating SWAP 10-2 visual field

loss, when analysed with both databases is shown in Figures 6.4 and 6.5. Both patients showed similar diffuse and focal loss, regardless of the database which was used to analyse the results.

The examination times for both SWAP and FDT were significantly shorter than white-white perimetry. Increased examination times have clinical implications as they may lead to a degradation in the quality of the data due to patient inattention and fatigue (Hudson *et al.*, 1994). Patients with epilepsy typically fatigue easily because of the condition itself, side effects of their medication or additional health problems. Both SWAP and FDT offer a shortened examination time when compared to white-white perimetry and their high sensitivities lend themselves as a more effective screening procedure. Nevertheless, to achieve maximum sensitivity FDT and SWAP need to be carried out in combination wherever possible.

6.7. Conclusions

The primary clinical outcome for any epilepsy treatment is complete seizure control without inducing effects from the controlling medication. For the majority of patients this outcome is unobtainable and the efficacy of any drug must be weighed against its toxic side effects. It is of critical importance that an effective and sensitive screening procedure is available for those patients that continue to receive VGB, as a prompt diagnosis will enable clinicians and patients to make informed choices about their treatment. The findings from this study indicate that the current screening guidelines using white-white perimetry fail to detect subtle and therefore, early abnormalities associated with VGB. This study suggests that the recommended guidelines be amended in order to yield the earliest detection of visual function deficit due to VGB therapy and that all recipients undergo a screening battery consisting of contrast sensitivity, SWAP (Program 10-2) and FDT (Program N-30). The empirical and extrapolated databases appear to be equally suitable methods for analysing visual field tests.

7. Detection of retinal abnormalities in multifocal electroretinogram (mfERG) 1: defining a normal database.

Aim: To collect a normal database of mfERG results, which may be used to calculate whether responses from VGB-treated patients fall outside a normal range. **Methodology:** The sample comprised 17 clinically normal subjects (mean age 36.7 years ± 17.7 years). Each participant underwent standard white-white automated perimetry on one randomly selected eye, using Program 30-2 Full Threshold algorithm on the Humphrey Field Analyser. The test eye then completed one mfERG examination on the Visual Evoked Response Imaging System (VERIS). Responses were used to collate a normal database of results with which to compare responses from VGB recipients. A Kolmogorov-Smirnoff test was used to investigate whether the data from the normal study exhibited a Gaussian distribution. **Results:** None of the 17 subjects demonstrated abnormal white-white 30-2 visual field tests, defined by shape probability analysis in STATPAC. The amplitudes of both first- and second-order components tended to decrease with increasing distance from the fovea ($p < 0.001$). The amplitudes of both first-order components were generally larger in the nasal ($p = 0.013$ for N1: $p = 0.004$ for P1) and inferior ($p = 0.017$ for N1: $p < 0.001$ for P1) visual hemi-fields. The implicit times of both second-order components tended to be longer in the nasal visual hemi-field ($p = 0.001$ for 2P1: $p = 0.009$ 2N1). Results from the Kolmogorov-Smirnoff test indicate that the majority of test parameters were normally distributed. **Conclusions:** Results are comparable with previous mfERG studies carried out on clinically normal subjects and suggest that the mfERG is capable of the detecting damage to inner and outer retinal layers. As the majority of the mfERG parameters were normally distributed it was subsequently possible to utilise mean and standard deviation to compare against responses from VGB recipients.

7.1. Introduction

Electrophysiological evidence suggests that VGB is associated with significant abnormalities in the retina. A full-field ERG recording is the mass potential representing the summed electrical response of the cells across the retina (Hood, 2000). Summing the electrical activity across the retina results in a failure to detect areas of localised damage. A focal ERG recording is the mass potential representing the summed electrical activity of the cells in specific retinal areas. Time restrictions have meant that it is not feasible to measure a large number of retinal areas with this technique. The mfERG is a relatively new technique, which simultaneously records the electrical activity from multiple cone-driven areas, allowing over 100 retinal areas to be measured inside seven minutes (Hood, 2000). The mfERG might represent an efficient method of investigating VGB associated abnormalities in the retina.

A large volume of information now exists to suggest that mfERG amplitudes and implicit times are useful parameters for detecting a wide range of retinal abnormalities including: age-Related Macular Degeneration (Bearse & Sutter, 1996; Kretschmann *et al.*, 1998a), Retinitis Pigmentosa (Chan & Brown, 1998; Kondo *et al.*, 1995; Seeligr *et al.*, 1998), myopia (Kawabata & Adachi-Usami, 1997) and glaucoma (Chan & Brown, 1999; Hasegawa *et al.*, 2000). Investigations of diabetic retinopathy have revealed that the mfERG was successful in detecting cases of sub-clinical abnormalities (Mita-Harris, 2001). In addition the technique is reported to yield good reproducibility (Meigen & Friedrich, 2002).

The mfERG might also provide some useful topographical information about the pathophysiology underlying the treatment. First-order responses are believed to reflect the activity from the outer retina layers (Sutter & Tran, 1992), while (Bearse & Sutter, 1996) second-order responses are believed to reflect the activity from the inner retina (Bearse & Sutter, 1996; Palmowski *et al.*, 1997). VGB elicits an anti-epileptic effect by irreversibly binding itself to the active site of GABA aminotransferase, resulting in the inhibition of GABA breakdown and increasing the GABA concentration levels in the brain and retina. The drug produces proportionally greater increases in the GABA levels in the retina, when contrasted to those of the brain (Sills *et al.*, 2001). This relatively new technique may help to determine whether VGB is associated with a widespread toxic effect across the retina or is more specific to certain GABA-ergic cells. Amacrine horizontal cells, interplexiform cells, Müller cells and ganglion cells have all been identified as GABAergic (Crooks & Kolb, 1992; Djamgoz, 1995; Lam, 1997).

Before carrying out any investigations, into ocular disease, it is vital that each laboratory establishes or confirms normal values for its own equipment and patient population. This is particularly important in an mfERG recording, as the responses are vulnerable to small changes in testing protocols because of their small signal amplitudes. Therefore normal

values may not be transferred between laboratories as they are not directly comparable. The first part of the present study concentrated on determining the limits of normality for a group of clinically normal subjects.

7.2. Aims

To collect a normal database of results to be used to calculate whether any responses from VGB-treated patients fell outside a normal range. To determine whether the normal topographical variation of the mfERG across the retina compares to previous studies that were carried out on clinically normal subjects.

7.3. Methodology

7.3.1. Participants and inclusion criteria

Twenty-three normal subjects: 12 female 11 male (mean age 38.3 years; ± 16.7 years; range 22 to 75) were invited to take part in the study. Inclusion criteria consisted of logMAR visual acuity of 0.1 or better ((6/6 Snellen equivalent), distance refractive error of not greater than ± 6.00 dioptres of sphere or ± 2.5 dioptres of astigmatism, lenticular changes not greater than NC3, N03, C1or P1 defined using the Lens Opacities Classification System (LOCS) III (Chylack *et al.*, 1993), intraocular pressure less than 22mmHg in either eye, nil retinal pathology found by digital fundus photography (Image Net), absence of tritanopic colour vision defect (Standard Pseudoisochromatic Plates), no systemic medication known to affect the visual field, no previous ocular surgery or trauma, no history of diabetes or no family history of diabetes mellitus or glaucoma.

7.3.2. Ethics approval and informed consent

Written informed consent was obtained from all the participants (see section 2.3).

7.3.3. Experimental procedures: visual fields

On the first visit each participant completed one visual field test using white-white perimetry (white-white) program 30-2 Full Threshold, Goldmann stimulus size III on the Humphrey Field Analyser (Carl Zeiss Ltd, Hertfordshire, UK). The assigned eye, alternated between subjects but remained constant over the two visits (visual field and mfERG). The alternate eye was occluded and the appropriate reading correction was placed in front of the fixating eye. All participants had previously carried out at least one successful visual field test, the results of which were not included in the study. Catch trials of less than 20% fixation losses, less than 33% false positives and less than 33% false negatives were employed to ensure

reliability of patient responses. If any participant's results fell outside these criteria, they were removed from the study.

7.3.4. Experimental procedures: mfERG

After successfully completing their visual field test, participants were invited back for a second visit. Tropicamide 1% was administered to the selected eye, resulting in pupil dilation to a diameter greater than seven mm. Topical anaesthetic 0.4% Benoxinate Hydrochloride was administered to anaesthetise the cornea and reduce the blink reflex. The responses were recorded monocularly using a Dawson-Trick-Lizkow (DTL) electrode, which was placed along the lower tarsal membrane of the eye. A gold cup reference electrode was attached 1cm from the outer canthus of the tested eye. A double gold cup ground electrode was clipped onto the ipsilateral ear lobe. Before attaching the gold cup electrodes the areas of contact were cleaned with Omniprep, which is a mildly abrasive soap solution, used to lower skin resistance. To improve conductivity a small amount of gel was placed inside the cups. The untested eye was occluded and the patient was asked to place their chin on the chin rest where a trial lens of the appropriate reading correction was placed. The testing distance was adjusted for each patient, in accordance with his or her reading correction.

The participant was asked to fixate on a stimulus of multiple hexagons located on a CRT monitor. Each hexagon was scaled inversely with the gradient of cone receptors (response density scaled), so that focal responses of approximately equal amplitude were obtained (Sutter & Tran, 1992). The stimulus consisted of an array of 61-hexagons. At a testing distance of 40cm the stimulus size subtended a visual angle of 53.1 degrees horizontally and 41.1 degrees vertically. The hexagon pattern alternated from black/white in accordance with a pre-determined binary m-sequence, set at a frame rate of 75Hz. Each hexagon started at a different location along the m-sequence, cross correlation between the response cycle and the m-sequence enabled an extraction of local response contributions. The maximum luminance was 200cd/m^2 (white segment) the minimum luminance 3 cd/m^2 (black segment), which resulted in a contrast of approximately 97%. The luminance of the surrounding screen was set to that of the mean stimulus luminance. The signals were amplified with a signal processor (Grass Neorodata Acquisition System, model 12; Quincy, MA) set at 50,000 Hz and band pass-filtered with the high cut of set at 300Hz and the low cut of set at 10Hz. The signals were received via a personal computer (Macintosh Quadra 650, Apple, Cupertino, USA) and analysed using VERIS software (VERIS Science version. 4.9; EDI) (EDI, San Francisco, CA, USA). Each mfERG examination lasted approximately four minutes and was broken up into 16 segments lasting exactly 13.83 seconds. Segments contaminated by blinks or eye movements were eliminated and re-recorded.

Each participant's data was run through one-iteration of the system's off-line artefact rejection procedure. This procedure removes any signals that are more than 2SD away from

predicted data. In order to reduce noise, one-iteration of spatial smoothing was used, whereby each local ERG trace was averaged with one sixth of its neighbour. This setting meant that 50% of each trace came from its adjoining neighbours. The above testing protocol met the currently recommended ISCEV guidelines for mfERG recordings (Marmor *et al.*, 2003).

7.4. Analysis

7.4.1. Visual fields

Visual fields were classified for abnormality based on the depth and locations of diffuse and focal loss.

7.4.2. mfERG

Within each mfERG waveform, a series of peaks and troughs were evident. The amplitude of the first-order N1-wave was calculated as the voltage difference between the baseline and the first trough of each trace. The amplitude of the first-order P1-wave was calculated as the voltage difference between the first trough (N1) and the first peak of each trace. The amplitude of the second-order (first slice) 2P1-wave was calculated as the voltage difference between the base line and the first peak of each trace. The amplitude of the second-order (first slice) 2N1-wave was calculated as the voltage difference between the first peak (2P1) and the first trough of each trace. The implicit time was defined as the period from the time of stimulation to the peak of each wave as shown in Figure 7.1. The amplitude in each waveform was scaled to compensate for stimulus (response density scaled: size unit = nV/deg^2), as this measurement was thought to be amore accurate view of the actual response amplitude. Analysing responses from the trace arrays is usually difficult because individual traces are frequently contaminated with noise or very small in amplitude. It is often more useful to average together traces, which show similar response characteristics. Traces were averaged together into rings and quadrants as shown in Figure 7.2. This procedure was previously used by Chan & Brown (1999) in order to determine the mfERGs normal topographical variation across the retina.

7.4.3. Statistics

Repeated measures analysis of variance was used to determine whether there was any difference in response amplitudes or implicit times with increasing retinal eccentricity. This calculation had 4 levels, one for each ring. Student's paired *t*-tests were used to determine whether there was any differences in response amplitudes or implicit times between hemi-fields (nasal versus temporal; superior versus inferior). The results from both analyses are presented in Table 7.1 and 7.2. Pearson's correlation coefficient was used to investigate the

effects of age, on the response amplitudes and implicit times, in each of the four rings. A Kolmogorov-Smirnoff test was used to determine whether response amplitudes and implicit times were normally distributed in each of the four rings. Each of the analyses was repeated for all of the following parameters (N1, P1, 2P1, 2N1).

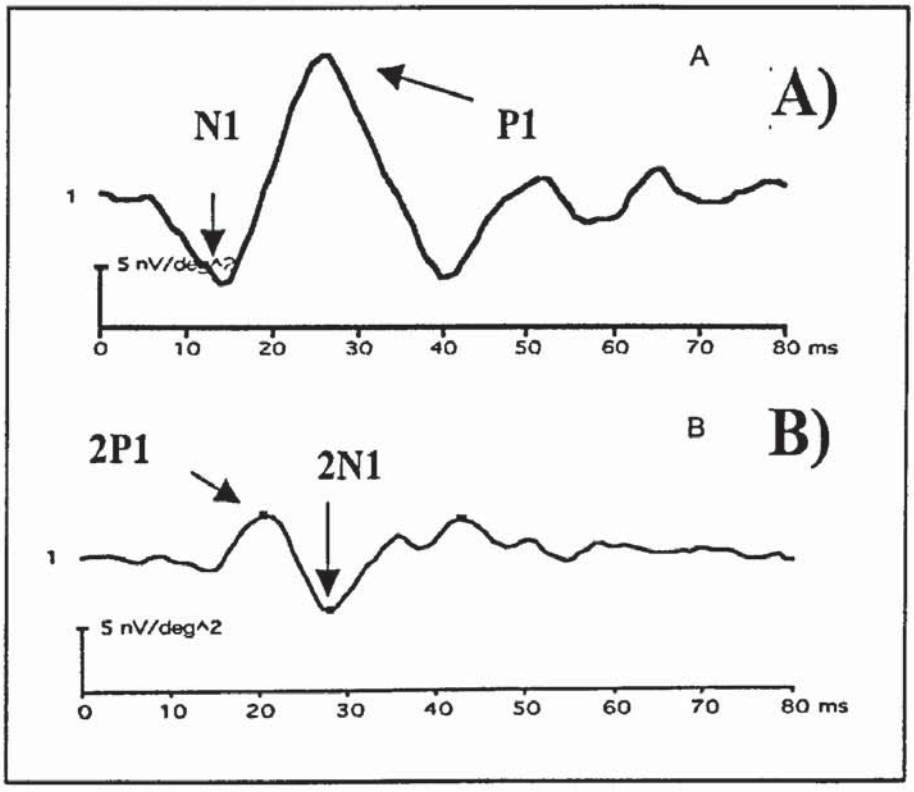

Figure 7.1. Multifocal electroretinograms from the left eye of a 26-year-old female. (**A**) An "All trace" wave obtained by averaging the sum of the waves of the first-order kernel. (**B**) An "All trace" wave obtained by averaging the sum of the waves of the second-order kernel.

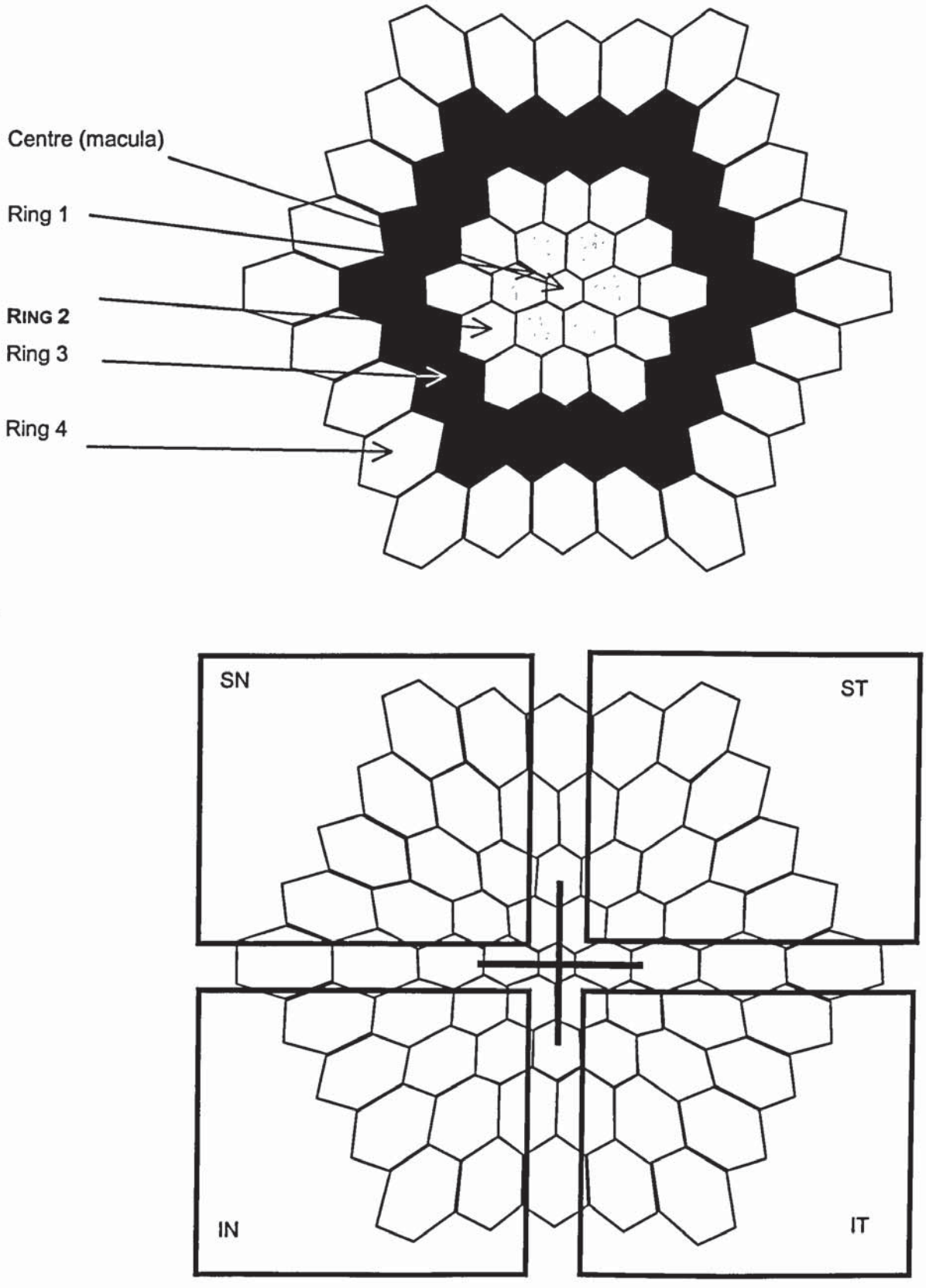

Figure 7.2. (Left) Schematic diagram of the 61 hexagonal stimulus pattern of the VERIS system with the four quadrant division (SN = superior nasal, ST = superior temporal, IN = inferior nasal, IT = inferior temporal visual field). (Right) The positions of the different regions (macula, rings 1 to 4) in the stimulus pattern adapted from Chan & Brown (1999).

7.5. Results

Six normal subjects were removed from the study, as they failed to successfully complete an mfERG recording due to repetitive blinking. Two subjects found the investigation uncomfortable and requested to leave, the other four subjects contaminated their records through repeated blinking. Consequently, 17 subjects: 12 female and 5 male (mean age 36.7 years; ± 17.7 years; range 22 to 75) remained in the study. On average the two visits were separated by 9 days; ± 5.8 days.

7.5.1. Visual fields

None of the 17 subjects demonstrated abnormal 30-2 visual field tests, defined by shape probability analysis in STATPAC and confirmed with Fundus photography.

7.5.2. mfERG

7.5.2.1. First order kernel: between rings

The amplitudes of both N1and P1 components tended to decrease with distance from the fovea 0 to 53.1 degrees (Figure 7.3). These differences were reported to reach statistical significance ($p < 0.001$ for both N1and P1). Inter-subject amplitude variation decreased with distance from the fovea as shown by the standard error bars in Figure 7.3. A statistical difference was also observed between the P1 implicit times and distance from the fovea ($p = 0.023$). No such difference was evident for N1.

7.5.2.2. First order kernel: between hemi-fields

The amplitudes of both first-order components were generally larger in the nasal and inferior visual hemi-fields (Figure 7.4). These differences reached statistical significance both nasally ($p = 0.013$ for N1: $p = 0.004$ for P1) and inferiorly ($p = 0.017$ for N1: $p < 0.001$ for P1). No statistical difference was observed between the implicit times for either component, across either visual hemi field See Table 7.1.

The amplitudes of all second order response components (2P1 and 2N1) were comparatively much smaller and more variable. In fact, in some central locations the waveform was unidentifiable. The central ring was subsequently not included in any analysis (first or second).

7.5.2.3. Second order kernel: between rings

The amplitudes of both second-order components tended to decrease with increasing distance from the fovea (Figure 7.5). These differences reached statistical significance ($p<0.01$ for 2P1 and 2N1). A statistical difference was also observed between the 2P1 implicit times across the retina ($p = 0.029$).

7.5.2.4. Second order kernel: between hemi fields

The amplitude of both components generally increased in the inferior visual hemi field Figure 7.6. These differences were reported to reach statistical significance ($p < 0.001$ for 2P1: $p = 0.039$ for 2N1). The implicit times of both components tended to be longer in the nasal visual hemi-field (Figure 7.7). These differences also reached statistical significance ($p = 0.001$ for 2P1: $p = 0.009$ 2N1). No statistical difference between superior and inferior hemi-fields and implicit times was evident.

7.5.2.5. Correlation with age

A null effect was found between age and all the parameters (N1, P1, 2P1, 2N1) in each of the rings that were investigated at the 5% significance level, with the exception of 2P1 amplitude ($p= 0.015$; adjusted $r^2=0.289$) in ring three and 2P1 amplitude ($p= 0.042$; adjusted $r^2=0.197$) in ring four.

	61 hexagon stimulus (first order)		
	Rings	Nasal/Temporal hemi field	Superior/Inferior hemi field
N1 amplitude	**p <0.001**	**p=0.013**	**p=0.017**
P1 amplitude	**p <0.001**	**p=0.004**	**p <0.001**
N1 latency	p=0.394	p=0.221	p=0.065
P1 latency	**p=0.023**	p=0.757	p=0.952

Table 7.1. Reporting the significant differences (p values) between the first-order waveforms across the retina.

	61 hexagon stimulus (second order)		
	Rings	Nasal/Temporal hemi field	Superior/Inferior hemi field
2P1 amplitude	**p<0.001**	**p =0.005**	**p=0.039**
2N1 amplitude	**p<0.001**	p =0.244	**p<0.001**
2P1 latency	p=0.072	**p =0.009**	p=0.123
2N1 latency	**p=0.029**	**p =0.001**	p=0.306

Table 7.2. Reporting the significant differences (p values) between the second-order waveforms across the retina.

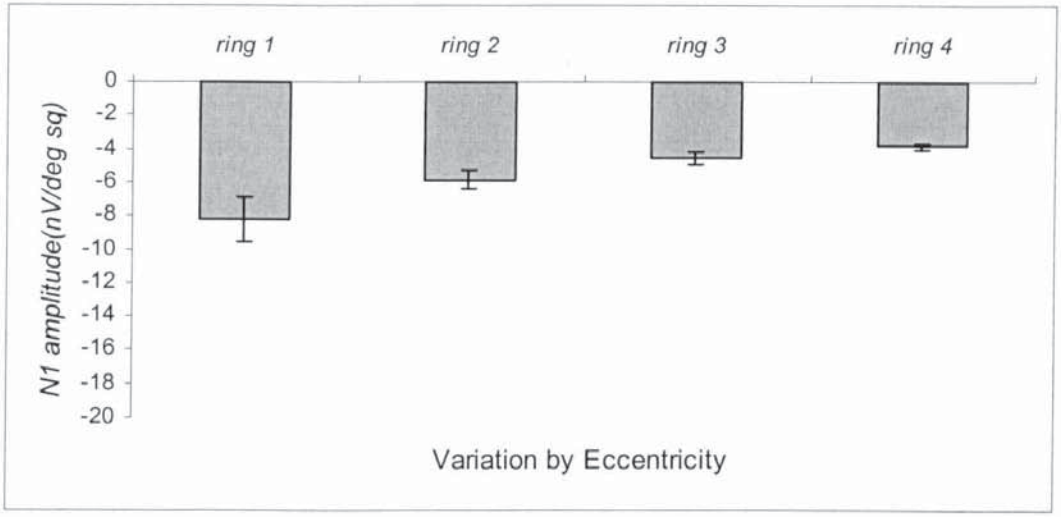

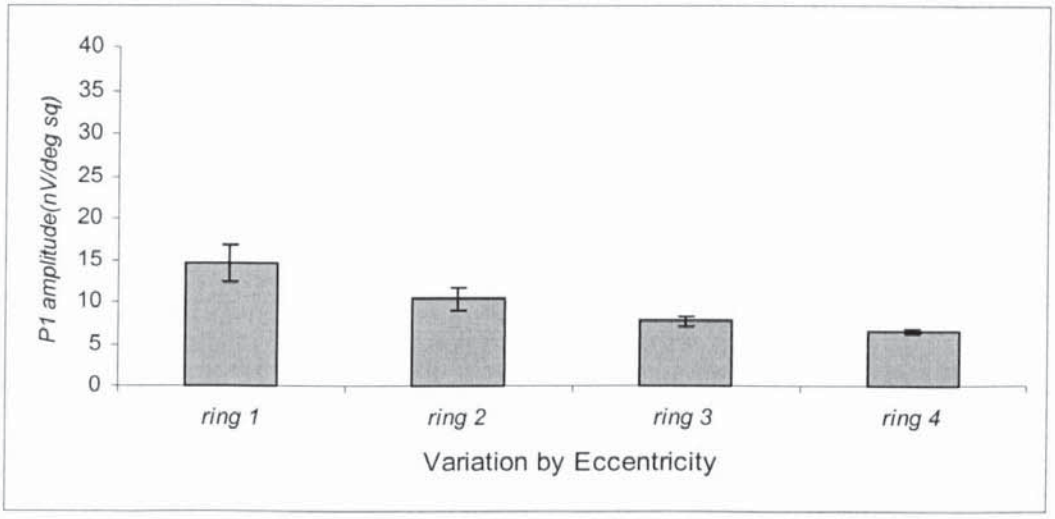

Figure 7.3. Mean and standard error of the N1-wave amplitude (upper) and the P1-wave amplitude (lower) in the 4 mfERG ringed locations

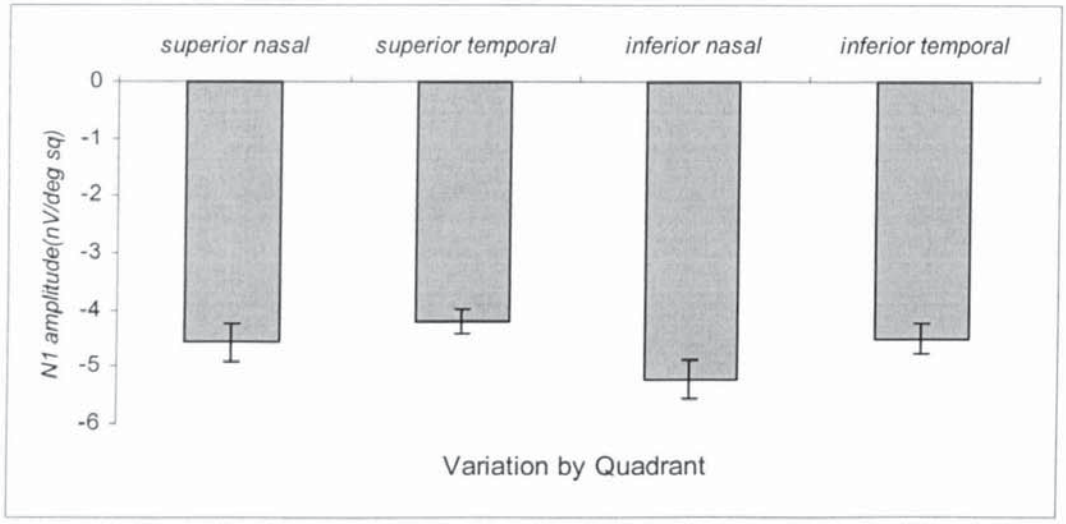

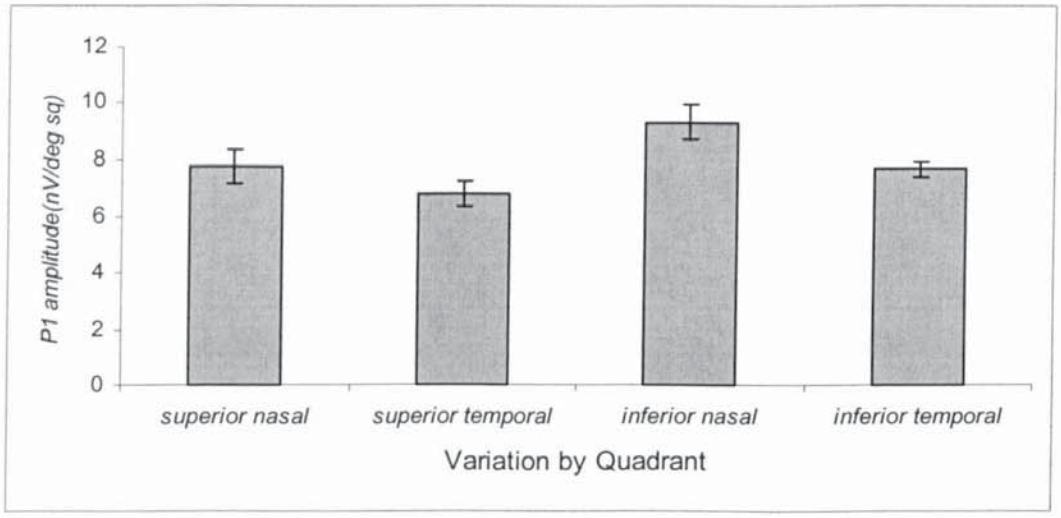

Figure 7.4. Mean and standard error of the N1-wave amplitude (upper) and the P1-wave amplitude (lower) in the mfERG 4 field quadrants.

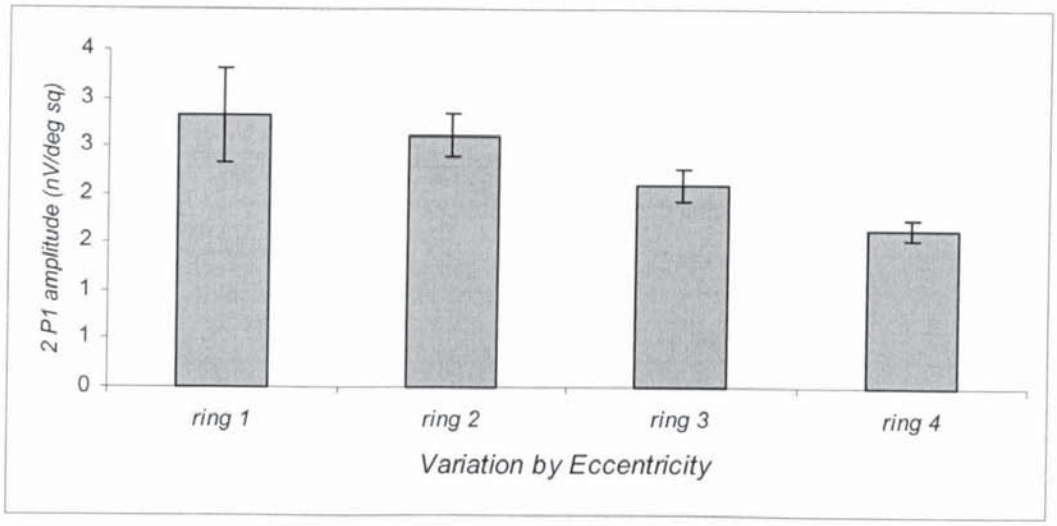

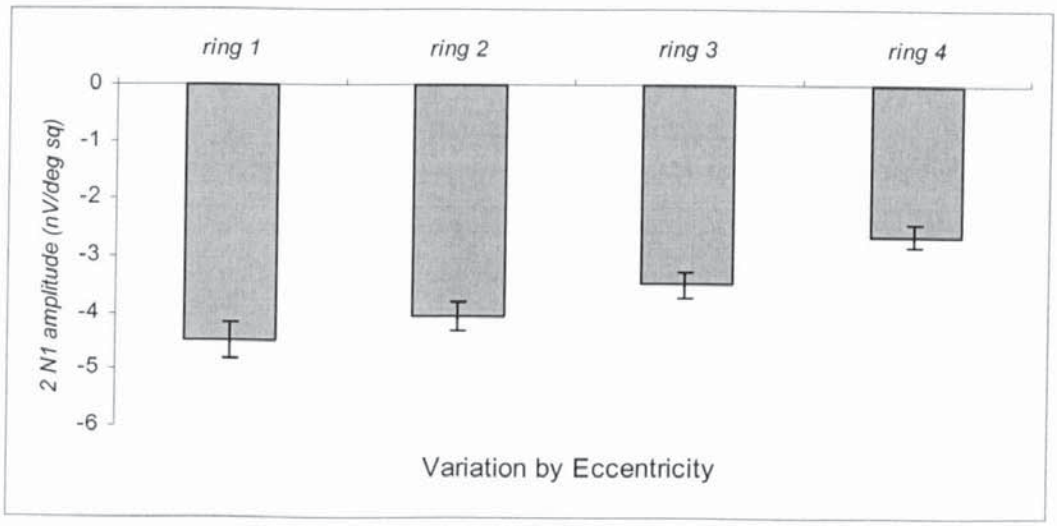

Figure 7.5. Mean and standard error of the 2P1-wave amplitude (upper) and the 2N1-wave amplitude (lower) in the 4 mfERG ringed locations.

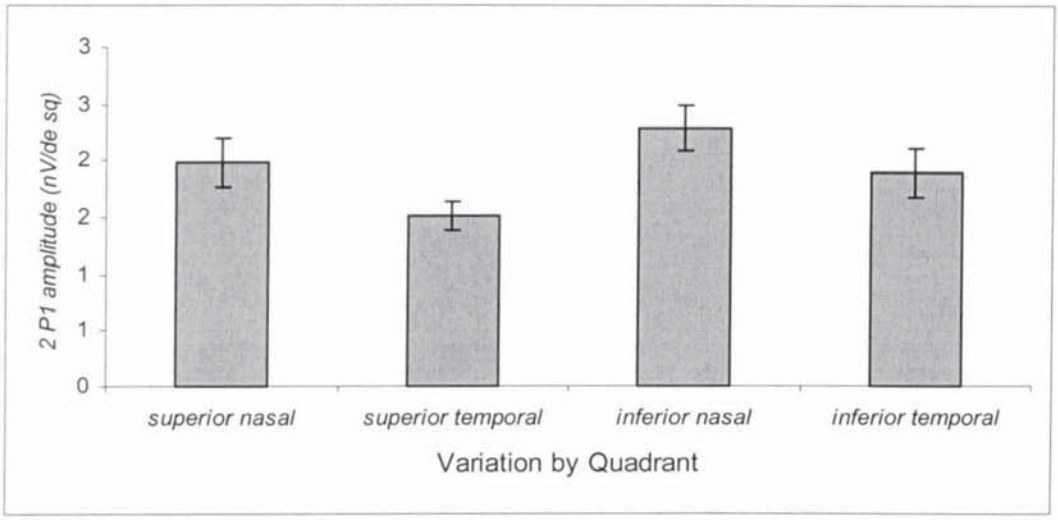

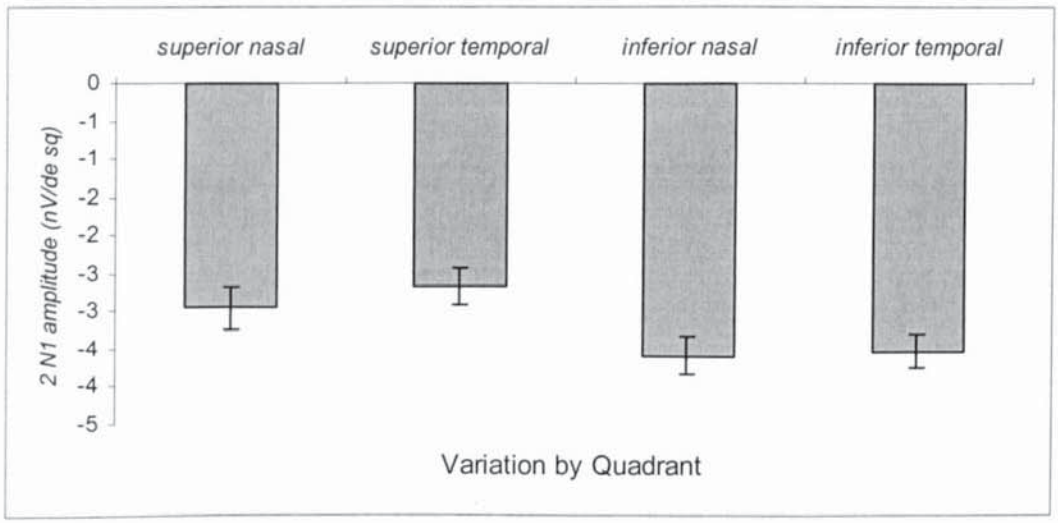

Figure 7.6. Mean and standard error of the 2P1-wave amplitude (upper) and the 2N1-wave amplitude (lower) in the 4 mfERG field quadrants.

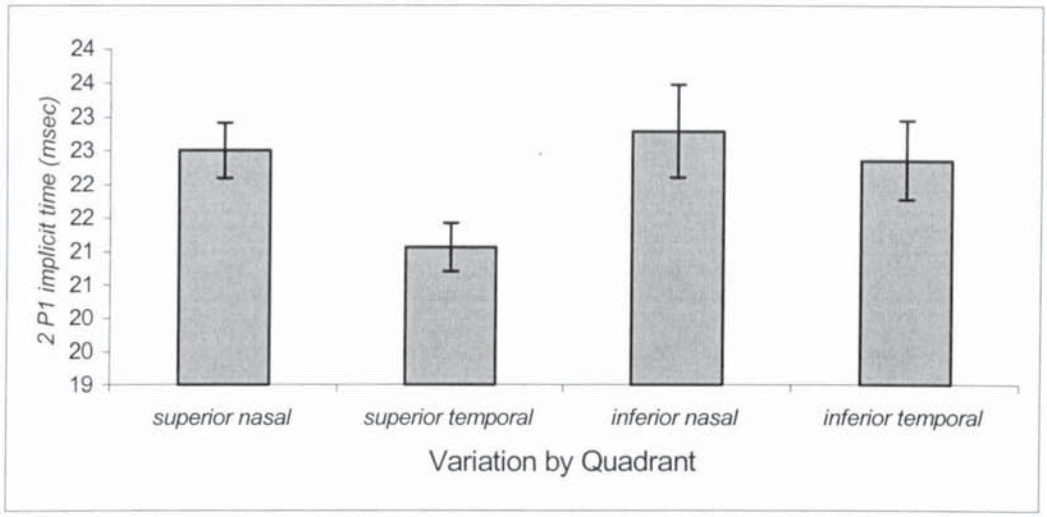

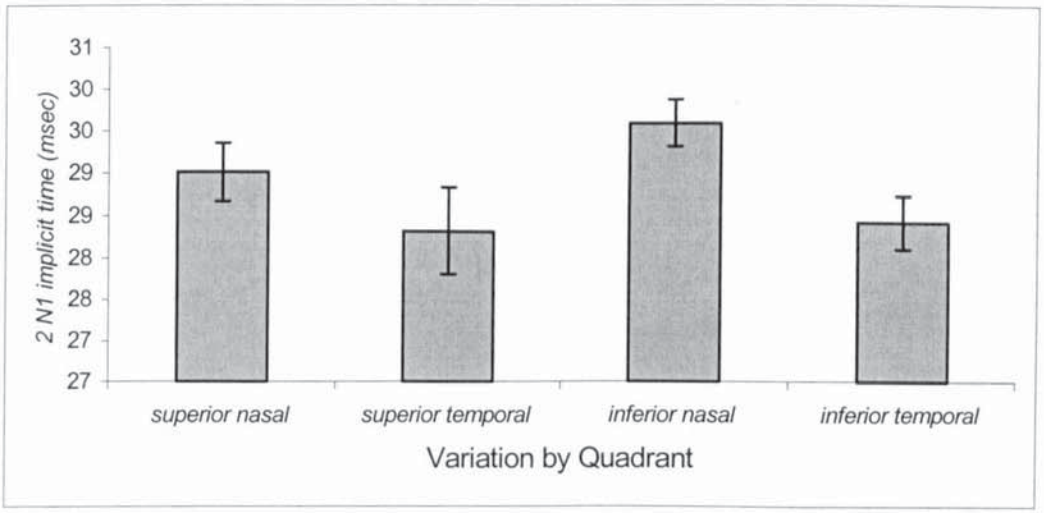

Figure 7.7. Mean and standard error of the 2P1-wave implicit time (upper) and the 2N1-wave implicit time (lower) in the 4 mfERG field quadrants.

7.5.2.6. Statistical test for normality

A Kolmogorov-Smirnoff test was used to determine whether the centiles of the observed data matched the centiles in a normal distribution. The results suggest that for all the test parameters in each ring the data was normally distributed, with the exception of the implicit time of N1 in ring three and 2 P1 in ring four. However, visual inspection of the frequency distribution curve for these two factors revealed that it was close to normal.

7.6. Discussion

The primary aim was to collect mfERG data, from clinically normal subjects, in order to provide a database with which to compare responses from VGB recipients. First-order (N1,P1) amplitudes and P1 implicit times were largest at the fovea and then decreased with increasing eccentricity. Present findings are concomitant with the majority of mfERG evidence from clinically normal subjects (Nagatomo *et al.*, 1998; Sutter & Tran, 1992). These authors have postulated that the amplitude reduction reflects the normal decline in cone photoreceptor densities across the retina. Second-order (2P1,2N1) amplitudes and 2P1 implicit times also decreased with eccentricity, the reduction appears to approximate the decline of human ganglion cell densities across the retina (Curcio *et al.*, 1990). Present findings along with a prior knowledge of normal topographic variation of cell populations across the retina, have suggested that the mfERG is a technique that is capable of detecting abnormalities in the inner and outer retinal layers. Conversely, Yoshii *et al.* (2001) concluded that second-order responses do not reflect inner retinal activity. Closer analysis of their methodology reveals that individual response amplitudes were plotted against ganglion cell density, which suggests that their experiment was particularly vulnerable to noise contamination.

Inter-subject amplitude variation was highest at the fovea and then decreased with increasing eccentricity. This finding is unsurprising, as the largest inter-subject cone density variation was reported at the fovea (Curcio & Allen, 1990). Alternatively, inter-subject variability might have decreased towards the peripheral field, as these waveforms were averaged with the largest number of hexagons and were consequently less vulnerable to artefacts caused by noise contamination. Lower inter-subject variability means that narrower confidence limits of normality are produced and a proportionately lower reduction in sensitivity is necessary before a reduction in sensitivity was recognised as abnormal. Present findings suggest that the mfERG might be a particularly sensitive tool for detecting peripheral abnormalities.

First (N1,P1) and second-order (2P1,2N1) amplitudes were significantly larger in the temporal retina (nasal visual hemi-field) and their waveforms became narrower and taller with increasing distance from the optic disc. Present variations concur with a number of

studies, whose protocols included a stimulus set at 50% contrast (Hood *et al.*, 1999; Hood *et al.*, 2000). Authors have suggested that these variations reflect an inner retinal contribution, which is generated by the ganglion and amacrine cells. They have also suggested that these contributions are accentuated when a stimulus of lower luminance or 50% contrast is used. The protocol that was used in the present study included a stimulus with high luminance and high contrast. The responses were recorded with DTL electrodes, which are known to reduce response amplitudes when compared to bipolar contact lens electrodes (Mohidin *et al.*, 1997). Present findings suggest that protocols that lower signal amplitudes also increase the detection of an inner retinal contribution, however, they also make each recording more vulnerable to noise.

First (N1,P1) and second-order (2P1,2N1) amplitudes were statistically larger in the upper retina (inferior visual hemi-field). Multifocal ERG studies (Chan & Brown, 1999; Nagatomo *et al.*, 1998; Parks *et al.*, 1997) focal ERG studies (Miyake *et al.*, 1989) and visual evoked potentials (Lehmann & Skrandies, 1979) concur with this finding, suggesting functional superiority in the upper retina. Lehmann & Skrandies (1979) have suggested that the superiority is an evolutionary adaptation to the greater importance of the inferior visual field to mammals. First-order (N1,P1) implicit times were similar across the entire retina, second-order (2P1, 2N1) implicit times were significantly longer in the temporal retina. Sutter & Bearse (1999) believe the second-order kernel originates from retinal ganglion cells as the implicit times were found to increase with distance from the optic nerve head. They have postulated that variations are caused by propagation delays (reduction in speed of signal transmission) in the unmyelinated fibres.

Correlations between age and the mfERG waveform have previously revealed controversial conclusions. Palmowski, Bearse, & Sutter (1997) have reported that age does not alter mfERG records (17 normal subjects aged 29-61). Conversely, Anzai *et al.* (1998) have documented a significant inverse correlation between amplitude and age in the central 2-8 degrees (33 subjects aged 14-72). Gerth *et al.* (2002) have recorded significant amplitude decreases and/or latency increases with age across the entire retina (71 subjects aged 9-80). Jackson *et al.* (2002) described amplitude reductions with increasing age, in the central 36-diameter field (46 subjects aged19-74). Present analysis appears to suggest that the majority of the investigated parameters (N1, P1, 2N1) were not influenced by age. The only exception to this finding was the 2P1amplitude in ring three and ring four. A normal age-decline in mfERG responses is expected to occur for several reasons: opacification and yellowing of the crystalline lens, pathology, senile miosis and cell loss. It is generally believed that a combination of both optical and neural factors produces the normal age-related changes (Gerth *et al.*, 2002). It is reasonable to assume that the present studies strict inclusion criteria, removed some of the normal age-decline, the small sample size might also have contributed to the failure to detect subtle age-related changes.

Second-order responses were noisy and considerably smaller in amplitude than first-order responses. Findings imply that care should be taken when analysing these waveforms because true pathology may resemble artefacts that are produced by noise. Future testing protocols could be designed to improve the signal-to-noise ratio by increasing the length of the m-sequence, lowering the number of stimulus elements or averaging together similar responses (Nabeshima, 2001; Yoshii *et al.*, 2001). Time pressures and limited patient numbers meant that repeat testing with the 61-hexagon stimuli was presently not possible. Averaging the traces into rings and quadrants however, helped to improve the detection of each signal.

The blind spot was not evident with any of the subjects recording. This finding is unsurprising as the optic nerve head is not expected to cover any one-stimulus patch particularly in the 61-heaxagon recording (Hood, 2000). An alternative postulation states that responses are detected at the optic nerve because this location reflects more light than other parts of the retina (Marmor *et al.*, 2003). The present studies modest sample size reflects the difficulty in recruiting subjects who were willing and capable of entering the study. Nevertheless, present numbers of subjects are comparable with previous mfERG studies where the controls ranged between five and 20 participants (Feigl, Haas, & El Shabrawi, 2002; Huang *et al.*, 2003; Meigen & Friedrich, 2002; Nagasaka *et al.*, 2003; Onozu & Yamamoto, 2003; Suzuki *et al.*, ; Yoshii *et al.*, 2001).

7.7. Conclusions

Present results are comparable with the majority of earlier mfERG studies carried out on clinically normal subjects and suggest that the mfERG is capable of the detecting damage to inner and outer retinal layers. The first–order responses appear to be correlated with the outer retinal layers the second-order responses appear to be correlated with the inner retinal layers. Care must be taken when analysing mfERG results, as the small amplitudes (second-order responses) are highly susceptible to contamination through noise. Analysis techniques which average traces which show similar response characteristics improves the detection of each signal and also make them less vulnerable to noise contamination (Palmowski *et al.*, 1997). Recently published mfERG ISCEV guidelines (2003) recommend that the median and 95% confidence interval limits are used, as electrophysiological data does not necessarily follow a normal distribution about a mean (Marmor *et al.*, 2003). Within the present study the majority of the mfERG parameters were normally distributed and it was subsequently possible to utilise mean and standard deviation to compare against responses from the VGB recipients. As parametric data affords the opportunity of identifying the position of a single point within the distribution, it was employed in the present study. This analysis technique was used successfully by Ponjavic & Andreasson (2001) to determine VGB-associated abnormalities. However, they only investigated the first-order kernel responses. Scalar

product analysis was also used, as this technique was reported to be less vulnerable to noise contamination (Keating *et al.*, 2000; Sutter & Tran, 1992).

8. Detection of retinal abnormalities in multifocal electroretinogram (mfERG) 2: VGB-attributed defects.

Aim: To evaluate the mfERG's ability for detecting VGB-attributed field loss and determine which parameters are primarily affected by VGB treatment. **Methodology:** The sample comprised 13 patients (mean age 40.2 years ±14.2 years) diagnosed with epilepsy and exposed to VGB therapy. Each participant underwent standard white-white automated perimetry on one randomly selected eye, using Program 30-2 Full Threshold algorithm on the Humphrey Field Analyser. The test eye then completed one mfERG examination on the Visual Evoked Response Imaging System (VERIS). The mean and standard deviation (SD) from the normal data was used to determine if any of the mfERG parameters fell outside the normal range. A participant's response was identified as defective if the averaged waveform in any ring was reduced by more than two standard deviations (SD) from normal. Scalar product field abnormality maps were also constructed by plotting reductions in waveforms that exceeded two and three standard deviations in scalar product (nV/deg sq) from normal. **Results:** Visual field defects were evident in five patients exposed to VGB treatment, these patients also demonstrated abnormal first- and second-order scalar product densities. In addition four patients, with normal visual fields, demonstrated abnormal second-order scalar product densities. The areas of visual field loss did not correspond to the defective scalar product areas. Abnormal mfERG responses were evident in both current and previously treated VGB recipients. **Conclusion:** The mfERG detects VGB-associated abnormalities which are not detected through investigations with white-white automated perimetry. The mfERG also provides useful topographical information about the pathophysiology underlying VGB. The location of the abnormalities indicates that VGB damages the photoreceptors, Müller, amacrine and ganglion cells.

8.1. Introduction

A number of studies have already investigated the mfERG responses in patients exposed to VGB (Besch *et al.*, 2000; Harding *et al.*, 2000a; Lawden *et al.*, 1999; Mackenzie & Klistorner, 1998; Ponjavic & Andreasson, 2001; Ruether *et al.*, 1998). The majority of evidence suggests that VGB is associated with reduced first-order amplitudes in the peripheral retina (Besch *et al.*, 2000; Harding *et al.*, 2000a; Lawden *et al.*, 1999; Mackenzie & Klistorner, 1998; Ponjavic & Andreasson, 2001; Ruether *et al.*, 1998). First-order kernel implicit times were reported as normal in two of the studies (Besch *et al.*, 2000; Lawden *et al.*, 1999). To date, only one study has attempted to investigate second-order kernel responses in VGB-treated subjects (Besch *et al.*, 2002). They reported delayed multifocal oscillatory potentials in all patients with confirmed visual field constriction and reduced first- and second-order kernel amplitudes in a proportion. The modest sample sizes, the majority of studies used less than 5 patients, and varied investigation parameters that are used in these studies suggest more research is still necessary with this technique. To date, none of the studies have suggested which parameter might be most useful for investigating subtle abnormalities associated with VGB.

8.2. Aims

To evaluate the ability of mfERG to detect VGB-attributed abnormalities and determine which parameters (retinal layers) act as primary indicators of damage.

8.3. Methodology

8.3.1. Patients and inclusion criteria

Seventeen patients: 14 female and 3 male (mean age 37.4 years; ± 15.78 years; range 18 to 65), presently or previously treated with VGB, were invited to take part in the study. Previous VGB recipients were included in order to determine whether the visual abnormalities were temporary side effects caused by VGB. Inclusion criteria included: logMAR visual acuity 0.1 or better (6/6 Snellen equivalent), distance refractive error of not greater than ±6.00 dioptres of sphere or ±2.5 dioptres of astigmatism or any known intra-cranial pathology which may effect the visual pathway or any unknown pathology which was unrelated to VGB therapy.

8.3.2. Ethics approval and informed consent

Written informed consent was obtained from all the participants. A detailed drug history was obtained from their hospital notes after requesting permission from the patient and their hospital consultant physician (see section 2.3).

8.3.3. Experimental Procedures: visual fields and mfERG

The protocol described for normal participants in section 7.3 was applied to epilepsy patients for visual field and mfERG examination. Results were compared to the normal database.

8.4. Analysis

8.4.1. Visual Fields

Visual fields were classified as normal or abnormal using criterion specifically designed for the interpretation of VGB-attributed visual field loss (Table 3.2; Wild *et al.*, 1999a).

8.4.2. mfERG

First and second-order responses were averaged into rings and their amplitudes and latencies measured using the same techniques that were described in section 7.4. Reponses were averaged into rings, as VGB is normally associated with concentric visual field loss. The mean and standard deviation (SD) from the normal data was used to determine if any of the mfERG parameters fell outside the normal range. A participant's response was identified as defective if the averaged waveform, in any ring, was reduced by more than two standard deviations (SD) from normal. Scalar product analysis was carried out as this type of analysis is advisable for studies that produce small amplitudes and poor signal-to-noise ratio (Keating *et al.*, 2000; Sutter & Tran, 1992). Scalar product field maps were constructed by plotting reductions in waveforms that exceeded two and three SDs in scalar product (nV/deg sq) away from normal.

8.5. Results

The mfERG responses were examined for all 17 patients exposed to VGB. Four patients were removed from the study, as they failed to successfully complete an mfERG recording due to repetitive blinking. Consequently, 13 patients: 10 female, 3 male (mean age 40.23 years; ±14.16 years; range 18 to 65) remained in the study. The two visits were separated on average by 10.76 days; ± 6.42 days. Patient's concomitant medication other than VGB is presented in Table 8.1.

8.5.1. Visual fields

All 13 subjects successfully completed their visual field examination. All visual fields were within the reliability criteria of <33% false positive and negative catch trials and <20% fixation losses. Five patients demonstrated visual field defects the results of which are presented in Table 8.2 & 8.3.

Patient number	Carbamazepine	Sodium Valporate	Clobazam	Levetiracetam	Topiramate	Lamotrogine	Phenytoin	Gabapentin	Other
1	X			X					
2							X		
3	X			X					
4						X			
5	X	X				X	X		X
6									
7				X					
8						X			
9	X	X				X	X		X
10					X				
11			X			X		X	
12	X								
13	X			X					X

Table 8.1. Concomitant epileptic medication (other than VGB).

8.5.2. mfERG

8.5.2.1. First-order responses

Normal first-order responses were evident for all patients with a normal visual field test. The results are presented in Table 8.2. P1 amplitudes were abnormal in four out of a possible five patients with confirmed visual field defects: the fifth produced an abnormally delayed P1 latency. N1 amplitudes were abnormal in two patients with confirmed field defects: a further four demonstrated abnormally delayed N1 latencies. All five patients with confirmed field defects also demonstrated abnormal first-order scalar product densities. For each participant the areas of visual field loss did not correspond to the defective scalar product areas (See Figures 8.1 & 8.2). Abnormal responses were evident in both current and previously treated VGB recipients.

8.5.2.2. Second-order responses

From the five patients with confirmed visual field defects: four demonstrated abnormal 2P1 amplitudes and latencies, three demonstrated reduced 2N1 latencies and 1 demonstrated abnormal 2N1 amplitude. The results are presented in Table 8.3. These patients also demonstrated abnormal second-order scalar product densities, however, the defective locations again did not correspond to the areas of visual field loss (See Figures 8.1 & 8.2). An additional four patients, with normal visual fields, demonstrated abnormal second-order scalar product densities. Abnormal second-order responses were evident in both current and previous VGB recipients.

Patient number	Age	Medication On/Off VGB	Visual field defect	First order kernel responses				
				N1 amplitude (nV/deg sq)	N1 latency (msec)	P1 amplitude (nV/deg sq)	P1 latency (msec)	Scalar product
1	49	On	-	-	-	-	-	-
2	18	Off	-	-	-	-	-	-
3	19	Off	-	-	-	-	-	-
4	40	Off	-	-	-	-	-	-
5	39	On	-	-	-	-	-	-
6	65	Off	-	-	-	-	-	-
7	24	On	-	-	-	-	-	-
8	42	Off	-	-	-	-	-	-
9	52	Off	Defect	-	Abnormal	Abnormal	-	Abnormal
10	29	Off	Defect	Abnormal	Abnormal	Abnormal	Abnormal	Abnormal
11	52	Off	Defect	Abnormal	Abnormal	Abnormal	Abnormal	Abnormal
12	45	On	Defect	-	Abnormal	-	Abnormal	Abnormal
13	49	On	Defect	-	-	Abnormal	-	Abnormal

Table 8.2. First–order results from the 13 VGB recipients, who successfully completed the study. Visual fields were classified using criteria which were specifically designed for the interpretation of VGB-attributed visual field loss (Wild *et al.*, 1999a). Multifocal ERG responses were identified as defective if the averaged waveform was reduced by more than 2 standard deviations (SD) from the normal in any ring.

Patient number	Age	Medication On/Off VGB	Visual field defect	Second order kernel responses				
				2P1 amplitude (nV/deg sq)	2P1 latency (msec)	2N1 amplitude (nV/deg sq)	2N1 latency (msec)	Scalar product
1	49	On	-	-	-	-	-	Abnormal
2	18	Off	-	-	-	-	-	-
3	19	Off	-	-	-	-	-	-
4	40	Off	-	-	-	-	-	-
5	39	On	-	-	-	-	-	Abnormal
6	65	Off	-	-	-	-	-	Abnormal
7	24	On	-	-	-	-	-	Abnormal
8	42	Off	-	-	-	-	-	-
9	52	Off	Defect	-	Abnormal	-	Abnormal	Abnormal
10	29	Off	Defect	Abnormal	-	-	Abnormal	Abnormal
11	52	Off	Defect	Abnormal	Abnormal	Abnormal	-	Abnormal
12	45	On	Defect	Abnormal	Abnormal	-	Abnormal	Abnormal
13	49	On	Defect	-	Abnormal	-	-	Abnormal

Table 8.3. Second-order results from the 13 VGB recipients, who successfully completed the study. Visual fields were classified using criteria which were specifically designed for the interpretation of VGB-attributed visual field loss (Wild *et al.*, 1999a). Multifocal ERG responses were identified as defective if the averaged waveform was reduced by more than 2 standard deviations (SD) from the normal in any ring.

8.6. Discussion

First-order amplitudes and/or latencies were abnormal in all the patients with confirmed visual field defects, suggesting that VGB damages the outer segment of the cone photoreceptors (Kretschmann *et al.*, 1998b). Findings are consistent with earlier reports of defective colour vision (Krauss *et al.*, 1998; Manucheri *et al.*, 2000; Mecarelli *et al.*, 2001), reduced visual acuity (Krauss *et al.*, 1998; Lawden *et al.*, 1999; Miller *et al.*, 1999), reduced 30Hz flicker (Harding *et al.*, 2000a; Harding *et al.*, 2002; Krauss *et al.*, 1998; Miller *et al.*, 1999) and reduced SWAP threshold sensitivity (Roff Hilton *et al.*, 2002).

Second-order responses were generally smaller in amplitude and more susceptible to noise contamination. Techniques such as ring averaging improved the quality of the responses and made the analysis less vulnerable to testing artefacts. Future studies might be designed to improve the signal quality further by using bipolar contact lens electrodes or increasing the recording time. However, as epileptic patients are particularly susceptible to fatigue the present study was limited by suitable examination times and the ability of the patients. Patient compliance was expected to worsen with the introduction of bipolar contact lens electrode, as they are inherently less comfortable than a DTL electrode. Present results indicate that the second-order amplitudes and/or latencies were defective in all the patients with confirmed visual field defects. Reduced second-order responses imply that VGB damages the inner retinal layers (ganglion, amacrine, Müller cells), a finding which concurs with the numerous reports of delayed oscillatory potential latencies (Besch *et al.*, 2002; Eke *et al.*, 1997; Harding *et al.*, 2000a). Other verification arises from animal studies which suggest that VGB leads to GABA accumulation in the glial Müller cells which exceeds their catabolic rate (Neal *et al.*, 1989) or a predominance of GABA transaminase in the peripheral glial cells (Pow & Rogers, 1996).

Abnormal first and second-order responses imply that VGB damages both the inner and outer retinal layers. Present findings are consistent with previous evidence from multifocal studies that have recorded abnormalities in the inner (Besch *et al.*, 2002) and outer (Harding *et al.*, 2000a; Lawden *et al.*, 1999; Ponjavic & Andreasson, 2001) retinal layers. Abnormal mfERG responses were evident in all patients with confirmed visual field loss, irrespective of whether the patients were currently receiving VGB. The evidence implies that the abnormalities were permanent retinal defects and not a temporary side effect such as an abnormal Arden Index (see section 1.11.5.1; Comaish *et al.*, 2002; Coupland *et al.*, 2001; Graniewski-Wijnands & Van der Torren, 2002; Harding *et al.*, 1999).

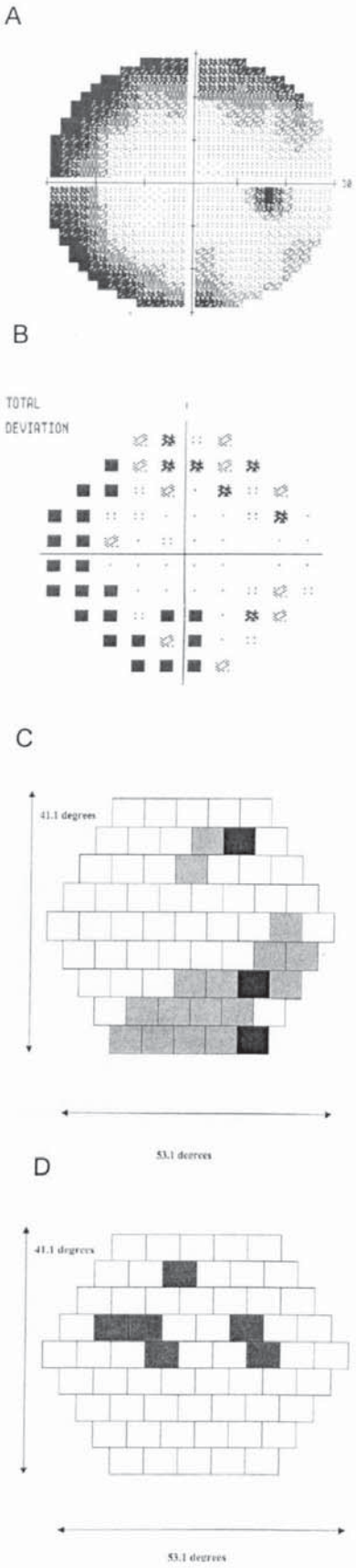

Figure 8.1. (A) The visual field (right eye) for a 54-year-old female patient showing moderate field loss attributed to VGB. (B) Total deviation probability map (C) Indicates abnormal first-order scalar response densities (D) Indicates abnormal second-order scalar response densities. White areas indicates responses in the normal range, grey areas indicates 2SD from normal and black areas indicates 3 SD from normal

A

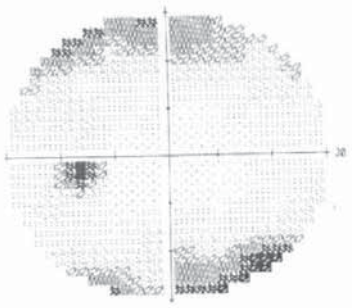

B

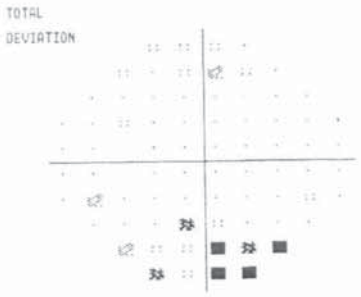

C

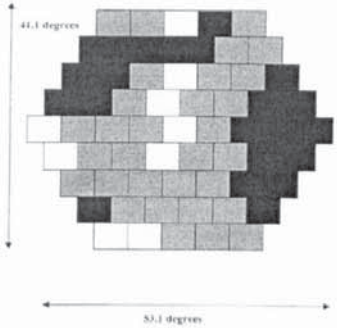

D

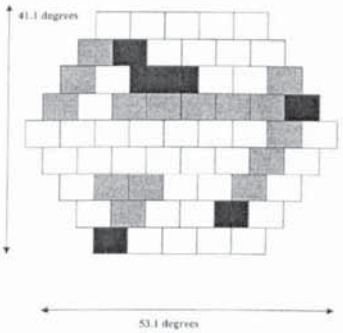

Figure 8.2. (A) The visual field (left eye) for a 51-year-old female patient showing mild field loss attributed to VGB. (B) Total deviation probability map (C) Indicates abnormal first-order scalar response densities (D) Indicates abnormal second-order scalar response densities. White areas indicates responses in the normal range, grey areas indicates 2SD from normal and black areas indicates 3 SD from normal.

First- and second–order scalar product abnormalities did not correlate with the areas of the visual field loss. In all cases, the scalar product abnormalities exceeded the areas of visual field loss (Figures 8.1& 8.2). These findings are unsurprising as the mfERG employs a different psychophysical design to white-white automated perimetry. White-white perimetry is thought to stimulate all the visual pathways, the mfERG in its present format, stimulates specific areas of the cone driven retina. The mfERG was consequently expected to yield higher sensitivity as it specifically targets a more redundant cell population in the retina (Johnson, 1994) and might therefore be more sensitive to mild abnormalities. Findings are consistent with two studies that reported either a reasonable (Harding *et al.*, 2000a) or similar (Lawden *et al.*, 1999) correlation between patient's first-order scalar product abnormalities and their visual field appearance. It is clearly evident from the patient examples documented in both studies (Harding *et al.*, 2000a; Lawden *et al.*, 1999) that mfERG first-order scalar product abnormalities exceeded the areas of visual field loss. All the patients who were classified with having visual field defects also demonstrated abnormal first- and second-order scalar product responses. It is of importance to note that abnormal second-order scalar product responses were identified in an additional four patients whose visual fields were classified as normal, these patients may be at risk of developing visual field defects on white-white perimetry. Findings probably indicate that the mfERG and in particular the second-order scalar responses are more sensitive than white-white perimetry in detecting the more subtle (possibly early) abnormalities. An alternative hypothesis is that second-order scalar responses are particular vulnerable to noise contamination and therefore false positive responses.

Four out of a possible 17 patients were not able to complete the recording because of repetitive blinking. The success of mfERG as a routine diagnostic tool appears to be slightly limited in certain participant groups (children or adults with learning disabilities). No statistical tests were attempted, as the small sample indicates that the results would have little scientific merit. Present numbers are comparable to the other studies which included an mfERG investigation (Besch *et al.*, 2002; Harding *et al.*, 2000a; Johnson *et al.*, 2000; Lawden *et al.*, 1999; Ponjavic & Andreasson, 2001) and their size probably reflects the difficulty in recruiting patients who are willing and capable of participating in such an investigation.

8.7. Conclusions

Present findings suggest that the mfERG is capable of detecting abnormalities associated with VGB treatment. Functional deficits in both the inner and outer retinal layers have implied that VGB damages the photoreceptors, Müller, amacrine and ganglion cells. Abnormal second-order scalar responses might indicate that the mfERG detects subtle abnormalities, which are not detected through investigations with white-white automated perimetry. Further

investigations using significantly larger numbers of VGB recipients however are needed to confirm this hypothesis. Different retinal layers may be affected at different stages within the disease however, with such small numbers this information was currently impossible to determine. Future investigative work should consequently aim to determine this information. The high sensitivity of mfERG must be weighed against its poor patient compliance (six participants failed to complete the normal study: four patients failed to complete the VGB study). The technique is consequently not advisable for use in routine clinical practice. As an investigative research tool however it does appear to have considerable advantages over white-white automated perimetry.

9. Discussion

9.1. Identification of risk factors for VGB-attributed visual field loss using a new quantitative algorithm for visual field classification.

It is clearly evident from this research that maximum VGB dose is significantly correlated with the severity of visual field loss measured using automated static white-white perimetry. This finding is of paramount importance because an immediate review of the manufacturer's recommended daily dose should take place. Currently, the maximum dose of VGB is based solely on the efficacy of the drug and not upon its toxicological side effects. There is a pressing need to carry out a longitudinal study which is specifically designed to investigate the pathological side effects of VGB, in relation to its maximum dose.

It is evident from the current literature that the design of research protocols needs to be more carefully considered. Previous investigations using perimetry to evaluate VGB therapy were open to examiner related bias, false positive results and the use of perimetric techniques which have long been established as having relatively poor sensitivity. To overcome many of these problems, a visual field protocol was designed in this work which included: exclusion criteria, reliability parameters, and methods for reducing an associated fatigue effect.

This research designed a quantitative method to classify the severity of visual field loss, which eliminates subjective judgements on the depth and severity of visual field loss and should therefore, overcome the limitations of the current visual field classification system. Using a standardised protocol should allow a more accurate comparison of the results between studies and enable a long-term analysis of the visual field progression, for those patients who continue to receive VGB. Analyses of a larger cohort of VGB-treated patients should enable statistically significant bandings differentiating between early, moderate or severe defects.

This research also highlights the importance of the application of the correct statistical procedures to the data. Previous investigators have failed to include maximum dose in their analyses and this omission has inevitably resulted in a number of incorrect assumptions being made about the significance of cumulative VGB dose. It is evident that all studies are limited to some extent by the numbers of participants who are of the required demographic and are willing to enter research studies. It is possible that this could have limited the statistical power with which these conclusions are drawn. The use of multi-centre studies, using standardised protocols is one method of increasing patient numbers, although this method could introduce increased variability into the examination procedure.

9.2. Evaluation of the SITA algorithm in the visual field analysis of patients exposed to Vigabatrin.

SITA Standard's reduced examination times, combined with excellent sensitivity and good specificity suggest that this algorithm is a useful alternative to the Full Threshold algorithm for the clinical diagnosis of VGB-attributed visual field loss. The algorithm may also prove to be an invaluable tool for the clinical investigation of other retinal abnormalities besides glaucoma. However, further investigations are necessary to investigate this hypothesis. The Full Threshold algorithm was the most sensitive algorithm in terms of repeatability followed by SITA Standard and SITA Fast, suggesting that the former algorithm is superior for monitoring the progression of those patients who continue to receive VGB treatment and are capable of carrying out the longer test. However, in a clinical situation where there are often time pressures, and in cases where the patient has a low level of concentration, SITA Fast offers a more rapid means of establishing VGB induced visual field loss. It should be remembered however, that the greater variability of the SITA Fast algorithm would be expected to make it more difficult to separate perimetric "noise" from visual field progression.

9.3. Validation of an empirically derived normal database for short-wavelength automated perimetry (SWAP) 10° visual fields: to classify VGB central defects.

SWAP has failed to gain wide spread acceptance in the routine clinical investigation of retinal disease due to its inherent greater between- and within-subject variability. It is known that this variability is lower in the central visual field (ten degrees). These results have shown that the 10-2 algorithm yielded lower between-subject variability, had lower examination duration and yielded less short-term fluctuation and between-subject variability than that previously documented for the SWAP 30-2 algorithm. These findings indicate that the SWAP 10-2 algorithm might yield higher sensitivity, superior efficiency and earlier diagnosis than its 30-degree counterpart and may therefore be particularly suited to the investigation of central retinal eye diseases, such as age-related macular degeneration, macular oedema and diabetes. It could also be applied to the investigation of other drug therapies which could potentially damage the central retina. Further research is still necessary to confirm this hypothesis.

The normal variation of threshold sensitivities between-subjects and within-subjects across the retina confounds the interpretation of visual field loss. The normal SWAP 10-2 database provided an effective method of differentiating SWAP defects in the VGB-treated population through enabling the calculation of age-corrected global perimetric indices and construction of probability maps for diffuse and focal visual field loss.

9.4. Investigation of Vigabatrin-attributed visual field defects with three clinical perimetric protocols.

This study has confirmed the clinical utility of Frequency Doubling Technology (FDT) and Short-Wavelength Automated Perimetry (SWAP) as techniques for detecting visual field loss attributed to VGB. Both tests offer a significantly shorter examination time and detected more VGB abnormalities when compared against conventional white-white automated static perimetry. SWAP has confirmed the presence of significant abnormalities in the central 10-degree visual field resulting from VGB therapy. Similarly, FDT yields more significant defects than conventional perimetry. These findings suggest that the prevalence of visual field damage in patients undergoing VGB therapy is significantly underestimated, as it was previously established with insensitive techniques which failed to detect these subtle abnormalities. Indeed, several patients exhibited normal visual fields with conventional perimetry but defective SWAP or FDT. Both findings are important as they considerably alter the risk-to-benefit ratio that is presently associated with the drug. Patients may not wish to continue treatment after being informed that the prevalence of VGB associated abnormalities is higher or that their central vision is also at risk to pathology. Further research to confirm the ability of SWAP and FDT for the detection of VGB abnormalities at an earlier stage than white-white perimetry is still necessary, using a larger sample of patients. Earlier diagnosis could therefore facilitate pathology detection prior to the irreversible abnormalities that are currently found when patients are investigated with conventional white-white automated static perimetry. If VGB therapy is withdrawn at this earlier stage, it might be possible to reverse the damage to the retina.

The empirically derived and the extrapolated normal databases are equally suitable methods for analysing VGB-attributed visual field loss. Extrapolating a normal database using the procedures described in (Cubbidge *et al.*, 2002) is a satisfactory alternative to collecting a normal database for the central ten degrees. The results suggest that the normal SWAP 30-2 database (currently provided in each Humphrey Field analyser) could be adapted to produce a normal SWAP 10-2 database using the same statistical techniques.

9.5. Detection of retinal abnormalities in multifocal electroretinogram (mfERG) 1: defining a normal database.

First- and second-order response amplitudes appear to be correlated with the distribution of photoreceptors and ganglion cells which are documented in the human retina (Curcio *et al.*, 1990; Curcio & Allen, 1990). This evidence in conjunction with the numerous articles which have reported the effects of various disease states on the inner and outer retina layers of the mfERG and the investigations of chemical isolation of cellular abnormalities using primate research all suggest that the mfERG is capable of detecting damage to inner and outer retinal layers (see Chapter 1). Abnormal first-order responses indicate that the pathology lies

within the outer retinal layers, abnormal second-order responses indicate that the pathology lies within the inner retinal layers. These findings indicate that the technique may be routinely used to help differentiate diseases that affect the outer retina from those that effect ganglion cell or the optic nerve. The technique enables quantification of the depth and severity of retinal abnormalities and may therefore be used to follow the progression of a disease or the effects of clinical intervention.

On the other hand, the mfERG is also known to suffer from a number of limitations. The technique requires a great deal of co-operation, several participants were removed from this study due to lack of comfort and/or repetitive blinking. The response amplitudes are particularly vulnerable to noise contamination. Further research is required to improve the mfERG's signal amplitudes as the second-order responses were particularly vulnerable to noise contamination. This could be achieved through increasing the length of the m-sequence, reducing the number of hexagons or using bipolar contact lens electrodes. Alternatively, greater contrast could be achieved using a different method of stimulus generation, e.g. using LED technology. LED technology could also lead to chromatic mfERG becoming a reality. The precise origins of the responses, in particular the non-linear (second-order) mechanisms, which shape the mfERG are currently unknown.

As the majority of the mfERG parameters yielded a normal Gaussian distribution, further studies can be analysed using standard parametric statistics. Other investigators have previously shown that the mfERG technique exhibits high reproducibility between-visits. There is however a pressing need to establish this finding using the equipment in the Department.

9.6. Detection of retinal abnormalities in multifocal electroretinogram (mfERG) 2: VGB-attributed defects.

The mfERG is a highly sensitive technique for identifying abnormalities associated with VGB therapy. The most sensitive parameter appears to be the second-order scalar response. These results suggest that this parameter could detect VGB pathology at an earlier stage than white-white perimetry, although a higher level of patient co-operation is required, which is often a problem in VGB patients. The abnormal first-order responses indicate that the VGB pathology is not specific to the GABAergic cells. Furthermore, the abnormal second-order responses suggest that the damage extends into the inner retinal layers. Damage to the Müller cells is particularly critical to VGB pathology, as GABA's inhibitory action is limited, via an active re-uptake into the pre-synaptic nerve terminals and surrounding glial cells. However, the reduced patient compliance of the mfERG technique unfortunately makes it less viable as a routine clinical tool. Nevertheless, future research is still required in order to determine the sequence of the damage to the different retinal layers in patients receiving

VGB. Establishing the mode of damage could enable VGB pathology detection before any irreversible damage has occurred.

9.6.1. Answering the original aims of the research

The findings of this research and existing literature (Chapter 1), suggest that it is highly probable that VGB affects the retina of a significant number of recipients to some extent. However, using current techniques, the pathology only becomes manifest after a considerable proportion of damage has already occurred. Pathological severity is correlated with maximum VGB dose, which is an unsurprising finding after considering the toxicological side effects which are regularly associated with the treatment. Elucidating the biological basis underlying the pathology is vital to understanding the visual field loss and preventing further abnormalities of this nature. It appears highly unlikely that the pathological occurrences relate to a direct action of the drug itself, as other GABA-T inhibitors have been associated with cases of intramyelinic oedema within a population of rats (John *et al.*, 1987). The most likely explanation is that inhibition of GABA-T augments a greater concentration of GABA in the retina and this increase results in the pathological changes. A particularly worrying aspect regarding this hypothesis is that the concentration of GABA within the retina might take several days to return to normal after administration of just a single dose of VGB (Richens, 1991). This sequence of events probably results in a cumulative build up of GABA in the retinal layers and excretion is highly dependent on a given patient's catabolic function. An investigation of GABA concentrations in the retina and the degree of pathological damage, could reveal a more complete relationship between severity of visual field loss and maximum VGB dose than has presently been reported. Such studies would necessitate finding accurate pathological markers in animal populations.

9.7. Future work

This research also suggests that alternative antiepileptic drugs (AEDs), particularly those based on the same principles as VGB (increasing GABA concentration), might also produce subtle abnormalities in visual function. Many of the currently prescribed antiepileptic drugs (AEDs) are already widely linked to various visual disturbances (Beran *et al.*, 1988; Cilio, Kartashov, & Vigevano, 2001; Fakhoury, Uthman, & Abou-Khalil, 2000; Foroozan & Buono, 2003; Kaufman, Lepore, & Keyser, 2001; Lopez *et al.*, 1999; Mecarelli *et al.*, 2001; Nousiainen *et al.*, 2000b; Paulus *et al.*, 1996).

9.7.1. Topiramate

Topiramate acts through a combination of different properties including modulation of the sodium channel activity and effects on the GABA and Alpha-amino-3hydroxy-5-mthyl-4-isoxazole receptors. This treatment was recently linked to several cases of acute myopia and

bilateral angle-closure glaucoma which was possibly linked to swelling of the ciliary body (Rhee, Goldberg, & Parrish, 2001; Sankar, Pasquale, & Grosskreutz, 2001). An isolated case of visual field loss in a 32-year-old female treated with Topiramate has been reported (Foroozan & Buono, 2003). However, after the treatment was discontinued the condition partially resolved.

9.7.2. Tiagabine

Tiagabine (TGB) is a new generation anti-epileptic medication whose mechanism of action results in selective inhibition of both neuronal and glial presynaptic GABA reuptake. The drug is frequently associated with symptoms such as: blurred vision, diplopia and difficulty in focusing (Fakhoury *et al.*, 2000). In one study abnormal colour perception was documented in approximately 50% of its recipients (Nousiainen *et al.*, 2000b). Occasional reports of visual field loss attributed to TGB have been produced since its introduction in the late 1990's (Beran *et al.*, 1988; Kaufman *et al.*, 2001). A retrospective review of 2531 clinical trial records reports that a total of eight patients demonstrated abnormal visual field loss when using visual field confrontation. For two of the patients the abnormalities were attributed to a brain lesion, for the other six patients the abnormality spontaneously resolved (Collins *et al.*, 1998). Using white-white automated static perimetry (Kalviainen *et al.*, 1999b) suggests that Tiagabine is not associated with any visual field loss.

9.7.3. Sodium Valporate

The effects of Sodium Valporate (VPA) are less well known. It has been shown to regulate the function of the T type calcium channel and/or the γ-aminobutyric acid-A receptor channel. A number of studies suggest that the treatment produces no adverse effects to retinal function (Bayer *et al.*, 1995; Lopez *et al.*, 1999). An isolated case of a 25-year-old female who presented with a visual field defect and was successfully treated firstly with Sodium Valporate and then later with Carbamazepine has been documented (Jung & Doussard-Lefaucheux, 2002). No other evidence of visual field loss attributed to the treatment is apparent.

9.7.4. Felbamate

This drug blocks currents evoked by N-methyl-D-asparate and facilitate GABAergic responses. Side effects such as diplopia (Cilio *et al.*, 2001) or blurred vision (Wilensky *et al.*, 1985) have been documented. In both studies, Felbamate was given as an add-on therapy, the side effects might therefore have been related to alternative AEDs.

9.7.5. Benzodiazepines

Benzodiazepine AEDs (diazepam, clonazepam and clobazam) enhance GABA-mediated increases in chloride conductance through increasing the frequency of the channel opening. In 1992, Elder (1992) reported on an isolated case of visual field loss which he attributed to diazepam treatment. The report was based on only two visual field examinations and might not have been very reliable. An investigation of 30 clinically normal volunteers that were administered single oral does of diazepam, revealed no obvious changes in their overall threshold sensitivity or short-term fluctuation, using standard white-white automated static perimetry using the Octopus perimeter. Occasional reports of acute glaucoma (Hyams & Keroub, 1977) and allergic conjunctivitis (Elmar & Lutz, 1975) have been reported. Stafanous *et al.* (1999) evaluated the log-term use of benzodiazepines on the eye and retina. They found that 63% of the investigated participants complained of irritation, burred vision or difficulty reading.

9.7.6. Barbiturates

Barbiturate AEDs (primidone phenobabrbitone) also enhance GABA-mediated increases in chloride conductance by increasing the frequency of the channel opening. Barbituates have been linked to pathology of the optic nerve (Hamard & Desbordes, 1982).

9.7.7. Carbamazepine

Carbamazepine is the standard anti-epileptic drug used for partial and generalised tonic-clonic seizures and works by inhibition of the voltage-dependent sodium channels. Reports of blurred vision (Meinardi, 1973), reduced contrast sensitivity (at all the spatial frequencies) (Tomson, Nilsson, & Levi, 1988) and abnormal colour perception (Lopez *et al.*, 1999; Mecarelli *et al.*, 2001; Nousiainen *et al.*, 2000b; Paulus *et al.*, 1996) have been documented. An accumulation of errors along the tritan axis (blue axis) is particularly evident when the Farnsworth Munsell 100-hue is carried out (Nousiainen *et al.*, 2000b; Paulus *et al.*, 1996).

9.7.8. Phenytoin

Phenytoin is a neuronal sodium channel agonist and tends to stabilise the hyper-excitability caused by excessive stimulation. Abnormal colour perception has been detected along the blue/yellow axis of the Farnsworth Munsell 100-hue in 77% of patients treated with Phenytoin (Lopez *et al.*, 1999). The results concur with those from Bayer *et al.* (1995) using both the Farnsworth Munsell 100-hue and the D-15 desaturated test. Other visual disturbances such as diplopia, oscillopsia (subjective sensation of oscillating objects; Remler *et al.*, 1990) and pathology of the optic nerve (Hamard & Desbordes, 1982), are occasionally reported.

9.7.9. Lamotrogine

Lamotrogine acts through inhibition of the voltage-dependent sodium channels, resulting in stabilisation of the presynaptic membrane and prevention of the release of excitatory neurotransmitters, especially glutamate. A study evaluating the efficacy of Lamotrogine in 566 patients diagnosed with refractory epilepsy reported that 8% of participants noticed episodes of transient diplopia (Arzimanoglou *et al.*, 2001). Cases of blurred vision also occur commonly (Burstein, 1995; Schachter *et al.*, 1995).

9.7.10. Gabapentin

Gabapentin was designed to be a GABA-mimetic drug, but its mechanism of action is not fully understood. The drug is used as a successful treatment for symptomatic pendular or gaze evoked jerk nystagmus (Bandini *et al.*, 2001). An open multi-centre study was used to investigate the efficacy and tolerability of Gabapentin in 599 patients diagnosed with epilepsy and uncontrolled seizures (Herranz, Sol, & Hernandez, 2000). A total of 19% of patients experienced adverse side effects including: somnolence (sleepiness), dizziness, headache, blurred vision, diplopia and nausea.

It is clearly evident from the studies outlined above, that most AEDs are associated with at least some visual disturbances. At the moment, it appears highly likely that the drugs that specifically act on the GABAergic pathway are particularly likely to cause visual disturbances. The most frequently reported symptoms appear to be blurred vision and diplopia. Despite these findings, there is little information available about a given recipients' contrast sensitivity or binocular control. To date, there is no consistent evidence to suggest that any of the AEDs, besides VGB, is associated with abnormal visual field loss. Nevertheless, it is important to remember that the majority of studies evaluating drug side-effects have used a questionnaire to evaluate the prevalence of visual disturbances. This method is insufficient for detecting mild-moderate visual field loss. Some studies have explored visual disturbances using white-white perimetry (manual or automated static), however this method most certainly failed at detecting subtle visual field loss. Abnormal colour perception was reported in a significant number of patients receiving various different AEDs. The Farnsworth Munsell 100-hue colour vision test appears to be the most sensitive technique for detecting these abnormalities. Results from section 6.5 suggest that both the SPP plates and the Ishihara will fail to detect mild abnormalities. Further research is still necessary to identify all of the visual side effects associated with each antiepileptic treatment and correlate them to the mode of action of the drug. Carefully designed protocols are required if the subtler abnormalities are to be detected. Suggested techniques would include an investigation of: ocular motility, colour perception (Farnsworth Munsell 100-hue), contrast sensitivity, FDT, SWAP using program 10-2 and the mfERG.

9.8. Conclusion

The *European Agency for the Evaluation of Medicinal Products* reviewed VGB in 1999. After investigating a pooled cohort of 335 VGB patients they suggested that prevalence of visual field constriction was approximately one third of the recipient adult population. This finding was based on the results of manual and automated white-white static perimetry alone. The pattern of visual field loss was described, as a concentric constriction of both eyes and central visual acuity was not impaired. From these findings, they recommended that the maximum daily dose of VGB should not exceed 3g/day. Additionally, each patient exposed to VGB should complete a visual field test with either standardised automated static perimetry (Humphrey or Octopus) or kinetic perimetry (Goldmann) before treatment is initiated and each patient be followed up at six-monthly intervals.

The findings from this thesis suggest that the maximum daily dose recommendation of 3g/day may be too high and that a prospective longitudinal study is necessary in order to determine the complete mechanism surrounding the pathology associated with VGB therapy. This work also confirms that the investigative procedures which are recommended by the European Agency fail to detect the subtler abnormalities induced by VGB therapy and thereby have significantly underestimated the prevalence of visual function deficits. Although high contrast visual acuity appears to remain intact, central visual function is not completely preserved. Findings suggest that contrast sensitivity is impaired at different spatial frequencies and this finding could explain the frequent reports of blurred vision that are presently associated with the drug. Overall, this thesis suggests at the very least, patients should be given more accurate information about the true nature of the defect (prevalence, location, severity), allowing them to weigh up a more realistic risk-to-benefit ratio, which is associated with the drug. Monitoring practices should be urgently reviewed, as the present techniques (white-white automated perimetry and Goldmann) are insufficient for detecting subtle abnormalities attributed to VGB. The optimal regimen for detecting visual field loss attributed to VGB should include contrast sensitivity measurement, SWAP using Program 10-2 and FDT.

10. References

Adams, AJ, Rodic, R, Husted, R, & Stamper, R (1982): Spectral sensitivity and color discrimination change in glaucoma and glaucoma-suspect patients. *Investigative Ophthalmology and Vision Science*, **23:** 516-524.

Advanced Glaucoma Intervention Study 2 (1994): Visual field test scoring and reliability. *Ophthalmology*, **101:** 1445-1455.

Agarwal, HC, Gulati, V, & Sihota, R (2000): Visual field assessment in glaucoma: comparative evaluation of manual kinetic Goldmann perimetry and automated static perimetry. *Indian Journal Of Ophthalmology*, **48:** 301-306.

Anderson, AJ & Johnson, CA (2003): Frequency-doubling technology perimetry. *Ophthalmology Clinics Of North America*, **16:** 213-225.

Anderson, DR & Patella, MV (1992): Introductory cocepts. In, Anderson, DR & Patella, MV (Eds.), *Automated static perimetry* (pp 10-29). St Louis: Mosby-Year Book Inc.

Anderson, RS & O'Brien, C (1997): Psychophysical Evidence for a Selective Loss of M Ganglion Cells in Glaucoma. *Vision Research* , **37:** 1079-1083.

Annegers, JF, Hauser, WA, & Elveback, LR (1979): Remission of seizures and relapse in patients with epilepsy. *Epilepsia*, **20:** 729-737.

Anzai, K, Mori, K, Ota, M, Murayama, K, & Yoneya, S (1998): Aging of macular function as seen in multifocal electroretinograms. *Nippon Ganka Gakkai Zasshi*, **102:** 49-53.

Appleton, RE (2001): West syndrome: long-term prognosis and social aspects. *Brain and Development*, **23:** 688-691.

Arden, GB & Barrada, A (1962): Analysis of the electro-oculograms of a series of normal subjects: the role of the lens in the development of the standing potential. *British Journal of Ophthalmology*, **46:** 468-482.

Arend, O, Remky, A, Evans, D, Stuber, R, & Harris, A (1997): Contrast sensitivity loss is coupled with capillary dropout in patients with diabetes. *Investigative Ophthalmology & Visual Science*, **38:** 1819-1824.

Arezzo, JC, Schroeder, CE, Litwak, MS, & Steward, DL (1989): Effects of vigabatrin on evoked potentials in dogs. *British Journal of Clinical Pharmacology*, **27:** 53-60.

Arndt, CF, Derambure, P, Defoort-Dhellemmes, S, & Hache, JC (1999): Outer retinal dysfunction in the patients treated with vigabatrin. *American Academy of Neurology*, **52:** 1201-1205.

Arndt, CF, Salle, M, Derambure, PH, Deefort-Dhellemmes, S, & Hache, JC (2002): The effect on vision of associated treatment in patients taking vigabatrin: carbamazepine versus valporate. *Epilepsia*, **48:** 812-817.

Arzimanoglou, A, Kulak, I, Bidaut-Mazel, C, & Baldy-Moulinier, M (2001): Optimal use of lamotrigine in clinical practice: results of an open multi-centre trial in refractory epilepsy. *Revue Neurologique*, **157:** 525-536.

Atchison, DA (1987): Effect of defocus on visual field measurement. *Ophthalmic & Physiological Optics*, **7:** 259-265.

Bailey, IL & Lovie, JE (1976): New design principles for visual acuity letter charts. *American Journal of Optometry and Physiological Optics*, **53:** 740-745.

Balwantry, CC & Johnson, CA (1999): Test-retest variability of frequency-doubling perimetry and conventional perimetry in glaucoma patients and normal subjects. *Ophthalmological Vision Science*, **40:** 648-656.

Bandini, F, Castello, E, Mazzella, L, Mancardi, GL, & Solaro, C (2001): Gabapentin but not vigabatrin is effective in the treatment of acquired nystagmus in multiple sclerosis: How valid is the GABAergic hypothesis? *Journal of Neurology, Neurosurgery, and Psychiatry*, **71:** 107-110.

Bayer, A, Thiel, H, Zrenner, E, Paulus, W, Ried, S, & Schmidt, D (1995): Disorders of colour vision perception and increase glare semsitivty in phenytoin and carbamazepine therapy: Ocular side effects of anticovulsants. *Der Nervenarzt*, **66:** 89-96.

Bayer, A, Zrener, E, Ried, S, & Schmidt, D (1990): Effects of Anticonvulsant Drugs of Retinal Function. Psychophysical and Electrophysiological findings in patients with epilepsy. *Ophthalmology and Vision Sciences*, **31:** 427.

Bearse, MA & Sutter, EE (1996): Imaging Localized retinal dysfunction with the multifocal electroretinogram. *Journal of the Optical Society of America.*, **13:** 634-40.

Ben-Menachem, E, Persson, L, Mumford, J, Haegele, K, & Huebert, N (1991): Effects of Long-Term Vigabatrin Therapy on Selected Neurotransmitter Concentrations on Cerebrospinal Fluid. *Journal of Child Neurology*, **6:** 11-16.

Bengtsson, B & Heijl, A (1998): SITA Fast, a new rapid perimetric threshold test. Description of the methods and evaluation in patients with manifest and suspect glaucoma. *Acta Ophthalmologica Scandinavica*, **76:** 431-437.

Bengtsson, B & Heijl, A (1999a): Inter-subject variability and normal limits of the SITA Standard, SITA Fast, and the Humphrey Full Threshold computerized perimetry strategies, SITA STATPAC. *Acta Ophthalmologica Scandinavica*, **77:** 125-129.

Bengtsson, B & Heijl, A (1999b): Comparing significance and magnitude of glaucomatous visual field defects using the SITA and Full Threshold strategies. *Acta Ophthalmologica Scandinavica*, **77:** 143-146.

Bengtsson, B, Heijl, A, & Olsson, J (1998): Evaluation of a new threshold visual field strategy, SITA, in normal subjects. *Acta Ophthalmologica Scandinavica*, **76:** 165-169.

Bengtsson, B, Olsson, J, Heijl, A, & Rootzen, H (1997): A new generation of algorithms for computerized threshold perimetry, SITA. *Acta Ophthalmologica Scandinavica*, **75:** 368-375.

Besch, D, Sarfan, A, & Kurtenbach, A (2000): Visual field defects and inner retinal dysfunction associated with vigabatrin. *Investigative Ophthalmology & Visual Science*, **41:** 892.

Beran, R, Currie, J, Sanbach, J, & Plunknell, M (1998): Visual field restriction with new antiepileptic medication. *Epilepsia* , **39:** 6.

Besch, D, Kurtenbach, A, Apfelstedt-Sylla., E, Sadowski, B, Dennig, D, Asenbauer, C, Zrenner, E, & Schiefer, U (2002): Visual field constriction and electrophysiological changes associated with vigabatrin. *Documenta Ophthalmologica*, **104:** 151-170.

Birch, A (2001): Tests for defective colour vision. In, Birch, A (Ed.), *Diagnosis of defective color vision* (pp 51-99). Oxford: Butterworth Heineman.

Birch, MK, Wishart, PK, & O'Donnell, NP (1995): Determining progressive visual field loss in serial Humphrey visual fields. *Ophthalmology*, **102:** 1227-1234.

Blumenthal, EZ, Sample, PA, Zangwill, L, Lee, AC, Kono, Y, & Weinreb, RN (2000): Comparison of long-term variability for standard and short-wavelength automated perimetry in stable glaucoma patients. *American Journal of Ophthalmology*, **129:** 309-313.

Budenz, DL, Rhee, P, Feuer, WJ, McSoley, J, Johnson, CA, & Anderson, DR (2002): Sensitivity and specificity of the swedish interactive threshold algorithm for glaucomatous visual field defects. *Ophthalmology* , **109:** 1052-1058.

Bullman, AG (1997): *Elementary Statistics: A Step by Step Approach*. New York: Mc Graw-Hill.

Burstein, AH (1995): Lamotrigine. *Pharmacotherapy*, **15:** 129-143.

Burnstein, Y, Ellish, NJ, & Higginbotham, EJ (2000): Comparison of frequency doubling perimetry with humphrey visual field analysis in a glaucoma practice: The reply. *American Journal of Ophthalmology*, **130:** 859-860.

Butler, W (1989): The Neuropathology of Vigabatrin. *Epilepsia*, **30:** 15-17.

Butler, W, Ford, GP, & Newberne, JW (1987): A Study of the Effects of Vigabatrin of the Central Nervous System and Retina of Sprague Dawley and Lister-Hooded Rats. *Toxicological Pathology*, **15:** 143-148.

Chan, HL & Brown, B (1998): Investigation of retinitis pigmentosa using the multifocal electroretinogram. *Ophthalmological Physiological Optometry*, **18:** 335-350.

Chan, HL & Brown, B (1999): Multifocal ERG changes in glaucoma. *Ophthalmic & Physiological Optics*, **19:** 306-316.

Chauchan, BC, Drance, SM, & Douglas, AR (1990): The use of visual field indices in detecting changes in the visual field in glaucoma. *Investigative Ophthalmology Vision Science*, **31:** 512-520.

Chiron, C, Dulac, O, Beaumont, D, Palacios, L, Pajot, N, & Mumford, J (1991): Therapeutic Trial of Vigabatrin in Refractory Infantile Spasms. *Journal of Child Neurology*, **6:** 52-59.

Chiron, C, Dumas, C, Jambaque, I, Mumford, J, & Dulac, O (1997): Randomized trial comparing vigabatrin and hydrocortisone in infantile spasms due to tuberous sclerosis. *Epilepsy Research*, **26:** 389-395.

Chylack, LT, Wolfe, JK, & Singer, DM (1993): The lens opacities classification system III. *Archives of Ophthalmology*, **111:** 831-836.

Cilio, MR, Kartashov, AI, & Vigevano, F (2001): The long-term use of felbamate in children with severe refractory epilepsy. *Epilepsy Research*, **47:** 1-7.

Cocchiarella, L & Anderson, G (2002): *Guides to the Evaluation of Permanent Impairment*. Chicago: American Medical Association.

Cohen, JA, Fisher, RA, Brigell, MG, Peyster, RG, & Sze, G (2000): The Potential for Vigabatrin-Induced Intramyelinic Edema in Humans. *Epilepsia*, **41:** 148-157.

Collins, SD, Brun, S, Kirstein, YG, & Somerville, K (1998): Absensce of visual field defects in peopkle taking tiagabine (Cabitril). *Epilepsia*, **39:** 146-147.

Comaish, IF, Gorman, C, Brimlow, GM, Barber, C, Orr, GM, & Galloway, NR (2002): The effects of vigabatrin on electrophysiology and visual fields in epileptics: a controlled study with a discussion of possible mechanisms. *Documenta Ophthalmologica*, **104:** 195-212.

Cossette, P, Riviello, JJ, & Carmant, L (1999): ACTH versus vigabatrin therapy in infantile spasms: A retrospective study. *American Academy of Neurology*, **52:** 1691-1694.

Coupland, SG, Zackon, DH, Leonard, BC, & Ross, TM (2001): Vigabatrin effect on inner retinal function. *Ophthalmology*, **108:** 1493-1496.

Crook, DK & Pow, DV (1997): Analysis of the distribution of glycine and GABA in amacrine cells of the developing rabbit retina: a comparison with the ontogeny of a functional GABA transport system in retinal neurons. *Visual Neuroscience*, **14:** 751-763.

Crooks, J & Kolb, H (1992): Localization of GABA, glycine, glutamate and tyrosine hydroxylase in the human retina. *The Journal of Comparative Neurology*, **315:** 287-302.

Cubbidge, RP, Hosking, SL, & Embleton, S (2002): Statistical modelling of the central 10-degree visual field in short-wavelength automated perimetry. *Graefe's Archive for Clinical and Experimental Ophthalmology*, **240:** 650-657.

Cubbidge, RP & Wild, JM (2001): The influences of stimulus wavelength and eccentricity on short-wavelength pathway isolation in automated perimetry. *Ophthalmic and Physiological Optics*, **21:** 1-8.

Curcio, CA & Allen, KA (1990): Topography of ganglion cells in human retina. *The Journal of Comparative Neurology*, **300:** 5-25.

Curcio, CA, Allen, KA, Sloan, KR, Lerea, CL, Hurley, JB, Klock, IB, & Milam, AH (1991): Distribution and morphology of human cone photoreceptors stained with anti-blue opsin. *The Journal of Comparative Neurology*, **312:** 610-624.

Curcio, CA, Millican, CL, Allen, KA, & Kalina, RE (1993): Aging of the human photoreceptor mosaic: evidence for selective vulnerability of rods in central retina. *Investigative Ophthalmology & Visual Science* , **34:** 3278-3296.

Curcio, CA, Sloan, KR, Kalina, RE, & Hendrickson, AE (1990): Human photoreceptor topography. *The Journal of Comparative Neurology*, **292:** 497-523.

Dacey, DM (1993): Morphology of a small-field bistratified ganglion cell type in the macaque and human retina. *Visual Neuroscience*, **10:** 1081-1098.

Dam, M (1989): Long-Term Evaluation of Vigabatrin (Gamma Vinyl GABA) in Epilepsy. *Epilepsia*, **30:** 26-30.

Daneshvar, H, Racette, I, Coupland, SG, Kertes, PJ, Guberman, A, & Zackon, A (1999): Symptomatic and Asymptomatic Visual Loss in Patients Taking Vigabatrin. *Ophthalmology*, **106:** 1792-1798.

Dimitrijevic, D, Whitton, PS, Domin, M, Welham, K, & Florence, AT (2001): Increased vigabatrin entry into the brain by polysorbate 80 and sodium caprate. *The Journal Of Pharmacy And Pharmacology*, **53:** 149-154.

Djamgoz, MBA (1995): Diversity of GABA receptors in the vertebrate outer retina. *Trends in Neurosciences*, **18:** 118-120.

Drance, SM, Lakowski, R, Schulzer, M, & Douglas, GR (1981): Acquired color vision changes in glaucoma: Use of 100-Hue and Pickfierd anomaloscope predictors of glaucomatous field change. *Archives of Ophthalmology*, **99:** 829-831.

Drance, SM, Wheeler, C, & Patullo, M (1967): The use of static perimetry in the early detection of glaucoma. *Canadian Journal of Ophthalmology*, **2:** 249-258.

Dulac, O, Chiron, C, Luna, D, Cusmai, R, Pajot, N, Beaumont, D, & Mondragon, S (1991): Vigabatrin in Childhood Epilepsy. *Journal of Child Neurology*, **6:** 30-37.

Eke, T, Talbot, JF, & Lawden, MC (1997): Severe persistant visual field constriction associated with vigabatrin. *British Medical Journal*, **314:** 180-181.

Elder, M (1992): Diazepam and it's effects and visual fields. *Australian and New Zealand Journal of Ophthalmolgy*, **20:** 267-270.

Elliott, DB, Hurst, MA, & Weatherill, J (1991): Comparing clinical tests of visual loss in cataract patients using a quantification of forward light scatter. *Eye,* **5:** 601-606.

Elliott, DB & Situ, P (1998): Visual acuity versus letter contrast sensitivity in early cataract. *Vision Research*, **38:** 2047-2052.

Elmar, G & Lutz, M (1975): Allergic conjunctivitis due to diazepam. *American Journal of Psychiatry*, **132:** 548.

Esterman, P (1968): Grids for scoring visual fields. II. perimeter. *Archives of Ophthalmology*, **79:** 400-406.

Fakhoury, T, Uthman, B, & Abou-Khalil, B (2000): Safety of long-term treatment with tiagabine. *Seizure*, **9:** 431-435.

Falk, G (1991): Retinal Physiology. In, Heckenlively, JR & Arden, GB (Eds.), *Principles and practice of clinical electrophysiology of vision* (pp 69-84). St Louis: Mosby Year Book.

Fankhauser, F, Koch, P, & Roulier, A (1972): On automation of perimetry. *Graefe's Archive For Clinical And Experimental Ophthalmology*, **184:** 126-150.

Feigl, B, Haas, A, & El Shabrawi, Y (2002): Multifocal ERG in multiple evanescent white dot syndrome. *Graefe's Archive for Clinical and Experimental Ophthalmology*, **240:** 615-621.

Flammer, J, Drance, SM, Fankhauser, F, & Augustiny, L (1984): Differential light threshold in automated static perimetry. Factors influencing short-term fluctuation. *Archives of Ophthalmology*, **102:** 876-879.

Flanagan, JG, Moss, ID, Wild, JM, Hudson, C, Prokopich, L, Whitaker, D, & O'Neill, EC (1993): Evaluation of FASTPAC: a new strategy for threshold estimation with the Humphrey Field Analyser. *Graefe's Archive for Clinical and Experimental Ophthalmology*, **231:** 465-469.

Foroozan, R & Buono, LM (2003): Foggy visual field defect. *Survey of Ophthalmology*, **48:** 447-451.

Fortune, B, Johnson, CA, & Cioffi, GA (2001): The topographic relationship between multifocal electroretinographic and behavioral perimetric measures of function in glaucoma. *Optometry and Vision Science*, **78:** 206-214.

Frankhauser, FBH (1979): Threshold fluctuations, interpolations and spatial resolution in perimetry. *Documenta Ophthalmologica Proceedings Series,* **19:** 295-309.

Frischman, LJ, Saszik, S, Harwerth, RS, Viswanathan, S, Li, Y, Smith, EL, Robson, JG, & Barnes, G (2000): Effects of experimental glaucoma in macaques on the multifocal ERG. *Documenta Ophthalmologica*, **100:** 231-251.

Gao, H & Hollyfield, JG (1992): Aging of the human retina. Differential loss of neurons and retinal pigment epithelial cells. *Investigative Ophthalmology & Visual Science*, **33:** 1-17.

Gerasimov, MR, Schiffer, WK, Brodie, JD, Lennon, IC, Taylor, SJC, & Dewey, SL (2000): [gamma]-Aminobutyric acid mimetic drugs differentially inhibit the dopaminergic response to cocaine. *European Journal of Pharmacology*, **395:** 129-135.

Gerth, C, Garcia, SM, Ma, L, Keltner, JL, & Werner, JS (2002): Multifocal electroretinogram: age-related changes for different luminance levels. *Graefe's Archive for Clinical and Experimental Ophthalmology*, **240:** 202-208.

Ghaith, AA, Daniel, J, Stulting, RD, Thompson, KP, & Lynn, M (1998): Contrast sensitivity and glare disability after radial keratotomy and photorefractive keratectomy. *Archives of Ophthalmology*, **116:** 12-18.

Gilchrist, J (1988): The psychology of vision. In, Edwards, K & Llewellyn, R (Eds.), *Optometry* (pp 25-43). London: Butterwoth & Co.

Ginsburg, AP & Cannon, MW (1984): Comments on variability in contrast sensitivity methodology. *Vision Research*, **24:** 287-287.

Giordano, L, Valseriati, D, Vignoli, A, Morescalchi, F, & Gandolfo, E (2000): Another case of reversibility of visual-field defect induced by vigabatrin monotherapy: is young age a favourable factor? *Neurological Sciences*, **21:** 185-186.

Glass, E, Schaumberger, M, & Lachenmayr, BJ (1995): Simulations for FASTPAC and the Standard 4-2 dB Full-Threshold Strategy of the Humphrey Field Annalyzer. *Investigative Ophthalmology and Visual Science*, **36:** 1847-1854.

Graham, D (1989): Neuropathology of vigabatrin. *British Journal of Clinical Pharmacology*, **27:** 43-45.

Gram, L, Klosterskov, P, & Dam, M (1985): Gamma-vinyl GABA; a double-blind palcebo-controlled trial in partial epilepsy. *Annals of Neurology*, **17:** 262-266.

Graniewski-Wijnands, HS & Van der Torren, K (2002): Electro-ophthalmological recovery after withdrawal from vigabatrin. *Documenta Ophthalmologica*, **104:** 189-194.

Greve, EL (1973): Single and multiple stimulus static perimetry in glaucoma; the two phases of perimetry. Thesis. *Documenta Ophthalmologica*, **36:** 1-355.

Gross-Tsur, V, Banin, E, Shahar, E, Shalev, SR, & Lahat, E (2000): Visual Impairment in Children with Epilepsy Treated with Vigabatrin. *Annals of Neurology*, **48:** 60-64.

Ham, WT, Meller, HA, Fugffolo, JJ, Guerry, D, & Guerry, RK (1982): Action spectrum for retinal injury from near UV radiation in aphakic monkey. *American Journal of Ophthalmology*, **93:** 299-306.

Hamard, H & Desbordes, JM (1982): Iatrogenic pathology of the optic nerve. *L'Annee Therapeutique Et Clinique En Ophtalmologie*, **33:** 185-202.

Hammond, BR, Jr. & Fuld, K (1992): Interocular differences in macular pigment density. *Investigative Ophthalmology & Visual Science*, **33:** 350-355.

Hammond, EJ, Rangel, RJ, & Wilder, BJ (1988): Evoked potential monitoring of vigabatrin patients. *British Journal Of Clinical Practice. Supplement*, **61:** 16-23.

Harding, GFA, Jones, LA, Tipper, VJ, Betts, TA, & Mumford, JP (1995): Electrortinogram, patterm electroretinogram and visual evoked potential assessment in patients receiving vigabatrin. *Epilepsia*, **36:** 108.

Harding, GFA, Robertson, KA, Edson, AS, Barnes, P, & Wild, J (1999): Visual electrophysiological effect of a GABA transaminase blocker. *Documenta Ophthalmologica*, **97:** 179-188.

Harding, GFA, Robertson, KA, Spencer, EL, & Holliday, I (2002): Vigabatrin; its effect on the electrophysiology of vision. *Documenta Ophthalmologica*, **104:** 213-229.

Harding, GFA, Wild, JM, Robertson, KA, Lawden, MC, Betts, TA, Barber, C, & Barnes, PMF (2000a): Electro-Oculography, Electroretinography, Visual Evoked Potentials, and Multifocal Electroretinography in Patients with Vigabatrin-Attributed Visual Field Constriction. *Epilepsia*, **41:** 1420-1431.

Harding, GFA, Wild, JM, Robertson, KA, Rietbrock, S, & Martinez, C (2000b): Separating the retinal electrophysiologic effects of vigabatrin: treatment versus field loss. *Neurology*, **55:** 6-15.

Hardus, P, Verduin, WM, Engelsman, M, Edelbroek, PM, Segers, JP, Berendschot, TTJM, & Stilma, JS (2001): Visual Field loss Associated with Vigabatrin: Quantification and Relation to Dosage. *Epilepsia*, **42:** 262-267.

Hardus, P, Verduin, WM, Postma, G, Stilma, JS, Berendschot, TTJM, & Van Veelan, CWM (2000a): Long term changes in the visual fields of patients with temporal lobe epilepsy using vigabatrin. *British Journal of Ophthalmology*, **84:** 788-790.

Hardus, P, Verduin, WM, Postma, G, Stilma, JS, Berendschot, TTJM, & Van Veelen, CWM (2000b): Concentric Contraction of the Visual Field in Patients with Temporal Lobe Epilepsy and its Association with the Use of Vigabatrin Medication. *Epilepsia*, **41:** 581-587.

Hart, WM, Hartz, RK, Hagen, RW, & Clark, KW (1984): Color contrast perimetry. *Investigative Ophthalmology and Vision Science*, **25:** 400-413.

Hasegawa, S, Takagi, M, Usui, T, Takadda, R, & Abe, H (2000): Waveform Changes of the First-Order Multifocal Electroretinogram in Patients with Glaucoma. *Investigative Ophthalmology and Visual Science*, **41:** 1597-1603.

Hauser, HA & Hesdorffer, DC (1990): *Epilepsy; frequency, causes and consequences.* New York: Demos and Epilepsy Foundation of America.

Hauser, WA, Annegers, JF, & Kurland, LT (1993): The incidence of epilepsy and unprovoked seizures in Rochester, Minesota, 1935-1984. *Epilepsia*, **34:** 453-468.

Hauw, JJ, Trottier, S, Boutry, JM, Sun, P, Sazdovitch, V, & Duyckaerts, C (1988): The neuropathology of vigabatrin. *British Journal Of Clinical Practice. Supplement*, **61:** 10-13.

Hawkins, AS, Szlyk, JP, Ardickas, Z, Alexander, KR, & Wilensky, JT (2003): Comparison of contrast sensitivity, visual acuity, and humphrey visual field testing in patients with glaucoma. *Journal of Glaucoma*, **12:** 134-138.

Hayley, MJ (1993): Basic principles of perimetry. In, Haley, MJ (Ed.), *The Field analyzer primer* (pp 3-12). San Leandro: Humphrey Instruments.

Heijl, A (1976): Automatic perimetry in glaucoma visual field screening. A clinical study. *Graefe's Archive For Clinical And Experimental Ophthalmology*, **200:** 21-37.

Heijl, A & Krakau, CE (1975): An automatic static perimeter, design and pilot study. *Acta Ophthalmologica*, **53:** 293-310.

Heijl, A, Lindgren, G, & Olsson, J (1987): A package for the statistical analyses of visual fields. *Documenta Ophthalmologica Proceedings Series, **49:*** 593-600.

Heijl, A, Lindgren, G, & Olsson, J (1987b): Normal Variability of Static Perimetric Threshold Values Across the Central Visual Field. *Archives of Ophthalmology*, **105:** 1544-1549.

Held, R (1988): Normal visual development and its deviations. In, Lennerstrand, G, von Noorden, GK & Campos, EC (Eds.), *Strabismus and Amblyopia, Wenner Gren International Symposium,* **49:** 247-258. London: Macmillan Press.

Herranz, JL, Areaga, R, Farr, IN, Valdizen, E, Beaumont , D, & Armijo, JA (1991): Dose-Response Study of Vigabatrin in Children With Refractory Epilepsy. *Journal of Child Neurology*, **6:** 45-51.

Herranz, JL, Sol, JM, & Hernandez, G (2000): Gabapentin used in 559 patients with partial seizures. A multicenter observation study. Spanish Gabapentin Work Group. *Revista de Neurologia*, **30:** 1141-1145.

Hess, RF (1984): On the assessment of contrast threshold functions for anomalous vision. *British Orthoptic Journal*, **41:** 1-15.

Hess, RF & Howell, ER (1977): The threshold contrast sensitivity function in strabismic amblyopia: evidence for a two type classification. *Vision Research*, **17:** 1049-1055.

Hodapp, E, Parish, RK, & Anderson, DR (1993): *Clinical decisions in glaucoma*. St Louis: Mosby.

Holmin, C & Krakau, CE (1979): Variability of glaucomatous visual field defects in computerized perimetry. *Graefe's Archive For Clinical And Experimental Ophthalmology*, **210:** 235-250.

Hood, DC (2000): Assessing Retinal Function with the Multifocal Technique. *Progress in Retinal Eye Research*, **19:** 607-646.

Hood, DC, Greenstein, V, Frishman, L, Holopigan, K, Viswanathan, S, Seiple, W, Ahmed, J, & Robson, JG (1999): Identifying inner retinal contributions to the human multifocal ERG. *Vision Research*, **39:** 2285-2291.

Hood, DC, Greenstein, VC, Holopigian, K, Bauer, R, Firoz, B, Liebmann, JM, Odel, JG, & Ritch, R (2000): An Attempt to Detect Glaucomatous Damage to the Inner Retina with the Multifocal ERG. *Investigative Ophthalmology and Visual Science*, **41:** 1570-1579.

Hood, DC & Li, Ju (1997): A Technique for Measuring Individual Multifocal ERG Records. *Optical Society of America*, **11:** 33-41.

Hood, DC, Seiple, W, Holopigian, K, & Greenstein, V (1997): A comparison of the components of multifocal and full field ERGs. *Visual Neuroscience*, **14:** 533-544.

Hopkins, A & Shorvon, S (1995): Definitons and epidemiology of epilepsy. In, Hopkins, A, Shorvon, S, & Cascino, G (Eds.), *Epilepsy* (pp 1-24). Chapman&Hall.

Hosking, SL, Roff Hilton, EJ, Embleton, SJ, & Gupta, AK (2003): Epilepsy patients treated with vigabatrin exhibit reduced ocular blood flow. *The British Journal Of Ophthalmology*, **87:** 96-100.

Huang, S, Wu, D, Jiang, F, Luo, G, Liang, J, Wen, F, Yu, M, Long, S, & Wu, L (2003): The multifocal electroretinogram in X-linked juvenile retinoschisis. *Documenta Ophthalmologica*, **106:** 251-255.

Hudson, C, Flanagan, JG, Turner, GS, Chen, HC, Young, LB, & McLeod, D (1998a): Influence of laser photocoagulation for clinically significant diabetic macular oedema (DMO) on short-wavelength and conventional automated perimetry. *Diabetologia*, **41:** 1283-1292.

Hudson, C, Flanagan, JG, Turner, GS, Chen, HC, Young, LB, & McLeod, D (1998b): Short-wavelength sensitive visual field loss in patients with clinically significant diabetic macular oedema. *Diabetologia*, **41:** 918-928.

Hudson, C, Wild, JM, & O' Neill, EC (1994): Fatigue Effects During a Single Session of Automated Static Threshold Perimetry. *Investigative Ophthalmology and Visual Science*, **35:** 268-280.

Hutchings, N, Hosking, SL, Wild, JM, & Flanagan, JG (2001): Long-term fluctuation in short-wavelength automated perimetry in glaucoma suspects and glaucoma patients. *Investigative Ophthalmology and Vision Science*, **42:** 2332-2337.

Hyams, SW & Keroub, C (1977): Glaucoma due to diazepam. *The American Journal Of Psychiatry*, **134:** 447-448.

Iester, M, Capris, P, Pandolfo, A, Zingirian, M, & Traverso, C (2000): Learning Effect, Short-term Fluctuation, and Long-term Fluctuation in Frequency Doublig Technique. *American Journal of Ophthalmology*, **130:** 160-164.

Iregren, A, Andersson, M, & Nylen, P (2002): Color Vision and Occupational Chemical Exposures: I. An Overview of Tests and Effects. *NeuroToxicology*, **23:** 719-733.

Jackson, GR, Ortega, J, Girkin, C, Rosenstiel, CE, & Owsley, C (2002): Aging-related changes in the multifocal electroretinogram. *Journal of the Optical Society of America. A, Optics, Image Science, and Vision*, **19:** 185-189.

Jeavons, PM & Bower, BD (1974): Infantile Spasms. In, Vinken, P & Bruyn, G (Eds.), *The Epilepsies, Handbook of Clinical Neurology* (pp 219-234). New York: Elsevier.

John, RA, Rimmer, EM, Williams, J, Cole, G, Fowler, LJ, & Richens, A (1987): Micro-vacuolation in rat brains after long term administration of GABA-transaminase inhibitors: comparison of the effects of ethanolamine-O-sulfate and vigabatrin. *Biochemical Pharmacology*, **36:** 1467-1473.

Johnson, CA (1994): Selective vs non-selective losses in glaucoma. *Journal of Glaucoma*, **3:** 32-44

Johnson, CA, Adams, AJ, & Brandt, JD (1993a): Progression of Early Glaucomatous Visual Field Loss as Detected by Blue-on-Yellow and Standard White-on-White Automated Perimetry. *Archives of Ophthalmology*, **111:** 651-656.

Johnson, CA, Adams, AJ, Casson, EJ, & Brandt, JD (1993b): Blue-on-Yellow Perimetry Can Predict the Development of Glaucomatous Visual Field loss. *Archives of Ophthalmology*, **111:** 645-650.

Johnson, CA, Adams, AJ, Twelker, JD, & Quigg, JM (1988): Age-related changes in the central visual field for the short-wavelength sensitive pathways. *Journal of the Optical Society of America. A, Optics, Image Science, and Vision*, **5:** 2131-2139.

Johnson, CA, Cioffi, GA, & Van Buskirk, ME (1999): Frequency Doubling Technology Perimetry Using a 24-2 Stimulus Presentation Pattern. *Optometry and Vision Science*, **76:** 571-581.

Johnson, CA, Howard, DL, Marshall, D, & Shu, H (1993c): A noninvasive video-based method for measuring lens transmission properties of the human eye. *Optometry and Vision Science*, **70:** 944-955.

Johnson, CA & Marshall, D (1995): Aging effects for the opponent mecahnisms in the central visual field. *Ophthalmological Vision Science*, **72:** 75-82.

Johnson, CA, Wall, M, Fingeret, M, & Lalle, P (1998): *A primer for Frequency Doubling Technology*. Dublin: Welch Allym.

Johnson, MA, Krauss, GL, Miller, NR, Medura, M, & Paul, SR (2000): Visual function loss from vigabatrin: Effect of stopping the drug. *Neurology*, **55:** 40-45.

Jonas, JB, Schneider, U, & Naumann, GO (1992): Count and density of human retinal photoreceptors. *Graefe's Archive for Clinical and Experimental Ophthalmology*, **230:** 505-510.

Jung, P & Doussard-Lefaucheux, S (2002): Visual field defect in a patient given sodium valporate then carbamazepine: possible effect of aminotransferase inhibition. *Revue Neurologique*, **158:** 477-479.

Kalviainen, R & Nousiainen, I (2001): Visual Field Defects with Vigabatrin Epidemiology and Therapeutic Implications. *CNS Drugs* , **15:** 217-230.

Kalviainen, R, Nousiainen, I, Mantyarvi , M, Nikoskelainen, E, Partanen, J, Partanen, K, & Riekkinen, P (1999a): Vigabatrin, a gabaergic antiepileptic drug, causes concentric visual field defects. *American Academy Neurology*, **53:** 922-926.

Kalviainen, R, Nousiainen, I, Mantyjarvi , M, & Riekkinen, P (1999b): Absensce of conecntric visual field defects in patients with initial tiagabine monotherapy. *Epilepsia*, **40:** 259.

Katz, J & Sommer, A (1986): Asymmetry and variation in the normal hill of vision. *Archives of Ophthalmology*, **104:** 65-68.

Katz, J, Tielsch, JM, Quigley, HA, & Sommer, A (1995): Automated perimetry detects visual field loss before manual Goldmann perimetry. *Ophthalmology*, **102:** 21-26.

Kaufman, KR, Lepore, FE, & Keyser, BJ (2001): Visual fields and tiagabine: a quandary. *Seizure*, **10:** 525-529.

Kawabata, H & Adachi-Usami, E (1997): Multifocal Electroretinogram in Myopia. *Investigative Ophthalmology and Visual Science*, **38:** 2844-2851.

Keating, D, Parks, S, & Evans, A (2000): Technical aspects of multifocal ERG recording. *Documenta Ophthalmologica*, **100:** 77-98.

Keltner, JL & Johnson, CA (1995): Short-wavelength automated perimetry in neuro-ophthalmologic disorders. *Archives of Ophthalmology*, **113:** 475-481.

Kemp, AM & Sibert, JR (1993): Epilepsy in children and the risk of drowning. *Archives Of Disease In Childhood*, **68:** 684-685.

King-Smith, PE, Grigsby, SS, Vingrys, AJ, Benes, SC, & Supowit, A (1994): Efficient and unbiased modifications of the QUEST threshold method: theory, simulations, experimental evaluation and practical implementation. *Vision Research*, **34:** 885-912.

Kline, RP, Ripps, H, & Dowling, JE (1978): Generation of b-wave currents in the skate retina. *Proceedings of the National Academy of Sciences of the United States of America*, **75:** 5727-5731.

Kondo, M, Miyake, Y, Horiguchi, M, Suzuki, S, & Tanikawa, A (1995): Clinical Evaluation of Multifocal Electroretinogram. *Investigative Ophthalmology and Visual Science*, **36:** 2146-2150.

Krakau, CE (1985): A statistical trap in the evaluation of visual field decay. *Acta Ophthalmologica*, **173:** 19-21.

Krakow, K, Polizzi, G, Riordan-Eva, P, Holder, G, Macleod, WN, & Fish, DR (2000): Recovery of visual field constriction following discontinuation of vigabatrin. *Seizure*, **9:** 287-290.

Krauss, GL, Johnson, MA, & Miller, NR (1998): Vigabatrin-associated retinal cone system dysfunction. *American Academy of Neurology*, **50:** 614-618.

Kretschmann, U, Bock, M, Gockeln, R, & Zrenner, E (2000): Clinical applications of multifocal electroretinography. *Documenta Ophthalmologica*, **100:** 99-113.

Kretschmann, U, Seeliger, MW, Ruether, K, Usui, T, Apfelstedt-Sylla, E, & Zreener, E (1998a): Multifocal electroretinography in patients with Stargardt's macular dystrophy. *British Journal of Ophthalmology*, **82:** 267-275.

Kretschmann, U, Seeliger, M, Ruether, K, Usui, T, & Zrenner, E (1998b): Spatial cone activity distribution in diseases of the posterior pole determined by multifocal electroretinography. *Vision Research*, **38:** 3817-3828.

Kwon, YH, Park, HJ, Jap, A, Ugurlu, S, & Caprioli, J (1998): Test-retest variability of blue-on-yellow perimetry is greater than white-on-white perimetry in normal subjects. *American Journal of Ophthalmology* , **126:** 29-36.

Lam, DM (1997): Neurotransmitters in the vertebrate retina. *Investigative Ophthalmology & Visual Science*, **38:** 553-556.

Landers, J, Goldberg, I, & Graham, S (2000): A comparison of short wavelength automated perimetry with frequency doubling perimetry for the early detection of visual field loss in ocular hypertension. *Clinical & Experimental Ophthalmology*, **28:** 248-252.

Lawden, MC, Eke, T, Degg, C, Harding, GFA, & Wild, JM (1999): Visual field defects associated with vigabatrin therapy. *Journal Neurology Neurosurgery Psychiatry*, **67:** 716-22.

Lehmann, D & Skrandies, W (1979): Multichannel evoked potential fields show different properties of human upper and lower hemiretina systems. *Experimental Brain Research.*, **35:** 151-159.

Lennerstrand, G & Lundh, BL (1984): Contrast sensitivity in amblyopia. In, Ravault, A. & Lenk, M. (Eds.), *Transactions of the Fifth International Orthoptic Congress* (pp77-84). Lyon: LIPS.

Liegeosis-Chauvel, C, Marwuis, P, Gisselbrecht, D, Pantieri, R, Beaumont, D, & Chauvel, P (1989): Effects of Long-Term Vigabatrin on Somatosensory-Evoked Potentials in Epileptic Patients. *Epilepsia*, **30:** 23-25.

Loiseau, P, Hardenburg, JP, Pestre, M, Guyot, M, Schechter, PJ, & Tell, GP (1986): Double-blind placebo controlled study of vigabatrin (gamma-vinyl-GABA) in drug-resistant epilepsy. *Epilepsia*, **27:** 115-120.

Lopez, L, Thompson, A, & Rabinowicz, A (1999): Assessment of Colour Vision in Epileptic Patients Exposed to Single-Drug Therapy. *European Neurology*, **41:** 201-205.

Lutze, M & Bresnick, GH (1994): Lens-corrected visual field sensitivity and diabetes. *Investigative Ophthalmology & Visual Science*, **35:** 649-655.

Lynn, JR (1969): Examination of the visual field in glaucoma. *Investigative Ophthalmology & Visual Science*, **8:** 76-84.

Mackenzie, R & Klistorner, A (1998): Asymptomatic as well as symptomatic defects occur within vigabatrin. *British Medical Journal*, **316:** 233-

Maddess, T & Henry, GH (1992): Performance of Non-linear Visual Units in Ocular Hypertension and Glaucoma. *Clinical Vision Science*, **7:** 371-383.

Maddess, T, James, AC, Goldberg, I, Wine, S, & Dobinson, J (2000): Comparing a Parallel PERG, Automated Perimetry, and Frequency-Doubling Thresholds. *Investigative Ophthalmology and Visual Science*, **41:** 3827-32.

Malmgren, K, Ben-Menachem, E, & Frisen, L (2001): Vigabatrin Visual Toxicity; Evoloution and Dose Dependence. *Epilepsia*, **42:** 609-615.

Manucheri, K, Goodman, S, Siviter, L, & Nightingale, S (2000): A controlled study of vigabatrin and visual field abnormalities. *British Journal of Ophthalmology*, **84:** 499-505.

Mare, M (1972): Clinical examination of the three color vision mechanisms in accquired color vision defects. *Modern Problems in Ophthalmology*, **11:** 224-227.

Marmor, MF, Arden, GB, ., Nilsson, SE, & Zreener, E (1989): Standard for clinical electrophysiology. *Archives of Ophthalmology*, **107:** 816-819.

Marmor, MF, Hood, DC, Keating, D, Kondo, M, Seeliger, MW, & Miyake, Y (1999): Standard for clinical electroretinography (1999 update). *Documenta Ophthalmologica*, **97:** 143-156.

Marmor, MF, Hood, DC, Keating, D, Kondo, M, Seeliger, MW, & Miyake, Y (2003): Guidelines for basic multifocal electroretinography (mfERG). *Documenta Ophthalmologica*, **106:** 105-115.

Martin, PR, White, AJ, Goodchild, AK, Wilder, HD, & Sefton, AE (1997): Evidence that blue-on cells are part of the third geniculocortical pathway in primates. *The European Journal Of Neuroscience*, **9:** 1536-1541.

Martinez, C & Noack, H (1997): *The risk of visual field defect and the use of vigabatrin.* Hoescht Marion Roussel (Internal Report). Kansas City.

Mattson, RH, Petroff, OA, Rothman, D, & Behar, K (1995): Vigabatrin: effect on brain GABA levels measured by nuclear magnetic resonance spectroscopy. *Acta Neurologica Scandinavica. Supplementum*, **162:** 27-30.

Mecarelli, O, Rinalduzzi, S, & Accornero, N (2001): Changes in Colour Vision after a Single Dose of Vigabatrin or Carbamazepine in Healthy Volunteers. *Clinical Neuropharmacology*, **24:** 23-26.

Meigen, T & Friedrich, A (2002): The reproducibility of multifocal ERG recordings. *Der Ophthalmologe: Zeitschrift Der Deutschen Ophthalmologischen Gesellschaft*, **99:** 713-718.

Meinardi, H (1973): Other antepileptic drugs: Carbamazepine. In, Woodbury, DM, Penry, JK, & Schimdt, RP (Eds.), *Antiepileptic Drugs* (pp 487-496). New York: Raven Press.

Meyer, DR, Stern, JH, Jarvis, JM, & Lininger, LL (1993): Evaluating the visual field effects of blepharoptosis using automated static perimetry. *Ophthalmology*, **100:** 651-658.

Miller, KM & Quigley, HA (1988): The clinical appearance of the lamina cribrosa as a function of the extent of glaucomatous optic nerve damage. *Ophthalmology*, **95:** 135-138.

Miller, NR, Johnson, MA, Paul, SR, Girkin, CA, Perry, JD, Endres, M, & Krauss, GL (1999): Visual dysfunction in patients receiving vigabatrin: Clinical and electrophysiologic findings. *American Academy of Neurology*, **53:** 2082-2087.

Mills, RP, Barnebey, HS, Migliazzo, CV, & Li, Y (1994): Does saving time using FASTPAC or suprathreshold testing reduce quality of visual fields? *Ophthalmology*, **101:** 1596-1603.

Mita-Harris, M (2001): Changes in the second-order kernel component obtained by the techniques of the multifocal electroretinogram in early stages of diabetes mellitus. *Nippon Ganka Gakkai Zasshi*, **105:** 470-477.

Miyake, Y, Shiroyama, N, Horiguchi, M, & Ota, I (1989): Asymmetry of focal ERG in human macular region. *Investigative Ophthalmology & Visual Science*, **30:** 1743-1749.

Mohidin, N, Yap, MKH, & Jacobs, RJ (1997): The repeatability and variability of the multifocal electroretinogram for four different electrodes. *Ophthalmic and Physiological Optics*, **17:** 530-535.

Munoz-Negrete, FJ, Rebolleda, G, Gonzalez Martin-Moro, J, & Cerio-Ramsden, CD (2003): Frequency doubling perimetry in terminal visual field defects. *Archivos de la Sociedad Espanola de Oftalmologia*, **78:** 203-210.

Nabeshima, T (2001): The Effect of Aging on the Multifocal Electroretinogram. *Japenese Journal of Ophthalmology*, **45:** 114-115.

Nagasaka, K, Horiguchi, M, Shimada, Y, & Yuzawa, M (2003): Multifocal electroretinograms in cases of central areolar choroidal dystrophy. *Investigative Ophthalmology & Visual Science*, **44:** 1673-1679.

Nagatomo, A, Nao-i, N, Maruiwa, F, Arai, M, & Sawada, A (1998): Multifocal Electroretinograms in Normal Subjects. *Japanese Journal of Ophthalmology*, **42:** 129-135.

Neal, MJ, Cunningham, JR, Shah, MA, & Yazulla, S (1989): Immunocytochemical evidence that vigabatrin in rats causes GABA accumulation in glial cells of the retina. *Neuroscience Letters*, **98:** 29-32.

Newman, WD, Tocher, K, & Acheson, JF (2002): Vigabatrin associated visual field loss: a clinical audit to study prevalence, drug history and effects of drug withdrawal. *Eye*, **16:** 567-571.

Nicolson, A, Leach, JP, Chadwick, DW, & Smith, DF (2002): The legacy of vigabatrin in a regional epilepsy clinic. *Journal of Neurology, Neurosurgery, and Psychiatry*, **73:** 327-329.

Nousiainen, I, Kalviainen, R, & Mantyjarvi, M (2000a): Contrast and glare sensitvity in epilepsy patients treated with vigabatrin carbamazepine monotherapy compared to healthy volunteers. *British Journal of Ophthalmology*, **84:** 622-625.

Nousiainen, I, Kalviainen, R, & Mantyjarvi, M (2000b): Color Vision in Epilepsy Patients Treated with Vigabatrin or Carbamazepine Monotherapy. *American Journal of Ophthalmology*, **107:** 884-888.

Nousiainen, I, Mantyjarvi , M, & Kalviainen, R (2000c): Visual function in patients treated with the GABAergic anticonvulsant Tiagabine. *Clinical Drug Investigation*, **20:** 393-400.

Nousiainen, I, Mantyjarvi, M, & Kalviainen, R (2001): No reversion in vigabatrin-associated visual field defects. *Neurology*, **57:** 1916-1917.

Onozu, H & Yamamoto, S (2003): Oscillatory potentials of multifocal electroretinogram retinopathy. *Documenta Ophthalmologica*, **106:** 327-332.

Owsley, C, Sekuler, R, & Siemsen, D (1983): Contrast sensitivity throughout adulthood. *Vision Research*, **23:** 689-699.

Palmowski, AM, Allgayer, R, Heinemann-Vernaleken, B, & Ruprecht, KW (2002): Influence of photodynamic therapy in choroidal neovascularization on focal retinal function assessed with the multifocal electroretinogram and perimetry. *Ophthalmology*, **109:** 1788-1792.

Palmowski, AM, Allgayer, R, Heinemann-Vernaleken, B, Scherer, V, Eich, W, & Ruprecht, KW (2001): A differentiated study of the retinal function in segmental retinitis pigmentosa by multifocal electroretinograms. *Der Ophthalmologe: Zeitschrift Der Deutschen Ophthalmologischen Gesellschaft*, **98:** 294-299.

Palmowski, AM, Bearse, M, & Sutter, EE (1997): Variability and repeatability of the ERG topography in normals. *Investigative Ophthalmology & Visual Science*, **38:** 877.

Palmowski, AM, Sutter, EE, Bearse, MA, & fung, W (1997): Mapping of Retinal Function in Diabetic Retinopathy Using the Multifocal Electroretinogram. *Investigative Ophthalmology and Visual Science*, **38:** 2586-2596.

Pammer, K & Wheatley, C (2001): Isolating the M(y)-cell response in dyslexia using the spatial frequency doubling illusion. *Vision Research*, **41:** 2139-2147.

Panda-Jonas, S, Jonas, JB, & Jakobczyk-Zmija, M (1995): Retinal photoreceptor density decreases with age. *Ophthalmology*, **102:** 1853-1859.

Parks, S, Keating, D, Evans, AL, Williamson, TH, Jay, JL, & Elliott, AT (1997): Comparison of repeatability of the multifocal electroretinogram and Humphrey perimeter. *Documenta Ophthalmologica Advances in Ophthalmology*, **92:** 281-289.

Paul, SR, Krauss, GL, Miller, NR, Medura, MT, Miller, TA, & Johnson, TA (2001): Visual Function is Stable in Patients Who Continue Long-Term Vigabatrin Therapy: Implications for Cliunical Decision Making. *Epilepsia*, **42:** 525-530.

Paulus, W, Scharwtz, G, & Steinhoff, BJ (1996): The effect of antiepileptic drugs on visual percep-tion in patients with epilepsy. *Brain*, **119:** 539-549.

Pederson, JE & Anderson, DR (1980): The mode of progressive disc cupping in ocular hypertension and glaucoma. *Archives of Ophthalmology*, **98:** 490-495.

Pederson, SA, Klosterskov, P, Gram, L, & Dam, M (1985): Long-term study of gamma-vinyl GABA in the treatment of epilepsy. *Acta Neurologica Scandanavia*, **72:** 295-298.

Perron, AM, Westall, CA, Mirabella, G, Buncic, JR, Logan, JW, & Snead, OC (2002): Contrast sensitivity changes in children prescribed the antiepileptic drug vigabatrin. *Investigative Ophthalmology and Vision Science*, **42:** 2091.

Piao, CH, Kondo, M, Tanikawa, A, Terasaki, H, & Miyake, Y (2000): Multifocal Electroretinogram in Occult Macular Dystrophy. *Investigative Ophthalmology and Visual Science*, **41:** 513-517.

Plummer, DJ, Sample, PA, Arevalo, JF, Grant, I, Quiceno, JI, Dua, R, & Freeman, WR (1996): Visual field loss in HIV-positive patients without infectious retinopathy. *American Journal of Ophthalmology*, **122:** 542-549.

Polo, V, Larrosa, JM, Pinilla, I, Perez, S, Gonzalvo, F, & Honrubia, FM (2002): Predictive value of short-wavelength automated perimetry; A 3-year follow-up study. *Ophthalmology*, **109:** 761-765.

Pomerance, GN & Evans, DW (1994): Test-retest reliability of the CSV-1000 contrast test and its relationship to glaucoma therapy. *Investigative Ophthalmology & Visual Science*, **35:** 3357-3361.

Ponjavic, V & Andreasson, S (2001): Multifocal ERG and full-field ERG in patients on long-term vigabatrin medication. *Documenta Ophthalmologica*, **102:** 63-72.

Pow, DV, Baldridge, W, & Crook, DK (1996): Activity-dependent transport of GABA analogues into specific cell types demonstrated at high resolution using a novel immunocytochemical strategy. *Neuroscience*, **73:** 1129-1143.

Pow, DV & Rogers, M (1996): GABA transamination regulates neuronal glutamate content in the retina. *Neuroreport*, **7:** 2683-2686.

Qiao, M, Malisza, KI, Bigio, MR, Kozlowski, P, Seshia, SS, & Tuor, UI (2000): Effect of Long-Term Vigabatrin Administration on the Immature Rat Brain. *Epilepsia*, **41:** 655-665.

Quigley, HA (1994): Comment. *British Journal of Ophthalmology*, **78:** 879-880.

Quigley, HA, Dunkelberger, GR, & Green, WR (1988): Chronic human glaucoma causing selectively greater loss of large optic nerve fibers. *Ophthalmology*, **95:** 357-363.

Quigley, HA, Dunkelberger, GR, & Green, WR (1989): Retinal ganglion cell atrophy correlated with automated perimetry in human eyes with glaucoma. *American Journal of Ophthalmology*, **107:** 453-464.

Radtke, ND, Seiler, MJ, Aramant, RB, Petry, HM, & Pidwell, DJ (2002): Transplantation of intact sheets of fetal neural retina with its retinal pigment epithelium in retinitis pigmentosa patients. *American Journal of Ophthalmology*, **133:** 544-550.

Ravindran, J, Blumbergs, P, Crompton, J, Pietris, G, & Waddy, H (2001): Visual field loss associated with vigabatrin: pathological correlations. *American Journal of Ophthalmology*, **132:** 809-809.

Reed, H & Drance, SM (1972): *The essentials of perimetry. Static Kinetic.* London, New York and Toronto: Oxford University Press.

Remler, BF, Leigh, RJ, Osorio, I, & Tomsak, RL (1990): The characteristics and mechanisms of visual disturbance associated with anticonvulsant therapy. *Neurology*, **40:** 791-796.

Remy, C & Beaumont, D (1989): Efficacy and safety of vigabatrin in the long-term treatment of refractory epilepsy. *British Journal of Clinical Pharmacology*, **27:** 125-129.

Remy, C, Favel, P, & Tell, G (1986): Double-blind, placebo-controlled crossover study of vigabatrin in drug resistant epilepsy in adults. *Bolletino Lega Italiana Contro L Epilessia*, **54/55:** 241-243.

Rhee, DJ, Goldberg, MJ, & Parrish, RK (2001): Bilateral angle-closure glaucoma and ciliary body swelling from topiramate. *Archives of Ophthalmology*, **119:** 1721-1723.

Richens, A (1991): Pharmacology and Clinical Pharmacology of Vigabatrin. *Journal of Child Neurology*, **6:** 7-10.

Riikonen, R & Donner, M (1980): ACTH therapy in infantile spasm:side effects. *Archive of disease in Childhood*, **55:** 664-672.

Rimmer, EM & Ritchens, A (1984): Double-blind study of gamma vinyl GABA in patients with refractory epilepsy. *British Journal of Clinical Pharmacology*, **27:** 189-190.

Rimmer, EM & Richens, A (1989): Interaction between vigabatrin and phenytoin. *British Journal of Clinical Pharmacology*, **27:** 27-33.

Ring, HA & Reynolds, EH (1992): Vigabatrin. In, Pedley, T & Meldrum, B (Eds.), *Recent advances in epilepsy* (pp 177-95). Edinburgh: Churchilll Livingstone.

Rodin, EA (1982): Epilepsy and work. In, Laidlaw, J & Richens, A (Eds.), *Textbook of epilepsy* (pp 496-506). London: Churchill Livingstone.

Roff Hilton, EJ, Cubbidge, RP, Betts, T, Comaish, IF, & Hosking, SL (2002): Epilepsy patients treated with vigabatrin exhibit central visual function defecits. *Epilepsia*, **43:** 1351-1359.

Rubin, GS (1988): Reliability and sensitivity of clinical contrast sensitivity tests. *Clinical Vision Science*, **2:** 169-177.

Ruether, K, Pung, T, Kellner, U, Schmitz, B, Hartmann, C, & Seeliger, M (1998): Electrophysiologic Evaluation of a patient With Peripheral Visual Field Contraction Associated With Vigabatrin. *Archives of Ophthalmology*, **116:** 817-819.

Russell-Eggitt, IM, Mackey, DA, Taylor, DSI, Timms, C, & Walker, JW (2000): Vigabatrin associated visual field defects in children. *Eye*, **14:** 334-339.

Sample, PA (2000): Short-wavelength automated perimetry: it's role in the clinic and for understanding ganglion cell function. *Progress in Retinal and Eye Research*, **19:** 369-383.

Sample, PA, Esterson, FD, Weinreb, RN, & Boynton, RM (1988): The aging lens: In vivo assessment of light absorption in 84 human eyes. *Investigative Ophthalmology & Visual Science*, **29:** 1306-1311.

Sample, PA, Johnson, CA, Haegestrom-Portnoy, G, & Adams, AJ (1996): Optimum parameters for short-wavelength automated perimetry. *Journal of Glaucoma*, **5:** 375-393.

Sample, PA, Taylor, JDN, Martinez, GA, Lusky, M, & Weinreb, RN (1993): Short-wavelength Colour Visual Fields in Glaucoma Suspects at Risk. *American Journal of Ophthalmology*, **115:** 225-233.

Sample, PA & Weinreb, RN (1990): Colour Perimetry for Assessment of Primary Open-Angle Glaucoma. *Investigative Ophthalmology and Visual Science*, **31:** 1869-1875.

Sample, PA & Weinreb, RN (1992): Progressive colour visual field loss in glaucoma. *Investigative Ophthalmology and Vision Science*, **33:** 2068-2071.

Sanabria, O, Feuer, WJ, & Anderson, DR (1991): Pseudo-loss of fixation in automated perimetry. *Ophthalmology*, **98:** 76-78.

Sankar, PS, Pasquale, LR, & Grosskreutz, CL (2001): Uveal effusion and secondary angle-closure glaucoma associated with topiramate use. *Archives of Ophthalmology*, **119:** 1210-1211.

Sankar, R & Wasterlain, CG (1999): Is the devil we know the lesser of the two evils? Vigabatrin and visual fields. *American Academy of Neurology*, **52:** 1537-1538.

Schachter, SC, Leppik, IE, Matsuo, F, Messenheimer, JA, Faught, E, Moore, EL, & Risner, ME (1995): Lamotrigine: A Six-Month, Placebo-Controlled, Safety and Tolerance Study. *Journal of Epilepsy*, **8:** 201-209.

Schiffer, WK, Gerasimov, MR, Bermel, RA, Brodie, JD, & Dewey, SL (2000): Stereoselective inhibition of dopaminergic activity by gamma vinyl-GABA following a nicotine or cocaine challenge: A pet/microdialysis study. *Life Sciences*, **66:** 169-173.

Schiffer, WK, Marsteller, D, & Dewey, SL (2003): Sub-chronic low dose gamma-vinyl GABA (vigabatrin) inhibits cocaine-induced increases in nucleus accumbens dopamine. *Psychopharmacologia*, **168:** 339-343.

Schmidt, T, Ruther, K, Jokiel, B, Pfeiffer, S, Tiel-Wilck, K, & Schmitz, B (2002): Is visual field constriction in epilepsy patients treated with vigabatrin reversible? *Journal of Neurology*, **249:** 1066-1071.

Schroeder, CE, Gibson, JP, Yarrington, J, Heydron, WE, Sussman, NM, & Arezzo, JC (1992): Effects of High-Dose Vinyl Gaba (Vigabatrin) Administration on Visual Somatosensory Evoked Potentials in Dogs. *Epilepsia*, **33:** 13-25.

Seeligr, MA, Kretschmann, UH, Apfelstedt-Sylla, E, & Zrenner, E (1998): Implicit Time Tomography of Multifocal Electroretinograms. *Investigative Ophthalmology Visual Science*, **39:** 718-723.

Sekhar, GC, Naduvilath, TJ, Lakkai, M, Jayakumar, AJ, Pandi, GT, Mandal, AK, & Honavar, SG (2000): Sensitivity of Swedish interactive threshold algorithm compared with standard full threshold algorithm in Humphrey visual field testing. *Ophthalmology*, **107:** 1303-1308.

Sharma, AK, Goldberg, I, Graham, SL, & Mohsin, M (2000): Comparison of the Humphrey Sweedish Interactive Thresholding Algorithm (SITA) and Full Threshold Strategies. *Journal of Glaucoma*, **9:** 20-27.

Sheu, SJ, Chen, YY, Chou, LC, Wu, TT, & Cheng, KK (2002): Frequency doubling technology perimetry in age-related macular degeneration. *Chinese Medical Journal;* **65:** 435-440.

Shirato, S, Inoue, R, Fukushima, K, & Suzuki, Y (1999): Clinical evaluation of SITA: a new family of perimetric testing strategies. *Graefe's Archive for Clinical and Experimental Ophthalmology*, **237:** 29-34.

Shorvon, SD (1982): *The drug treatment of epilepsy.* Unpublished Thesis. University of Cambridge, 1982.

Shorvon, SD (1991): Medical assessment and treatment of chronic epilepsy. *British Medical Journal (Clinical Research Ed.)*, **302:** 363-366.

Sills, GJ, Patsalos, PN, Butler, E, Forrest, G, Ratnaraj, N, & Brodie, MJ (2001): Visual field constriction: accumulation of vigabatrin but not tiagabine in the retina. *Neurology*, **57:** 196-200.

Soliman, MAE, de Jong, LAMS, Ismaeil, AA, van den Berg, TJTP, & de Smet, MD (2002): Standard achromatic perimetry, short wavelength automated perimetry, and frequency doubling technology for detection of glaucoma damage. *Ophthalmology*, **109:** 444-454.

Sperling, HG, Johnson, C, & Harwerth, RS (1980): Differential spectral photic damage to primate cones. *Vision Research*, **20:** 1117-1125.

Sponsel, WE, Arango, S, Trigo, Y, & Mensah, J (1998): Clinical classification of glaucomatous visual field loss by frequency doubling perimetry. *American Journal Of Ophthalmolgy*, **125:** 830-836.

Stafanous, SN, Clarke, MP, Ashton, H, & Mitchell, KW (1999): The effect of long-term use of benzodiazepines on the eye and retina. *Documenta Ophthalmologica*, **99:** 55-68.

Sutter, EE & Bearse, MA (1999): The optic nerve head component of the human ERG. *Vision Research*, **39:** 419-436.

Sutter, EE & Tran, D (1992): The Field Topography of ERG Components in Man-I. The Photopic Luminance Response. *Vision Research*, **32:** 433-446.

Suzuki, K, Hasegawa, S, Usui, T, Ichibe, M, Takada, R, Takagi, M, & Abe, HMultifocal electroretinogram in patients with central serous chorioretinopathy. *Japanese Journal of Ophthalmology*, **46:** 308-314.

Tartara, A, Manni, R, Galimberti, CA, Hardenberg, A, Orwin, J, & Perucca, E (1986): Vigabatrin in the treatment of epilepsy: a double-blind, placebo- controlled study. *Epilepsia*, **27:** 727-723.

Tassinari, CA, Michelucci, R, Ambroseto, G, & Salvi, F (1987): Double-blind study of vigabatrin in the treatment of drug resistant epilepsy. *Archives of neurology*, **44:** 688-692.

Teesalu, P, Airaksinen, PJ, Tuulonen, A, Nieminen, H, & Alanko, H (1997): Fluorometry of the crystalline lens for correcting blue-on-yellow perimetry results. *Investigative Ophthalmology & Visual Science*, **38:** 697-703.

Teesalu, P, Tuulonen, A, & Airaksinen, PJ (2000): Optical coherence tomography and localized defects of the nerve fibre layer. *Acta Ophthalmologica Scandinavica*, **78:** 49-52.

Tennis, P, Cole, TB, Annegers, JF, Leestma, JE, McNutt, M, & Rajput, A (1995): Cohort study of incidence of sudden unexplained death in persons with seizure disorder treated with antiepileptic drugs in Saskatchewan, Canada. *Epilepsia*, **36:** 29-36.

Theodossiadis, G, Theodossiadis, P, Malias, J, Moschos, M, & Moschos, M (2002): Preoperative and postoperative assessment by multifocal electroretinography in the management of optic disc pits with serous macular detachment. *Ophthalmology*, **109:** 2295-2302.

Thomas, D, Thomas, R, Muliyil, JP, & George, R (2001): Role of frequency doubling perimetry in detecting neuro-ophthalmic visual field defects. *American Journal of Ophthalmology*, **131:** 734-741.

Toggweiler, S & Wieser, HG (2001): Concentric visual field restriction under vigabatrin therapy: extent depends on the duration of drug intake. *Seizure*, **10:** 420-423.

Tomson, T, Nilsson, BY, & Levi, R (1988): Impaired visual contrast sensitivity in epileptic patients treated with carbamazepine. *Archives Neurology*, **45:** 897-900.

Townsend, JC (2003): Brightness and colour comparison. In, Eskridge, JB, Amos, JF, & Bartlett, JD (Eds.), *Clinical Procedures in Optometry* (pp 493-503). Philadelphia: Lipcott Comany.

Traquair, HM (1938): *An introduction to clinical perimetry*. London: Henry Klimpton Publishers.

Tsai, CS, Zangwill, L, Sample, PA, Garden, V, Bartsch, DU, & Weinreb, RN (1995): Correlation of peripapillary retinal height and visual field in glaucoma and normal subjects. *Journal of Glaucoma*, **4:** 110-116.

Tzekov, R & Arden, GB (1999): The Electroretinogram in Diabetic Retinopathy. *Survey of Ophthalmology*, **44:** 53-60.

Uldall, P, Alving, J, Gram, L, & Beck, S (1991): Vigabatrin in Paediatric Epilepsy- An Open Study. *Journal of Child Neurology*, **6:** 38-44-

Vaegan & Buckland, L (1996): The spatial distribution of ERG losses across the posterior pole of glaucomatous eyes in multifocal recordings. *Australian and New Zealand Journal of Ophthalmolgy*, **24:** 28-31.

Vaegan & Sanderson, G (1997): Absence of ganglion cell subcomponents in multifocal luminance electroretinograms. *Australian and New Zeland Journal of Ophthalmology*, **25:** 87-90

Van der Torren, K, Graniewski-Wijnands, HS, & Polak, BCP (2002): Visual field and electrophysiological abnormalities due to vigabatrin. *Documenta Ophthalmologica*, **104:** 181-188.

Vanhatalo, S, Nousiainen, I, Eriksson, K, Rantala, H, Vainionpaa, L, Mustonen, K, Aarimaa, T, Alen, R, Aine, MR, & Byring et, a (2002): Visual field constriction in 91 Finnish children treated with vigabatrin. *Epilepsia*, **43:** 748-756.

Verrotti, A, Lobefalo, L, Petitti, MT, Mastropasqua, L, Morgese, G, Chiarelli, F, & Gallenga, PE (1998): Relationship between contrast sensitivity and metabolic control in diabetics with and without retinopathy. *Annals Of Medicine*, **30:** 369-374.

Versino, M & Veggiatt, P (1999): Reversibility of vigabatrin-induced visual-field defect. *The Lancet*, **354:** 486.

Vigevano, F & Cilio, M (1997): Vigabatrin Versus ACTH as First-Line Treatment for Infantile Spams: A randomized, Prospective Study. *Epilepsia*, **38:** 1270-1274.

Vingrys, AJ & Pianta, MJ (1999): A new look at threshold estimation algorithms for automated static perimetry. *Optometry and Vision Science*, **76:** 588-595.

Wall, M, Neahring, RK, & Woodward, KR (2002): Sensitivity and specificity of frequency doubling perimetry in neuro-ophthalmic disorders: a comparison with conventional automated perimetry. *Investigative Ophthalmology & Visual Science*, **43:** 1277-1283.

Wall, M, Punke, SG, Stickney, TL, Brito, CF, Withrow, KR, & Kardon, RH (2001): SITA standard in optic neuropathies and hemianopias: a comparison with full threshold testing. *Investigative Ophthalmology & Visual Science*, **42:** 528-537.

Watson, AB & Pelli, DG (1983): QUEST: a Bayesian adaptive psychometric method. *Perception & Psychophysics*, **33:** 113-120.

Werner, EB, Krupin, T, Adelson, A, & Feitl, ME (1990): Effect of patient experience on the results of automated perimetry in glaucoma suspect patients. *Ophthalmology*, **97:** 44-48.

White, AJR, Sun, H, Swanson, WH, & Lee, BB (2002): An examination of physiological mechanisms underlying the frequency-doubling illusion. *Investigative Ophthalmology & Visual Science*, **43:** 3590-3599.

Wild, JM, Cubbidge, RP, Pacey, IE, & Robinson, R (1998): Statistical Aspects of the Normal Visual Field in Short-Wavelength Automated Perimetry. *Investigative Ophthalmology Visual Science*, **39:** 54-63.

Wild, JM & Hudson, C (1995): The attenuation of blue-on-yellow perimetry by the macular pigment. *Ophthalmology*, **102:** 911-917.

Wild, JM, Hutchings, N, Hussey, MK, Flanagan, JG, & Trope, GE (1997): Pointwise univariate linear regression of perimetric sensitivity against follow-up time in glaucoma. *Ophthalmology*, **104:** 808-815.

Wild, JM, Martinez, C, Reinshagen, G, & Harding, GFA (1999a): Characteristics of a Unique Visual Field Defect Attributed to Vigabatrin. *Epilepsia*, **40:** 1784-1794.

Wild, JM, Moss, ID, Whitaker, D, & O'Neil, EC (1995): The statistical interpretation of blue-on-yellow visual field loss. *Investigative Ophthalmology and Vision Science*, **36:** 1398-1410.

Wild, JM, Pacey, IE, Hancock, SA, & Cunliffe, IA (1999c): Between-Algorithm, Between-Individual Differences in the Normal Perimetric Sensitivity: Full Threshold, FASTPAC, and SITA. *Investigative Ophthalmology and Visual Science*, **40:** 1152-1160.

Wild, JM, Pacey, IE, O' Neill, EC, & Cunliffe, IA (1999b): The SITA Perimetric Threshold Algorithms in Glaucoma. *Investigative Ophthalmology and Vision Science*, **40:** 1998-2009.

Wildberger, H & Junghardt, A (2002): Local visual field defects correlate with the multifocal electroretinogram (mfERG) in retinal vascular branch occlusion. *Klinische Monatsblatter Fur Augenheilkunde*, **219:** 254-258.

Wilensky, AJ, Friel, PN, Ojemann, LM, Kupferberg, HJ, & Levy, RH (1985): Pharmacokinetics of W-554 (ADD 03055) in epileptic patients. *Epilepsia*, **26:** 602-606.

Wood, JM, Wild, JM, Bullimore, MA, & Gilmartin, B (1988): Factors affecting the normal perimetric profile derived by automated static threshold LED perimetry. I. Pupil size. *Ophthalmic & Physiological Optics,* **8:** 26-31.

Wood, JM, Wild, JM, Hussey, MK, & Crews, SJ (1987): Serial examination of the normal visual field using Octopus automated projectionperimetry: evidence for a learning effect. *Acta Ophthalmologica (Copenh)*, **65:** 326-333.

Yamashiro, H, Tanaka, M, Saito, M, & Shirato, S (2001): The ability of frequency doubling technology to detect abnormality of visual function in early glaucoma. *Nippon Ganka Gakkai Zasshi*, **105:** 488-493.

Yoshii, M, Yanashima, K, Wada, H, Sakemi, F, Enoki, T, & Okisaka, S (2001): Analysis of Second-order Kernel Response Components of Multifocal Elelctroretinograms Eliciated From Normal Subjects. *Japanese Journal of Ophthalmology*, **45:** 247-251.

Zielinski (1974): Epilepsy and mortality rate and cause of death. *Epilepsia*, **15:** 191-201.